

# **Generation and Analysis of a Mouse Model for Conditional Inactivation of CTLA-4**

**José Ignacio Saldaña**

A THESIS SUBMITTED FOR THE DEGREE OF  
DOCTOR OF PHILOSOPHY OF THE UNIVERSITY OF LONDON  
AND FOR THE  
DIPLOMA OF MEMBERSHIP OF IMPERIAL COLLEGE

DIVISION OF CELL AND MOLECULAR BIOLOGY  
FACULTY OF NATURAL SCIENCES

IMPERIAL COLLEGE LONDON

September 2006.

---

*To my Father*

---

---

## Abstract

CTLA-4, a receptor for the B7 family of costimulatory molecules, is one of the main regulators of T-cell activation. The ligation of this glycoprotein with its ligands CD80 or CD86, produces a negative signal that down regulates IL-2 production, and causes cell cycle arrest. The main *in vivo* evidence that further substantiates the negative role of CTLA-4, is that mice deficient for this molecule, develop a lethal lymphoproliferative disorder that leads to death between 3 or 4 weeks after birth. The characteristics of this phenotype produce a very important limitation to study adult-stage immunity in the absence of CTLA-4.

To overcome this problem, we generated a mouse model in which conditional *Ctla-4* inactivation can be performed using the *Cre-loxP* system. We are interested in studying the peripheral immune system of animals in which the inactivation of CTLA-4 can be temporally controlled, in order to gain access of adult-stage lymphoid tissue in the absence of this costimulatory molecule.

In this thesis we report the generation and phenotypical characterization of mice bearing a targeted *Ctla-4* allele. Homozygous individuals develop lymphadenopathy with no signs of tissue damage. T cells from these mice over express CTLA-4 upon polyclonal activation and show qualitative differences in the expression of the transcripts corresponding to the main CTLA-4 splice variants.

Further modifications to the targeted CTLA-4 allele, by Cre-mediated recombination in the germ cells, yielded mice having an allele that lacks the coding sequences for two of the most important domains of this molecule. Mice with this genotype, develop a fatal autoimmune disorder very similar to that present in previously generated CTLA-4 knock out models. The nature of the sequence deletion generated in these mice makes them an interesting model for further experimental work.

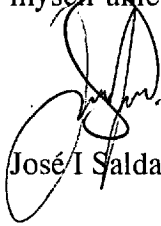
We discussed the implications of these data with respect to the current literature in the field.

---

---

## Declaration

I, José I Saldaña, hereby declare that the work presented in this thesis was carried out by myself unless otherwise stated



José I Saldaña

---

## **Acknowledgments.**

I am deeply thankful to Maggie Dallman for providing me with the opportunity to undertake research in this fantastic project, for the express yet very thorough reading of this document, but above all for the experience I gained while working in her research group.

I would also like to thank Professor Dan Davis, Professor Miguel Seabra, Dr Rosemary Boyton, Dr Rita Tewari, Dr Tessa Crompton, Professor Danny Altmann for the learning obtained while discussing with them as well as for their support.

I am particularly thankful to Professor Ita Askonas for her invaluable support and equally for the opportunities for discussion.

Much appreciation and gratitude goes to Laurence Bugeon for all her advice and support during work but also for the enjoyable discussions, normally over a nice pint of Ale.

To Alan Ahern and Jenny Rowland for being close and almost collaborators when introducing me to the art of “Gene Targeting”. Not forgetting the past and present members of staff in the Dallman lab and the SAF building; Carol, Susan, Leanne, Ian, Bruce, Charlie, Ursula, Rachel, Nel, Niam and Will, your advice, help and company was invaluable.

As far as my friends in Mexico and elsewhere is concerned; Lorena, Diego, Quique, Ivan, Carlos, Enrique, Augusto, Christian, Benjamin, Nuria, Santiago, Bruno, Rodrigo, Toni, Alex, Tim and Iratxe. I would like to say that it seems that neither The Atlantic, Europe nor Down Under are as far as they seem to be.

Thanks to my contemporary and non-contemporary fellow PhD students; particularly Catherine Reynolds for being the perfect friend anyone requires while working mad hours. It has always been fantastic to find you there by your bench when I thought I was going to be on my own on a Sunday evening. To Divya, Clare, Sabrina, Bebhinn, Damiano, Mowe, Nikky, Geoff, Javier and also specially Emma, it was great to work with you all.

To the “local family” Irene and Jordi (The Unforgettables) and to “the other local family”: Cristina, Julia, Gaby and Fernando my deepest gratitude.

All my love to the closest people to me: Juan, Emma, Isabel and Milagros your support made this happen.

---

---

The financial resources to cover my tuition fees and living expenses were provided, in joint agreement, by CONACyT-Mexico and The Foreign and Commonwealth Office under a Chevening scholarship (grant 167474), The Secretary of Education-Mexico and The French Swiss Association of Mexico. I am very thankful for their support.

---

---

## Table of Contents

Title page	i
Dedication	ii
Abstract	iii
Declaration	iv
Acknowledgments	v
Table of contents	vi
Abbreviations	vii
List of figures	viii
List of tables	ix

### ***Chapter 1. Introduction*** 1

#### **1.1 T cell activation: the two signal model.** 2

1.1.1 Antigen-MHC interaction is insufficient for T cell activation.

1.1.2 The components of the second signal of T cell costimulation.

#### **1.2 Costimulation receptors: their structure, interactions and expression.** 5

1.2.1 CD28 and CTLA-4.

1.2.2 The B7 ligands.

1.2.3 Costimulation as defined by surface plasmon resonance studies and gene expression.

i. Affinity and kinetics of binding.

ii. Gene expression of costimulatory receptors.

iii. The functional hypothesis.

#### **1.3 Other important costimulatory molecules.** 17

1.3.1 ICOS.

1.3.2 The PD1-PD-L pathway.

1.3.3 B7-H3 and B7-H4.

---

---

1.3.4	BTLA.	
<b>1.4</b>	<b>Negative regulation by CTLA-4.</b>	<b>21</b>
<b>1.5</b>	<b>Molecular genetics of <i>Ctla-4</i>.</b>	<b>24</b>
1.5.1	CTLA-4 genomic organization and splicing.	
1.5.2	<i>Ctla-4</i> is polymorphic and its locus associates with autoimmunity.	
<b>1.6</b>	<b>Mechanisms of CTLA-4 costimulation.</b>	<b>29</b>
1.6.1	Competition with CD28 for ligands.	
1.6.2	CTLA-4 negative signaling.	
1.6.3	CTLA-4 and CD4 <sup>+</sup> CD25 <sup>+</sup> regulatory T cells.	
<b>1.7</b>	<b>The role of CTLA-4 in the induction of peripheral tolerance.</b>	<b>32</b>
<b>1.8</b>	<b>Targeted mutagenesis in mice.</b>	<b>35</b>
1.8.1	The history of gene targeting.	
1.8.2	The methodology of gene targeting.	
1.8.3	The targeting vectors.	
i.	The length of the homologous region of the targeting vector.	
ii.	Degree of Polymorphism and isogeneity of the homologous sequence.	
iii.	Positive selection.	
iv.	Negative selection.	
1.8.4	Screening for homologous recombination.	
1.8.5	Chimera production and germline transmission of the targeted mutation.	
<b>1.9</b>	<b>Site Specific Recombination.</b>	<b>47</b>
1.9.1	The Cre-loxP system.	
1.9.2	The FLP – <i>FRT</i> system.	
1.9.3	Site specific recombinases in gene targeting.	
<b>1.10</b>	<b>Conditional gene targeting.</b>	<b>51</b>

---



---

<b>1.11 Conclusions and aims.</b>	55
<b>1.12 General Aims.</b>	56
<b><i>Chapter 2. Materials and Methods</i></b>	57
<b>2.1 Materials</b>	58
2.1.1 Buffers, solutions and media.	58
i. Molecular Biology.	
ii. Techniques for protein analysis.	
iii. Tissue culture techniques.	
iv. Flow cytometry.	
v. Tamoxifen Treatment.	
2.1.2 Heat shock competent bacteria.	60
2.1.3 Enzymes.	61
2.1.4 Kits for Molecular Biology.	
2.1.5 Plasmid vectors.	
i. <i>pBluescript II KS+</i>	
2.1.6 Oligonucleotides.	62
2.1.7 Kits used for the techniques of protein analysis.	63
2.1.8 Antibodies used for tissue culture, Western blot and flow cytometry.	63-64
i. Antibodies used for western blot.	
ii. Purified Antibodies used for tissue culture.	
iii. Anti mouse monoclonal and isotype antibodies control used for flow cytometry.	
<b>2.2 Methods</b>	65
<b>2.2.1 Molecular Biology.</b>	65
i. Agarose gel electrophoresis.	
ii. Small and large scale plasmid DNA purification.	
iii. Extraction of DNA from agarose gels.	
iv. Plasmid purification and genomic DNA extraction using Phenol/Chloroform or as crude lysates.	
v. RNA extraction for Reverse Transcriptase - PCR.	

---

- 
- vi. UV spectrophotometry.
  - vii. Restriction enzyme digestion of plasmid and genomic DNA.
  - viii. Alkaline phosphatase treatment of DNA.
  - ix. Restriction overhangs modification or "end filling".
  - x. DNA precipitation.
  - xi. Oligonucleotide annealing.
  - xii. Ligation of DNA fragments.
  - xiii. Transformation of E.coli.
  - xiv. Design and synthesis of oligonucleotide primers for PCR.
  - xv. Polymerase chain reaction.
  - xvi. Southern Blot, hybridization, removal of radio-labeled probes and autoradiography.

**2.2.2 Techniques for protein analysis. 75**

- i. SDS-PAGE.
- ii. Western blotting.

**2.2.3 Tissue culture. 76**

- i. Preparing single cell suspensions from peripheral, thymus lymph nodes and spleen.
- ii. Viable cell count.
- iii. Isolation of CD3 cells by paramagnetic beads.
- iv. Total lymph node or primary T cells cultures.
- v. Measuring cell proliferation by radioactive thymidine uptake.

**2.2.4 Flow cytometry. 78**

- i. Surface stain.
- ii. Intracellular stain.
- iii. Acquisition and analysis.

**2.2.5 Experimental animals and animal husbandry. 79**

- i. Experimental animals.
- ii. Tamoxifen inductions.

**2.2.6 Histological analysis. 80**

**2.2.7 Statistical analysis. 80**

---

---

<b>Chapter 3. Generation of mice bearing a targeted <i>Ctla-4</i> allele.</b>	81
<b>3.1 Background.</b>	82
<b>3.2 General characteristics and construction strategy of the targeting vector.</b>	84
<b>3.3 Molecular cloning of pMKSB7K.</b>	90
<b>3.4 Generation of p4KBH4NEO.</b>	94
<b>3.5 Screening for homologous recombination among neomycin-resistant ES cell clones by PCR.</b>	107
3.5.1 Screening for homologous recombination at the 3' end of <i>Ctla-4</i> .	109
3.5.2 Screening for homologous recombination at the 5' end of <i>Ctla-4</i> .	109
<b>3.6 Screening for a single gene replacement by Southern blot analysis, Chimera production and germ-line transmission analysis.</b>	117
3.6.1 Screening for a single gene replacement by Southern blot analysis.	117
3.6.2 Chimera production from ES cell sample 1A1 and analysis of germ line transmission.	124
3.6.3 Screening for a single gene replacement by Southern blot analysis of ES cell samples 4A11 and 3B5.	125
3.6.4 Chimera production from ES cell samples 4A11 and 3B5 and analysis of germ line transmission.	134
<b>3.7 Concluding remarks.</b>	138
3.7.1 Estimation of the frequency of homologous recombination at the <i>Ctla-4</i> locus.	138
3.7.2 Towards a model for conditional inactivation of <i>Ctla-4</i> .	138
3.7.3 Phenotypic analysis of mice bearing a targeted <i>Ctla-4</i> allele prior any modification.	139

---

---

<b>Chapter 4. The phenotype of <i>Ctla-4</i> targeted mice.</b>	140
<b>4.1 Background.</b>	141
<b>4.2 Generation of heterozygous and homozygous mice bearing a targeted <i>Ctla-4</i> allele.</b>	143
<b>4.3 Histological analysis of CTLA-4 targeted mice.</b>	143
<b>4.4 Homozygous <i>Ctla-4</i> targeted mice develop lymphadenopathy.</b>	145
<b>4.5 Homozygous mice have an increased proportion of CD4 single positive thymocytes and lower numbers of double positive thymocytes.</b>	151
<b>4.6 <i>Ex vivo</i> analysis of the activation state of T cells from experimental animals.</b>	154
<b>4.7 T cells from homozygous mice over-express CTLA-4 upon polyclonal activation.</b>	156
<b>4.8 CTLA-4 over-expression is not associated to genetic background heterogeneity.</b>	161
<b>4.9 Activated lymph node cells from homozygous mice express higher levels of CD25 but do not proliferate differentially.</b>	165
<b>4.10 Analysis of the expression of known <i>Ctla-4</i> splice variants.</b>	167
<b>4.12 Discussion.</b>	172

---

---

<b><i>Chapter 5. Cre-mediated recombination and Ctla-4</i></b>	176
<b>5.1 Background.</b>	177
<b>5.2 The generation of mice bearing two <i>loxP</i> sites flanking exons 2 and 3 of <i>Ctla-4</i>.</b>	179
<b>5.3 Generation of mice with a <i>Ctla-4</i> allele lacking exons two and three.</b>	185
<b>5.4 Analysis of the phenotype of del/del mice.</b>	189
<b>5.5 Discussion.</b>	198
i. Generation of a model for conditional inactivation of CTLA-4	
ii. The phenotype of mice lacking exons 2 and 3 of CTLA-4.	
<b><i>Chapter 6. Concluding discussion</i></b>	201
<b>6.1 The rationale of generating a model for conditional inactivation of CTLA-4.</b>	202
<b>6.2 Key findings.</b>	204
<b>6.3 Inducible Cre transgenics suitable to inactivate <i>Ctla-4</i>.</b>	206
<b>6.4 The uses and the value of a <i>Ctla-4</i> conditional knock out</b>	207
<b><i>Bibliography</i></b>	209

---

---

## Abbreviations

bp:	Base pair.
Kb:	Kilobase.
BSA:	Bovine Serum Albumin
Ci:	Curie
CIAP:	Calf Intestinal alkaline phosphatase.
Cre:	Cyclisation recombination gene.
kDa:	Kilo Dalton.
dNTP:	Deoxynucleotide triphosphate.
dCTP:	Deoxycytosine triphosphate.
dATP:	Deoxiadenine triphosphate.
dGTP:	Deoxiguanine triphosphate.
dTTP:	Deoxithymidine triphosphate.
DNA:	Deoxyribonucleic acid.
ES:	Embryonic Stem.
EDTA:	Ethylendiaminetetraacetic acid.
FRT:	flp recognition target.
g:	Acceleration due to gravity or grams.
FACS:	Fluorescence activated cell sorting.
G418:	Geneticin.
HCl:	Hydrochloric acid.
L:	Litre.
LB:	Luria-Bertani.
LIF:	Lukaemia inhibition factor.
<i>LoxP</i> :	Locus of crossing over P1
M:	Molar
mRNA:	Messenger ribonucleic acid.
NaCl:	Sodium chloride.
NaOH:	Sodium hydroxide.
<i>neo</i> :	Neomycin
PBS:	Phosphate Buffered Saline.
PCR:	Polymerase chain reaction.
RT-PCR:	Reverse transcriptase polymerase chain reaction

---

---

PGK:	Phosphoglycerate kinase-1
RNA:	Ribonucleic acid.
IL:	Interlukin
SDS:	Sodium dodecyl sulphate.
V:	Volts
TAE:	Tris-acetate.
Taq:	<i>Thermophilus acuaticus</i>
TBE:	Tris-borate acetate.
TE:	Tris-EDTA.
Tris:	Tris[hydroxymethyl]aminoethane.
CM:	Centi Morgan
Tam:	Tamnoxifen
UV:	Ultra violet.
V:	Volts
MAb:	Monoclonal antibody
IgSF:	Immunoglobulin superfamily.
$\mu$ :	micro
IgV:	Immunoglobulin variable
IgC:	Immunoglobulin constant
APC :	antigen presenting cell
MLR:	Mixed lymphocyte reaction
MHC:	Major histocompatibility complex
CTL:	Cytotoxic lymphocyte
TCR:	T cell receptor
cDNA:	Complementary DNA
CHO:	Chinese hamster ovary
DKO:	Double knock out
Treg:	Regulatory T cell
IDO:	Indoleamine 2,3-dioxigenase
Kd:	Dissociation constant
n:	Nano
hr:	Hour
min:	minute
sec:	second
CTLA-4:	cytotoxic T lymphocyte antigen 4

---

---

ICOS: Inducible costimulator  
ICOSL: Inducible costimulator ligand  
PD-1: Programme death 1  
PD-1L: Programme death 1 ligand  
SNP: single nucleotide polymorphism  
OVA: Ovalbumin  
HPRT: Hypoxanthine phosphoribosyl transferase  
LCR: Locus control region  
CFSE: Carboxy-fluorescein diacetate, succinimidyl ester  
MFI: Mean fluorescence intensity  
FICTLA-4: Full length CTLA-4  
LiCTLA-4: Ligand independent CTLA-4  
sCTLA-4: soluble CTLA-4  
CD: cluster of differentiation

All units are standard SI units.

---



---

## ***List of figures***

### ***Chapter 1***

<b><u>Figure</u></b>	<b><u>Page number</u></b>
1.1 The “two signal” model of T cell activation.	3
1.2 Structure of the costimulatory receptors in the plasma membrane and their interactions.	9
1.3 Diagram of the quaternary structures of costimulatory and inhibitory complexes formed between CD28, CTLA-4 and B7.	16
1.4 <i>Ctla-4</i> and its splice variants.	26
1.5 Localization of 7 single nucleotide polymorphisms (SNP) and the (AT) <sub>n</sub> repeat sequence within the 2q33 human CTLA-4 locus.	28
1.6 Scheme of replacement and insertion vectors and their products of recombination.	38
1.7 Integration of a replacement vector.	45
1.8 The <i>loxP</i> site	48
1.9 Spatio-temporal control of gene inactivation through Cre –mediated recombination in cells and mice.	54

### ***Chapter 3***

<b><u>Figure</u></b>	<b><u>Page number</u></b>
3.1 Diagram of the targeting construct compared with wild type <i>Ctla-4</i> allele.	86
3.2 Restriction map of the 129Sv <i>Ctla-4</i> genomic region compared with the targeting vector and the modified alleles after Cre-mediated recombination.	87
3.3 Restriction digest of the plasmids, p4KHBHB and p4KBH4 containing the 129Sv CTLA-4 genomic sequence used for the construction of the targeting vector,	88
3.4 Cloning strategy for the construction of the <i>Ctla-4</i> targeting vector.	89

---

---

<b>3.5</b> Characterization by restriction digest of clone pMKSb7K.	91
<b>3.6</b> The insertion of the first <i>LoxP</i> into pMKSb7K using a synthetic oligonucleotide.	93
<b>3.7</b> Ligation of an adaptor (EcoR1BglII) to p4KBH4.	96
<b>3.8</b> Insertion of the floxed PGKneo cassette into the modified p4KBH4.	97
<b>3.9</b> Elimination of a 1.2 Kb region downstream exon 4.	99
<b>3.10</b> Generation of pLoxCTLA-4.	101
<b>3.11</b> Sequencing analysis of exons 1 and 2 of pLoxCTLA-4.	102
<b>3.12</b> Sequencing analysis of exons 3 and 4 of pLoxCTLA-4.	103
<b>3.13</b> Sequence analysis of the <i>LoxP</i> immediately upstream exon 1.	104
<b>3.14</b> Sequence analysis of the <i>LoxP</i> sites flanking the neo cassette.	105
<b>3.15</b> Circular restriction map of the targeting construct pLoxCTLA-4.	106
<b>3.16</b> PCR strategy to detect homologous recombination (HR) between the targeting vector and the wild-type <i>Ctla-4</i> locus.	108
<b>3.17</b> Assessment of homologous recombination of the targeting vector in the <i>Ctla-4</i> locus by a PCR on the 3' end.	110
<b>3.18</b> PCR amplification of a 7.3 Kb region across the 5' region of the <i>Ctla-4</i> locus.	112
<b>3.19</b> Diagram of the insertion of the regions of homology of pLoxCTLA-4 by homologous recombination into the <i>Ctla-4</i> allele.	113
<b>3.20</b> Assessment of a complete or partial insertion of pLoxCTLA-4 into the <i>Ctla-4</i> allele.	115
<b>3.21</b> Restriction map of the WT and targeted <i>Ctla-4</i> alleles for Southern blot analysis.	118
<b>3.22</b> Southern blot analysis using the 5' external probe hybridized to ES cell genomic DNA digested with <i>EcoR1</i> .	121
<b>3.23</b> Southern blot analysis using the 3' external probe hybridized onto ES cell genomic DNA digested with <i>HindIII</i> .	122

---

---

3.24. Southern blot analysis using the internal probe hybridized to ES cell genomic DNA digested with <i>EcoR</i> I.	123
3.25 Assessment of complete or partial insertion of pLoxCTLA-4 into the <i>Ctla-4</i> allele.	126
3.26 Southern blot analysis using the 5' external probe hybridized to ES cell genomic DNA digested with <i>EcoR</i> I.	128
3.27 Southern blot analysis using the 3' external probe hybridized onto ES cell genomic DNA digested with <i>Hind</i> III.	131
3.28 Southern blot analysis using the internal probe hybridized onto ES cell genomic DNA digested with <i>Hind</i> III.	132
3.29 Southern blot analysis using the 3' external probe, performed on genomic DNA digested with <i>EcoR</i> I from ES cells after amplification and before blastocyst injection.	133
3.30 Southern blot analysis of tail genomic DNA of agouti offspring from chimeric animals generated by blastocyst injections of ES cell sample 4A11.	135
3.31 Southern blot analysis of agouti animals heterozygous for the <i>Ctla-4</i> targeted allele.	137

## ***Chapter 4***

<b><u>Figure</u></b>	<b><u>Page number</u></b>
4.1 Intercross of heterozygous animals bearing a targeted <i>Ctla-4</i> allele to produce homozygote mutants.	144
4.2 Histologic analysis of organs from <i>Ctla-4</i> targeted mice.	146
4.3 The lymphadenopathy observed in homozygous mice is reflected in increased cell numbers.	147
4.4 Total cell counts in the spleen of wild-type, heterozygous and homozygous animals.	149
4.5 Increased lymph node cellularity observed in homozygous <i>Ctla-4</i> targeted mice results from an increased proportion of B cells.	150
4.6 Homozygous animals have a distinct CD4-CD8 profile in thymus when compared to WT or heterozygous individuals.	152

---

---

4.7 Percentage of CD4+ and CD8+ T cells in lymph nodes from CTLA-4 targeted mice.	153
4.8 Percentage of lymph node cells expressing the activation markers CD69 and CD25 is similar between experimental animals.	155
4.9 Resting total lymph node cells do not express CTLA-4 intracellularly.	157
4.10 Lymphocytes of homozygous mice over-express intracellular CTLA-4 upon activation.	158
4.11 Purity assessment after CD3+ T cell negative isolation with paramagnetic beads.	159
4.12 Intracellular expression of CTLA-4 increased in homozygotes as compared with littermates.	160
4.13 Generation of a line of CTLA-4 targeted mice on a 129SvPAS pure background.	162
4.14 Intercross of heterozygous animals bearing a targeted <i>Ctla-4</i> allele on a 129SvPAS background to produce homozygote mutants.	163
4.15 Intracellular expression of CTLA-4 is also increased in 129SvPAS homozygotes as compared with littermates.	164
4.16 Homozygous CD3+ cells express higher levels of CD25 but do not proliferate differentially.	166
4.17 Li-CTLA-4 expression is similar in homozygous targeted mice as as compared to littermates.	168
4.18 <i>Ctla-4</i> and its splice variants.	169
4.19 The kinetics of expression of all splice variants are altered in homozygous targeted mice as compared with littermates.	170

## ***Chapter 5***

<b><u>Figure</u></b>	<b><u>Page number</u></b>
5.1 Outcomes of Cre-mediated recombination on the <i>Ctla-4</i> targeted allele.	178
5.2 Generation of mice bearing <i>LoxP</i> sites flanking exons 2 and 3 for use in experiments for conditional inactivation of CTLA-4.	181

---

---

<b>5.3</b> Generation of mice heterozygous for a targeted <i>Ctla-4</i> allele and positive for a transgene encoding an inducible form of Cre (MerCreMer).	182
<b>5.4</b> Schematic representation of the PCR strategy to detect Cre-mediated deletion of <i>Ctla-4</i> .	183
<b>5.5</b> In vivo inducible Cre mediated deletion of <i>Ctla-4</i> .	184
<b>5.6</b> Generation of <i>Ctla-4</i> del/del mice by Cre mediated deletion.	187
<b>5.7</b> Generation of mice bearing a deleted <i>Ctla-4</i> allele by Cre mediated recombination.	188
<b>5.8</b> Genotyping of del/del mice.	190
<b>5.9</b> del/del mice show a lethal phenotype and die 4 weeks after birth.	191
<b>5.10</b> CTLA-4 expression analysis by flow cytometry and western blot of cells from del/del mice compared with wt/wt and/or wt/del littermates.	192
<b>5.11</b> Histologic analysis of organs from del/del mice as compared the littermates.	195
<b>5.12</b> Flow cytometric analysis of thymocytes and lymph node cells from <i>Ctla-4</i> del/del mice as compared with littermates.	196
<b>5.13</b> Flow cytometry analysis of lymph node cells from del/del mice compared with wt and wt/del littermates.	197
<b>5.14</b> Breeding strategy to generate mice suitable to conditionally inactivate CTLA-4.	199

---

---

## *List of tables*

### *Chapter 2*

<u>Table</u>	<u>Page number</u>
2.1 Oligonucleotides used for PCR and sequencing.	62
2.1 Primary and secondary antibodies used for Western blot	63
2.4 Mouse monoclonal antibodies used for flow cytometry	64
2.5 Mouse anti TNP isotype control antibodies	64
2.6 Conditions for the PCR performed	73

### *Chapter 3*

<u>Table</u>	<u>Page number</u>
3.1 Blastocyst injection sessions performed with ES cell sample 1A1 and chimeras produced	124
3.2 The results of the blastocyst injections performed with ES cells form sample 4A11	134
3.3 The results of the blastocyst injections performed with ES cells form sample 3B5	134

### *Chapter 5*

<u>Table</u>	<u>Page number</u>
5.1 Viable cell count form lymph nodes of wt/wt, wt/del and del/del mice.	193

---

***Chapter 1. Introduction***

## **1.1 T cell activation: the two signal model.**

### **1.1.1 Antigen-MHC interaction is insufficient for T cell activation.**

The production of a successful adaptive immune response requires the activation and clonal expansion of rare antigen specific lymphocytes, a decrease in the number of these cells and finally a mechanism to establish long-term memory once the antigen has been eliminated. Among those lymphocytes, T cells play a major role as effectors, coordinators and regulators of such responses to specific antigens. T cell activation is a complex process that involves a variety of interactions between adhesion molecules and receptors on the cell surface of the T cells and the antigen presenting cells (APC). The activation of a T cell depends on the association of the T cell receptor with an antigenic peptide bound to the major histocompatibility complex (MHC) on the surface of the APC (Zinkernagel., *et al* 1944). Although this interaction determines the generation of an antigen-specific T cell immune response, itself it is not sufficient to fully activate T cells, as initially demonstrated by the activation studies of cytotoxic T lymphocytes (CTL) to allogeneic transplant antigens (Laferty., *et al* 1975, reviewed in Laferty., *et al* 1977). Laferty and co-workers showed, in a transplant model, that successful CTL responses could not be triggered by all the cells carrying alloantigens (abundant in the transplant), but only by haematopoietic cells having allogenic MHC antigen, and a second stimulatory signal (co-stimulatory). Later, it was further postulated that in the absence of an antigen independent costimulatory signal, T cells become hyporesponsive or anergised rather than activated (Jenkins., *et al* 1987; Jenkins., *et al* 1988).

The two signal model is schematically described in figure 1.1.

Jenkins and Schwartz in the eighties suggested that the costimulatory signal was fundamentally independent to the signals provided by the TCR and this led to the search for cell surface receptors present on resting T cells, that had signaling properties distinct from the TCR.



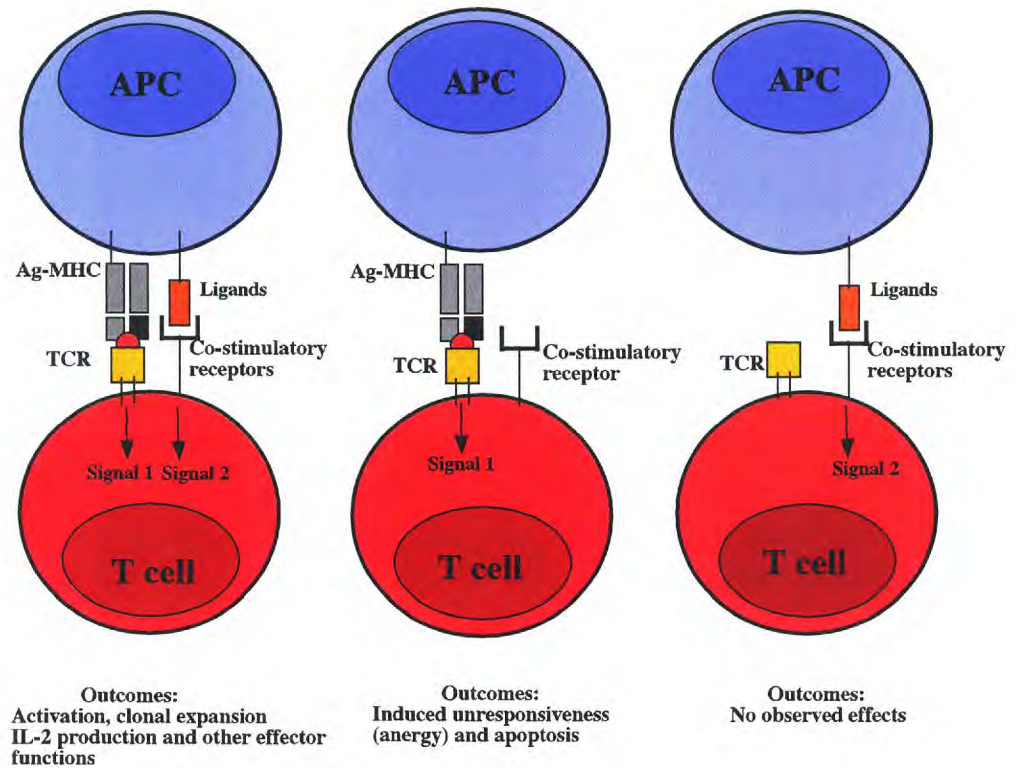


Figure 1.1.- The “two signal” model of T cell activation. Antigen presenting cells can display antigen bound to the MHC and/or costimulatory ligands to provide two fundamentally independent signals to T cells.

Given the nature of this model, three different outcomes can be expected: clonal expansion of T cells and effector functions will only develop upon ligation of both, Ag-MHC (signal 1) and costimulatory ligands and receptors (signal 2). In the absence of signal 2, T cells will be rendered unresponsive (anergic). Provision of only signal two, has produced no observed effects. We now today that this binary interactions are not the only mode of costimulation and that interactions “in trans” happen.

Figure adapted from (Bretscher., *et al* 1970) and (June., *et al* 1994).

## 1.1.2 The components of the second signal of T cell costimulation.

The components of the second signal of T cell activation were identified in the late eighties using antibody reagents and various in vitro cell culture assays. One of the first costimulatory molecules to be identified was CD28. It was initially characterized and defined as a T cell costimulatory receptor in experiments where the activation of human T cells and T cell clones by antigen primed APC or in mixed lymphocyte reactions (MLR) were blocked using Fab fragments of antibodies reactive with the molecule. Here the activation of those T cells clones could not only be blocked by the CD28 antibodies, but also the cells were rendered unresponsive to subsequent antigen challenges (Damle., *et al* 1988 and Harding., *et al* 1992). The now well characterized ligand for CD28 on the APC, CD80, was identified using blocking monoclonal antibodies against B7-1 (or CD80) on B cells to show the failure of these cells to adhere to chinese hamster ovary cells transfected with CD28 (Linsley., *et al* 1990).

In previous years, the search for activated cytotoxic T cell surface antigens through the screening of a subtracted complementary DNA (cDNA) library, resulted in the identification of a structure homologue of CD28, the Cytotoxic T Lymphocyte antigen 4 (CTLA-4) (Brunet., *et al* 1987). This molecule was soon associated with the T cell costimulatory pathway, as a fusion protein of the  $\gamma$  immunoglobulin constant region and the extra-cellular domain of CTLA-4 (CTLA-4-Ig) was found to bind B7-1 on the surface of transfected CHO cells (Linsley., *et al* 1991). The evidence that the immune response - otherwise not compromised in CD80 knock out mice- could be suppressed by administering CTLA-4-Ig, together with the *in vivo* studies comparing the effects of the CTLA-4-Ig with the administration of a B7-1 (CD80) specific antibody led to the discovery of an additional ligand for both CD28 and CTLA-4, namely B7-2 (CD86).

The costimulatory ligands of the B7 family - CD80 and CD86, as defined under the cluster of differentiation nomenclature - are also referred as B7-1 and B7-2 throughout the literature. In this thesis, the term B7 will be used in reference to both molecules, otherwise their individual CD nomenclature will be used.

## 1.2 Costimulation receptors: their structure, interactions and expression.

### 1.2.1 CD28 and CTLA-4.

CD28 and CTLA-4 are structurally very similar yet they are not functionally redundant. CD28 provides positive costimulation and survival signals by promoting the production of IL-2, the expression of the IL-2 receptor and consequently T cell proliferation (Martin., *et al* 1986), together with the expression of the anti-apoptotic gene such as Bcl-x<sub>L</sub> (Boise., *et al* 1995) CTLA-4 ligation on T cells inhibits the up-regulation of activation markers like CD69 and CD25, decreases IL-2 accumulation and restricts cell cycle progression from G1 to S phase through inhibition of cell cycle proteins (Krumel., *et al* 1996). The differential action of these two T cell receptors has been solidly demonstrated by the study of the phenotypes of mice bearing targeted null mutations for both molecules. These evidence will be extensively discussed in subsequent sections.

*Cd28* locates adjacent *Ctla-4* on chromosome 1 in mice and 2 in humans and they share similar gene structures. Evidence suggests that both genes probably evolved by duplication from a common ancestral sequence (Harper., *et al* 1991). The degree of sequence conservation of both proteins is high between human mouse and even in the *rat*. This is particularly clear when comparing the intracellular domain where the sequence is identical between human and mouse (Clark., *et al* 1992). They are both type-1 membrane proteins and members of the immunoglobulin superfamily (IgSF). They consist of an extracellular IgV-like domains, a transmembrane domain and a highly conserved short intracellular tail without intrinsic enzymatic activity, which bears tyrosine-dependent signaling motifs substrate for phosphorylation.

CTLA-4 and CD28 have a disulphide-linked homodimeric quaternary structure, comprising 44kDa and 33-37kDa monomers respectively. (Gros., *et al* 1990, Brunet., *et al* 1987 and reviewed in Carreño., *et al* 2002).

CTLA-4 dimerizes through cysteine (Cys 122) residues at towards the transmembrane domain. This mode of dimerization allows for a coligation with both B7 ligands

around an axis orthogonal to the membrane, thus making the interaction of CTLA-4 to B7 molecules bivalent and avidity-enhanced (Schwartz., *et al* 2001 and Stamper., *et al* 2001) (see figure 1.2).

Similar crystallographic data, where the interaction of CD28 and the B7 ligands is studied, are not available yet. Nevertheless amino acid sequence analysis show that despite the facts that is a high degree of sequence conservation between CD28 and CTLA-4, the residues responsible for dimerization in CTLA-4 are not conserved in CD28, suggesting an independent mode of dimerization for CD28 monomers.

Given the relatively high level of sequence conservation and the structural similarities between CD28 and CTLA-4, it has been assumed that CD28 homodimers are also bivalent on the cell surface (i.e. Greene., *et al* (1996)). The comparison of the stoichiometry of binding of soluble B7-1 (sB7-1) molecules to immobilized CD28 and CTLA-4-Ig fusion proteins (CD28-Fc or CTLA-4-Fc), performed by surface plasmon resonance, showed that CTLA-4-Fc bound twice the amount of sB7-1 than that bound by CD28-Fc (Collins., *et al* 2002). Recent crystallographic data indicate that the observed CD28 dimer has the overall shape and dimensions of that of CTLA-4. It is, however, of interest that their dimerization modes are fundamentally different.

Whereas in CTLA-4 the residues that mediate contact between dimers are adjacent and include the stalk region, in CD28 crystals the contact is formed by the small 3-stranded A,G, F  $\beta$  sheet present in all IgV IgSF domains.

An additional general difference in both structures is that the interface of contact between monomers of CTLA-4 allows the possible interaction of putative residues that mediate dimerization; the area containing a fraction of such conserved residues in the interface between CD28 monomers is buried. CD28-like homodimerization of CTLA-4 is prevented by the substitution of His116 by Tyr115 and Ile114 by Gln113 and vice-versa by the change of Ile117 by Pro119. The resemblance of the native CD28 dimeric structure to the crystals resolved was further confirmed by Cryo-electron microscopy and mutagenesis (Davis., *et al* 2005).

The CTLA-4 homodimers are further stabilized by the interface between both monomers through 19 hydrogen bonds and 48 contacts forming van der Waals interactions (Ostrov., *et al* 2000). In vivo dimerization also depends on the N-glycosylation of

two sites on the extracellular domains proximal to the membrane (N78, N110) (Darlington., *et al* 2005 ). A very important structural hydrophobic motif found in the complementary determining region 3 of the IgV-like domain in both CD28 and CTLA-4 is the hexamer MYPPPY (in single letter aminoacid code) (Harper., *et al* 1991). CD28 and CTLA-4 fusion proteins generated with variants of this motif (generated by site directed mutagenesis) have shown impaired binding to B7, thereby establishing this conserved motif as critical for ligand-binding (Linsley., *et al* 1995).

### 1.2.2 The B7 ligands.

CD80 and CD86 are both, transmembrane glycoproteins members of the immunoglobulin super-family. Both B7 molecules have a chimeric structure as far as their extracellular domain is concerned, they comprise an IgV-like domain similar to those present in conventional recognition receptors like CD4 and a membrane proximal IgC1-like domain with a structure like antigen receptors and the MHC (Ikemizu., *et al* 2000).

In crystal lattices and in solution, CD80 forms bivalent homodimers able to bind to CTLA-4 in a periodic and linear array which gives this interaction the characteristic mentioned above of enhanced avidity. In addition, there is no evidence for covalent dimerization of CD80 (Stamper., *et al* 2001).

In spite of the fact that crystallographic data shows a plausible dimeric structure for CD86, monomer asymmetry, the presence of hydrophilic residues in its putative dimerization interface and the evidence that neither non-glycosylated nor fully glycosylated soluble CD86 dimerizes in solution, favors the idea that dimerization under physiological conditions is unlikely (reviewed in van der Merwe., *et al* 2003 ). Studies using soluble forms of CD86 show that glycosylation at the area of interface between monomers may impede dimerization (Collins., *et al* 2002). Schwartz., *et al* previously proposed the existence, in physiological conditions, of dimeric CD86. However they used dimeric CD86 proteins expressed by bacteria which will be non-glycosylated and perhaps able to form dimers. This situation may have given a false impression of what may actually be occurring at the cell surface (Schwartz., *et al* 2001).

The monomeric state of CD86 on the surface of APC has also been confirmed by imaging studies using photobleaching based fluorescence energy transfer (FRET) (Bhatia., *et al* 2005; reviewed in Bhatia., *et al* 2006).

All these data imply that CD86 is monovalent and not able to form periodical arrays with CTLA-4 (reviewed in Davis., *et al* 2003).

Figure 1.2 shows a scheme of these four costimulatory molecules and their interactions. The figure highlights the mode of interaction by which bivalent CTLA-4 homodimers form avidity enhanced interactions, particularly with CD80, in the form of stable periodical arrays.

Signaling through the B7 molecules has not been fully characterized yet but several reports provide evidence to allocate signaling properties to the intracellular domains of these receptors. B7 receptors, expressed on T cells, may be involved in transmitting inhibitory signals by CD4<sup>+</sup> CD25<sup>+</sup> regulatory T cells (Treg) (Paust., *et al* 2004). CD80/CD86<sup>-/-</sup> double knock out (DKO) CD4<sup>+</sup> CD25<sup>-</sup> T cells were resistant to suppression by concentrations of wild type Tregs able to suppress the activity of wild type CD4<sup>+</sup> CD25<sup>-</sup> T cells. Interestingly suppression was only restored by the expression of full length B7 molecules but not by expressing truncated B7 receptors lacking the intracellular domain.

In support of the idea that B7 molecules can signal, more convincing experiments show the ability of B7 receptors to deliver signals to the expressing APC upon ligation with CTLA-4 on the surface of T cells. Engagement of B7 molecules can initiate the immunosuppressive pathway of tryptophan catabolism through the production of IFN $\gamma$  and induction of the enzyme indoleamine 2,3-dioxygenase (IDO). Consequent production of tryptophan metabolites can suppress T cell proliferation. (Grohmann., *et al* 2002, Fallarino., *et al* 2003 and Munn., 2004 reviewed in Greenwald., *et al* 2005).



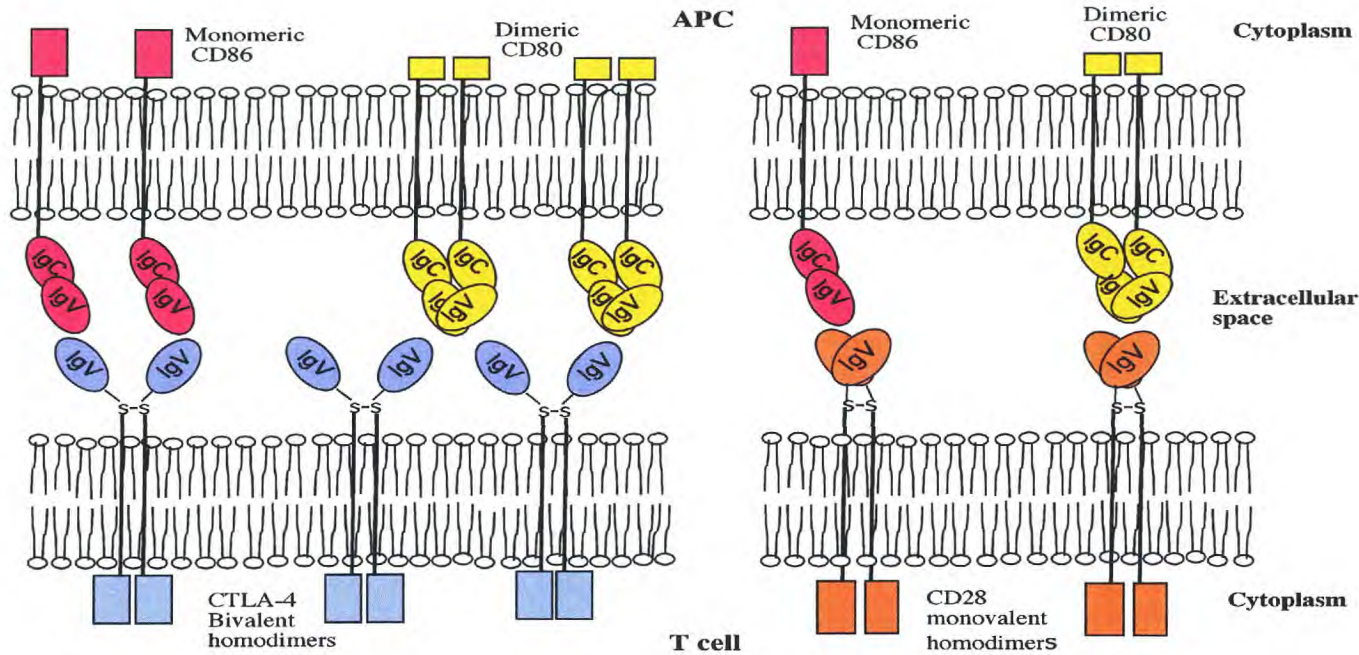


Figure 1.2.- Structure of the co-stimulatory receptors in the plasma membrane and their interactions.

CD86, monomeric on the surface of APC, interacts with CTLA-4 with low affinity and this interaction is not enhanced in avidity. In contrast, bivalent dimers of CD80 interact with CTLA-4 with relatively high affinity and forming periodic arrays increasing the avidity of the complex and making the interaction more stable. CD28 homodimers are monovalent, they as well interact with B7 ligands with low affinity, and no affinity enhancement. The four receptors are transmembrane proteins members of the IgSF; CD28 and CTLA-4 have one extracellular IgV-like domain, a transmembrane domain and a cytoplasmic signalling domain. CTLA-4 has two putative phosphorylation sites in the intracellular domain. CD80 and CD86 have both two extracellular domains one (IgV and IgC-like) a transmembrane domain and a cytosolic signalling domain longer in the case of CD86 and with 3 putative phosphorylation sites (adapted from Davis, S.J., *et al* 2003).

As shown in figure 1.2, the intracellular domain of CD86 is longer than that of CD80 and contains 3 putative phosphorylation sites for protein kinase C suggesting its potential signaling capabilities. (Azuma., *et al* 1993).

The function of B7 molecules and their T cell ligands, are determined by the above-mentioned structural characteristics.

In the the following part we will discuss how these interactions have been defined, in particular by studies using surface plasmon resonance technology.

### **1.2.3 Costimulation as defined by surface plasmon resonance studies and gene expression.**

#### **i.- Affinity and kinetics of binding.**

The functional differences between CD28 and CTLA-4 have been well established, nevertheless, the reason why two different ligands, CD80 and CD86, are necessary has been not very clear. Preservation of both genes across mammalian species suggests that they have been subjected to independent selective pressures.

Initial structural and binding studies provided limited molecular basis for the functional differences between these molecules. In fact the prevailing view was that CD80 and CD86 had similar structures and comparable rather high affinities of binding for CD28 and CTLA-4 (Lindsey., *et al* 1994, reviewed in Carreño., *et al* 2002 and Sharpe., *et al* 2002). None of these studies gave a clear and accurate view of the interactions between costimulatory molecules, but more recently Surface plasmon resonance technology has shown, that the costimulatory receptors and ligands form complexes of diverse structure and binding properties, providing an explanation for the existence and functional differences between B7 ligands.

The initial Plasmon resonance analyses used recombinant sCD80 produced in an eukaryotic expression system (CHO cells) to ensure proper glycosylation of the recombinat products. They measured the affinities and kinetics of binding to immobilized recombinant CTLA-4 and CD28-Ig fusion proteins at physiological temperature and



reported binding affinities as dissociation constants ( $K_d$ ) in micro molar concentrations units, an inverse magnitude of the strength of interaction.

The measured binding affinities of CD80 with CD28 and CTLA-4 ( $K_d = 4\mu\text{M}$  and  $0.42\mu\text{M}$  respectively) resulted much lower than previously estimated using soluble CD80-Ig fusion proteins ( $K_d = 200\text{ nM}$  and  $12\text{ nM}$  respectively) (Linsley, et al 1991). This lower affinity observed was the result of a fast kinetics of binding (van der Merwe, et al 1997).

Complete analysis of the affinities and kinetics of binding between the four components of the costimulatory pathway produced the following key findings: CD86 binds 13-fold more weakly to CTLA-4 than CD80; relative to its CTLA-4 binding affinity CD86 binds CD28 two to three fold more effectively than CD80 and finally, neither CD28 or CD86 can participate in avidity-enhanced interactions as the ones proposed for CTLA-4. These indicate that relative to CD80, the binding of CD86 is biased against CTLA-4 suggesting that there is a reduced likelihood that CD86-CD28 interactions will be attenuated by simultaneous CTLA-4 ligation, thus favouring positive costimulation under conditions where only CD28, CD86 and CTLA-4 are expressed. The reverse applies for CD80, for instance its predominant inhibitory activity when ligated to CTLA-4 is less likely to be affected by the presence of CD28 (Collins, et al 2002, reviewed in van der Merwe, et al 2003).

## **ii.- Gene expression of costimulatory receptors.**

CD28 is constitutively expressed at high levels by all mouse mature T cells and thymocytes (Gross, J.A. et al 1992) whereas in humans, it is only expressed constitutively on CD4<sup>+</sup> T cells and approximately 50% of CD8<sup>+</sup> T cells (Damle, et al 1983).

CD28 transcripts and protein expression increases upon TCR engagement but following ligation by CD80 is transiently down regulated at the mRNA level. This data are consistent with the predominant inhibitory role of CD80 (Linsley, et al 1993). In addition, CD28 is rapidly internalized by endocytosis and a proportion of the product targeted for degradation, the remainder is recycled to the cell surface.

The process of endocytosis may be mediated via phosphatidylinositol 3-kinase (PI3-K) which binds actively to the cytoplasmic tail of CD28 and was previously considered to be involved in the CD28 signaling cascades (Cefai., *et al* 1998).

CTLA-4 is expressed on the T cell surface only following activation of CD4<sup>+</sup> and CD8<sup>+</sup> T cells in both mice (Brunet, J.F., *et al* 1987) and humans (Linsley., *et al* 1992; Lindsten., *et al* 1993). It's expression is tightly controlled and dependent on ligation of CD28; activated CD28 deficient mouse T cells express very low levels of CTLA-4 unless exogenous IL-2 is provided (Wallunas., *et al* 1994). In fact, the increase in the expression of CTLA-4 correlates with the CD28 expression levels when transcripts are analyzed (Freeman.,*et al* 1992; Lindsten., *et al* 1993).

Upon activation, mouse and human CTLA-4 transcripts have been shown to peak between 24 and 48 hours post activation but are detectable as early as 1 hour (Linsley., *et al* 1992; Lindsten., *et al* 1993) and functionally effective at 12 hours (Krumel., *et al* 1996). Regardless of the abundance of mRNA, CTLA-4 protein appearance at the cell surface is delayed and in most T cells only reaches levels 1/30 to 1/50 of that of CD28 on the same cell (Linsley., *et al* 1992). Most CTLA-4 appears to be dynamically localized in post-Golgi vesicles polarized towards the synapse region (Alegre., *et al* 1996). CTLA-4 molecules are efficiently translocated to the cell surface following T cell activation and rapidly endocytosed through a clathrin, AP-1, AP-2-mediated pathway dependent on the binding of AP complexes to the dephosphorylated intracellular domain. (Chuang., *et al* 1997). This post-translational mechanism of regulation and the differences observed in human and mouse T cell subsets with respect to their CTLA- expression will be discussed in detail later in this chapter.

The mechanisms underlying the transcriptional regulation of CTLA-4 expression are still been studied but it is known that the expression is initiated about 335 bp upstream from the start codon (Ling., *et al* 1999) and that it may be dependent on the transcription factor N-FAT (nuclear factor of activated T cells), as inhibition of N-FAT activation with Cyclosporin A causes a marked decrease in CTLA-4 gene expression (Finn., *et al* 1997).

Other sites for transcriptional regulatory elements (STAT, GATA1, NF- $\kappa$ B and the IL-4 negative regulatory element) (Perkins., *et al* 1996) have been found in the 5' region of the gene.

B7- expression on the surface of the APC is also modulated in accordance with the activation state of the cell. APC show a constitutive expression of CD86 that is up-regulated rapidly upon activation (Hathcock., *et al* 1994). In contrast, surface levels of CD80 are virtually undetectable, before maturation and activation. This costimulatory ligand is induced to expression levels of approximately 10% of the levels of CD86 on the same cell (Inaba., *et al* 1994).

The kinetics of expression of these molecules are as follows: CD86, which is detectable at low levels on the surface of APC, is rapidly up-regulated upon activation, its expression reaches a maximum at 48 hours and is sustained for several days. CD80, in contrast, is not detected on resting cells and it is slowly induced after activation. It reaches a peak at 72 hours lasting, as well for several days (Hathcock., *et al* 1994 and Lenschow., *et al* 1994).

Maturation and activation stimuli for APC include CD40 ligation, peptide-MHC II-TCR ligation in T-B interactions, B cell receptor cross linking, toll-like receptor binding, and growth factors such as granulocyte-macrophage colony stimulating factor (GM-CSF) (De Smedt., *et al* 1996; Ranheim., *et al* 1993; Lenschow., *et al* 1994; Hathcock., *et al* 1994; Witmer-Pack., *et al* 1987).

Some cytokines like IL-2 or IL-4 appear to enhance the induction (Valle., *et al* 1991; Stack., *et al* 1994) whereas IL-10 mediates the specific down-regulation of costimulatory molecules (CD86) suggesting a tolerogenic effect of such cytokine (Akbari., *et al* 2001).

The structural data of all the costimulatory molecules together with their patterns of gene expression have allowed the proposal of a functional hypothesis for this pathway of T cell activation.

### iii.- The functional hypothesis.

The intriguing question of why two similar ligands exist on the surface of the APC, which both bind to two functionally independent receptors on the surface of T cells, may now be explained if one considers the structure, dimerization patterns, binding properties and kinetics of expression of these four costimulatory molecules.

As mentioned before, the oligomeric state and comparative affinities of binding of the B7 molecules to CD28 and CTLA-4 has provided evidence to propose a differential role for these two molecules. The observation that CD86 has a weaker interaction with CTLA-4 than CD80, that relative to its CTLA-4 binding affinity CD86 binds more effectively to CD28 and CD86 is constitutively expressed and up-regulated after APC activation, supports the idea that this molecule favors positive costimulation and also indicates that the most immediate interactions following peptide-MHC-TCR ligation may predominantly lead to T cell activation.

The subsequent upregulation in the expression of CD86 may sustain positive costimulation, but the induction of CD80 on the APC, although able to transduce a positive signal through CD28, may tip the balance of positive costimulation to inhibition of T cell responses as CD80 has a much higher affinity for CTLA-4; newly expressed or translocated to the T cell surface after CD28 costimulation. An inhibitory interaction seems to be predominant at this stage as bivalent CTLA-4 homodimers can bind a higher density of CD86 molecules on the surface of the APC as well as forming very stable and affinity enhanced periodic interactions with CD80. CD28 monovalent dimers are, in contrast, unable to produce such enhanced interactions (reviewed in van der Merwe., *et al* 2003). Figure 1.3 summarizes these costimulatory interactions. Absolute affinities of binding are shown as equilibrium dissociation constants and the comparative differences in binding affinities that define this hypothesis is reported as  $K_d$  ratios of interaction.

Important questions arise from this functional hypothesis of costimulatory interaction; it is known that the stability of binding of CTLA-4-CD80 complexes is 10,000 fold higher than that of CD28-CD86 (Collins., *et al* 2002), so why do such differences exist between very similar molecules?. A plausible explanation could be that, if weak

interactions between CD28 and CD86 are enough to activate T cells after peptide-MHC-TCR ligation, long lasting inhibitory interactions may be necessary to control the response. The higher stability of interaction observed between CD80 and CTLA-4 fulfills this characteristic, therefore it is likely that these molecules, once expressed in the cell surface, they would stay longer in the synapse providing active control of T cell responses (van der Merwe., *et al* 2003).

*In vivo* studies are consistent with and support this functional hypothesis, for instance it has been reported that treatment of mice of the diabetes susceptible strain, NOD, with blocking anti CD86 mAb protects from diabetes. In contrast CD80 mAb exacerbates the disease in female mice and induces it in resistant males (Lenschow., *et al* 1995). Tolerance induction requires CD80 and CTLA-4 in a murine model of allo-transplantation, whereas CD86 is an activation requirement for allo-reactive T cells (Judge., *et al* 1999).

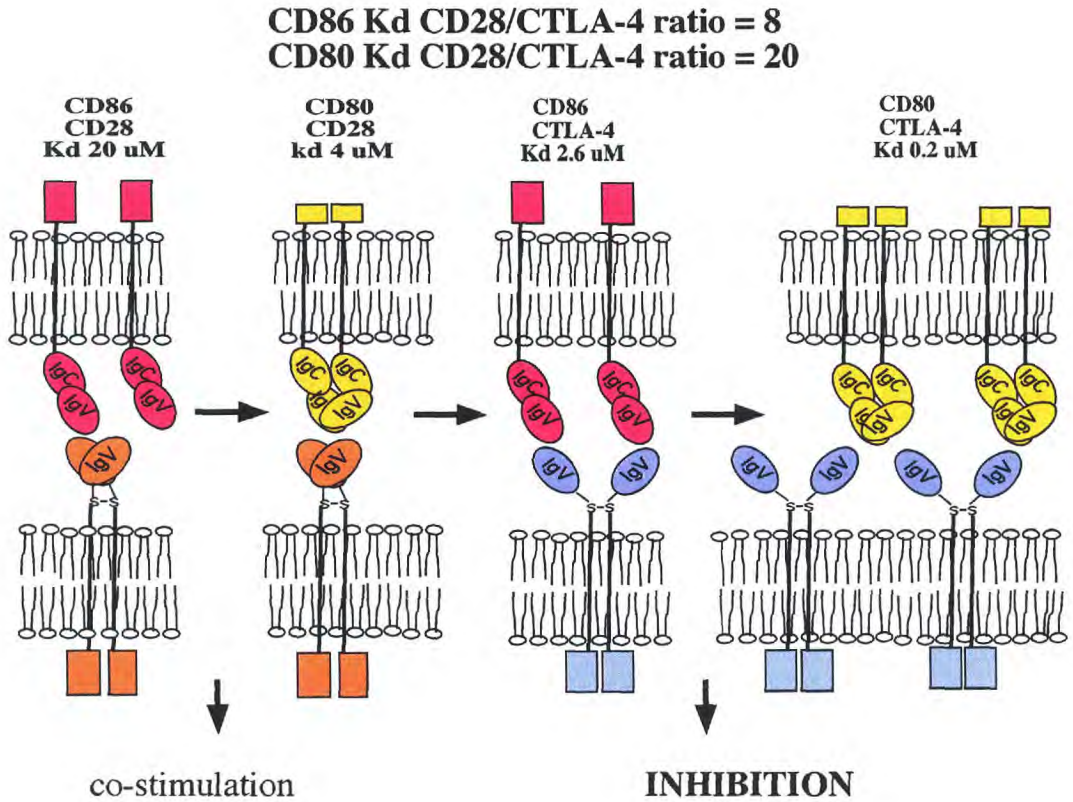


Figure 1.3.- Diagram of the quaternary structures of co-stimulatory and inhibitory complexes formed between CD28, CTLA-4 and B7. The equilibrium dissociation constants (kd), determined in solution by surface plasmon resonance, and the kd ratio between B7 receptors are shown. Adapted from (van der Merwe, P.A *et al* 2003).

Recently, Manzotti and co-workers, have shown, using CD80 or CD86 CHO transfectants, that CD80, despite being a more potent co-stimulator to human resting CD4+CD25- T cells than CD86, as measured in terms of numbers of cells that undergo cycles of division, induce significantly slower kinetics of T cell proliferation. At initial stages no CTLA-4 expression was detected but later in the cultures, when CTLA-4 expression was identified, blocking with anti CTLA-4 mAb significantly increased the number of divisions of the CD80-stimulated T cells (Manzotti., *et al* 2006).

The existence of functional ligands for CD28 and CTLA-4 other than CD80 and CD86 is unlikely as CTLA-4, CD80 and CD86 triple null mutant mice have a normal phenotype instead of the lymphoproliferative phenotype observed in CTLA-4 deficient mice. This rules out the possibility of uncontrolled T cell activation that could possibly be mediated by the interaction of CD28 with another putative costimulatory ligand. (Mandelbrot., *et al* 1999). The existence of other ligands for B7 on T cells other than CD28 and CTLA-4 may, however, be possible (Mandelbrot., *et al* 2001).

### **1.3. Other important costimulatory molecules.**

Various new members of the B7 family have been identified and a significant amount of work has accumulated in the last years allowing us to understand their functions.

Two main new pathways can be delineated: one involving ICOS on the surface of T cells and its ligand ICOSL on the APC. The other; involving PD1 on T cells and two new ligands on the APC, PD-L1 and PD-L2.

Additional B7 homologs (B7-H3 and B7-H4 together with a CD28 homologue, BTLA, expressed on T cells and B cells have also been identified and studied. Structural and functional studies on these molecules have been extensively reviewed (Greenwald., *et al* 2005). Here their functional characteristics will be briefly reviewed with emphasis on their potential to inhibit T cells responses, as it is important for the argument of this thesis to highlight any additional negative regulators that can act synergistically with or in the absence of CTLA-4.

### 1.3.1 ICOS.

The inducible co-stimulator (ICOS) is a glycosylated disulfide-linked homodimeric transmembrane member of the IgSF encoded just adjacent to CTLA-4. Although it is similar with CD28, several structural differences result in their diverse functional effects (Hutloff., *et al* 1999). At its cytoplasmic tail, one of the most important differences is the lack of the YMFM motif that for CD28 recruits Grb2 and is crucial for signals leading to IL-2 production (Okamoto., *et al* 2003) therefore the ligation of this receptor does not induce the production of this cytokine. ICOS is up-regulated on CD4<sup>+</sup> and CD8<sup>+</sup> T cells only following activation and CD28 costimulation, although this is not dependent on costimulation as its blockade in CD28<sup>-/-</sup> mice inhibits one of ICOS primary functions, the differentiation of T cells to Th1 or Th2 cells and the production of the corresponding cytokines (IL-4, IL-5 and IFN $\gamma$ ) (Kopf., *et al* 2000). ICOS is also present on effector and memory T cells (Coyle., *et al* 2000).

ICOS ligand is expressed on various non-lymphoid cells such as kidney, liver and lung as well as on B cells, macrophages and dendritic cells (Yoshinaga., *et al* 1999; Nkazawa., *et al* 2004).

Apart of the influence of ICOS ligation on Th differentiation, costimulation through this molecule provides critical T cell help to B cell activation and thus humoral responses.

Perhaps the clearest evidence to support this view is the fact that ICOS deficient mice show reduced germinal centres and defects in their formation upon primary or secondary immunizations together with impaired IgG class switching (McAdam., *et al* 200; Tafuri., *et al* 2001).

Altogether, functional studies have shown that ICOS provides a key positive second and later signal that promotes T cell differentiation and effector functions such as T cell-mediated B cell help. No effects of ICOS are likely to affect T cell activation as ICOS does not induce IL-2.



### 1.3.2 The PD1-PD-L pathway.

Programmed death-1 (PD-1) is another monomeric IgSF member. (Freeman, G.L., *et al* 2000). Signaling through this molecule is mainly mediated through 2 tyrosines, one forming an immunoreceptor tyrosine based switch motif (ITSM) and the second one an immunoreceptor tyrosine-based inhibitory motif (ITIM) (Okazaky, T., *et al* 2001).

PD-1 is expressed by double negative thymocytes,  $\gamma\delta$  double negative thymocytes and it is induced on CD4<sup>+</sup> and CD8<sup>+</sup> T cells, B cells and monocytes in the periphery (Agata., *et al* 1996). The ligands, PD-L1 and 2 are expressed differentially; PD-L1 is expressed on resting T cells including Tregs, B cells, non lymphoid cells and dendritic cells and is up-regulated after activation. In contrast PD-L2 expression is only inducible on dendritic cells and macrophages (Liang., *et al* 2003).

The main function of these pathway is the inhibition of T cells as illustrated by the propensity of PD-1 knock out mice to develop late onset autoimmunity. PD-1 deficient mice on the C57BL/6 background develop progressive arthritis and lupus-like glomerulonephritis. PD-1 knock out mice on BALB/c background develop late cardiomyopathy (Nishimura., *et al* 1999; Nishimura., *et al* 2001).

As opposed to CTLA-4, the broad pattern of expression of PD-1 and the ligands, together with its participation in controlling tissue-restricted autoimmunity point to a role in controlling inflammatory responses in the periphery. This may be mediated mainly through interaction between PD-1 and PD-L1 as PD-L2 is lymphoid-restricted, suggesting an overlapping function with other B7 costimulatory molecules.

### 1.3.3 B7-H3 and B7-H4.

B7-H3 is expressed by lymphoid and non-lymphoid tissue and in the mouse B7-H3 gives rise to two different splice variants (4Ig-B7-H3 and 2Ig Steinberger., *et al* 2004; Ling., *et al* 2003). These costimulatory molecules are not constitutively expressed but thus induced under conditions of cytokine stimulation (IFN $\gamma$ , GM-CSF or LPS, Steinberger., *et al* 2004).

A ligand for B7-H3 has not yet been identified. Although studies using B7-H3<sup>-/-</sup> APC in an mixed lymphocyte reaction (MLR) have shown an increase in alloreactive T cell proliferation (Suh., *et al* 2003), other similar experiments have reported opposing evidences (Wang., *et al* 2005).

B7-H4 a gpi-linked molecule, is expressed broadly in both lymphoid and non lymphoid tissue including the lung, liver skeletal muscle and pancreas. On B cells, DC and T cells, it is not expressed at resting but it can be induced upon activation . As well, its receptor remains to be identified, but the function of this molecule has been postulated from experiments where transfectants or immobilized B7-H4-Ig have shown to deliver a negative signal that inhibits TCR-mediated proliferation and IL-2 production (Sica., *et al* 2003).

#### **1.3.4 BTLA.**

A member of the CD28 family this last costimulatory receptor has shown functions similar to PD-1 and CTLA-4. BTLA is a monomeric protein selectively expressed only in lymphocytes (B and T) and, for T cells, only in Th1 cells . It is induced upon activation, but in contrast to ICOS, BTLA remains expressed in Th1 but not in Th2 subsets (Watanabe., *et al* 2003). The negative regulatory role of this molecule has been proven using mice with targeted null mutations. These animals are similar to PD-1 knock outs as they develop increased antibody responses and susceptibility to autoimmunity. Both KO models develop more subtle phenotypes than CTLA-4 deficient mice (Watanabe., *et al* 2003).

## 1.4 Negative regulation by CTLA-4.

The structural similarities of CD28 with CTLA-4 and the fact that both receptors share ligands had suggested that both molecules could deliver positive stimulation upon ligation. The phenotype of the CD28 deficient mice, however, did not support the idea that these two molecules have similar functions.

T cells From CD28<sup>-/-</sup> mice show significantly lower proliferative responses than wt mice, and exogenous stimulation with lectins (Concanavalin A) did not induce IL-2 production and or expression of the IL-2 receptor  $\alpha$  chain. In addition, basal IgG concentrations, and helper T cell responses were dramatically reduced in CD28 deficient mice, as compared with wild type littermates. Interestingly no effects were found in the induction of cytotoxic T cell responses suggesting that CD28 is not required for all T cells responses (Shahinian., *et al* 1993). This evidence contradicts the idea that CTLA-4 could have a positive costimulatory activity as the previously mentioned defects that are present in CD28<sup>-/-</sup> T cells would have otherwise been compensated through CTLA-4.

Another strategy that further confirmed the negative costimulatory potential of CTLA-4 used monoclonal antibodies and antibody Fab fragments *in vitro*. Although initial studies that used anti CD28 and costimulatory anti CTLA-4 antibodies proposed a synergy between these receptors in promoting proliferation and IL-2 production, CTLA-4 ligation alone did not replicate the effect on proliferation and cytokine production observed after TCR stimulation and anti CD28 treatment (Linsley., *et al* 1992). Subsequently, the use of Fab fragments of these antibodies was shown to have an enhancing effect on T cell responses and, in accordance with this, crosslinking CTLA-4 after *in vitro* CD3 and CD28 stimulation, reduced such proliferative responses (Wu., *et al* 1997 and Walunas., *et al* 1994). Altogether this proved that the initial synergy observed was the result of a block in the inhibitory signals provided to the T cells through CTLA-4 and B7.

The evidence that clearly defined a negative role for CTLA-4 came from the generation of mice bearing a targeted deletion of this gene. To date, three independent CTLA-4 knock-out mice models have been published providing much evidence on the function of this molecule (Waterhouse., *et al* 1995; Tivol., *et al* 1995 and Chambers., *et al* 1997). CTLA-4<sup>-/-</sup> mice develop a lethal lymphoproliferative disorder characterized by the accumulation and a massive infiltration of T lymphocytes in spleen, lymph nodes, heart, pancreas and lung. This lymphocytic infiltration or hyperproliferation leads to lymphadenopathy, splenomegaly and multiorgan damage, particularly myocarditis and pancreatitis that is fatal within 3 to 4 weeks of birth (Waterhouse., *et al* 1995 and Tivol., *et al* 1995).

Mice lacking CTLA-4 are born healthy but 5 to 6 days after birth a large proportion of T cells become activated. The phenotype of these T cells is CD44<sup>hi</sup>, Mel<sup>lo</sup> and CD45RB<sup>hi</sup> which suggest they have been activated *in vivo*. In addition a large proportion of cells blast transform and express CD69, an early activation marker and CD25, all indications of recent activation. *Ex vivo* proliferation in response to lectins, anti CD3 stimulation or anti-TCR $\alpha\beta$  stimulation are increased in CTLA-4<sup>-/-</sup> T cells when compared with cells from wt and heterozygous littermates. In fact CTLA-4 null T cells proliferate spontaneously in culture, although at "low levels". IFN $\gamma$  and IL-4 production by T cells from homozygous mutant animals is also enhanced (Waterhouse., *et al* 1995).

One of the hypotheses to explain this phenotype relied on the assumption that alterations in the process of negative selection in the thymus, could allow a large proportion of auto-antigen specific T cells into the periphery. To address this, Waterhouse., *et al* analyzed negative selection in CTLA-4 deficient mice using a TCR transgenic line specific for the male H-Y antigen. In the thymus of male animals, a homogeneous population of T cells undergo synchronous negative selection, when transgenics were crossed with CTLA-4 deficient mice. T cells in the offspring of this cross had a resting phenotype indicating that the dysregulation was not due to alterations in negative selection (Waterhouse., *et al* 1997). CTLA-4 may, however, fine tune negative selection (Takahashi., *et al* 2005).

In one of the previous CTLA-4 knock out models generated (Tivol, EA., et al 1995) a gross dysbalance in the CD4/CD8 thymic profile of mutant mice was observed when compared with wt littermates. This suggested abnormalities during T cell development. A third CTLA-4 knock out model where thymocytes were analyzed during their entire ontogeny indicated that the altered CD4/CD8 profile previously observed was due to an imprecision in the dissection techniques for thymi collection and an that enlarged parathyroid lymph node had been harvested together with the thymus (Chambers., *et al* 1997).

Further research has shown that the severe proliferation of peripheral T lymphocytes in CTLA-4 knock out mice is mediated by CD28-dependent activation of CD4<sup>+</sup> T cells, as antibody depletion of CD4<sup>+</sup> cells rescues the phenotype. Similar evidence was not found for CD8<sup>+</sup> cells although the predominant role of CD4<sup>+</sup> T cells in producing the phenotype observed is not reflected in an altered CD4/CD8 ratio in the periphery. (Chambers., *et al* 1997, Mandelbrot., *et al* 1999).

To further support the dependence of the lymphoproliferative response, associated with the CTLA-4 deficiency with costimulation through both CD80 and CD86, Mandelbrot., *et al* crossed CTLA-4<sup>-/-</sup> mice with animals deficient for CD80, for CD86 and for both CD80 and CD86. The results obtained showed that either CTLA-4/CD80<sup>-/-</sup> or CTLA-4/CD86<sup>-/-</sup> mice developed a severe lymphoproliferative disorder, but in contrast, CTLA-4/CD80/CD86<sup>-/-</sup> mice appeared normal (Mandelbrot., *et al* 1999). Moreover the inhibitory effects of CTLA-4 appear to be required to control positive costimulation via CD28 as CTLA-4<sup>-/-</sup> CD28<sup>-/-</sup> double knock out mice do not develop a lymphoproliferation (Mandelbrot., *et al* 2001).

Treatment of CTLA-4 deficient mice with CTLA-4 Ig, which binds to B7 molecules preventing costimulation, has proven to protect these animals from lymphoproliferation, rulling out a defect in the TCR signaling machinery in CTLA-4<sup>-/-</sup> mice (Tivol., *et al* 1997).

Putting all these data together, there is unequivocal evidence to point out the requirement of CD28 and both B7 ligands to provide essential costimulation which under conditions of CTLA-4 absence triggers in the development of the autoimmunity.

A final rather puzzling observation is that the autoimmunity observed in CTLA-4 deficient mice is not cell autonomous. Reconstituted RAG 1<sup>-/-</sup> mice with equal numbers of wild type and CTLA-4<sup>-/-</sup> T cells do not develop autoimmunity and remain healthy. This is not only explained by an inhibition provided by wild type T cells as in these mice the CTLA-4<sup>-/-</sup> T cells undergo normal activation and expansion.

This indicates that although the inhibition exerted through CTLA-4 is T cell autonomous, suppressive cytokines or negative stimuli produced by other cells or by CTLA-4 expressing cells (perhaps Tregs) can protect CTLA-4<sup>-/-</sup> animals from autoimmunity (Tivol., et al 2002).

All the data described above point out that CTLA-4 is a major T cell costimulatory molecule involved in controlling T cell immunity. Despite the fact that most of the data point in such direction and only few reports have generated controversial evidence to consider the opposite, the precise mechanisms of action of CTLA-4 are still not fully understood.

## **1.5 Molecular genetics of *Ctla-4*.**

### **1.5.1 CTLA-4 genomic organization and splicing.**

*Ctla-4* is located on chromosome 1 in mice and on 2 in humans. Mouse CTLA-4 maps to cytoband C at 30.1 cM (location between 61212315-61219120 bp on the sense strand). In humans this corresponds to the syntenic genomic region of chromosome 2 coded as 2q33.

Encoded adjacent to mouse *Ctla-4* is *Cd28* (band C10-C3, location between 61049756-61076649 bp + strand) and *Icos* (30.2 cM at 61281213-61302409 bp on the sense strand) (Mouse genome informatics, Jackson Laboratories <http://www.informatics.jax.org/>).

*Ctla-4* consists of 4 exons: exon 1 encodes the leader peptide, exon 2 the extracellular ligand binding domain, exon 3 the transmembrane domain and exon four the cytoplasmic tail (Dariavach., et al 1988 and Ling., et al 1999).

Upon transcription, the resulting mRNA can undergo splicing, various splice variants are expressed and they differ between man and mouse. For human *Ctla-4* is possible to detect a full-length mRNA transcribed from all exons, a transcript coding for a soluble form of CTLA-4 (sCTLA-4) that does not contain exon 3 and a transcript containing only exons 1 and 4. In mice, the expression of a fourth splice variant has been detected and its mRNA encodes for exons 1, 3 and 4. This last variant is called ligand-independent CTLA-4 (LiCTLA-4) as it lacks the B7 binding domain (Ling, V., *et al* 1999; Ueda., *et al* 2003; Magistrelli., *et al* 1999 and Oaks., *et al* 2000) (see figure 1.4). Li CTLA-4 is a functional CTLA-4 isoform strongly linked to type-1 diabetes in non-obese-diabetic mice. It is expressed on primary mouse T cells and it has shown higher expression in memory and regulatory T cells from congenic diabetes resistant NOD mice as compared with diabetes susceptible NOD animals. Biochemical studies have demonstrated that LiCTLA-4 dephosphorylates TCR-zeta chain thereby inhibiting T cells responses and regulating autoimmunity (Vijaykrishnan., *et al* 2004).

### **1.5.2 *Ctla-4* is polymorphic and its locus associates with autoimmunity.**

Given the importance of CTLA-4 as a negative costimulator, its role in determining peripheral tolerance and its specific pattern of expression in functionally different T cells subsets, transcriptional or translational changes in expression can have important consequences for immune homeostasis. For this reason the investigation of polymorphisms associated with autoimmune diseases has had CTLA-4 as obvious target.

The first CTLA-4 polymorphism detected was a microsatellite marker corresponding to a (AT)<sub>n</sub> repeat in the 3' untranslated region (UTR) downstream exon 4 producing significant odds ratio for development of Graves' disease (Yanagawa., *et al* 1995). This marker is not conserved in mice (Ling., *et al* 1996) and, in fact, locates in the area with the smallest sequence similarity between mice and human, suggesting it is not important for protein function or expression and that genetic susceptibility to Graves' may therefore be caused by an alternative mechanism.

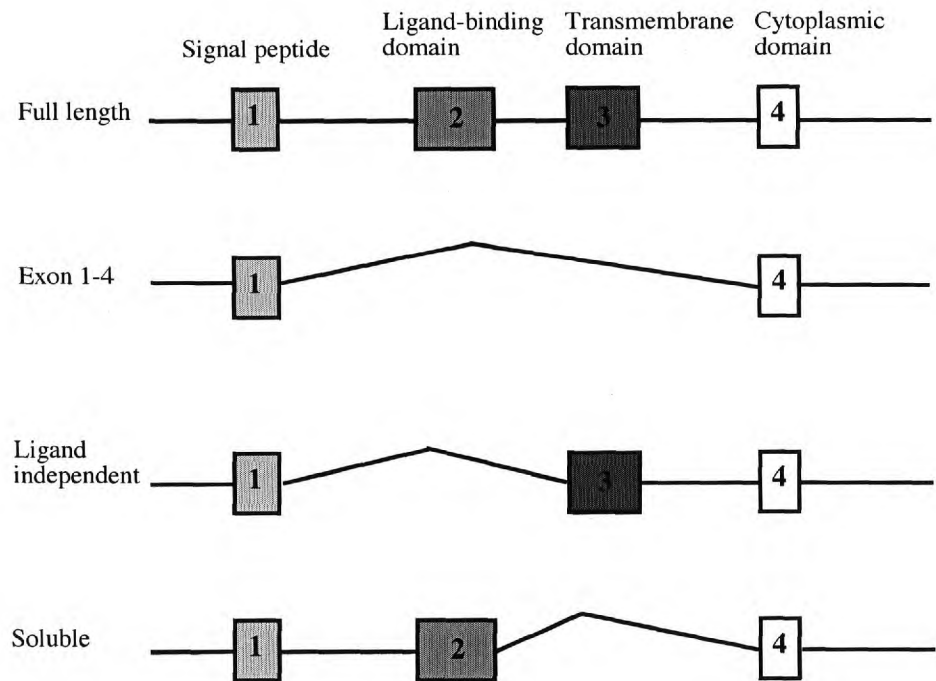


Figure 1.4.- *Ctla-4* and its splice variants. *Ctla-4* has four exons encoding different polypeptide chains (top). Four different splice variants have been identified at the level of mRNA. Humans express full length *Ctla-4*, exons 1-4 *Ctla-4* and soluble *Ctla-4* (exons 1,2,4). In mice an alternative variant (liCTLA-4) is expressed lacking exon 2. Taken from (Teft., *et al* 2005)



This sequence alteration could indeed become a good etiological candidate as AT rich sequences in 3' UTR may generate mRNA instability (Conne., *et al* 2000).

Genome-wide searches identified in type-1 diabetes and less clearly in Graves' linkage with regions of the chromosome 2 (2q31-q35), and within the regions locus IDDM7 (the CTLA-4 locus) was included (Copeman., *et al* 1995).

Later the first single nucleotide polymorphism (SNP) in *Ctla-4*, an A-G change at position 49 in exon 1, was reported to be associated with the two diseases already mentioned (Nistico., *et al* 1996).

This substitution (Thr to Ala in the protein) would not affect the function of the leader peptide but may alter intracellular trafficking of CTLA-4 by causing differences in glycosylation (Bradshaw., *et al* 1997). This SNP was further associated with numerous autoimmune diseases.

Two independent SNPs have also been identified within CTLA-4; C-T at position + 1822 in intron 1 and C-T at - 318 in the promoter region. The first of these has been associated with type 1 diabetes and Graves' disease (Marron., *et al* 2000; Vaidya., B *et al* 2003), the second has not shown disease association. Subsequent mapping of a greater area of the genome, that includes CD28, CTLA-4 and ICOS, together with regression analysis on Graves' cases, identified a significant number of polymorphisms (108) of which 4 were highly disease associated. These variations, CT 60, JO31, JO30 and JO27-1, span a 6.1Kb region 3' of CTLA-4, a common autoimmune disease locus (Ueda, H., *et al* 2003 reviewed in Gough., *et al* 2005), see figure 1.5.

Establishing how the CTLA-4 polymorphisms trigger or contribute to pathophysiology of autoimmunity is still not clear, researchers have observed differences in T-cell activation and proliferation, *in vitro*, between patients possessing susceptibility alleles as compared to controls. Hypotheses to explain such observations have also been proposed including alterations in the levels or patterns of CTLA-4 expression or CTLA-4 trafficking, but no clear links with disease causes or progression have been determined (reviewed in Gough., *et al* 2005). A clearer picture in this respect comes from studies where the abundance of mRNA of full length CTLA-4 transcripts and the soluble isoform (sCTLA-4) were compared between homozygous disease protective haplotypes and heterozygous individuals.

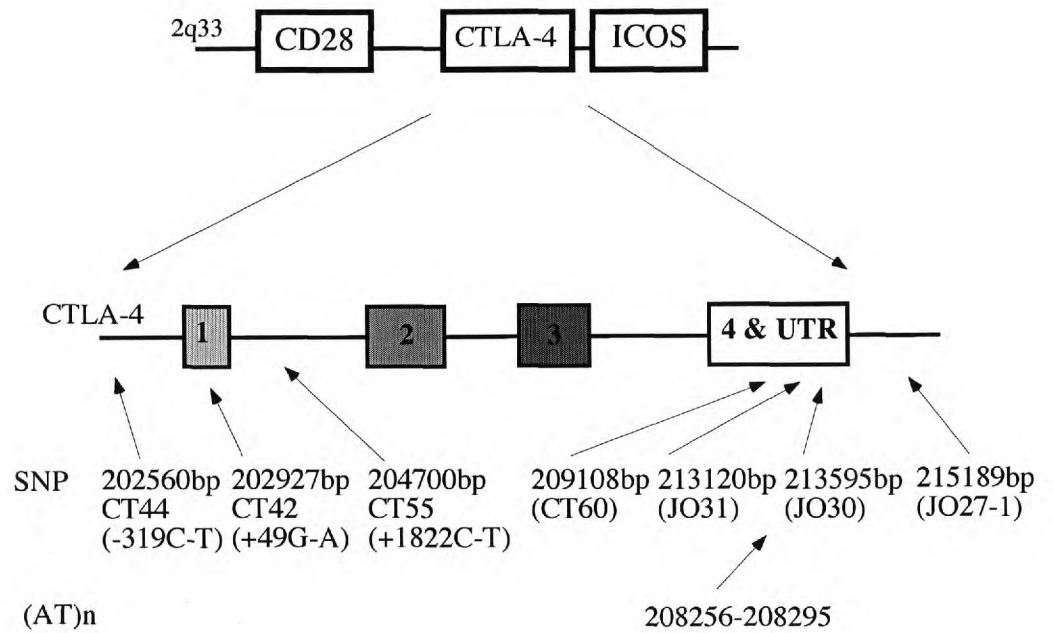


Figure 1.5.- Localization of 7 single nucleotide polymorphisms (SNP) and the (AT)<sub>n</sub> repeat sequence with in the 2q33 human CTLA-4 locus. Taken from Gough., *et al* 2005.

No differences were observed in the mRNA levels of FICTLA-4 but higher levels of sCTLA-4 were observed in the disease protective haplotype as compared with the susceptible one. Subsequent analysis by quantitative RT-PCR showed that the sCTLA-4/FICTLA-4 mRNA ratio was 50 % lower in homozygous susceptible individuals compared with homozygous protected subjects. These data show that the 6.1Kb 3' region of CTLA-4 determines the efficacy of splicing leading to sCTLA-4 production (Magistrelli., *et al* 1999). Higher sCTLA-4 serum levels have additionally been found in patients with autoimmune thyroid disease when compared to healthy controls (Oaks., *et al* 2000).

Lastly, mouse orthologues to the 2q33 susceptibility region have been identified, these regions (Idd5.1 and 5.2) determining susceptibility to diabetes in NOD mice. Region Idd5.1 includes *Icos* and *Ctla-4* but not *Cd28* and approximately 62 SNPs have been identified, only 2 being in coding regions. One of those SNP maps to exon 2 of CTLA-4 and has an A at position 77 in the diabetes resistant strains C57BL/10 and C57BL/6, and a G in the diabetes-prone strain NOD. This sequence substitution has been postulated to be a modulator of the splicing of CTLA-4 reducing the abundance of its ligand-independent isoform (LiCTLA-4) highly expressed in T cells from diabetes resistant strains by favouring the inclusion of exon 2 in the final transcript (Ueda., *et al* 2003; Vijaykrishnan., *et al* 2004)

## **1.6 Mechanisms of CTLA-4 costimulation.**

### **1.6.1 Competition with CD28 for ligands.**

As mentioned in section 1.2.3, the greater affinities and avidities of binding of CTLA-4 to B7 ligands is consistent with the possibility that upon T cell activation once CTLA-4 is translocated to the surface it may sequester the available ligands limiting essential CD28 signals.

In a study where mutant forms of CTLA-4, either with truncations, modifications or absence of the intracellular domain were produced and expressed as transgenes in

mice, the authors show that these CTLA-4 mutants can still exert a negative function. (Masteller., *et al* 2000). This could also be the mechanism of action of sCTLA-4, as once secreted it could block binding of CD28 to B7. However the evidence that the soluble CTLA-4 fusion protein CTLA-4 Ig can trigger the IDO pathway (Grohmann., *et al* 2002) and that some agonistic CTLA-4 antibodies are also inhibitory (Fallarino., *et al* 1998; Krummel., *et al* 1995), complicates this scenario as it is then difficult to ascertain when each individual mechanism is likely to come into action.

### **1.6.2 CTLA-4 negative signaling.**

Antibody crosslinking of both CTLA-4 and TCR, under CD28 costimulation, is sufficient to induce the canonical CTLA-4 effector mechanisms, cell cycle arrest and inhibition of IL-2 production (Baroja., *et al* 2000). CTLA-4 may interfere with TCR proximal events by recruiting phosphatases (i.e. PP2A) to the TCR/CD28 complexes and therefore inhibiting early phosphorylation (Lee., *et al* 1998). A second mechanism that has been postulated, involves as well, interference with TCR signaling but now by exclusion from lipid rafts of the TCR $\zeta$  chain limiting complete TCR signaling (Darlington., *et al* 2002).

Finally analysis of the expression of lipid rafts have suggested CTLA-4 as an inhibitor of raft formation in the cell surface, therefore again limiting TCR organization at the immune synapse (Martin., *et al* 2001).

Signaling through CTLA-4 may not require ligand binding, at least in mice and evidence for that comes from the observations that LiCTLA-4 is an active isoform able to induce the dephosphorilation of TCR $\zeta$  chain (Vijaykrishnan., *et al* 2004).

### **1.6.3 CTLA-4 and CD4<sup>+</sup> CD25<sup>+</sup> regulatory T cells.**

CD4<sup>+</sup> CD25<sup>+</sup> Regulatory T cells include a subset of naturally occurring T cells that express high levels of the IL-2 receptor  $\alpha$  chain (CD25). These cells derive from the thymus, suppress T cell proliferation and cytokine production and they possess constitutive

expression of CTLA-4, all these observations have suggested that CTLA-4 may have an individual functional role through T regs (Takahashi., *et al* 2000; Read., *et al* 2000).

The mechanism of action of CTLA-4 in T regs is still quite controversial and researchers have used monoclonal blocking antibodies in an approach to understand its function. Several groups have shown that Treg suppression can be inhibited by blocking CTLA-4, indicating an important role of this molecule for Treg activity (Takahashi., *et al* 2000, Tang., *et al* 2004). In contrast opposing evidence has also been published, indicating the limitations posed by this strategy (Thornton., *et al* 2004). Blocking antibodies, although one of the only strategies available to analyze the function of specific markers on specific cells, are limited in functional studies for reasons such as inaccessibility to the T cell immune synapse in the culture setup due to size, the predominant location of CTLA-4 in cytosolic vesicles and finally the fact that antibodies can also block CTLA-4 on the surface of activated effector T cells making the analysis of experimental data complicated. All these limitations complicate the analysis of CTLA-4 on this subset of T cells as the lack of inhibition can not always refute a possible functional role of CTLA-4 in these T cells.

In Tregs CTLA-4 may have actually a role to enhance function (Takahashi, T., *et al* 2004). In disagreement with this view is the observation that CTLA-4 knock out mice have T cells that express the canonical T reg transcription factor Foxp3 and are able to suppress (Tang., *et al* 2004). This last observation does not rule out a possible functional role for CTLA-4, instead suggesting that it may not be essential.

The observation that the enzyme IDO (see above) can trigger the tryptophan catabolism pathway in APC to indirectly inhibit T cell responses, has now been also considered as a potential mechanism of action for T regs (Mellor., *et al* 2004). High expression levels of CTLA-4 on the surface of Tregs can produce a signal to dendritic cells to produce IDO and subsequently inhibit 3rd party T cells responses (reviewed in Sansom., *et al* 2006).

In conclusion it is attractive to consider that CTLA-4 might play a role in T cell regulation by Tregs. The reasons to consider that are that it is expressed constitutively, that the phenotype observed in CTLA-4<sup>-/-</sup> is not cell autonomous and secondary suppressive signals (cytokines) provided by Tregs may coexist, and finally, that the phenotype seen in CTLA-4<sup>-/-</sup> mice is similar to the phenotype observed in Foxp3 deficient mice which lack T regs (Khattari., *et al* 2003). Important limitations hamper our understanding of the function of CTLA-4 in Treg biology and although much has been done, novel strategies are required to overcome such limitation.

## **1.7 The role of CTLA-4 in the induction of peripheral tolerance.**

The disease phenotype present in CTLA-4 deficient mice has provided an invaluable system to test the role of this molecule as a negative costimulator. It has been postulated that the hyper activation of T cells observed in these mice is the result of reactivity to self antigens present in the periphery which otherwise would be under control of CTLA-4 inhibition.

In order to study the the role of CTLA-4 in peripheral tolerance, approaches such as the use of blocking mAbs have also been useful, yet they have also produced conflicting conclusions as to the role of negative regulatory properties of this protein.

Studies using blocking CTLA-4 mAb in the response to a superantigen demonstrated that this receptor is essential for tolerance induction in both CD4<sup>+</sup> and CD8<sup>+</sup> cells, antibody-treated individuals showing increased numbers of superantigen-specific T cells and a lac3232k of tolerance induction. (Walunas., *et al* 1998). Others have demonstrated that the use of blocking CTLA-4 mAb during and after a tolerogenic stimulus, using antigen-coupled splenocytes as APC as a system for tolerance induction to experimental autoimmune encephalomyelitis EAE, showed a potent activity of CTLA-4 during tolerogenesis, indicating an important participation of this receptor in maintaining a tolerant state (Eagar., *et al* 2002).

There is evidence to suggest CTLA-4 as one of the key molecules mediating allograft tolerance, this has been performed by analyzing ligation, by membrane bound

anti-CTLA-4 antibodies (Hwang., *et al* 2002). However, several other groups have produced opposing evidence particularly at the level of CD8 T cell responses.

In a model of inducible anergy, Frauwirth, *et al* have shown, using CTLA-4/B7 blocking antibodies, that primary CTLA-4<sup>+/+</sup> T cells as well as CTLA4<sup>-/-</sup> T cells are equally anergized when injected with soluble antigenic peptide (Frauwirth., *et al* 2000 and Frauwirth., *et al* 2001). This evidence has also been produced in a system of tumour antigen specific tolerance induction (Sotomayor., *et al* 1999).

An interesting approach to understand the function of CTLA-4 in establishing peripheral tolerance, comes from experiments where CTLA-4 deficient mouse cells are transferred into RAG-2 deficient mice. Under these circumstances researchers are able to transfer the lymphoproliferative disorder seen in CTLA-4<sup>-/-</sup> mice and, in addition, it is possible to revert the phenotype when wild type T cells are concomitantly transferred. This shows that the role of CTLA-4 in the establishment of peripheral tolerance is more complex than the simple transmission of inhibitory signals to self reactive T cells, and may involve the presence of other cell populations within a regulatory network (Tivol., *et al* 2002).

The study of tolerance induction requires the employment of *in vivo* models as the multifactorial cellular interactions that determine the tolerance state cannot be reproduced *in vitro*. With this in mind and aiming to further dissect the role of CTLA-4 in tolerance induction to a tissue restricted self antigen and also to compare this in a scenario where the self antigen is present systemically, Eggena. *et al* develop a system using Rag deficient TCR transgenics. In their experiments T cell from DO11.10/Rag<sup>-/-</sup> and in a CTLA-4<sup>-/-</sup> or WT background were transfer into transgenic recipients (also on the Rag<sup>-/-</sup> background) able to express ovalbumin specifically in  $\beta$ -cells in pancreatic islets. Upon transfer of DO11.10/Rag<sup>-/-</sup>/CTLA-4<sup>-/-</sup> T cells, recipient mice developed severe insulinitis and diabetes. This pathology was mediated by CTLA-4<sup>-/-</sup> CD4<sup>+</sup> cells spontaneously or in an induced fashion through DO11.10/Rag<sup>-/-</sup>/WT T cells only if animals were challenged with exogenous OVA plus adjuvant (Eggena., *et al* 2004). These data indicate that in the presence of CTLA-4, self antigen is not able to activate autoreactive

CD4<sup>+</sup> T cells, whereas in its absence self antigen is sufficient to trigger autoimmunity, This is consistent with the idea that CTLA-4 increases the activation threshold of T cells. A variation of the system in which OVA is not expressed in a tissue restricted fashion but as a soluble protein and therefore systemically, was used to compare the role of CTLA-4 deficient and wt T cells to break tolerance. CTLA-4 appeared not to have the same role in determining tolerance to an antigen with systemic expression (Lohr., *et al* 2004) and other mechanisms of regulation may exist to achieve tolerance for instance through regulatory T cells.



---

## 1.8 Targeted mutagenesis in mice.

### 1.8.1 The history of gene targeting.

Mouse Genetics and years of intensive breeding have generated a large number of mouse strains, many of which serve as models to understand genotype-phenotype interactions. More recently, gene targeting has made it possible to introduce precise mutations in the mouse genome, facilitating the reproduction of both genocopies and phenocopies of such mutations with either basic biological relevance or identified in diseases, sometimes also in human disorders.

The technology of gene targeting started with the isolation and culturing of pluripotent ES cells from the inner cell mass of the mouse blastocyst, (Evans., *et al* 1981 and Martin., *et al* 1981). A crucial observation that made possible the implementation of this technique was that these ES cells, retained their capacity to colonize the germline of chimeric mice created by injection of the cells into blastocysts following prolonged culture *ex vivo* (Bradley., *et al* 1984). Subsequently, the demonstration that a fragment of genomic DNA introduced into a mammalian cell can undergo random integration or recombination with the endogenous sequence with which it shares a degree of homology provided a mean to produce specific genetic alterations in the mouse genome. This later process is known as gene targeting by homologous recombination and involves the occurrence of pairing and cross-over events between the homologous sequence of the exogenous fragment of DNA and the chromosomal target site, whereupon only the homologous region of the exogenous DNA recombines with the genome.

The first evidence of the occurrence of gene targeting in mammalian cells came from the studies of a fibroblast cell line harboring a truncated - therefore dysfunctional- copy of the thymidine kinase (TK) gene. The activity of this gene was restored when the missing sequence, sharing an area of homology with the chromosomal TK gene, was introduced as a exogenous fragment of DNA (Lin., *et al* 1985).

Homologous recombination was also demonstrated at the endogenous  $\beta$ -globin locus (Smithies., *et al* 1985). The previous observation and the ability to culture and inject

ES cells into blastocysts led (Thomas and Capecchi. 1987) and (Doetschman., *et al* 1987) to perform the first experiments of gene targeting by homologous recombination in ES. In the first case the sequence of the selectable neomycin phosphotransferase gene (neo) was inserted into an exon of a cloned fragment of the hypoxanthine phosphoribosyl transferase (HPRT) gene and transfected into murine ES cells. After recovery of G418 resistant colonies of ES cells, approximately 1 in every  $10^3$  cells showed an *Hprt*<sup>-/-</sup> phenotype, as analyzed by resistance to the base analog 6-thioguanine (6-TG). In the later instance, it was demonstrated that homologous recombination could be used to correct a mutant form of HPRT in an ES cell line.

Two years later Koller's group, generated chimeric mice from the ES cells bearing a corrected HPRT gene, subsequently demonstrating the germline transmission of such genetic modification (Koller., *et al* 1989).

### **1.8.2 The methodology of gene targeting.**

The principal applications of gene targeting have been the generation of animals harbouring null mutations in a desired locus (knock outs), the introduction of point mutations into specific genomic loci or the site-specific insertion of exogenous coding sequences in what is known as "Knock in" strategies.

Overall the strategy involves the construction of a targeting vector, comprising a modified mouse genomic sequence that is designed to either replace or insert into a specific homologous sequence in ES cells, by homologous recombination. Once an event of insertion or replacement is identified, a preparation of so called "targeted" ES cells is injected to pre-implantation blastocysts, followed by the generation of chimeric animals from those embryos. The final step involves the transmission of the targeted mutation through the germline by crossing the chimeric mice.

### **1.8.3 The targeting vectors.**

Targeting vectors generally include a region homologous with the desired chromosomal recombination site, a selectable marker gene able to drive position dependent expression

of antibiotic resistant and a plasmid backbone. Two different vector designs can be employed to achieve the desired mutation; replacement and insertion vectors each yielding different types of recombination products (figure 1.6).

Replacement vectors are typically used to generate null mutations and require linearization within the plasmid backbone prior cellular transfection, whereupon recombination replaces the targeted chromosomal DNA sequence with that of the targeting vector (Figure 1.6 A). Insertion vectors are linearized within the region of homology, so the plasmid undergoes a single reciprocal recombination event resulting in the integration of the entire plasmid into the chromosomal locus (Figure 1.6 B).

Insertion vectors can be used in experiments aiming to disrupt alleles, however, replacement vectors are more commonly used as the screening for positive homologous recombination events is less complex (Hasty, *et al.*, 1991).

In order to translate targeted mutations to whole animals, pluripotent ES cells are electroporated with a preparation targeting vector and cultured under selection conditions. ES cells that integrated the construct will develop antibiotic resistance (due to the selection maker) and therefore survive to clonally expand.

During the culture of ES cell, normally performed for short periods of time to keep low passaged cells, the differentiation ability of the cells is impeded using leukemia inhibiting factor.

At this stage ES clones can be independently isolated for screening, as two different phenomena could have occurred. On the one hand, the targeting vector could have recombined within its region of homology on the target locus (either replacing the wild type gene or as an insertion) and on the other, the vector could have also integrated somewhere else in the genome. The first case is known as a homologous recombination event and the later a random integration.

It is important to mention that those events are not mutually exclusive as copies of the construct can randomly integrate at the same time as the locus of interest has been targeted. Initial experiments demonstrated a very low frequency of gene targeting by homologous recombination in mammalian cells relative to the levels observed in yeast. This is probably due to the proficient competing pathway of random integration of exogenous DNA versus a homologous recombination event (Hasty, *et al.*, in Joyner, A 2000).

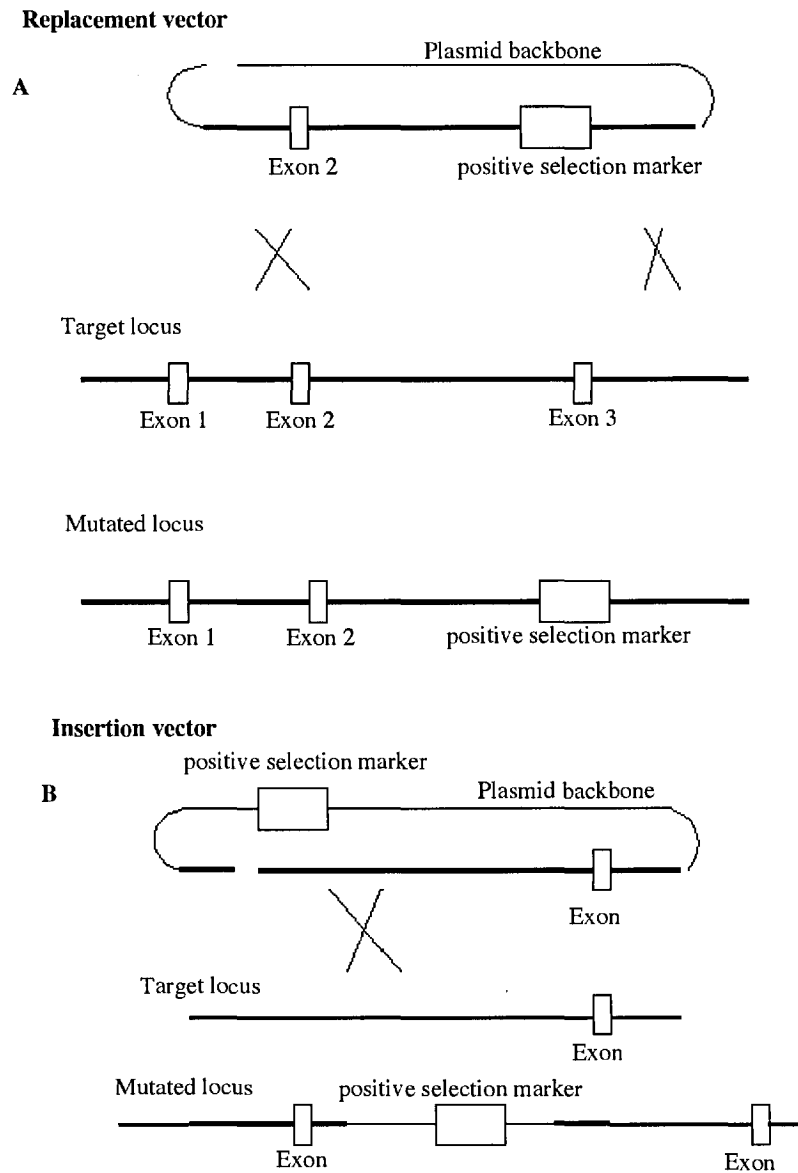


Figure 1.6.- Scheme of replacement and insertion vectors and their products of recombination. (A) shows a typical replacement vector, normally linearized within the plasmid sequence, that integrates into the target locus by two reciprocal events of crossover replacing the region of homology (thick line). Insertion vectors (B) are linearized within the region of homology and after recombination, by a single event of crossover, all vector components are integrated duplicating the homologous sequences (vector and locus differentiated by lines of different thickness). Figure adapted from (Joyner, A.L. 2000).

Observations of the critical characteristics of targeting vectors together with advances in their construction, have been made possible to enrich for and improve the ratio of gene targeting events. Among these characteristics the most important ones are:

*i. The length of the homologous region of the targeting vector.*

The homologous region of the vector with its target locus is the most important factor affecting the frequency of gene targeting. Targeting experiments done at the *Hprt* locus have shown that the efficiency of homologous recombination was strongly dependent and proportional to the length of homology of both insertion and replacement vectors (Thomas., *et al* 1987). Generally, regions of homology of 5Kb to 10Kb are used in gene targeting experiments (Hasty., *et al* 1991). However, with an increase in size of the targeting construct, difficulty arises due several reasons: the cloning and handling of big constructs is sometimes inconvenient because the plasmid yield is inversely proportional to its size when amplified by bacteria during transformations. Very large homology may also limit the availability of unique restriction sites for both linearization and Southern blot analysis of recovered neo resistant clones, in addition, very large restriction fragments are difficult to resolve by normal electrophoresis.

Finally PCR screening strategies can become complicated with large homology, as the amplification of very long products is not always reliable.

In order to tackle this last limitation imposed by the size of the area of homology, the selectable marker cassette can be placed towards one side of the construct, albeit creating a short and a long arm of homology, facilitating the screening of targeted ES cell clones by a diagnostic PCR.

Despite the requirement of large regions of homology for successful targeting constructs, it has been experimentally established that a minimum arm of homology of 0.5kb can render homologous recombination events at frequencies high enough to select a clone within hundreds screened (Thomas., *et al* 1992).

---

*ii. Degree of Polymorphism and isogeneity of the homologous sequence.*

The 129 mouse strain initially proved the most permissive in the yielding of embryonic stem cell lines in contrast to other strains.

129 mice have a relatively high prevalence of rare germ cell tumours in the testes (Stevens, 1983). These tumours progress to form teratocarcinomas in embryos and this characteristic helped the derivation of ES cells directly from embryos.

The ES cells isolated by Martin. *et al* in 1981 were derived from the ICM of blastocysts that were cultured in medium conditioned by an established teratocarcinoma cell line. Thus the advantage given by that tissue culture methodology determined that most ES cell lines generated to date and used for gene targeting experiments are of 129 origin. However, efforts have yielded ES cell lines in several “nonpermissive” strains, for example, the C57Bl/6J (Doetschman., *et al.*, 1985), CBA/Ca inbred strains and PO and MF-1 random-bred strains (Brook., *et al* 1997).

An important disadvantage of using this strain for gene targeting experiments is that the degree of polymorphisms among the 129 mouse substrains, at a given genomic target site, varies widely from locus to locus. Analysis of simple sequence length polymorphisms (SSLP) at randomly chosen DNA loci, revealed that a high degree of genetic variation exists within the 129 mouse substrains and ES cells. Overall, 65% of the SSLP markers differed between the 129 substrains examined and in addition, the 129/SvJ substrain was demonstrated to be accidentally contaminated with genomic segments of non-129 origin (Simpson., *et al* 1997).

These evidence, together with the previous empiric observation that variable frequencies of recombination can be expected when 129 DNA and ES cells from different strains are used, strongly encourages the researcher to perform a careful selection of the source of DNA used to construct the targeting vector as well as the substrain of mouse ES cells used to produce chimeric mice (Deng., *et al* 1992). In ideal circumstances, gene targeting plasmids are best constructed from a genomic library of the strain of the ES cells chosen for transfection, although this is not always practical.

### *iii. Positive selection.*

Following transfection, the targeting vector can either integrate into its target locus or into a random chromosomal location. The ratio of these events depend upon several factors, such as the location of the target locus in the genome and in most cases, random insertions can happen with a higher frequency than homologous recombination events. In fact, both phenomena are considered to be competing events and this competition determines the frequency of homologous recombination of the targeting vector.

Cloning, within the region of homology of the vector, a drug resistance gene (i.e. the neomycin analog G418, spectinomycin, puromycin) is essential to enrich for ES cell clones that have a stable insertion of the vector. Therefore after transfection, the sample of ES cells is cultured in the presence of the corresponding antibiotic and drug-resistant colonies selected. Drug resistance can be triggered in ES cells either because the construct underwent homologous recombination, or if random insertions of at least the sequence of the resistance gene have occurred.

As an advantage, positive selection cassettes can have a dual function, once they primarily serve as a mechanism to enrich for the insertion of the targeting vector, they are also actively used as tools to disrupt coding sequences when knock out models are generated. It is important to note that the insertion into the genome, of resistance cassettes driven by strong and very active promoters, can also be disadvantageous. This has been demonstrated in gene targeting experiments aiming to introduce and retain a neomycin resistance cassette in various loci. An example of this was reported in mice bearing an insertions of a pGK neo cassette in the granzyme B locus. This mutation significantly reduced the expression of downstream sequences encoding other granzymes, even when the insertion site lies as far as 100 Kb away from the affected gene (Pham., *et al* 1996). The exact mechanisms underlying this phenomena are not well known yet, however, the insertion of selection cassettes in the  $\beta$ -globin gene locus control region (LCR), have demonstrated that pGK-neo cassettes can disrupt the normal interaction between the LCR and downstream gene promoters or regulatory elements either by potentiation or competition. Subsequent deletion of the cassette restores gene expression suggesting the specificity of the effect (Hugh., *et al* 1996).

These effects could be influenced by the position where the selection marker is inserted, in another report, the same group demonstrated that targeting at a different location in the  $\beta$ -globin locus does not produced alterations in neighbour genes (Kaufman., *et al* 2001). These effects, often called hypomorphic or neighbourhood effects, are to be considered as part of the strategy to generate knock out models; altered phenotypes can sometimes be the outcome of targeted mutations that keep the selection markers, and this may mask or complicate the phenotypic characterization of the model.

Several strategies are available to overcome this problems, for instance, the use of selection cassettes flanked by site-specific recominase sites (LoxP or FRT) allow to selectively excise such cassettes either in the ES cells (i.e. by transient transfection of Cre) or in mice by crosses with transgenics that express the appropriate recombinases.

#### *iv. Negative selection.*

Random integration of the gene targeting vector typically involves the insertion of both genomic and bacterial plasmid sequences into the genome, a situation that can lead to disruption of additional coding sequences in the genome. This problem can be resolved by using negative selection. This involves the incorporation of a cassette within the plasmid sequence, such that the cassette is lost upon homologous recombination but retained when the vector inserts into a random location. Drug selection against this cassette then enriches for targeted clones. For example inclusion of the Herpes simplex thymidine kinase (HSVtk) gene in the plasmid backbone of the targeting construct and application of the selection drug ganciclovir, negatively selects against clones that have retained this cassette. Negative selection has been reported to enrich for gene targeting events by up to 20-fold (Hasty., *et al*, in Joyner, A. 2000)

### **1.8.4 Screening for homologous recombination.**

In this section we will describe the recombinant alleles produced by replacement vectors, the undesirable targeted products that can occur as well as the main strategies used to screen and confirm events of homologous recombination among drug-resistant ES cell clones. The desired genetic exchange when a replacement vector is used in a gene



targeting experiment is one in which the full sequence of homology and other elements of the vector replace the homologous region in the genome. However, undesirable targeted mutations can happen. Some of those incorrect targeted insertions are formed when vector ends join together or the construct re-circularizes following insertion into the region of homology by two events of cross over. The final recombination product of this phenomena is the insertion of all the elements of the targeting vector including the plasmid, in a single or multiple fashion. Figure 1.7 shows these as compared with an event of gene targeting or simple gene replacement.

An initial screening to select ES cell clones for homologous recombination utilizes the technique of Polymerase chain reaction. This strategy is logistically very useful as it provides the possibility to narrow down the amount of positive selection-resistant ES cell clones selected after electroporation, before confirmation of targeting is performed by Southern blot. PCR screens rely on the use of primers that will amplify a specific junction fragment produced following a cross-over event of an arm of the targeting vector. For example, one primer locates within the positive selection cassette and the other within the genomic target locus but outside the homologous sequence of the vector. This type of PCR will only produce a product if the targeting vector (or at least the corresponding arm of homology) has undergone homologous recombination.

This type of PCR may not be able to amplify following the insertion of a concatamer as the presence of the plasmid backbone or other duplicated sequences may increase the distance between primers (see figure 1.7B). Another type of insertions that result in inappropriate targeting and that may or may not be detected by PCR are the insertions following only one event of crossover. In this case, only the region of homology integrates into the locus but the endogenous sequence is not replaced and is actually duplicated.

As we can see in figure 1.7 an event of simple gene replacement requires that the vector recombines following two reciprocal events of crossover, one on each arm of homology.

If the integration happens through crossover on only one arm of homology, the construct integrates in either a 5' or a 3' duplicate increasing the size of the locus.

The insertion of all the elements of the targeting vector after concatamer formation or re-circularization, as well as insertions in 5' or 3' duplicate can be readily discriminated by Southern blot analysis. This type of screening technique relies in the generation of

altered restriction fragments within the locus if an event of simple gene replacement has occurred. This is detected with a set of external probes (one at either end of the sequence targeted) homologous to the sequence of the target gene, but outside the area of homology of the construct.

These probes are insensitive to events of random integration that can happen with significant frequencies. To discriminate ES cell clones with such integrations, a probe internal to the construct (i.e homologous to the positive selection marker) can be used which will illuminate restriction fragments of the expected size corresponding to targeted alleles together with, extra fragments if random integrations are present simultaneously.

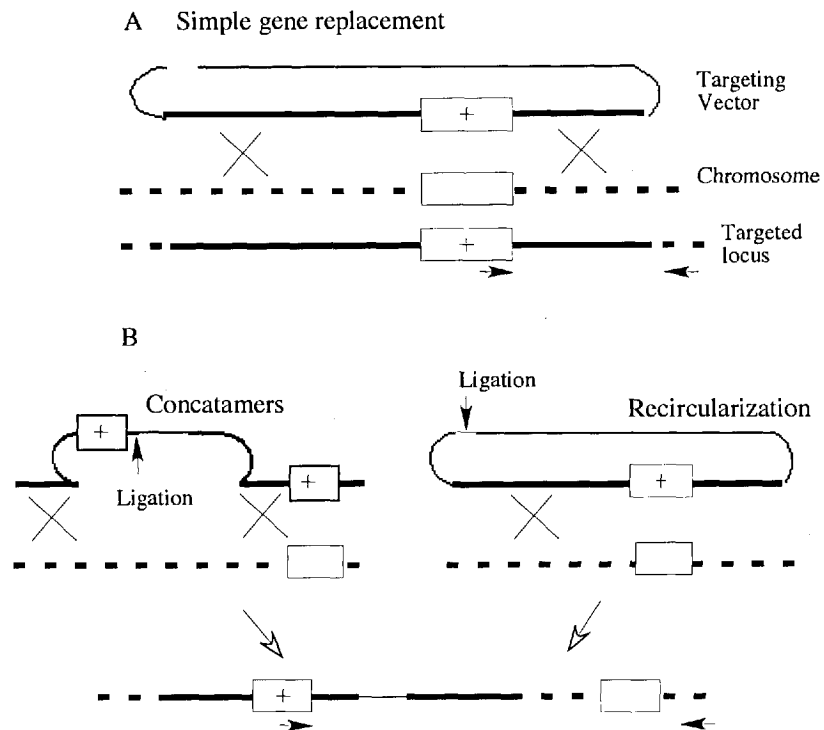


Figure 1.7.- Integration of a replacement vector. In (A) the figure illustrates a simple gene replacement of the targeting vector and the homologous sequence. Crosses represent points of crossover, thick line the homologous sequence of the vector and dashed lines its counterpart in chromosomal DNA. Screening PCR primers are represented as horizontal arrows. (B) represents targeted mutations where either by re-ligation of one copy of the vector or more, the mutation results in the insertion of all the elements of the targeting vector. Figure adapted from (Joyner. 1999).

### **1.8.5 Chimera production and germline transmission of the targeted mutation**

Mutations created by gene targeting in ES cells can be transmitted through the germline of the mouse by chimera production. The most common method in use today to produce such chimeric mice, involves the microinjection of ES cells of a particular mouse strain, into the blastocoele cavity of pre-implantation blastocysts belonging from a different strain (Moustafa., *et al* 1972).

Following the microinjection the chimeric embryos are grown in culture and then implanted into a pseudo-pregnant foster mother to continue the development until birth.

The objective of using blastocysts of a different mouse strain is to facilitate the assessment of the potential transmission of the targeted mutation to the germline of the mouse. For example; when ES cells corresponding to the 129 strain, which carry a dominant agouti-coat colour, are injected into blastocysts of the C57BL6/J background (of black coat colour), the contribution of the ES cells to the embryo can be assessed by simply analyzing the level of agouti colour in the fur of the chimeric offspring. This gives an indication of the potential that those ES cells have had to colonize the germline of this chimera and therefore to transmit the mutation. The degree of coat-colour chimerism in these mice can only give an indication of the potential germline transmission of the mutation, contributed by the population of the targeted 129 ES cells in the embryo. To test that, chimeric mice are backcrossed to C57BL6/J mice and then the appearance of a complete agouti coat-colour in the offspring confirms germline transmission.

It is important to consider that fifty percent of these mice are statistically predicted to be heterozygous for the recombinant mutated allele, which can be tested for by Southern blot screening of tail DNA.

## 1.9 Site Specific Recombination.

There are several prokaryotic organisms as well as yeast species that encode site-specific recombinases able to catalyze the cleavage of DNA at a single site and its ligation to another single independent target site. Among those enzymes two important ones are Cre and Flp.

### 1.9.1 The Cre-loxP system.

The Cre recombinase is a 38 kDa monomeric product of the *cre* gene of bacteriophage P1 (Sternberg., *et al* 1986). It is a member of the  $\lambda$  integrase superfamily of site specific recombinases (Argos., *et al.* 1986). The normal function of this gene is the maintenance of the P1 genome in monomeric circular form in a bacterial host. The Cre recombinase recognises a 34 bp sequence (see figure 1.8 A) and referred to as *loxP* (locus of cross-over (x) in P1), which consists of two 13 bp inverted repeat sequences flanking an 8 bp non-palindromic core sequence. The 13 bp sequences act as binding sites for recombinase monomers and the 8 bp core confers directionality to the *loxP* site and hence, directionality on the recombination reaction. It is at this A:T-rich asymmetric core sequence that strand cleavage and reciprocal ligation happen. Upon binding of the recombinase monomers to each palindromic half of the *loxP* site, two such 13 bp target sites come together to form a synaptic complex, figure 1.8 C. A Holliday intermediate is formed initially by the cleavage, exchange and ligation of one DNA strand. This sequence is repeated for the second strand of DNA to resolve the Holliday junction into two recombinant DNA strands.

The Cre recombinase can interact with its respective target sites to give a variety of outcomes, depending on the positioning of the sites. Recombination between two unidirectional target sites in a head-to-tail orientation excises the intervening DNA as a circular molecule.

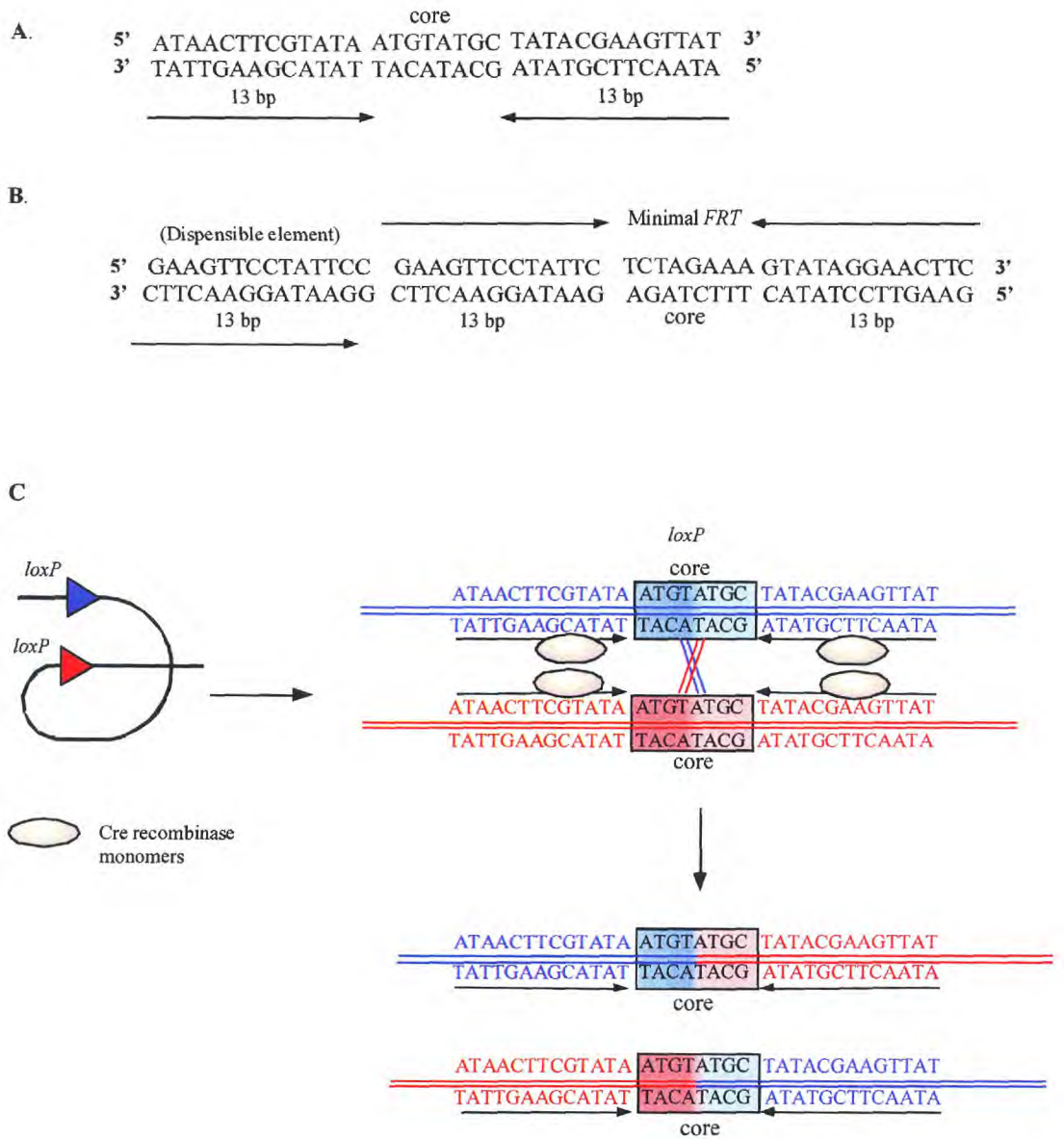


Figure 1.8.- A The *loxP* site sequence, Cre target site. B. The FRT site, Flp recombinase target site and the dispensable element. C. Recombination between 2 unidirectional *loxP* sites mediated by Cre recombinase. Adapted from (Joyner, 2000).

Alternatively, recombination between target sites in an inverted head-to-head orientation inverts the direction of the intervening DNA sequence. Moreover, these reactions are reversible depending on the availability of the recombinase. The demonstration that efficient recombination can occur between altered Cre recombinase sites has led to the development of mutated sequences that change the equilibrium of the reaction towards generation of recombination products, for example, the *loxP* 511 and *loxP* 514 sequences (Hoess *et al.* 1986). Such mutant *loxP* sites can recombine with wild-type sequences, but recombination between mutant substrates is extremely inefficient. Single base-pair mutations at either end of the 8 bp spacer of wild-type *loxP* cassettes were demonstrated to have little effect on recombination between the mutant and wild-type *loxP* sequences but the efficiency of recombination was much lower between two mutant sequences (Lee., *et al* 1998). Double substitution mutations within the spacer region were also tolerated, but led to drastically reduced levels of recombination.

### **1.9.2 The FLP – *FRT* system.**

The Flp recombinase is a 43 kDa protein encoded by the 2 $\mu$  circular plasmid of the budding yeast *Saccharomyces cerevisiae* (Gerbaud, C., *et al* 1979; Broach., *et al* 1980). The target site of the Flp recombinase, designated *FRT* (Flp recognition target sequence), comprises structural elements similar to the *loxP* sequence (Figure 1.8). The dispensable element is present in the 2 $\mu$  plasmid, but is not essential for Flp mediated recombination (Sadowski. 1995).

### **1.9.3 Site specific recombinases in gene targeting.**

Recombinase systems have been used in gene targeting for the design of targeting constructs, the efficient removal of the selectable markers from targeted alleles and for conditional gene targeting. Furthermore, conventional gene knockout experiments that generate null alleles, by insertion of the positive selection marker into a coding sequence of the gene, may, in several instances, generate abnormal but functional targeted products, due to alterations in the alternative splicing or the induction of hypomorphic

alleles effects. These effects are caused by the elements of targeting constructs, such as strong viral promoter-driven antibiotic resistance cassettes, which can alter the expression of proximal and sometimes distant genes- (Nagy., *et al* 1998; Meyers., *et al* 1998) . This problem may be overcome with the inclusion of recombinase sites in the gene targeting vector, flanking the selection marker, so that it can be removed subsequent to a homologous targeting event. In addition, by flanking the region to be deleted within the targeting vector with recombinase sites, it is possible to use recombinase systems to bypass the embryonic lethality of some conventional null mutations and provides a route to conditionally modify genes *in vivo*.

A potential disadvantage of using such recombinase target sites within sequences of the targeting vector is that the recombinase leaves behind the heterologous sequence of the target site, for example, the 34 bp loxP sequence recognised by the Cre recombinase. However, the sequence appears sufficiently small so as to be neutral towards gene expression when positioned in non-coding genomic DNA. Depending on the gene targeting strategy, retaining such recombinase sites is useful if further deletions are required.

At present recombinase systems like Cre-loxP and Flp-FRT are commonly used as genetic engineering tools to manipulate endogenous sequences and transgenes *in vivo*. Cre has demonstrated a higher efficiency of recombination than Flp. This may be due to discrepancies in optimal working temperatures as Cre recombinase works at 37°C, but Flp recombinase has an optimum temperature of 30°C. In consequence, Flp currently seems to be the recombinase of choice to perform *in vitro* eviction of FRT-flanked marker sequences (Dymecki. 1996) while Cre recombinase is commonly utilized for *in vivo* gene manipulation in mice (Orban., *et al* 1992). Both Cre and Flp can mediate recombination between target sites over very large genomic distances, although variable recombination frequencies have been observed depending on different factors.

Vooijs. *et al* have shown that for various alleles (*R26R* and *Brca2*), the distance between loxP sites has an impact on the recombination frequencies using a system where the activity of a mutant form of Cre was temporally regulated by an estrogen derivate 4-hydroxy Tamoxifen (Vooijs., *et al* 2001).



Cre transgenic mice are valuable tools to perform *in vivo* modifications to targeted alleles such as the elimination of positive selection cassettes or the generation of intermediate alleles required for conditional gene targeting strategies. Among these transgenics the so called “germ line deleters” are particularly useful as their expression of Cre in embryological tissues facilitates the generation of the genotypes needed, simply by performing a cross with animals bearing the *loxP* sites flanking the DNA sequences of interest, an example of these transgenic mice is the EIIa-Cre. In this line, Cre expression is driven by the EIIa adenoviral promoter, which targets Cre expression to the early mouse embryo (Lakso., *et al* 1996). Another very potent and reliable Cre deleter line, in this case with expression driven by the early acting PGK-1 promoter, possesses Cre expression under dominant maternal control, meaning that when females are crossed with males that carry a gene flanked by *loxP* sites (“floxed”), deletion is observed even in the offspring negative in genotype for Cre (Lallemand., *et al* 2004).

Finally another strategy to deliver Cre and to induce recombination on *loxP* site-bearing sequences, comprises the transient delivery of Cre through viral transduction using Adenoviral strains encoding Cre. These tools are valuable to turn on or off “floxed” genes by transient expression of Cre and subsequent temporal recombination in genetically modified cell lines. They have also proven efficient for deletion in embryos kept in culture before implantation. One of such strains that has shown successful viral transduction in cells and embryos is AxCanCre (Kanegae., *et al* 1995).

Several other specific Cre transgenics have been generated by pronuclear injection and knock-in strategies. These reagents are thoroughly described in this online database; <http://www.mshri.on.ca/nagy/Cre-pub.html>.

## **1.10 Conditional gene targeting.**

The generation of null mutants can result in severe early phenotypes or even lethality at the developmental stages, therefore several strategies aimed at gaining spatial and temporal control of the process of gene ablation have been developed.

One of the most widely used strategy uses the Cre-lox system, where Cre is controlled in its temporal and spacial expression.

Cre-loxP conditional gene targeting requires the generation of a mouse harbouring a loxP-flanked segment of the gene to be altered and a second mouse strain expressing the Cre recombinase from a transgene which is under the control of a particular promoter with a desired tissue expression profile, and/or with the ability to deliver an active form of Cre, only in the presence of an inducing agent or drug.

Crossing the two strains produces double transgenic offspring with a Cre-loxP induced temporally and/or spatially restricted genetic modification, thus generating a conditional mutant.

The spatial control of the targeted mutation affords the study of gene function in specific tissues or cell lineages to permit the dissection of particular components of a disease phenotype. Tissue-specific gene ablation was first demonstrated by (Gu., *et al* 1994) who generated a mouse harbouring a floxed promoter and first exon of the DNA polymerase  $\beta$  gene (*pol*  $\beta$ ). This gene-targeted mouse was mated with a Cre transgenic mouse that expressed Cre recombinase in T cells only. The consequence was DNA *pol*  $\beta$  gene ablation in about 40% of T cells but not any other tissues in offspring mice.

Temporal control of the mutation provides a means of inducing a mutant genotype at a particular stage of development. Such control is able to negate adaptive or gene redundancy mechanisms which have been observed in conventional knockout models, often obscuring precise genotype-phenotype relationships (Suemori., *et al* 2000).

This enables the differentiation between the phenotype of chronic versus acute ablation of a protein. Spatial and temporal control of Cre-mediated recombination has been performed through several strategies. Adenoviral expression of Cre have been used to by several groups (Akagi., *et al* 1997 and Shibata., *et al* 1997). However the immune response of animals infected has made difficult the analysis and has affected the health status of animals studied. Another method used to gain temporal control of Cre *in vivo*, has utilized elements of the Tetracycline operon, but these has not always provided tight and reliable control of Cre expression and such leakiness complicates the analysis (Utomo., *et al* 1999). Finally interferon inducible Cre expression systems have also been employed to control Cre recombination *in vivo* (Khun., *et al* 1995).

An alternative approach takes advantage of recombinases fused with either one or two domains of a mutated estrogen receptor. These fusion protein becomes active only in the presence of the synthetic estrogen agonist Tamoxifen (as well as 4-hydroxy tamoxifen) instead of its natural ligand 17 $\beta$ -estradiol (Feil., *et al* 1996). This system has proven to deliver a very tight control of the expression of Cre, and several transgenics have been generated where the system is driven by tissue specific promoters (Brocard., *et al* 1997; Schwenk., *et al* 1998; Vasioukhin., *et al* 1999). However one of the main problems observed still with these animal models is that random insertions of the transgene, generate a mosaic expression limiting the control of Cre expression (Garrick., *et al* 1998). This obstacle can be overcome with the generation of tissue-specific, inducible Cre expressing mice through knock in strategies, where single copy transgenes can be introduced into stable loci that are ubiquitously express throughout the mouse development and adult stages (Vooijs., *et al* 2001). Figure 1.9 shows how the estrogen-dependent Cre inducible system works.

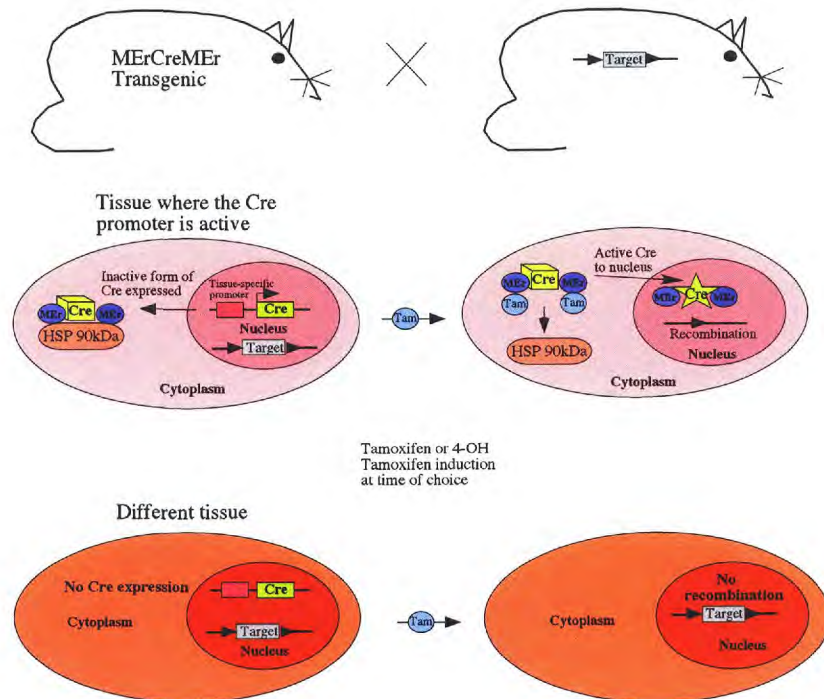


Figure 1.9.- Spatio-temporal control of gene inactivation through Cre-mediated recombination in cells and mice. In (A) the figure illustrates the two genetically modified animals required for the system. First; a transgenic mouse having tissue restricted expression of the fusion protein Cre recombinase is crossed with an animal bearing a floxed gene of interest. B shows that at the level of the cells in the specific tissue where Cre is expressed, only the presence of Tamoxifen or 4-hydroxy tamoxifen, can induce the dissociation of the heat shock protein (HSP90) that keeps Cre inactive in the cytoplasm. After such dissociation, Cre can use the nucleo-localization sequences of the mutated estrogen domains to translocate to the nucleus and excise the gene of interest. In other tissues (C), Cre is not expressed and no effect is observed.

## 1.11 Conclusions and aims

It has been approximately 20 years since CTLA-4 was first identified and a vast amount of data is already available which allow us to understand its predominant role as a negative costimulatory molecule. From genetic mapping to structural characterization and biologically functional experiments, the methodologies used are diverse and very powerful but all have important limitations when studying the mechanisms of action of a molecule like CTLA-4.

Perhaps the clearest image obtained about the function of CTLA-4 as a negative costimulatory molecule, has been elucidated by analyzing the immunity of CTLA-4<sup>-/-</sup> mice. However the lethality of this phenotype limits the study of the mechanisms of action of this molecule at the adult-stage peripheral T cell regulation. This problem could be overcome by using conditional gene targeting.

Gaining temporal control of CTLA-4 deficiency will not only allow us to study the immune system in the absence of this gene at different stages of life, but also will be useful to extend the knowledge already obtained from other mouse models, for instance, the above-mentioned autoantigen systemic and tissue restricted transgenic system

Another advantage would be the ability to obtain T cell subsets (i.e. CD4<sup>+</sup> CD25<sup>+</sup> regulatory T cells) in which a *Ctla-4* deletion can be induced at later stages, to use them in *in vitro* assays.

In the process of making such model for conditional inactivation, animals bearing a targeted CTLA-4 allele can also be employed to address questions on the genetic regulation of this gene. Sequence modifications required for targeting can produce hypomorphic alleles that may alter the expression of the gene of interest or neighboring genes, a situation that for CTLA-4 is of interest for two reasons: First, *Ctla-4* is adjacent to two of the most important T cell costimulatory molecules; ICOS and CD28. Second, due to what is already known on its polymorphic variants and their association with autoimmunity, targeting *Ctla-4* without inactivation may result in an interesting phenotype.

In this project we will apply conditional gene targeting with the aim of selectively inactivating CTLA-4 expression in a temporal and spacial fashion in animals. Our essential aim is to analyze the peripheral immune system of animals in which conditional inactivation has been achieved particularly in adult stage.

### **1.12 General Aims.**

- Generate a mouse in which conditional *Ctla-4* inactivation can be achieved using the Cre-*loxP* system.
- Perform a phenotypic analysis of mice homozygous for a targeted *Ctla-4* allele, as well as mice with a *Ctla-4* allele in which exons 2 and 3 have been deleted by Cre-mediated recombination.
- To study the peripheral immune system of animals in which a conditional CTLA-4 inactivation has been achieved, particularly later in the development or in adult stage.

***Chapter 2. Materials and Methods***

## 2.1 Materials.

### 2.1.1 Buffers, solutions and media.

#### *i. Molecular Biology.*

- Ampicilin: (Amp; A9518 Sigma) was prepared as a 50mg/ml stock solution and added to LB media to a final concentration of 50 $\mu$ g/ml when media was at 50 °C. Amp aliquots were stored at -20 °C
- Luria Bertani medium (LB): 1% (w/v) Bacto-tryptone (0123-17-3, Difco), 0.5% (w/v) yeast extract (0127-17-9; Difco), 0.25 mM NaCl (S9625, Sigma). 1.5% w/v agar for plates (0145-17-0, Difco).
- Loading Buffer (6x): 0.25% bromophenol blue (B5525, Sigma), 50% (v/v) Glycerol (101186, BDH).
- Tris-EDTA (TE) buffer: 10mM Tris-HCl pH 8.0 (T3252, Sigma), EDTA pH 8.0 (E5134, Sigma).
- 10X Tris-borate buffer (TBE) buffer: 0.89M Tris-borate (T1503, Sigma), 20mM EDTA pH 8.0.
- 10X Tris-acetate-EDTA (TAE) buffer: 400mM Tris-acetate, 10mM EDTA, pH 7.0
- Hybridization buffer: Ultrahybe buffer™ (8669, Ambion).
- 20X Salt Sodium Citrate (SSC): 5M NaCl, 0.3M Tri-sodium citrate (C7254, Sigma)
- 10X TNE: 50mM Tris pH 8.0, 150mM NaCl, 100mM EDTA.
- Depurination solution 1X: 250mM HCl (H1758, Sigma).
- Denaturing solution 1X: 1.5M NaCl, 0.5M NaOH (480878, Sigma).
- Neutralising solution 1X: 1M Tris-HCl, pH 8.0, 1.5M NaCl.
- GNTK buffer, (50 mM KCl (P9333, Sigma), 1.5 mM MgCl<sub>2</sub>, 10 mM Tris-HCl, pH 8.5, 0.01% gelatin (G2500, Sigma), 0.45% Nonidet P-40 (21-3277, Sigma), 0.45% Tween-20 (P1379, Sigma).
- Dyethyl pyro-carbonate treated H<sub>2</sub>O (9916, Ambion).
- Ethidium Bromide: 10mg/ml stock (E2515, Sigma).



- Radioisotopes: [ $\alpha$ - $^{32}\text{P}$ ] dCTP, 3000 Ci/mmol 250 $\mu\text{Ci}$  (A0005, GE Healthcare formerly Amersham Biosciences).
- DNA Molecular weight markers: 1Kb plus<sup>TM</sup> DNA ladder 100bp-12Kb range (SM1331 250, Invitrogen).
- Deoxynucleotide triphosphates (dNTP): Set of 4, 100mM each (U1330, Promega).

Autoclaving of solutions was performed at 121°C, 15lb/in<sup>2</sup> for 20 min or by filtration through a 0.2 $\mu\text{m}$  Millipore membrane.

*ii. Techniques for protein analysis.*

- Tris glycine running buffer: 0.025M Tris pH 8.3, 0.192M glycine (G7126, Sigma), 0.1% SDS (L4390, Sigma).
- 2X Sample buffer: 0.125M tris-HCl pH 6.8, 4% SDS, 20% glycerol, 0.1% bromophenol blue, 10% 2-mercaptoethanol (M7522, Sigma).
- Towbin transfer buffer: 0.025M Tris pH 8.3, 0.192M glycine, 20% methanol (10158, BDH).
- Coomassie blue staining solution: 10% glacial acetic acid, 10% methanol 0.01% Coomassie Brilliant Blue R (B0149, Sigma).
- Coomassie destain solution 10% glacial acetic acid, 10% methanol.
- 1X Phosphate buffered saline (PBS): 10 Dulbecco's A phosphate buffered saline tablets (BR14a; Oxoid) were dissolved in 1 litre of distilled water to give a final concentration of: 8g/L NaCl, 0.2g/L KCl, 1.15g/L Disodium hydrogen phosphate and 0.1g/L Potassium hydrogen phosphate.
- Blocking/antibody buffer: 1X PBS, 5% skimmed milk (domestic).
- Membrane washing buffer: 1X PBS, 0.1% Tween-20.
- 40% Bis/Acrylamide solution (A3574, Sigma).
- Benchmark<sup>TM</sup> pre-stained molecular weight markers 6.0 kDa to 181.1kDa (10748-010, Invitrogen).
- Restore<sup>TM</sup> Western blot stripping solution (21059, Pierce).
- Protease inhibitors Complete mini EDTA free (1836170, Roche).
- Phosphosafe<sup>TM</sup> Cell lysis buffer (71296-3, Novagen).

### *iii. Tissue culture techniques.*

- Cell culture medium: RPMI-1640 (31870-108, Gibco BRL-Invitrogen), 0.58g/L L-glutamine (25033-010, Gibco BRL-Invitrogen), 0.2U/ml Penicillin-streptomycin (15070-022, Gibco BRL-Invitrogen), 10% to 15% heat inactivated foetal calf serum (FCS) (253500; Harlan) and  $2.5 \times 10^{-5}$ M 2-mercapto ethanol.
- Tritiated thymidine: 5% v/v stock solution ( $[^3\text{H}]$ -thymidine; 2407005, ICN Biochemicals).
- Sodium and potassium free Dulbecco's tissue culture PBS (P5368, Sigma).
- Trypan blue: 0.4% working solution in PBS (T6146, Sigma).
- Erythrocyte lysis buffer: 8.34g Ammonium chloride (A-9434, Sigma), 0.037g EDTA, 1g Sodium bicarbonate (S6014, Sigma). Sterilized by autoclaving.

### *iv. Flow cytometry.*

- Staining buffer: Ice cold PBS, 10% Bovine serum albumin (BSA)(A2153, Sigma), 10% normal mouse serum (M5905, Sigma).
- Washing buffer: Ice cold PBS, 10%BSA.

### *v. Tamoxifen Treatment.*

- Preparation for injections: Tamoxifen; (T5648-1G, Sigma). Stock  $100 \mu\text{g}/\mu\text{L}$  Tamoxifen in 100% ethanol and emulsified in 2ml sunflower oil (domestic) to give an approximate final concentration of  $50 \mu\text{g}/\text{ml}$ .
- Preparation for oral administration was prepared with the required amount directly in sunflower oil.

## **2.1.2 Heat shock competent bacteria.**

The *Escherichia coli* strain used for all clone propagations was XL 10-Gold (Stratagene). Genotype: TetR,  $\Delta(\text{mcrA})183$ ,  $\Delta\text{mcrCB-hdsSMR-mrr}173$ , endA1, supE44, thi-1, recA1, gryA96, relA1, lac, Htr, (F', proAB, lacqZ  $\Delta\text{M15tn}10$ , (TetR), Amy, Cam)a.

### 2.1.3 Enzymes.

- Restriction endonucleases (Promega and New England Biolabs).
- T4 DNA ligase (M180, Promega).
- Taq polymerase (M2035, Promega).
- Calf intestinal alkaline phosphatase (M1821, Promega).
- DNA polymerase I (Klenow fragment) (Y01396, Invitrogen).
- Proteinase K (P2308, Sigma), DNA free recombinant Proteinase K (3115836, Roche).

### 2.1.4 Kits for Molecular Biology.

- GeneClean by NaI-glass beads method: Easypure, (390001, Biozym Inc)
- Plasmid DNA isolations: Maxirep Kit endotoxin free (C-12362, Qiagen) and Miniprep Kit (C-27106, Qiagen).
- DNA labeling by random priming: RadPrime DNA labelling kit (18428-011, Invitrogen)
- Probe cleaning: Sephadex SH-200 HR MicroSpin columns (27-5120-01, GE Healthcare).
- Absolute RNA<sup>TM</sup> mini-prep kit (400800, Stratagene).
- High capacity cDNA archive kit (ABI, 432217).
- Expand Long<sup>TM</sup> PCR kit (1681834, Roche)

### 2.1.5 Plasmid vectors.

#### *i. pBluescript II KS<sup>+</sup>*

This vector, from Stratagene, is a colony producing phagemid, derived from the pBS phagemid. It contains a synthetic polylinker, a fragment of the LacZ gene to facilitate blue/white colony screening and an ampicilin resistance gene.

All the constructs produced, including pGKneo which contains the sequence of the neomycin resistance gene flanked by loxP sites, had pBluescript as backbone. pGKneo was kindly provided by Dr Yuri Mishima at NIH USA.

## 2.1.6 Oligonucleotides.

Primer name	5'-3' Sequence
LoxF	GTATACACCACTCTACCACAGTGA
LoxR	GGCAAATAATTCTTCCTTTCATTTATT
E4F	CTTGGGCATTTTGGTTGTTC
E4R	ACGCGTCGACTCCTTCTTCTTCATAAACGGC
E3EcoR1F	CACCATGTCTGTGTAAGGCT
E4EcoR1R	TCCCTCCCCAGCAAAAATAA
BpAF	CCCTGGAAGGTGCCACTCCC
Neo2R	CAGAAGACAGGAGTTGGATTCCCAGC
Neo2F	GAAGACAATAGCAGGCATGC
E1R	AGCAAGCTGCTGTGGCTAGT
E2F	CAAAGGGTGAAGGGAGTGAT
GR	CAGAAGACAGGAGTTGGATTCCCAGC
5'pF	TGCTGAGGTATATGAACTACGT
5'pR	CTTTGATCCAAGGTACGTGTGCTA
Neo1	TGCCGCGCTGTTCTCCTC
Neo2	AAGCGGCCATTTTCCGCCAT
PGKR	GGTGGATGTGGAATGTGTGC
E4NeoR	AACTGAGCTAGTCAAATTCACC
Exon1F	CTTGTCTTGGACTCCGGAGG
E4R	ACGCGTCGACTCCTTCTTCTTCATAAACGGC
HPRTF	TCGTGATTAGCGATGATGAACC
HPRTR	CTGGCAACATCAACAGGACTCC
Cre1	CGCAGAACCTGAAGATGTTTCGCGA
Cre2	GGATCATCAGCTACACCAGAGACG

Table 2.1.- Oligonucleotides used for PCR and sequencing were selected from the mouse genomic sequence (*Ctla-4*: NCBI accession #AF142145, *Hprt*:accession # NM013556) and synthesized by Sigma Genosys.

### 2.1.6 Kits used for the techniques of protein analysis.

- Protein concentration: BCA™ protein assay kit based on the Biuret reaction (23227, Pierce).
- Chemio-luminescence detection of proteins: Western Pico ECL kit (34080, Pierce).

### 2.1.7 Antibodies used for tissue culture, Western blot and flow cytometry.

#### *i. Antibodies used for western blot.*

Reference & source	Specificity	Species isotype	Format	Clone	Dilution
Santa Cruz s-1628	Mouse CD152 C terminus	Goat poly-clonal IgG	Serum	C19	1:200
Sigma A5420-1ML	Goat IgG	Rabbit IgG	Purified HRP conjugated	--	1:8000
Chemicon MAB 1501R	Pan actin	Monoclonal	Purified	C4	1:1000
GE Healthcare NA931	Mouse IgG	Sheep poly-clonal IgG	Purified HRP conjugated	--	1:1000

Table 2.2.- Primary and secondary antibodies used for Western blot.

#### *ii. Purified Antibodies used for tissue culture.*

Reference	Specificity	Species isotype	Clone
553238	Mouse CD3e	hamster IgG2	500A2
553294	Mouse CD28	hamster IgG2	37.51

Table 2.3.- Mouse purified (azide free) monoclonal antibodies used for stimulation of T cells. All antibodies were purchased from BD and used at a final concentration of 1 µg/ml.

*iii .Anti mouse monoclonal and isotype antibodies control used for flow cytometry.*

Reference	Specificity	Fluorochrome	Species isotype	Clone
553062	CD3e	FITC	hamster IgG1	145-2C11
553050	CD4 (1:400)	PE-Cy5	rat IgG2a	RM4-5
553031	CD8a (Ly-2)	FITC	rat IgG2a	53-6.7
557399	CD19	R-PE	rat IgG2a	1D3
553866	CD25	R-PE	rat IgG1	PC61
553297	CD28	R-PE	hamster IgG2	37.51
553237	CD69	R-PE	hamster IgG1	H1.2F3
553720	CD152 (CTLA-4)	R-PE	hamster IgG1	UC10-4F10-11
552146	CD278 ( ICOS )	R-PE	rat IgG2b	7E.17G9
551892	CD279 ( PD-1 )	R-PE	hamster IgG2	J43

Table 2.4.- Mouse monoclonal conjugated antibodies used for flow cytometry. All antibodies were purchased from Beckton Dickinson (BD) and used at a 1:100 dilution or otherwise stated.

Reference	Fluorochrome	Species isotype	Clone
553953	FITC	hamster IgG1	G235-2356
553954	R-PE	hamster IgG	G235-2356
557078	R-PE	rat IgG1	A110-1
550085	R-PE	hamster IgG2	B81-3
553929	FITC	rat IgG <sub>2a</sub>	R35-95
553930	R-PE	rat IgG <sub>2a</sub>	R35-95
553989	R-PE	rat IgG <sub>2b</sub>	A95-1

Table 2.5.- Mouse anti TNP isotype control antibodies. All antibodies were purchased from BD and used at a 1:100 dilution.

## 2.2 Methods.

### 2.2.1 Molecular Biology

#### *i. Agarose gel electrophoresis.*

DNA samples were mixed with loading buffer and subjected to electrophoresis through 0.8% to 2% agarose gel (A5643, Sigma, LMP4327, Appligen Oncor) for low melting point) in TBE or TAE with ethidium bromide. Gels were visualized with a UV transilluminator (Herolab). Documentation was performed using a UV sensitive camera (Herolab) and a thermal paper printer (Sony).

DNA fragments sizes were estimated using the 1Kb plus DNA ladder (100,200,300,400,500,650,800,1000, 1650,2000bp with increments of 1Kb up to 12Kb).

#### *ii. Small and large scale plasmid DNA purification.*

The “maxi” and “mini” prep kits (Qiagen,) were used to isolate plasmid DNA from bacteria. For a “maxi-prep” 10 mL LB containing 100 µg/mL ampicillin were inoculated with a single bacterial colony and grown overnight at 37°C, shaking at 250 rpm. The overnight culture was used to inoculate 500 mL of LB broth containing ampicillin, and grown overnight. Bacteria were pelleted by centrifugation for 15 min at 6000 g, at 4°C. The pellet was resuspended in 10 mL of Buffer P1 containing 100 µg/mL RNase A. 10 mL Buffer P2 was added to the bacterial suspension, mixed gently and incubated at room temperature for 5 min. 10 mL chilled Buffer P3 was added, mixed gently and stored on ice for a further 20 min. Precipitated protein and chromosomal DNA were removed by centrifugation at 4°C for 30 min at 20 000 g. Another centrifugation step of 20 000 g at 4°C for 15 min was applied to the supernatant to remove the remaining particulate material.

A Qiagen-tip 500 resin column was equilibrated with 10 mL Buffer QBT, and allowed to empty by gravity flow. The supernatant containing the plasmid DNA was applied to the column and again allowed to enter by gravity flow. The column was washed twice

with 30 mL Buffer QC, and the DNA eluted with 15 mL Buffer QF. Nucleic acids were precipitated with 0.7X volumes of isopropanol and pelleted by centrifugation at 10,000 g for 30 min at 4°C. The DNA pellet was washed with 5mL of room-temperature 70% ethanol, and centrifuged at 10,000 g for 10 min. The supernatant was carefully decanted and the pellet air-dried for 5-10 min. The DNA was resuspended overnight at 4°C, in 500 µL TE. DNA concentration was determined by spectrophotometry.

The small scale preparation or, “mini-prep,” of plasmid DNA was performed in a similar manner to that of the previously described DNA “maxi-prep”. 5 mL of overnight culture was harvested by centrifugation at 5,000 g for 5 min. The Qiaprep “mini” prep kit from Qiagen was used for the isolation of plasmid DNA. The bacterial cells were resuspended in 250 µL of Buffer P1 containing 100 µg/mL RNase A and lysed by addition of 250 µL Buffer P2. 350 µL of Buffer N3 was added to the lysate, mixed gently and the precipitated protein and chromosomal DNA removed by centrifugation for 5 min at 13,000 rpm. The supernatant was applied to a Qiaprep silica-gel column and centrifuged for 60 sec at 13,000 g. The column was washed with 750 µL Buffer PE containing 80% ethanol, with an additional subsequent centrifugation step to remove residual wash buffer. The Qiaprep column was placed in a 1.5 mL microfuge tube, and 50 µL TE applied to the silica-gel membrane, allowed to stand for 1 minute, and eluted by centrifugation at 13,000 g for 60 sec.

Stocks of recombinant bacteria were kept frozen using glycerol: 750µL of bacterial culture in LB was mixed with 250µL of sterile 80% glycerol-H<sub>2</sub>O in a vial, snap frozen and kept at -70 °C. Cells were grown from the frozen stock by taking a stab.

### *iii. Extraction of DNA from agarose gels.*

Gene clean was used to isolate DNA from agarose gels (Easypure kit). Following electrophoresis in a TAE agarose gel, the DNA was excised from the gel, and the volume of the gel slice was assessed. 3X volumes of NaI were added to the gel slice, and incubated at 50°C until the agarose melted. 5µL of Glassmilk solution (an aqueous suspension of



silica beads) was added to the mix, and incubated on ice for 10 min, with gentle intermittent shaking. The DNA/glassmilk was briefly spun at 13 000 g and the pellet washed three times with New wash solution (a solution of NaCl, Tris, EDTA and ~50% ethanol). The DNA was eluted from the Glassmilk by addition of 10 $\mu$ L TE and centrifugation at 17 500 g for 30 sec in a bench-top centrifuge. The TE containing the DNA was transferred to a fresh tube.

*iv. Plasmid purification and genomic DNA extraction using Phenol/Chloroform or as crude lysates.*

Phenol/chloroform extractions were performed to remove contaminating traces of protein from plasmid DNA samples. An equal volume of TE-saturated phenol (RP3024, Rathum Chemicals) was added to the DNA sample, mixed by vortexing, and phases separated by centrifugation at 10,000g for 1 min. The aqueous phase is separated from the organic phase and extracted once with an equal volume of chloroform/isoamyl alcohol (24:1 v/v) (277106P; BDH and 1-9392; Sigma).

After phenol/chloroform extraction or to concentrate a particular sample, DNA was precipitated by adding 2.5 volumes of 100% ethanol and 10% sodium acetate (pH 5). The mixture was then incubated at -20°C for 15 min and spun for 15 min at 10,000 g. The DNA pellet was then washed with 70% ethanol, air-dried and resuspended in an appropriate volume of TE.

ES cell genomic DNA was extracted from two different culture conditions based on the analysis to be performed in each case, on the one hand, 96-well plate cultures yielded approximately 800ng and were used for PCR, on the other, 24-well plate cultures yielded approximately 30 $\mu$ g which was enough to perform Southern blots.

To extract genomic DNA from a 96-well plate culture, cells were initially lysed by adding 50 $\mu$ L of a 10mM Tris-HCl pH 7.5, 10mM EDTA, 10mM NaCl, 0.5% SDS 1mg/ml proteinase K buffer. After an overnight incubation at 55°C in a humid environment, DNA was precipitated in a mixture of ice cold 100% ethanol, 75mM NaCl for 2h until precipitated DNA was visible. DNA will bind to the tissue culture plastic allowing us to eliminate the solution in each well by inverting the plate over several layers of paper towels.

Finally each sample was washed twice with 200 $\mu$ L 70% ethanol and spun for 5 min in a bench top tissue culture centrifuge at 2800 g for 5 min. Ethanol was eliminated in each wash by inverting the plates on paper towels and air dried for 10 min after the last wash. Each sample was resuspended in 50 $\mu$ L of TE and quantified by running an aliquot against a quantitative marker in an agarose gel.

From a 24-well plate, cells were resuspended in 1ml of TNE for 30 min at 37°C. After incubation the cell suspension was transferred to a 2ml eppendorf tube, 50 $\mu$ L of 10%SDS and 10 $\mu$ L of 20mg/ml of proteinase K were added and the mixture incubated overnight at 55°C.

The next day DNA was phenol-chloroform extracted three times using initially 1 volume of TE saturated phenol only, then 1 volume of phenol-chloroform 1:1 and finally 1 volume of TE saturated chloroform to eliminate traces of phenol.

The sample was precipitated with 0.7 volumes of isopropanol (10062;Sigma), spun at 10,000 g for 10 min, eliminating the alcoholic phase without disturbing the pellet.

Pellets were washed twice with 500 $\mu$ L 70% ethanol and resuspended in 200 $\mu$ L of TE.

Crude lysates from mouse tail biopsies were prepared as follows:

Approximately 5mm of tail tip biopsy was submerged in 200 $\mu$ L of GNTK buffer and digested with 0.1mg/ml proteinase K overnight at 56°C.

After complete digest samples were centrifuged at 10,000 g and 0.5 $\mu$ L to 1 $\mu$ L used for PCR. In each case proteinase K was inactivated by incubating the DNA template at 95°C for 5 min before any PCR.

#### *v. RNA extraction for Reverse Transcriptase - PCR.*

RNA extractions from cell lysates were performed using the Absolute RNA™ mini-prep kit. Between  $1 \times 10^6$  to  $1 \times 10^7$  cells were lysed with 350 $\mu$ L of lysis buffer containing 2-mercapto ethanol and vortexed. At this point, if necessary, samples were stored at -70 °C, or processed as follows. Cell-lysates were diluted with an equal volume of 70% ethanol (10107; BDH) in DEPC treated water and mixed by inversion. Lysates are then passed through a spin filter column and centrifuged at 10,000 g to eliminate cell debris,

filtrates are then passed through a spin binding column and centrifuged at the same speed. RNA binds to the column so it is kept and filtrate discarded. The column is then washed with 700 $\mu$ L of low salt buffer, centrifuged, and subsequently digested with 1 $\mu$ g/ml of RNase-free DNase I to eliminate genomic DNA. After 15 min at 37 °C, spin columns are washed sequentially with 700 $\mu$ L of high salt buffer, 700 $\mu$ L of low salt buffer and 300 $\mu$ L of low salt buffer, spinning in between, after the last wash spin columns are spun empty do allow drying. Spin columns are then transferred to a fresh tubes and RNA eluted with 60 $\mu$ L of elution buffer at 60 °C.

RNA is quantified by spectrophotometry and its quality evaluated by visualization of ribosomal RNA (28S and 18S) on an agarose gel. Previous to the electrophoresis the tank was washed with 1% SDS to inactivate any contaminating RNAses.

*vi. UV spectrophotometry.*

DNA concentrations were determined by spectrophotometry spectrophotometer. A 100 $\mu$ L sample was scanned at 260nm and 280nm to determine the absorbance ratio (A260/A280), as this ratio indicates the level of purity of the sample.

DNA concentration was calculated considering that an OD 260nm of 1 is equivalent to a concentration of 50 $\mu$ g/ml for dsDNA and 40 $\mu$ g/ml for RNA.

*vii. Restriction enzyme digestion of plasmid and genomic DNA.*

Different amounts of DNA were digested in a reaction volume of 20-50  $\mu$ L for 2-4 hrs, using 1-10 units of restriction enzyme per  $\mu$ g of DNA. Digestions were performed in the appropriate restriction buffer and at the optimum temperature according to manufacturer's specifications.

Genomic DNA restriction digests were performed as follows.

10X RE buffer	5 $\mu$ L
Restriction enzyme	5-10U
40mM Spermidine	1.25 $\mu$ L
10mg/ml RNase A	0.5 $\mu$ L
5mg/ml BSA	1 $\mu$ L
10-15 $\mu$ g of DNA +H <sub>2</sub> O up to	50 $\mu$ L

*viii. Alkaline phosphatase treatment of DNA.*

Alkaline phosphatase was used to eliminate 5' phosphate groups left by restriction enzymes, and therefore to diminish self-religation of the vector during cloning experiments. An appropriate amount of Calf intestinal alkaline phosphatase (0.01U per pmol of 5' ends, 1 $\mu$ g of a 1Kb DNA fragment equals to 3.03pmol of ends) was added to a sample of DNA, resuspended in Tris-HCl pH 8, and the reaction incubated at 30°C for 30 min.

The phosphatase was inactivated by adding a solution of 10mM Tris-HCl, 1mM EDTA, 200mM NaCl and 0.5% SDS.

After inactivation nucleic acids were isolated by phenol/chloroform extraction and ethanol precipitation.

*ix. Restriction overhangs modification or "end filling".*

The modification of incompatible DNA using restriction overhangs was performed by DNA polymerization using the bacteriophage T4 DNA polymerase, known as the Klenow Fragment.

DNA "end filling" reactions comprised as follows:

Digested DNA	2 $\mu$ g
DNA polymerase Klenow fragment	2U
dNTP	2mM for each one
10X Klenow Buffer (0.5M Tris-HCl, 0.1M MgCl <sub>2</sub> )	2.5 $\mu$ L
H <sub>2</sub> O to a final volume of	25 $\mu$ L

*ix. DNA precipitation.*

DNA precipitation was done using the salt-ethanol method. 0.1 volume of 3M sodium acetate (S2889; Sigma) was added to the DNA sample, 2 volumes of 100% ethanol were then added and the sample incubated at 4 °C for 15 min to allow the precipitate to form. DNA was then pelleted by centrifugation at 10,000 g for 15 min.

After discarding the supernatant, DNA was washed in 70% ethanol and spun again for 5 min before solubilization in TE.

*x. Oligonucleotide annealing.*

When an adaptor or linker is needed, either to add a restriction site or to clone an exogenous sequence into a DNA clone, chemically synthesized oligonucleotides can be used. In this case each complementary oligonucleotide was resuspended in 100 $\mu$ L of sterile H<sub>2</sub>O at 4°C. An equimolar concentration of both oligos were mixed, heated at 95°C, allowed to slowly cool to room temperature and finally kept at -20°C until ready to use.

*xi. Ligation of DNA fragments.*

Bacteriophage T4 ligase was used to clone DNA fragments in to plasmids.

Ligation efficiency was determined by the ratio of vector to insert and the nature of templates for ligation.

Ligation reactions comprised as follows:

Vector	50-100ng
insert	50-150ng
10X ligase buffer	1 $\mu$ L
T4 ligase 1:4	1 $\mu$ L
H <sub>2</sub> O to a final volume of	10 $\mu$ L

*xii. Transformation of E.coli.*

5-25ng of ligated DNA was added to 50 $\mu$ L of competent cells, mixed gently and incubated on ice for 30 min. Cells were then subjected to heat-shock for 45 sec at 42°C, followed by quenching on ice for 2 min. 250 $\mu$ L of LB broth was added and cells incubated for 1 hr at 37°C for 1 hr. 50-150 $\mu$ L of the transformed cells was then spread onto LB-agar plates with the correspondent antibiotic. Plates were incubated at 37°C overnight.

*xiii. Design and synthesis of oligonucleotide primers for PCR.*

PCR primers were selected with a length between 21 to 27 bases, and with annealing temperatures in the range of 55 to 62°C, this temperature was determined by calculating the dissociation temperature as shown in (a) and the annealing temperature as in (b).

$$(a) \quad Td (\text{°C}) = 4(C+G) + 2(A+T).$$

$$(b) \quad \text{Annealing temperature} = Td - 5\text{°C}.$$

G-C content of primers was generally 50% and, when possible, oligonucleotides had G or C at the end.

*xiv. Polymerase chain reaction.*

Amplification of target DNA sequences during the screening of ES cells was performed using the Expand Long Kit from Roche, this kit consists of a Taq polymerase mixture that has been optimized to efficiently amplify long PCR products from genomic DNA. The PCR reaction mixture consisted of 100ng of template DNA, 10pmol of each primer, 1.5 units of Taq, 1X PCR buffer including the optimal concentration of MgCl<sub>2</sub> and each dNTP at 0.1mM.

Each reaction (50µL) was amplified following the specific conditions needed for each pair of primers (see table 2.1). The first stage of the reaction was an initial denaturation of the DNA template at 94°C for 2 min. following this, 35 cycles of amplification were performed in a thermocycler (PTC-100, MJResearch).

Each cycle consisted of three steps: 94°C for 30 sec: 30 sec at the appropriate temperature to allow the annealing of the primers to the DNA template: and 3 min at 72°C for the extension of DNA strands. At the end of the previous cycles a 10-minute extension step at 72°C was allowed for the final extension of the DNA strands.

A negative control containing no DNA template (NTC) was always included to monitor any exogenous DNA or cross-contamination during the reactions.

Other PCR reactions including amplifications from cDNA were performed using Taq and supplied buffers from Promega. Reaction volumes (25µL) included: 100ng of template, primers at 0.4µM each and dNTP at a final concentration of 0.1mM for each.

Number of cycles of amplification were 35 except 40 for Cre genotyping). Table 2.6 shows temperatures and extension times for each primer set and PCR reaction.

Reverse transcription from RNA was performed using the High Capacity Archive kit from ABI. 400ng previously quantified by spectrophotometry and each sample standard amounts verified by electrophoresis, were mixed in a 100 $\mu$ L reaction as follows:

2X Master mix for 50 $\mu$ L:

10X RT Buffer 10 $\mu$ L

25X dNTP mix 4 $\mu$ L

10X Random primers 10 $\mu$ L

Reverse transcriptase 5 $\mu$ L (25 Units)

RNA in DEPC-H<sub>2</sub>O to 50 $\mu$ L

Experiment	Primers	Product (Kb)	Extension Time (sec)	[MgCl <sub>2</sub> ] (mM)	Annealing Temp (°C)
ES cell screening	5'pF-Neo2R	7.3	7 min 20 sec	Unknown	60
ES cell screening	Neo2F-GR	2.1	20	Unknown	65
ES screening Genotyping	LoxF-LoxR	0.3 WT 0.34 Mutant	20	3	61
Internal probe	Neo1-Neo2	0.6	40	1.5	60
5' external probe	5'pF-5'R	0.72	45	1.5	59
Cre genotyping	Cre1-Cre2	0.45	45	1.6	65
Cre-mediated deletion	LoxF-PGKR	0.29	15	1.6	60.5
Cre-mediated deletion	E3EcoR1F E4NeoR	0.58 WT 0.63 Mutant	35	1.6	60.5
Cre-mediated deletion	LoxF-E4NeoR	0.36	20	1.6	59
CTLA-4 RT-PCR	E1F-E4R	0.73, 0.65 0.42, 0.3	45	1.5	63
HPRT RT-PCR	HPRTF-HPRTR	0.65	30	1.5	60

Table 2.6 Conditions for the PCR performed.

*xv. Southern Blot, hybridization, removal of radio-labeled probes and autoradiography.*

Southern Blot is a technique used to detect sequences of interest from a restriction genomic DNA digest.

In this case ES cell genomic DNA was digested as previously mentioned and then separated by electrophoresis in a 0.8% agarose gel at 50V overnight. The gel was further treated 10 min with depurination buffer to hydrolyse DNA and facilitate transfer of large (>10Kb) fragments, followed by a 30 min incubation in denaturation buffer and a final 30 min incubation in neutralizing buffer.

The denaturalized product of the separation was transferred for at least 18h by capillary action on to a solid support membrane (Hybond N+ RPN203B, GE Healthcare) using 20X SSC.

Membranes were then rinsed with SSC 20X, pre-hybridized at 50°C, for at least 30min. DNA fragments longer than 500bp were radio-labeled by random prime labeling using the T4 DNA polymerase known as Klenow fragment. A 25ng sample of probe was made up to 21µL in molecular biology grade water and denatured at 95°C for 5 min. Finally, the probe was quenched on ice and a labeling reaction set up as follows:

Denatured DNA	21µL
5X Rad-prime buffer	20µL
5U Klenow Fragment	1µL
[α- <sup>32</sup> P] dCTP	5µL
0.5mM of each dATP, dGTP and dTTP	3µL

The 50µL reaction was incubated at 37°C for 1h and the unincorporated nucleotides were removed by fractionation through a TE pre-equilibrated S200 HR MicroSpin column. Each column was resuspended by vortexing and placed in a microfuge tube. The column was spun at 4000g for 30 sec to eliminate the storage buffer and the labeling reaction applied to the centre of the column. After spinning at 4000g for 30 sec the labeled product was collected in a tube and added to the pre-hybridization buffer before an overnight incubation at the same temperature as the pre-hybridization step.



Membranes were initially washed with a large volume of 3X SSC to eliminate traces of unbound probe followed by sequential washes of increasing stringency to minimize non-specific binding of the probe. Generally, membranes were washed once with 3X SSC, 0.1% SDS, 15 min in 1X SSC, 0.1% SDS and finally for 15 min in 0.1X SSC, 0.1% SDS. All washes were performed at 65°C.

To perform the autoradiography, the membranes were covered in cling-film and exposed to an Biomax X-ray film (8326886; Kodak). Exposure time varied according to signal intensity from 1-4 days.

The removal of hybridized probes from membranes was done by washing the membrane in 0.4M NaOH at 45°C for 30 min followed by a second 15 min wash in 0.1X SSC, 0.1% SDS, 0.2M Tris-HCl pH7.5 at 45°C.

### **2.2.3 Techniques for protein analysis.**

#### *i. SDS-PAGE.*

A 12% acrylamide resolving gel solution were poured into plastic cassettes (NC2010:Invitrogen) and allowed to set covered with a volume of 100% 2-propanol (10062, BDH). The alcohol was then eliminated and a solution of 5% acrylamide was poured on top of the resolving gel to act as stacking gel and to form the required lanes. Samples were mixed 1:1 with reducing loading buffer, boiled for 2 min and then loaded into the gel. Samples were run into the stacking gel for 20 min at 60V and then resolved at 120V until the dye front migrated out after approximately 90min, using a mini tank (X-cell, Invitrogen). The gel was then processed for electrotransfer.

#### *ii. Western blotting.*

After electrophoresis the gel is processed for electrotransfer. The stacking gel and lanes are cut away and the remaining portion of gel superimposed on a sheet of PVDF (Hybond P RPN303F, GE Healthcare) membrane. Both the gel and membrane, without any bubbles in between, are covered with two foam sheets and placed in the corresponding

plastic frames inside the electroblotting apparatus (Mini-protean; Biorad). The correct polarity was always observed.

Transfer was performed at 40 milli Amperes overnight in Towbin buffer and the gel stained with Comassie to evaluate transfer.

Membranes after transfer were stained with the reversible dye Ponceau red (c0644, Sigma) and after a quick wash with PBS the blot was treated with blocking solution at RT for 1 hr. After that period, blots were incubated with the primary antibodies (in blocking buffer). After the primary antibody incubation blots were washed 3 times for 15 min with washing solution, treated with the appropriate secondary reagents for 1 to 2 hrs, washed again and taken for chemio-luminescence detection following manufacturers indications.

Exposure to photosensible film (03E220, Fuji) was performed at varying exposure times and developed in an automated developing system (Curix, Agfa).

### **2.2.3 Tissue culture.**

#### *i. Preparing single cell suspensions from peripheral, thymus, lymph nodes and spleen.*

Thymy, inguinal, popliteal, brachial, mesenteric and cervical lymph nodes were harvested immediately after the sacrifice of the animal. Single cell suspensions were prepared by gentle maceration through a 70 $\mu$ m nylon strainer (F-2350, BD) into complete RPMI media. Cells were recovered by centrifugation at 530 g for 10 min and resuspended in 10ml of RPMI. Cell suspensions from spleen were prepared as before but processed for erythrocyte lysis. After centrifugation, cells were resuspended in 5ml of lysis buffer and incubated for 2 min at 4°C. After this step cells were washed once with complete RPMI, centrifuged at 530 g for 10 min and resuspended in the same media.

#### *ii. Viable cell count.*

The number of viable cells in a suspension was determined by uptake of trypan blue. 10 $\mu$ L of cells suspension was treated with an equal number of dye and half of this

volume counted in a haemocytometer. Two diagonally opposite sectors were fully counted and cell number determined as shown in (c).

(c) Cells/ml = total number of trypan negative cells x 10,000 x dilution factor

*iii. Isolation of CD3 cells by paramagnetic beads.*

Negative selection was used to isolate intact CD3<sup>+</sup> T cell populations for use in tissue culture. Selection was done with beads coated with antibodies specific for mouse (110.02, Dynal) or rat (110.07, Dynal) IgG isotypes.

Each type of beads were used individually in sequential steps to eliminate first; cells expressing surface IgG (B cells) and then in combination with other (home made) antibodies such as a rat anti MHC-II, to eliminate cells expressing those markers (DC).

Cells in media were spun at 530 g and resuspended in 3ml RPMI supplemented with 10% FCS. 150µL of anti mouse beads were added and cells incubated at 4 °C for 15 min in a rotating wheel (SB1, Stuart Scientific). After this step unwanted cells, bound to beads, were eliminated by collection inside a strong magnet (MPC-1, Dynal).

The supernatant from this step was then treated with 1ml of rat anti MHC-II, (clone M5114) for 15 min at 4 °C. Later cell pellets were recovered by centrifugation, resuspended in 3ml of RPMI-FCS and further treated with 75µL of anti mouse IgG beads and 75µL anti rat IgG beads. After a third incubation, unwanted subpopulations (extra IgG expressing cells or MHC-II expressing cells) were removed by collection of supernatants under the magnetic field. CD3<sup>+</sup> T cells, up to 98.5% purity, were recovered by a final centrifugation step counted and analyzed phenotypically by flow cytometry.

*iv Total lymph node or primary T cells cultures.*

96 or 24 well plates (Falcon, BD) were pretreated with either 100µL/well or 500 µL/well respectively of 1µg/ml anti mouse CD3 antibody in sterile PBS overnight at 4 °C. The day of experiment the PBS was aspirated and wells washed once with PBS. After either cell preparations from lymph nodes or negative selection, cells were diluted to numbers of 2x10<sup>5</sup> cells in 100µL to be added to 96 well plates or 3x10<sup>6</sup> cells per

---

500 $\mu$ L for cultures on 24 well plates. When necessary (i.e. on cultures of isolated T cells) an aliquot of anti mouse CD28 soluble antibody was added to a final concentration of 1 $\mu$ g/ml in media.

*v. Measuring cell proliferation by radioactive thymidine uptake.*

Tritiated thymidine was diluted in complete media and stored at 4 °C. Assays in 96 well plate format were pulsed with 1 $\mu$ Ci/well in 20 $\mu$ L, for the final 8 to 12 hr of culture. After that time plates were either frozen or cells lysed on to a glass fiber matt, using a harvester (Mach III: Tomtec). The amount of incorporated thymidine was measured using a liquid scintillation counter (1450 Microbeta, Wallace).

## **2.2.4 Flow cytometry.**

*i. Surface stain.*

2x10<sup>5</sup> cells were harvested, washed twice with PBS and placed in 96 “V” bottom plates to perform the antibody staining. 50 $\mu$ L of blocking solution was added to each cell sample and incubated on ice for 15 min. Another aliquot of 50 $\mu$ L of blocking solution, including the proper amount of each antibody (see materials) was added and incubated on ice for 15 min. Finally each cell sample was washed twice with washing buffer spun at 650 g, transferred to FACS tubes and acquired using a FACS Calibur™ cytometer (Beckton Dickinson).

*ii. Intracellular stain.*

4x10<sup>5</sup> cells were processed for surface stain as mentioned before. After staining, the cells are fixed with 50 $\mu$ L to 100 $\mu$ L of a 1:20 dilution of fixative (CellFix, BD) for 20 min at RT. Subsequently, each well was filled with washing buffer to remove the fixative by centrifugation. The cells are then permeabilized for 20 min with 100 $\mu$ L of a commercial solution of saponin (Cytoperm, BD), cells washed and spun before adding the staining antibody diluted in fresh permeabilization solution. The stain proceeded

for not less than 35 min. Before transfer to tubes for acquisition, cells are washed once again with washing buffer.

*iii. Acquisition and analysis.*

Acquisition (a minimum of 30,000 events collected) and analysis was done using the software Cell Quest™ from Beckton Dickinson.

## **2.2.5 Experimental animals and animal husbandry**

*i. Experimental animals*

C57BL/6, 129SVPAS and mice with a mixture of both backgrounds were initially generated at GenOway (Lyon, France) and kept at Charles River animal facilities.

Animals sent to our laboratory were housed in specific pathogen free facilities at the Central Biomedical Services, Imperial College London.

Breeding tail biopsy collection and ear marking was performed under the standard regulations and as determined in a personal and project Home Office license.

Two Cre expressing transgenic strains of mice were employed in this project:

The first strain, named  $\beta$ -70 expresses Cre in a Tamoxifen-dependent, inducible fashion, was kindly provided by Dr Laurence Bugeon from Imperial College. This strain expresses the estrogen receptor fused with Cre under the control of the ubiquitous Chicken  $\beta$ -actin promoter.

The second strain is a Cre transgenic that expresses the recombinase under the control of the early acting PGK-1 promoter (Lallemand. Y., *et al* 2004). This strain was kindly provided by Dr Tanya Tomachova at the Seabra Laboratory, Imperial College London.

Both strains were on the C57BL/6 background.

All animals used in experiments were of 16 weeks of age or older.

---

*ii. Tamoxifen inductions.*

Adult male and females were treated with tamoxifen either orally or by intraperitoneal injection following these schemes: 2mg of tamoxifen administered daily for 4 days, a single injection of 1 mg or 2 mg, or a single oral administration of 5mg.

**2.2.6 Histological analysis.**

Histological sections were obtained and haematoxylin-eosin stains performed by the Histology Laboratory, Section of Leukocyte Biology Imperial College London.

Slides were visualized and digital photography taken in an optical microscope coupled to an imaging system (Olympus).

**2.2.7 Statistical analysis.**

The data corresponding to the phenotypic characterization of mice bearing a targeted *Ctla-4* allele was collected from independent experiments with groups of 1 individual per genotype in each experiment. Results were tested for normality using the Kolmogorov-Smirnov goodness of fit test and if considered normal, the mean of multiple replicas of the experiments was compared between groups. When differences were observed, they were statistically analyzed by a one-way ANOVA with Bonferoni multiple comparison post test. If the goodness of fit test could not be applied to the data (when only few replicas were available), the data was analyzed by a non parametric Kruskal-Wallis test with a Dunnett's post test comparison. Other data is only reported representative of several replicas. These analyses were done using the Instat<sup>TM</sup> software (GraphPad).

***Chapter 3. Generation of mice bearing a targeted Ctla-4 allele.***

### 3.1 Background.

In chapter one we discussed the experiments and evidences that led to the development of the methodologies of gene targeting and conditional gene targeting in mice. It is however, important to briefly recapitulate the main aspects of this techniques before describing the results concerning the generation of mice bearing a targeted *Ctla-4* allele.

A gene targeting experiment starts by the construction of a targeting vector that comprises a modified mouse genomic sequence, designed to recombine with and mutate a specific genomic locus in pluripotent ES cells. Subsequently the ES cells that have been transfected with the construct are screened to detect events of homologous recombination and once a clone of ES cells is identified, chimeric animals are then generated from those targeted ES cells by blastocyst injection. Finally the transmission of the characterized mutation through the germline is assessed by crossing the chimeric animals and screening for targeting among the offspring of that cross.

The vectors used in gene targeting have the following basic elements: a bacterial plasmid backbone, a sequence homologous to the target gene of interest and a selectable marker such as a neomycin resistance cassette. There are two types of targeting vectors: replacement and insertion vectors and both yield different recombination products. A description of the characteristics of both vectors can be found in chapter 1.

The type of construct we used to generate the CTLA-4 targeted mice is a replacement construct. This type of vectors are commonly used to generate mice harboring null mutations in a desired locus or *knock outs*, this is done by introducing the selectable cassette into the sequence of an exon critical for the function of he corresponding polypeptide. Nonetheless “non disruptive” locus-specific modifications for instance; insertion of selectable markers or recombination sites (FRT & *loxP*) into non coding regions, can also be achieved using replacement constructs. In this case we have designed a replacement vector to introduce, into non-coding regions of the *Ctla-4* allele two main elements. First a neomycin resistance cassette, essential to select ES cells that have integrated the targeting construct and second, the sequence of 3 *loxP* sites which will allow us to modify and later conditionally eliminate, by Cre-mediated recombination,



segments of the coding and non-coding sequences of this gene as well as the selection marker. The purpose of this last genetic modification is not only to eliminate the sequence of the neo cassette, which if retained, can result in a hypomorphic allele and a possible alteration in the levels of expression of *Ctla-4* or other important neighbour genes (i.e. *Icos* or *Cd28*). More importantly this vector design will allow us to achieve the ultimate goal of producing an animal having both a deleted allele and the second allele with two *loxP* sites flanking exons 2 and 3, which are critical for the activity of CTLA-4. Mice having these modifications at the the *Ctla-4* locus can subsequently be crossed with transgenic animals that express Cre in an inducible fashion (under the control of a inducible promoter, such as the interferon dependent Mx-1 (Kuhn., *et al* 1995) to gain temporal control of the *Ctla-4* disruption.

In summary this chapter describes: the construction of a CTLA-4 targeting vector by molecular cloning, the transfection and screening of targeted ES cells, the production of chimeric mice and finally, the generation of mice heterozygous for a targeted *Ctla-4* allele. These mice were produced with the ultimate aim of generating a model for conditional inactivation of this key negative regulator of T cell immunity.

### 3.2. General characteristics and construction strategy of the targeting vector.

The homology of a targeting construct with its target sequence is pivotal to achieve effective pairing and crossover with the homologous target gene sequence. Our construct was designed to share a total homology with the wild type mouse CTLA-4 locus of 6.8 Kb (4.1 Kb on the 5' arm of homology and 2.7Kb on 3' arm of homology). These figures are much higher than the values observed to be required to obtain an acceptable frequency of recombination, from 500bp-2Kb, (Moens., *et al* 1992). The total length of construct excluding the plasmid backbone is 8.65 Kb.

Figure 3.1 shows a diagram of the targeting construct, compared with wild type *Ctla-4* allele, and the regions of homology shared by both arms are described with respect to the location where events of crossover can happen. The insertion of the construct into the *Ctla-4* allele will depend on two reciprocal crossover events. The regions of homology of the construct are represented in figure 3.1.

The main elements of this targeting vector are a *loxP* site downstream of exon 1 and a neomycin resistance gene flanked by two *loxP* sites downstream exon 3. The location of these elements, in relation to the coding sequences of the gene, is important to achieve our ultimate purpose. We are interested in generating animals bearing an allele where exons 2 and 3 are flanked by *loxP* sites as well as animals having a null allele for experimental work (see figure 3.2, C and D). Mice having such genotypes will be subsequently generated from animals heterozygous for the targeted allele, by Cre recombination in the germ-line, using an inducible Cre transgenic mouse line already developed in the lab. It is of interest to generate and analyze mice bearing a targeted allele (as in figure 3.2B) as these mice may develop a hypomorphic allele and a possible phenotype of interest.

To make the construct, the *Ctla-4* genomic sequence was obtained from a 129/Sv genomic DNA library. This library had previously been screened in the lab by Dr Laurence Bugeon.

The sequence was isolated and subcloned into four plasmids with pBluescript II KS+ backbone and kindly provided for the construction of the targeting vector as well by Dr Bugeon. Two clones comprising a genomic sequence of 8.3Kb in total length, were selected to proceed with the cloning strategy and a characterization by restriction digest is shown in figure 3.3. A diagram of the overall strategy to generate the targeting construct is shown in figure 3.4 and the cloning process is describe to detail in the next two sections.

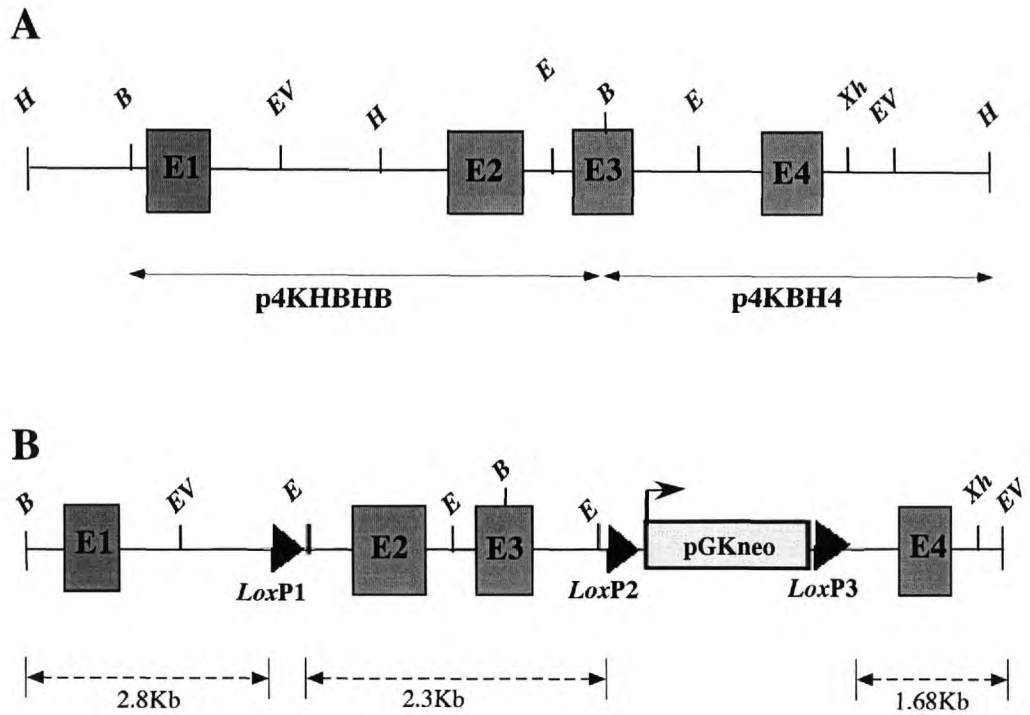


Figure 3.1 Diagram of the targeting construct compared with wild type *Ctla-4* allele. In A, the figure shows a representation of the wild type *Ctla-4* genomic region, homologous to the targeting vector. In B, the figure illustrates a diagram of the construct; solid arrows indicate the sequence of the plasmids employed to make the targeting vector, dashed arrows indicate the segments and size of the sequence of the construct homologous to *Ctla-4*. Restriction sites indicated as; H: *Hind*III, B: *Bam*HI, E: *Eco*R1, EV: *Eco*RV, Xh: *Xho*I.

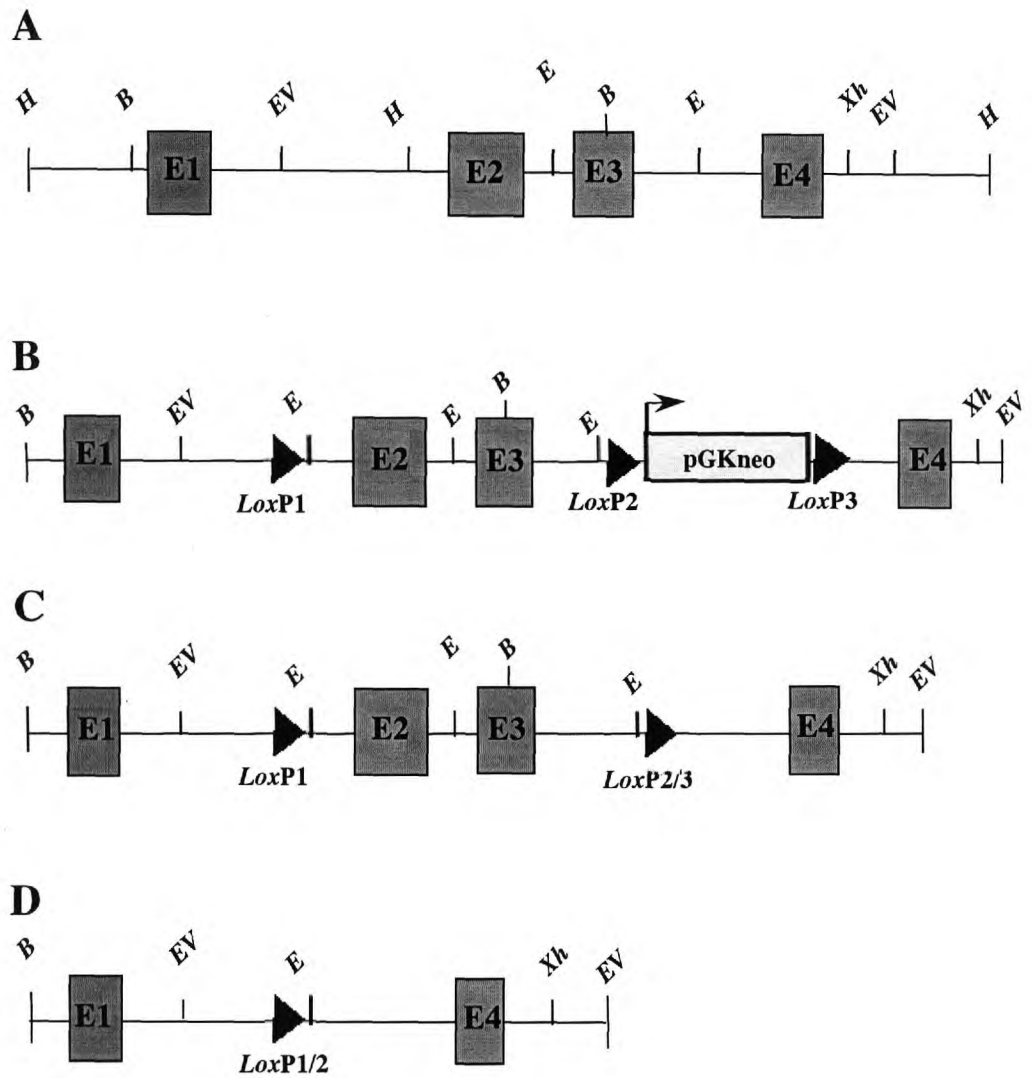


Figure 3.2.- Restriction map of the 129Sv *Ctla-4* genomic region compared with the targeting vector and the modified alleles after Cre-mediated recombination. The figure illustrates in A, the 129Sv *Ctla-4* genomic region. in B, the targeting vector. C and D show two different modified alleles of interest, obtained after Cre-mediated recombination. Restriction sites indicated as; H: *HindIII*, B: *BamHI*, E: *EcoRI*, EV: *EcoRV*, Xh: *XhoI*.

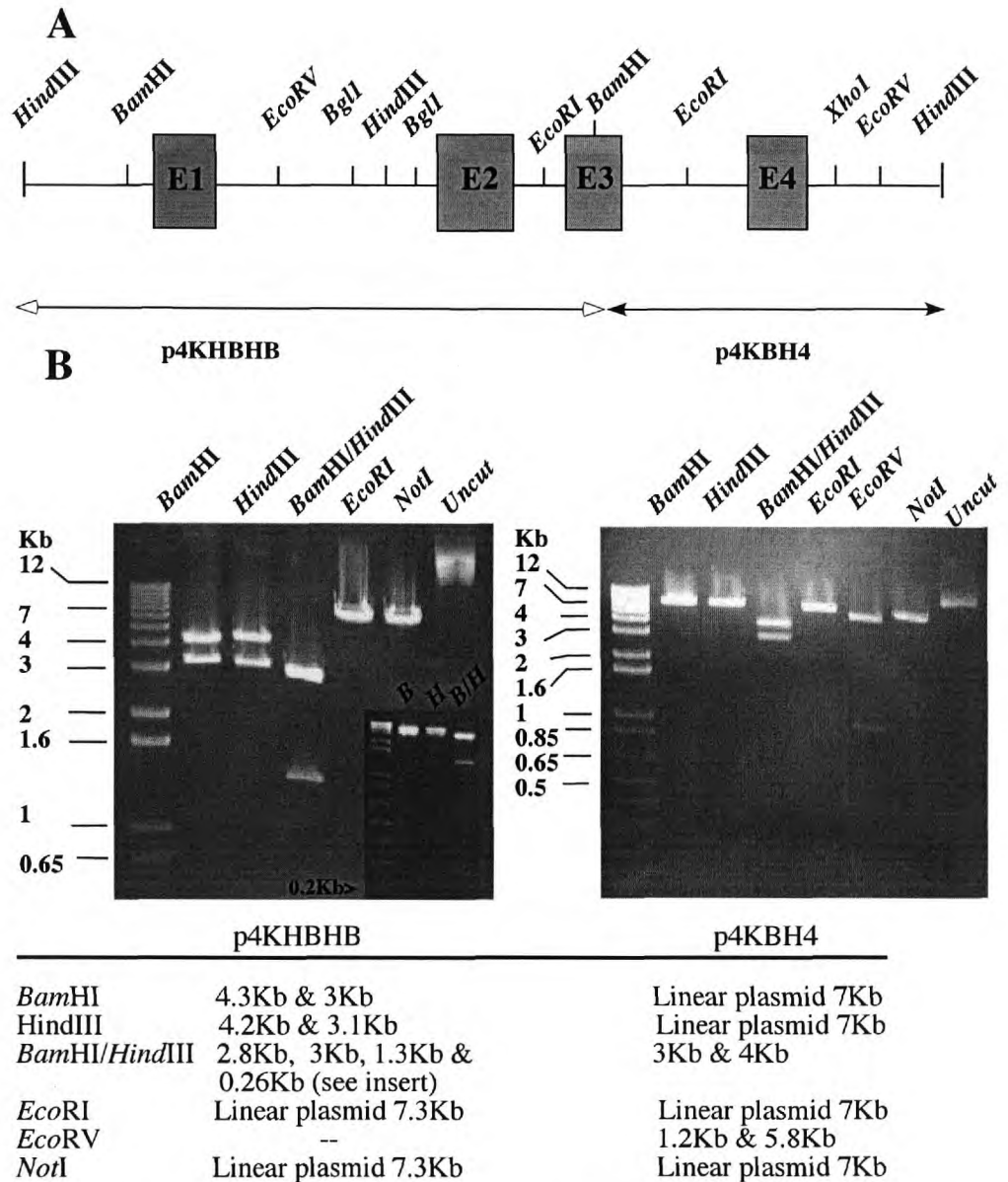


Figure 3.3.- Restriction digest of the plasmids, p4KHBHB and p4KBH4 containing the 129Sv CTLA-4 genomic sequence used for the construction of the targeting vector. A, diagrammatic representation of the CTLA-4 region isolated from a mouse 129Sv DNA library and subcloned into pBluescript II KS+. B, 5 $\mu$ g of maxiprep DNA was digested with *Bam*HI, *Hind*III, *Eco*RI, *Eco*RV, *Not*I and subjected to an agarose gel electrophoresis (1% agarose). Inserted picture shows the 0.26Kb fragment on p4KHBHB visible earlier in the electrophoresis. Uncut plasmids (last lanes) are show. C, Predicted sizes of restriction fragments were obtained from the sequence published (NCBI Ac#AF142145).

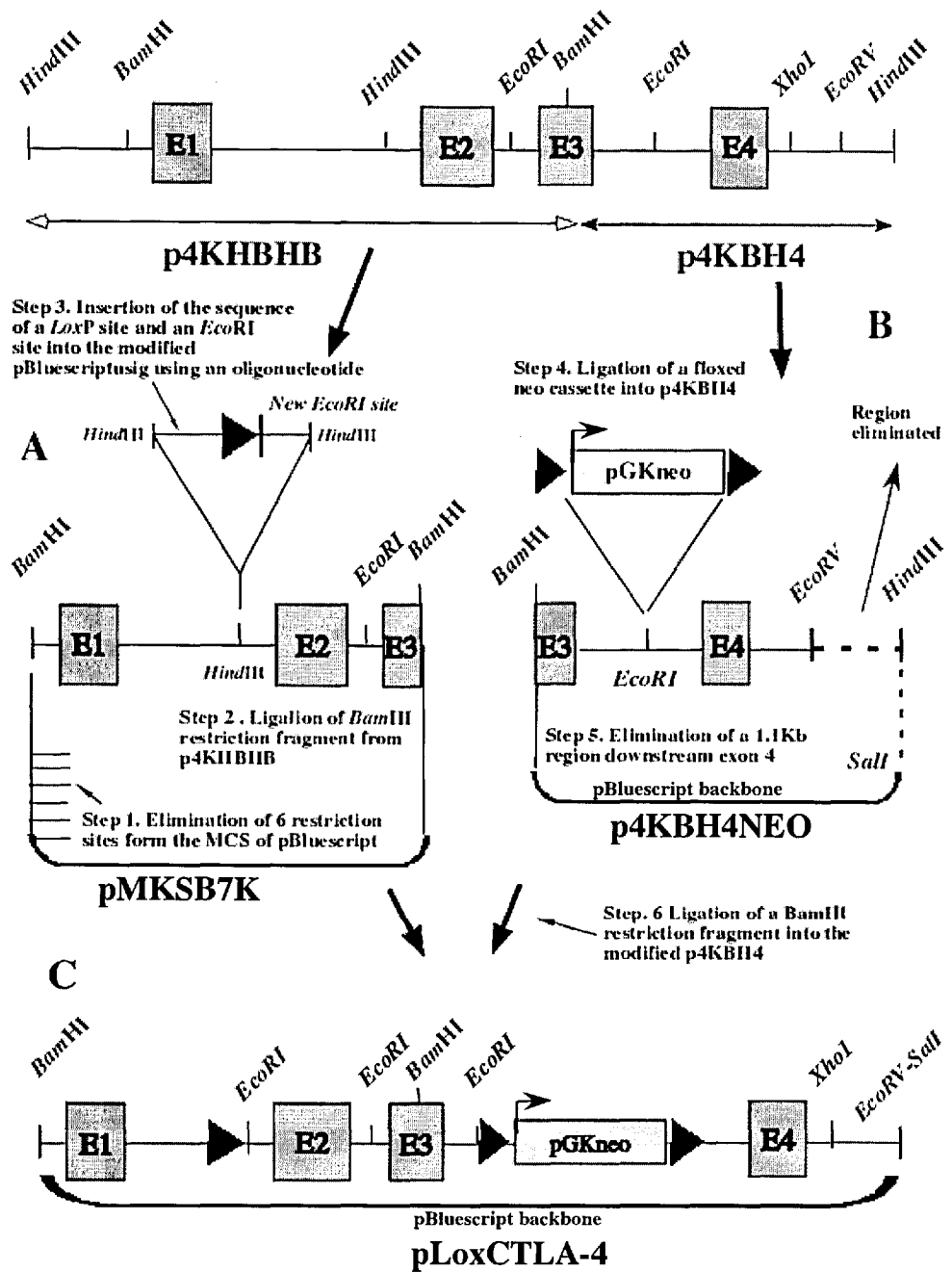


Figure 3.4.- Cloning strategy for the construction of the *Ctla-4* targeting vector. A fragment of 8.36Kb, corresponding to the 129Sv mouse genomic sequence of *Ctla-4*, was sub-cloned into 2 different plasmids and used to generate an 8.65 Kb targeting construct. A, construction of pMKSB7K. B, generation of p4BH4NEO. C, final targeting vector. The cloning methodology is indicated for each step.

### 3.3 Molecular cloning of pMKS7K.

Initially, an aliquot of pBluescript without insert was modified by excising the sequence of 6 restriction enzyme sites from the multiple cloning site (MCS). The rationale of this modification was to avoid the presence the *EcoRI* and *HindIII* restriction sites, as they will interfere with the subsequent cloning steps.

Approximately 10 µg of pBluescript were simultaneously digested with *SmaI* and *HincII*, after digestion, the sample was purified and then ligated, taking advantage of the two blunt ends produced by the two restriction enzymes used.

The next step in the strategy, was to ligate a 4.14 Kb *BamHI* fragment from the CTLA-4 genomic clone (p4KHBHB) to the modified pBluescript. This fragment was isolated by digesting approximately 10 µg of p4KHBHB with *BamHI* and purifying the fragment from an agarose gel. The fragment was then ligated into the modified pBluescript which was previously dephosphorylated. Figure 3.5 shows a restriction digest characterization performed on miniprep DNA from antibiotic resistant *E. coli*. This cloning step was not directional and it was possible then to obtain plasmids with the insert in any orientation, The restriction digest performed shows that the insert in the selected clone was in the 3' to 5' orientation (see section C on figure 3.5). This was considered not a problem because after completing all the modifications planned, the insert will be excised again and ligated to complete the targeting vector. This resulting clone, designated pMKS7K, includes introns 1,2 and 3 as well as exons 1, 2 and half the sequence of exon 3. It represents approximately half of the region of homology of our targeting vector.

pMKS7K was then modified by inserting, on its unique *HindIII* site, a 44 bp synthetic oligonucleotide. The sequence of this double stranded oligo included the first *loxP* site as well as a new *EcoRI* site introduced to change the size of the restriction fragments when the construct undergoes HR and the targeted allele is digested with this enzyme.



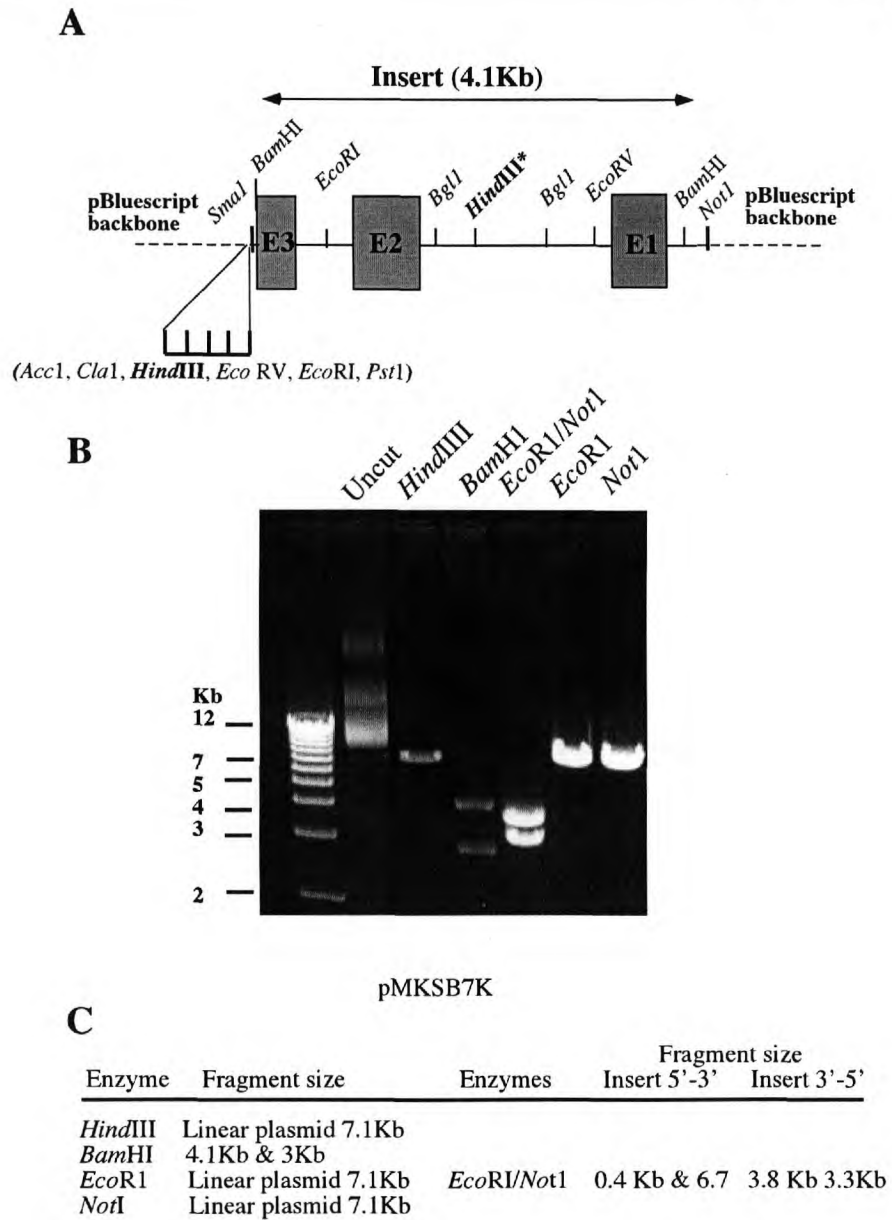


Figure 3.5.- Characterization by restriction digest of clone pMKS7K. The figure illustrates in A, a diagram showing the ligation of a 4.1Kb fragment into pBluescript. This vector was previously modified to eliminate six restriction sites in the MCS (sites in brackets). B, DNA from one representative clone was digested with *HindIII*, *BamHI*, *EcoRI*, *NotI* and *EcoRI-NotI* and fragments resolved by a 1.5% agarose gel electrophoresis in order to assess the orientation of the insert after ligation. C, Expected restriction fragment sizes if the insert ligated in either of the two possible orientations.

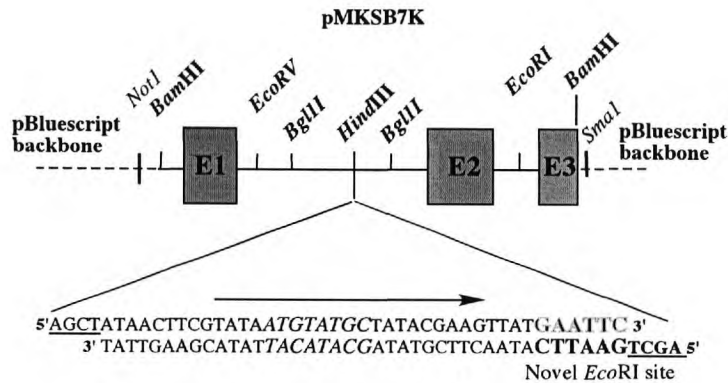
In addition, the oligo had a base pair change in each one of its ends to change the sequence of the *HindIII* site upon ligation. This modification will avoid the regeneration of site, and therefore altering the pattern of restriction fragments produced after *HindIII* digest of genomic DNA from putative targeted ES cells. These alterations will be essential for the Southern blot strategy to confirm the HR of our construct in the *Ctla-4* genomic locus.

pMKS7K was digested with *HindIII*, and the linear DNA purified by ethanol precipitation and 50ng of the annealed oligonucleotide containing the loxP site sequence was ligated to pMKS7K. Before transformation, the ligation product was digested with *HindIII* to diminish the uptake of non recombinant pMKS7K by bacteria. This was possible since the insertion of such oligo will not recreate the previous *HindIII* site and only religated vector will be digested. This step proved crucial for this cloning procedure as commercial oligonucleotides lack phosphate groups and dephosphorylation of the recipient vector would have been detrimental for the efficiency of ligation.

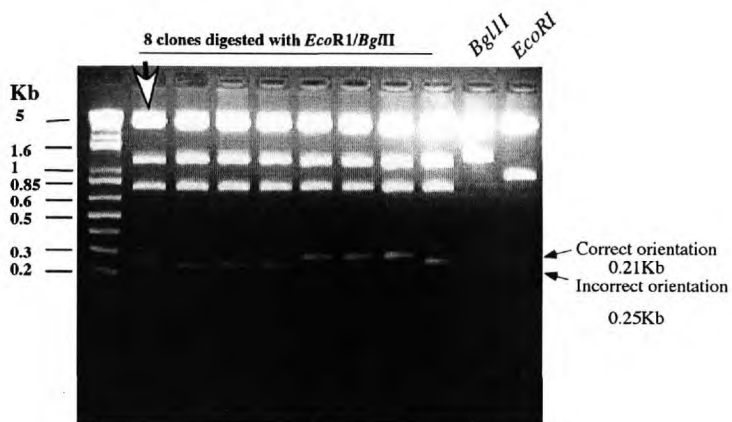
The orientation of the inserted oligo containing the loxP sequence, was tested by simultaneously digesting the positive clones isolated with *EcoRI* and *BglII*. According to the sequence of the oligo and the genomic CTLA-4 sequence published (NCBI Ac#AF142145), this digest would generate fragments of various sizes but the presence of a 0.21 Kb fragment rather than one of 0.25 Kb will discriminate between clones having the insert in a correct 5' to 3' orientation, irrespective of the orientation of the 4.1Kb insert of pMKS7K (figure 3.6).

4 clones were found to have the correct orientation and one was selected for further molecular cloning. The presence of a complete loxP sequence as well as its orientation was confirmed by sequencing (data not shown).

A



B



C

Enzymes	LoxP site insertion into pMKSb7K	
	LoxP 5'-3'	LoxP 3'-5'
<i>EcoRI</i> / <i>BglIII</i>	0.75 Kb	0.75 Kb
	1.21 Kb	1.17Kb
	0.21 Kb	0.25 Kb
	4.82 Kb	4.82 Kb
<i>EcoRI</i>	0.96 Kb & 6.2 Kb	
<i>BglIII</i>	1.42 Kb & 5.78 Kb	

Figure 3.6.- The insertion of the first *LoxP* into pMKSb7K using a synthetic oligonucleotide. A, shows diagram of pMKSb7K and the sequence of the *LoxP* site (the orientation of the site is represented by an arrow). The sequence in bold correspond to the novel *EcoRI* site inserted, underlined are the modified *HindIII* overhangs and in larger fonts, the Cre recombinase core of the *LoxP* site. In B, 8 different clones collected were digested with *EcoRI* and *BglIII* to assess the orientation of the *LoxP* site with respect to the *Ctla-4* genomic sequence, single digests were also performed on DNA from one clone to control for the activity of the enzymes (shown to the left). Restriction fragments were separated by agarose gel electrophoresis (2% agarose). The clone marked was used for further molecular cloning and arrows to the right show the representative bands indicating the correct or incorrect orientation of the double stranded oligo in pMKSb7K. C, The table shows the expected restriction fragment sizes according to the orientation of the oligo in pMKSb7K.

### 3.4 Generation of p4KBH4NEO.

One of the most important steps towards the construction of this plasmid was the introduction of the sequence of a PGK-driven Neomycin resistance gene flanked by two *LoxP* sites into the *EcoRI* site downstream exon 3 of the CTLA-4 genomic clone p4KBH4. This neo cassette will confer neomycin resistance to any ES cell that integrates our targeting construct, therefore allowing us to select them using the neomycin analog, G418. Additionally, the presence of two *LoxP* sites flanking this gene will allow its excision by Cre-mediated recombination. The fact that this type of recombination leaves a single *LoxP* site behind, will allow the generation of an allele bearing exons 2 and 3 flanked by *LoxP* sites (see figure 3.2 C).

The floxed neo cassette was kindly provided by Dr Yuri Mishina, NIH, USA already cloned into pBluescript. Digesting the plasmid with *BamHI* and *EcoRI* to excise the cassette was the strategy of choice, but this produced two incompatible ends making it impossible to directly clone it into the *EcoRI* site of p4KBH4. To overcome this problem, p4KBH4 was modified by adding a dsDNA adaptor (*EcoRI**BglII*). This adaptor included on its 5' end an *EcoRI* site and on its 3' end an additional *BglII* site. *BglII* produces compatible ends with *BamHI* but the resulting restriction site, after cloning, is incompatible with *BamHI*. This was necessary as introducing a new *BamHI* site would have been inconvenient when this part of the construct is ready for subsequent ligation to pMKS7K. The 3' *EcoRI* overhang of the adaptor has a nucleotide modification which upon ligation, will avoid the recreation of a novel 3' *EcoRI* site in this region (see figure 3.7).

p4KBH4 was digested with *EcoRI* and dephosphorylated with CIAP. Approximately 50ng of double stranded adaptor (*EcoRI**BglII*) was ligated into the plasmid (figure 3.7). The modification of p4KBH4 with *EcoRI**BglII* allowed, the insertion of an *EcoRI*-*BamHI* digestion fragment containing the floxed neo cassette.

The fragment containing the neo cassette was excised from pBluescript and isolated from an agarose gel. Modified p4KBH4 was digested with *EcoRI* and *BglII*, the linear plasmid purified by the GeneClean method and both DNA segments ligated. The ligation mix was used to transform *E. coli*. A *BamHI*/*EcoRI* screening of miniprep DNA samples coming from antibiotic resistant bacteria showed a high frequency of insertion of

the neocassette confirming the efficiency of the adaptor strategy (data not shown). The selected plasmid, designated p4KBH4NEO, was characterized by restriction digest as shown in figure 3.8. The fragments obtained after simultaneous digestion with *Bam*H1+*Eco*R1 and *Eco*R1+*Hind*III, yielded fragments with the expected sizes (see figure 3.8 C) in accordance with the sequence published (NCBI Ac#AF142145). Single *Eco*R1, *Hind*III and *Bam*H1 digest were also included as controls and to assess the possibility of insertion of novel restriction sites within the sequence of the neo cassette. This situation could have altered the Southern blot ES cell screening strategy. The integrity of both exons as well as the orientation of both *loxP* sites in this intermediate construct were assessed by sequencing and found to be as expected (data not shown).

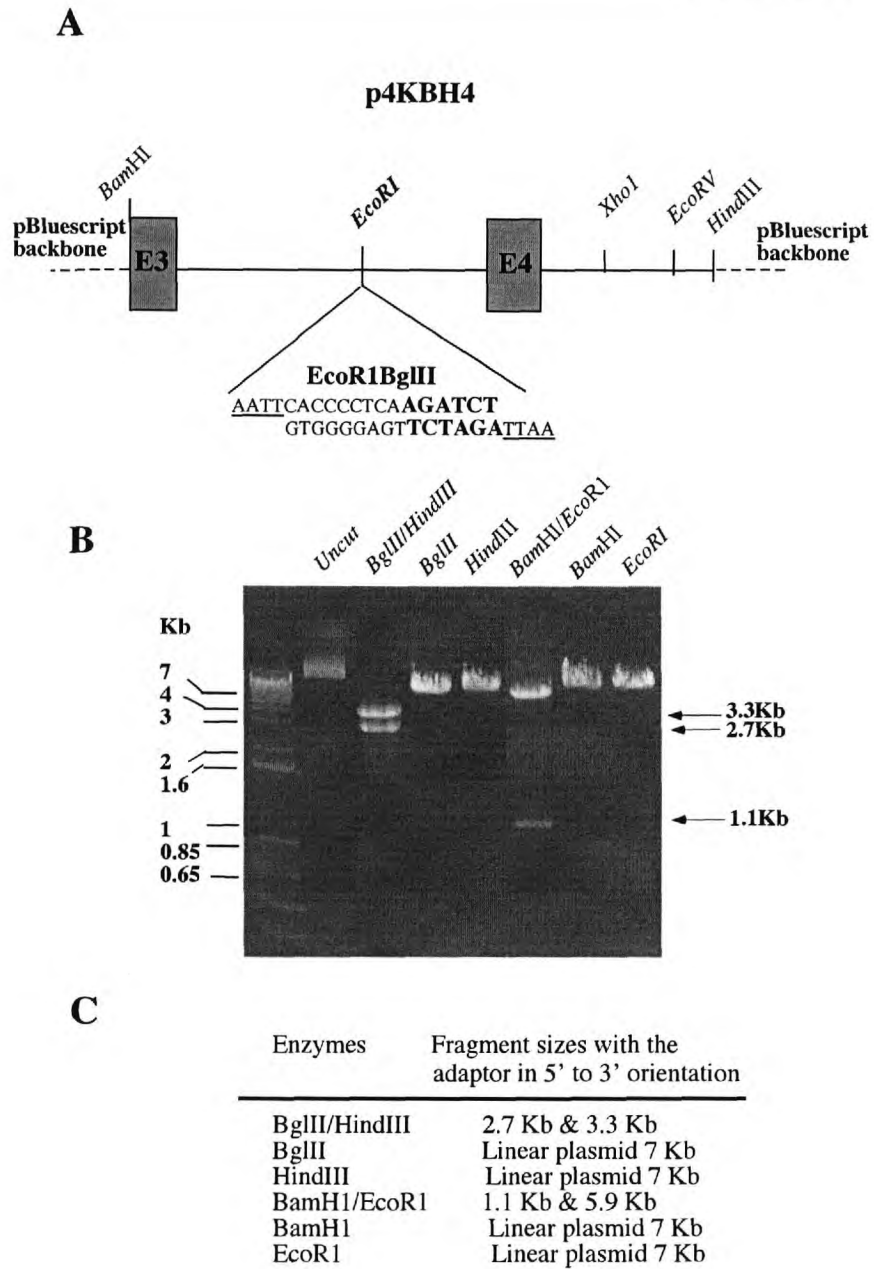


Figure 3.7.- Ligation of an adaptor (*EcoRI**Bgl*III) to p4KBH4. In A, the figure shows a diagram of p4KBH4 and the sequence of (*EcoRI**Bgl*III). A novel *Bgl*III site (shown in larger fonts) was inserted in the sequence of (*EcoRI**Bgl*III). B, double and single digests were performed with *Bgl*III, *Hind*III and *Bam*HI, *Eco*R1 on DNA from a representative clone and the corresponding restriction fragments (C) separated in a 1% agarose gel electrophoresis. Arrows on the right show the sizes of restriction fragments that confirm the orientation of the insert

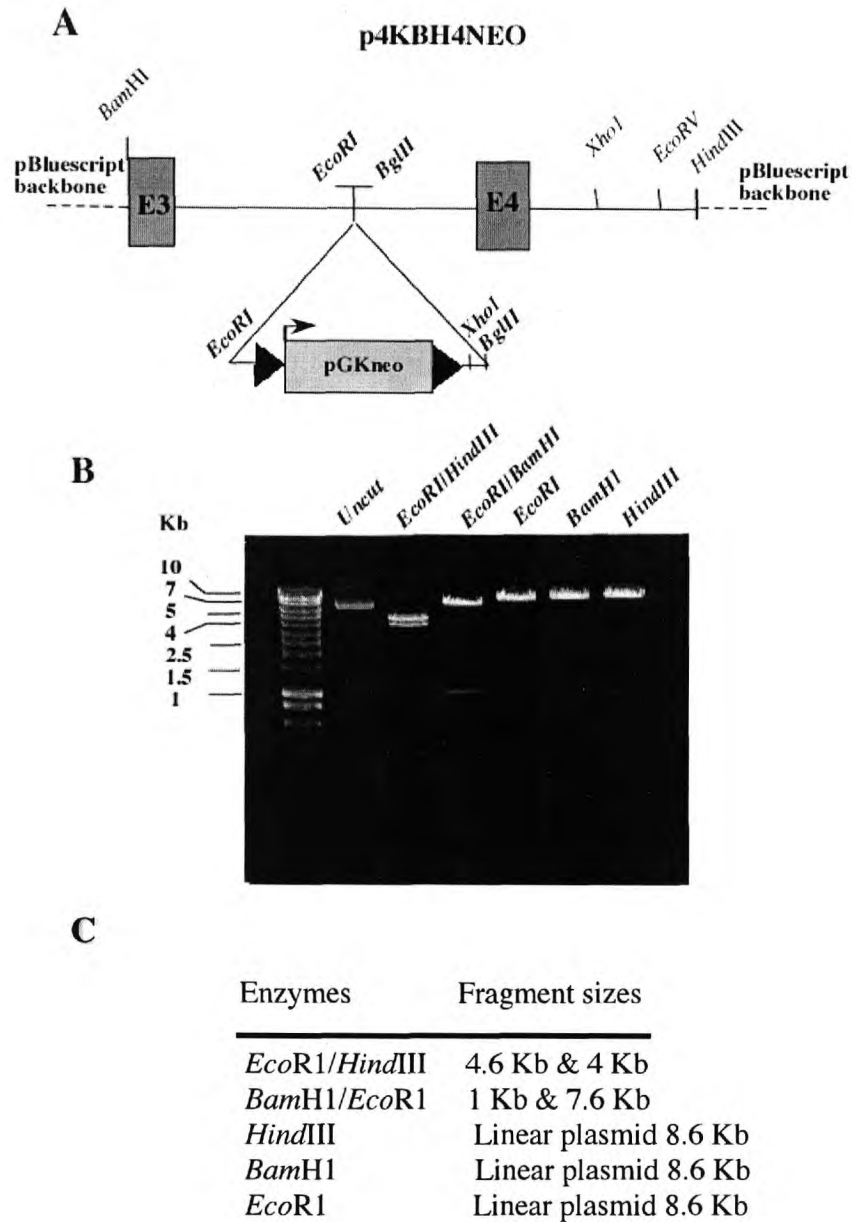


Figure 3.8.- Insertion of the floxed PGKneo cassette into the modified p4KBH4. Schematically described in A, an aliquot of the plasmid containing the PGK neo cassette was digested with *EcoR1* and *BglII* and the corresponding fragment ligated to p4KBH4 containing the adaptor (*EcoR1BglII*). In B, a representative clone was digested either individually or simultaneously with *EcoR1*, *HindIII* and *BamHI* to confirm the ligation of the fragment. The corresponding restriction fragments were separated by agarose gel electrophoresis (1% agarose) In C, the table shows the restriction fragment sizes expected for this digest.

The last modification to p4KBH4NEO comprised the elimination of a 1.25 Kb segment downstream of exon 4. Eliminating this region will shorten the distance between the neo cassette and the 3' end of the construct, leaving an area with a distance suitable to be amplified by PCR (2.1Kb). p4KBH4NEO was digested with *EcoRV* and *SalI* and the fragment of interest (7Kb) was purified from an agarose gel by the. As these two enzymes generate incompatible ends, a restriction overhang modification was performed using the T4 polymerase I Klenow fragment. This enzyme was able to fill the *SalI* cohesive restriction overhang to generate a blunt end that was compatible with *EcoRV*. After the Klenow reaction, the DNA was extracted with phenol/chloroform, ethanol-precipitated and religated. A small aliquot of the ligation reaction was used for *E.coli* transformation.

Figure 3.9 shows the screening characterization of successful clones obtained after this step. Miniprep DNA from antibiotic resistant bacteria was digested with *XhoI* to verify the elimination of the 3' area of this plasmid. Expected restriction fragment sizes between modified and unmodified plasmids is shown in figure 3.9 C.



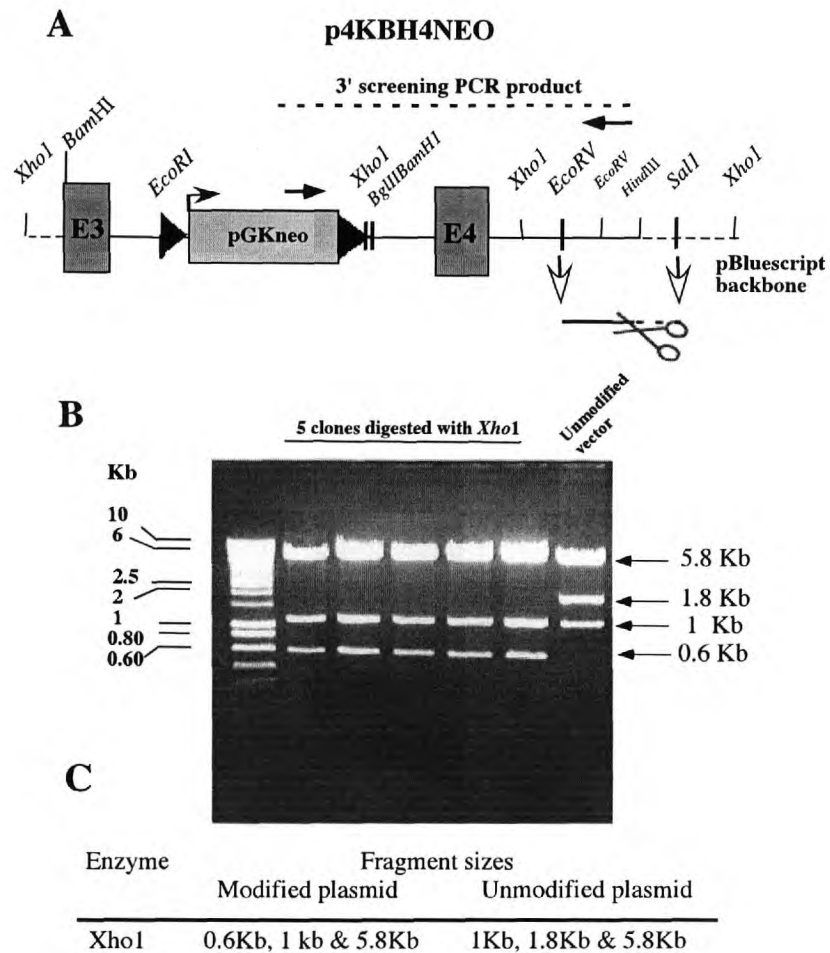


Figure 3.9.- Elimination of a 1.2 Kb region downstream exon 4. p4KBH4NEO was digested with *EcoRV* and *SalI* and the corresponding 2.1Kb fragments eliminated from the plasmid. In A, the figure shows a diagram of the area eliminated as well as the primer location and product size for the screening PCR at the 3' end of the construct. B, DNA from 5 individual clones was digested with *XhoI* and the restriction fragments separated by electrophoresis (fragments sizes shown to the right). The unmodified plasmid digested with the same enzyme is also shown. In C, the figure shows the expected sized of the *XhoI* restriction fragments corresponding to clones with or without the 2.1K region.

The final step to generate the targeting construct comprises the ligation of the two modified plasmids, the modified p4KBH4NEO and pMKS7K containing the sequence of the *loxP* site. This last plasmid was digested with *Bam*HI and further purified from an agarose gel. The modified p4KBH4NEO was also digested with *Bam*HI, dephosphorylated to avoid religation and purified by phenol chloroform extraction followed by ethanol precipitation. Finally both fragments were ligated to generate a 11.6 Kb targeting vector and a clone selected from 25 miniprep DNA samples from antibiotic resistant *E. coli* (data not shown) was subjected to a final characterization by restriction digest. Figure 3.10 shows a diagram of this cloning step together with a 1% agarose gel electrophoresis of a *Not*I, *Bam*HI and *Eco*R1 single restriction digests performed on the selected clone. All restriction fragments were found to be of the correct size (see figure 3.10 C), the integrity of the 4 exons and the orientation of the 3 *loxP* were again verified by sequencing. The location of primers used and segments of the sequence obtained showing both the correct 5' to 3' orientation of the 3 *loxP* sites together the integrity of each exon are shown in figures 3.11 to figure 3.14.

Validating the 5' to 3' orientation of the 3 *loxP* sites is crucial if these sequences are to be recognized by Cre to produce the projected modifications of the *Ctla-4* allele illustrated in figure 3.2.

The final construct was designated pLoxCTLA-4 and a circular restriction map is shown in figure 3.15.

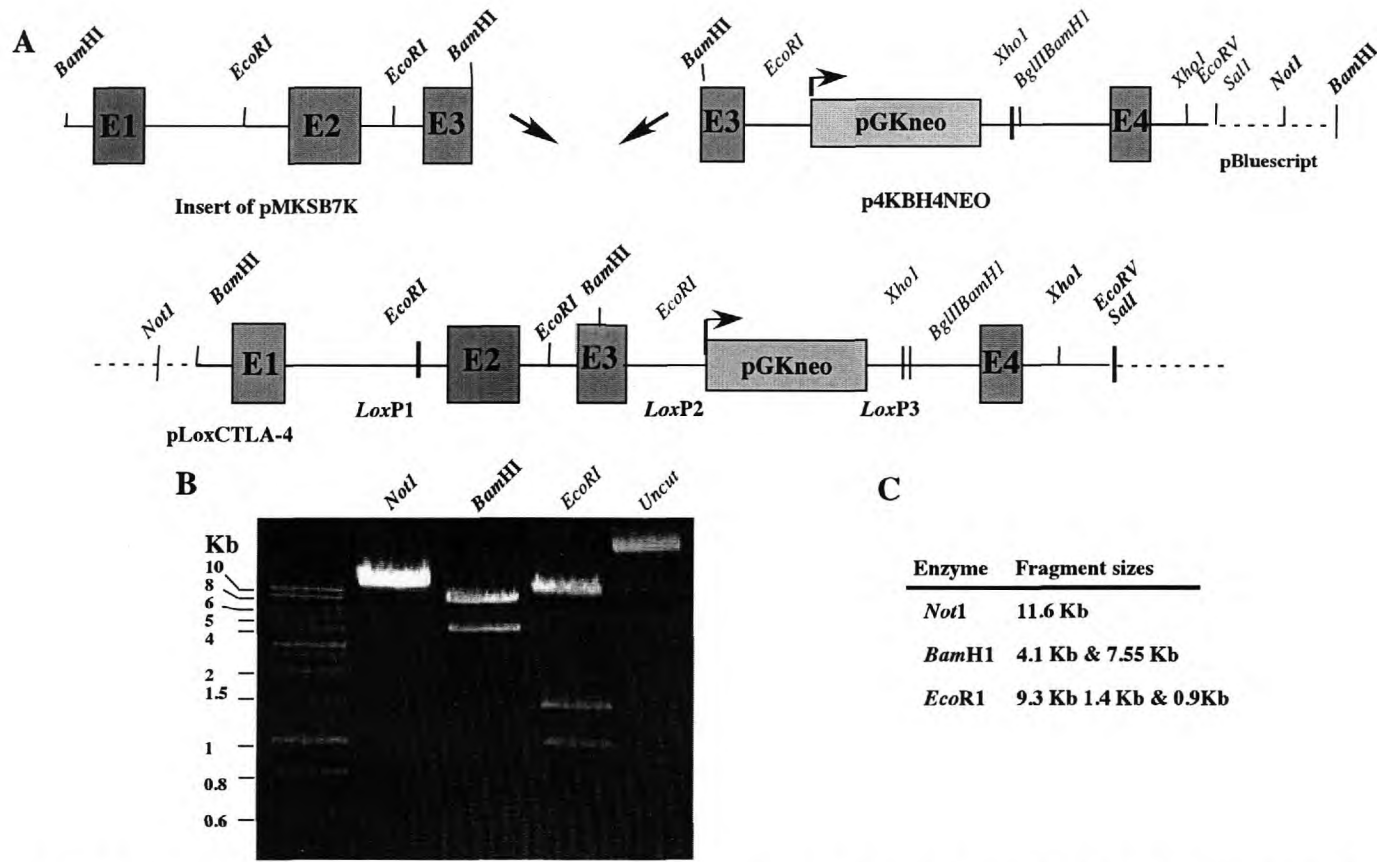


Figure 3.10.- Generation of pLoxCTLA-4. A 4.1Kb *BamHI* restriction fragment from pMKS7K, bearing the sequence of a *loxP* site, was excised from the plasmid and ligated to p4KBH4NEO to generate the CTLA-4 targeting vector. In A, the figure shows a scheme of the cloning procedure. In B, DNA from the clone amplified for ES cell transfection, was digested with *NotI*, *BamHI* and *EcoRI* for characterization and the corresponding restriction fragments separated by electrophoresis. C, the table reports the expected sizes for the restriction fragments. The overall homology of the construct to the *Ctla-4* genomic sequence is 6.84 Kb; 4.1 Kb upstream exon 3 and 2.7 Kb downstream the same exon.

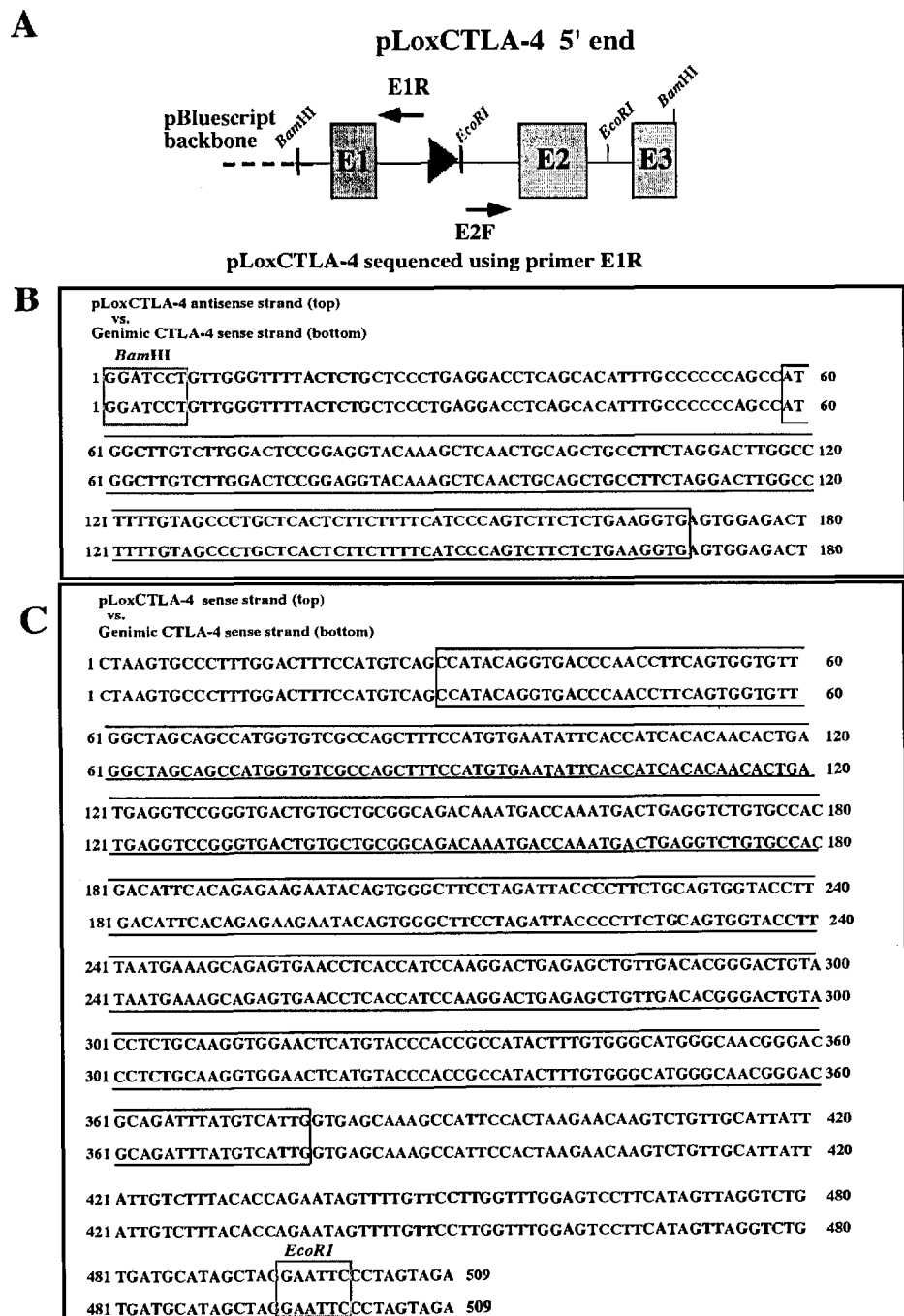


Figure 3.11.- Sequencing analysis of exons 1 and 2 of pLoxCTLA-4. In A, the figure shows a diagram of a fragment of the 5' end of the construct and the location of the primers (E1R & E2F) used for sequencing. A pairwise alignment between the sequences obtained using the primers mentioned and the CTLA-4 genomic sequence, was performed to confirm the integrity of exons 1 (B) and 2 (C). The coding sequences (in boxes) were determined according to Ling, V., *et al* (1999) and the sequence published (NCBI Ac#AF142145). Relevant restriction sites shown within a grey box.

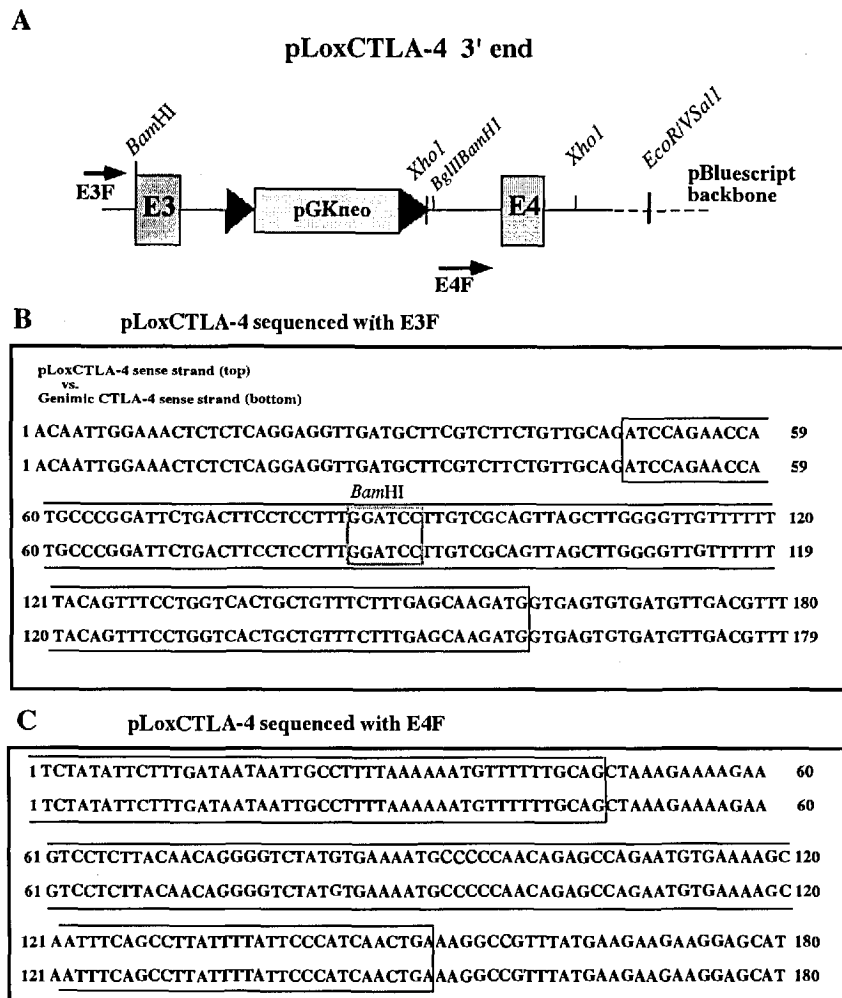


Figure 3.12.- Sequencing analysis of exons 3 and 4 of pLoxCTLA-4. In (A) the figure shows a diagram of the 3' end of the construct and the location of the primers (E3F & E4F) used for sequencing. A pairwise alignment between the sequences obtained using the primers mentioned and the CTLA-4 genomic sequence was performed to confirm the integrity of exons 3 (B) and 4 (C). The coding sequences (in boxes) were determined according to Ling, V., *et al* (1999) and NCBI Ac#AF142145. Relevant restriction sites shown within a grey box.

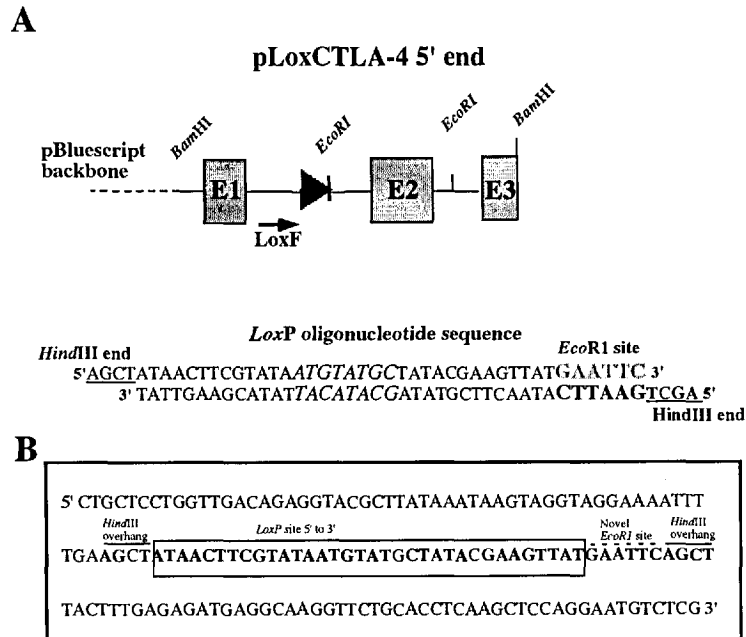


Figure 3.13.- Sequence analysis of the *LoxP* immediately downstream exon 1. In A, the figure shows a diagram of the 5' end of the construct and the location of the primer (*Lox1F*) used for sequencing. The the oligonucleotide used to introduce the sequence of this *LoxP* site is also shown. A segment of the sequences corresponding to the sense strand of pLoxCTLA-4 is shown in B. The sequence of the *LoxP* site is shown within a box *HindIII* overhangs and the new *EcoRI* sites are also indicated.

A

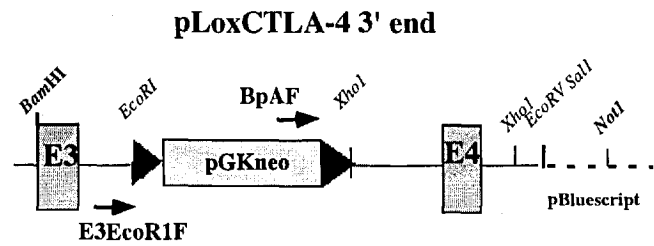
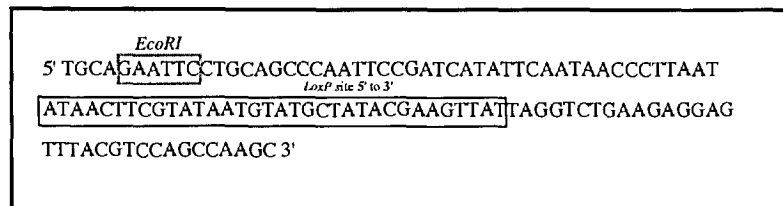
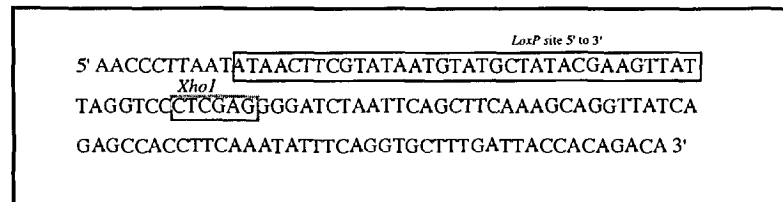
B **pLoxCTLA-4 sequenced with E3EcoR1F**C **pLoxCTLA-4 sequenced with BpAF**

Figure 3.14.- Sequence analysis of the *LoxP* sites flanking the neo cassette. In A, the figure shows a diagram of the 3' end of the construct and the location of the primers (E3EcoR1F & BpAF) used for sequencing. The sequence of the *LoxP* site in 5' to 3' orientation is also shown. Two segments of the sequences corresponding to the sense strand of pLoxCTLA-4, as sequenced with the above primers, are shown in (B) and (C). Relevant restriction sites are indicated in grey boxes.

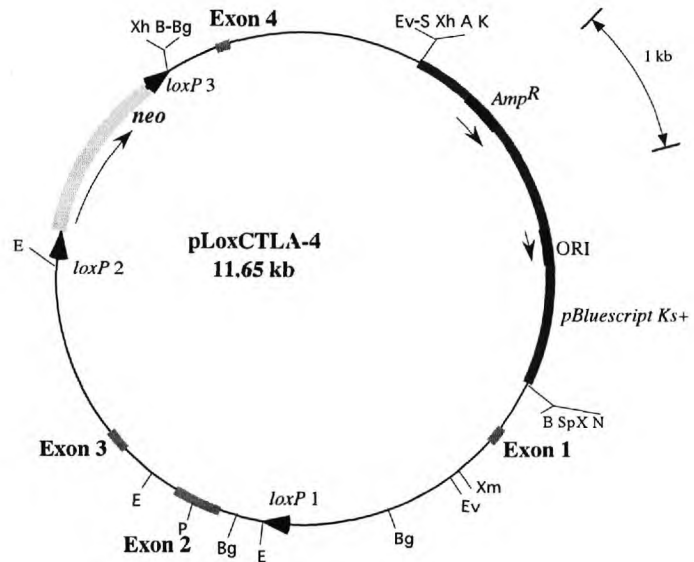


Figure 3.15.-. Circular restriction map of the targeting construct pLoxCTLA-4.  
 A; *Apa*I, B; *Bam*HI, Bg; *Bgl*II E; *Eco*RI, Ev; *Eco*RV K; *Kpn*I, N; *Not* I, Sp; *Spe*I, Xm;  
*Xmn*I, Xh; *Xho* I, P; *Pst*I, Ev-S; *Eco*RV-SalI *AMP<sup>R</sup>*; ampicillin resistance gene, *neo*; neo-  
 mycin transferase gene, ORI; origin of replication.



### 3.5. Screening for homologous recombination among neomycin-resistant ES cell clones by PCR.

A volume of pLoxCTLA-4 was re-transformed and a maxi-prep performed from a single colony of antibiotic resistant *E.coli*. Restriction digest verified the authenticity of this clone. Concentration and purity of the preparation was assessed by UV spectrophotometry, and approximately 200 µg of DNA were linearised by digestion with the unique *Not1* site present in the pBluescript backbone.

An aliquot was analyzed by agarose gel electrophoresis to ensure complete digestion of the DNA, following by extraction, ethanol precipitation and re-suspension ( to an estimated concentration of 1 µg/µL). 40 µg of this preparation was used to electroporate  $5 \times 10^6$  129SvPAS ES cells in serum-free media under the following parameters: a voltage of 260 V, a capacitance of 500 µF in a 4mm cuvette. Cells were immediately plated in a 10 cm tissue culture Petri dish containing a monolayer of fibroblast feeder cells and allowed to recover for 48 hours prior to supplementation of the ES medium with 200 µg/ml of G418.

The plating of the transfected ES cells at low density permitted the clonal expansion of individual cells and after a period of positive selection, G418 resistant ES cell colonies were of sufficient size to be individually picked and cultured in wells of 96 multi-well plates coated with 2% porcine skin gelatin.

These ES colonies were subsequently split into two plates, and one multi-well plate was frozen at -80°C in freezing media to preserve ES cell colonies alive. From this plate, ES cell cultures where homologous recombination is detected by PCR, will be amplified for Southern blot analysis and also for blastocyst injection.

The plasmid DNA maxi-prep, ES cell transfection and cell culture was performed at genOway LTD in Lyon France ([www.genoway.com](http://www.genoway.com)) and 96-well plates containing dry frozen ES cells were sent to our lab for PCR screening.

A PCR screening strategy was designed to select a small number of ES cells cultures, from the 221 initially received from genOway, for subsequent amplification and Southern blot analysis. This strategy is summarized in figure 3.16 and comprises 2 PCRs one across each 5' and 3' ends of *Ctla-4*.

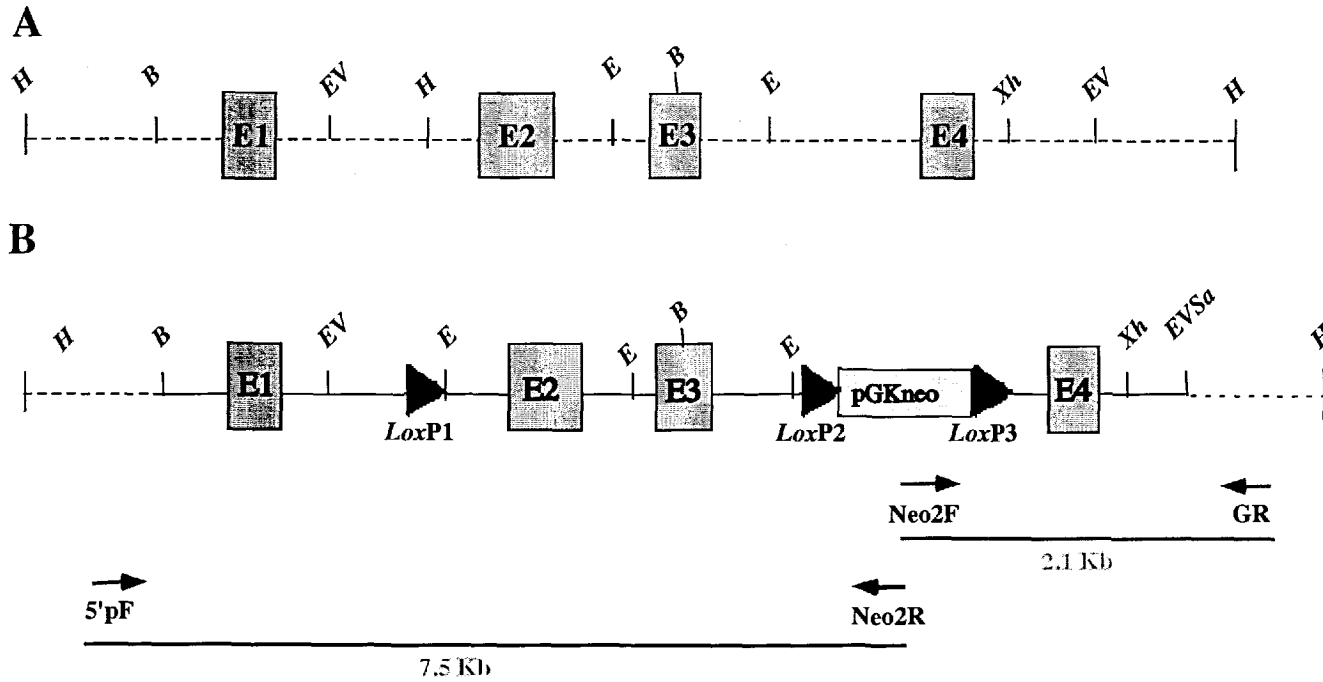


Figure 3.16.- PCR strategy to detect homologous recombination (HR) between the targeting vector (in solid line) and the wild type *Ctla-4* locus (in dashed lines) in ES cells. In A, the figure illustrates the wild type *Ctla-4* locus. In B, the same locus after homologous recombination with the targeting vector. 2 different PCR were designed to confirm HR after electroporation and selection of ES cells. The location of the primers and the sizes of the expected PCR products across the regions amplified are shown.

### **3.5.1 Screening for homologous recombination at the 3' end of *Ctla-4*.**

221 ES cell cultures in 96-well plates were sent in the first instance by genOway to our laboratory. ES cells were lysed, *in situ*, with 200  $\mu$ L of 50mM Tris, 10% SDS, 20  $\mu$ g/ml proteinase K and the genomic DNA extracted from each well by ethanol/NaCl precipitation followed by re-suspension in TE. The DNA yield of the extractions from each plate was relatively homogeneous (see example in figure 3.17) and between 1  $\mu$ L to 5  $\mu$ L were used as template for the PCR.

The 221 ES cell cultures were first screened using primers Neo2F and GR. The conditions of amplification of this PCR are reported in chapter two. The expected 2.1Kb product was obtained in 14 individual ES cell cultures out of 221. Figure 3.17 shows an agarose gel electrophoresis of a sample of ES cell cultures representative of the total lysates processed. The first ES cell lysate that produced the specific 2.1Kb product, was included as positive control in all subsequent reactions. Non template controls were also always included to rule out false positive amplification due to DNA contamination or carry-over of a positive sample. Finally, in order to verify if this PCR will amplify a fragment that is not specific, the reaction was performed using wt mouse DNA and no product was detected (data not shown).

### **3.5.2 Screening for homologous recombination at the 5' end of *Ctla-4*.**

The appearance of the 2.1 Kb PCR product in the previous experiment indicates that, at least, the region of the construct amplified by the PCR has undergone homologous recombination. This PCR, however, does not show whether the entire construct or a segment of its sequence longer than the 3' arm of homology replaced the target *Ctla-4* allele after 2 reciprocal events of crossover (see figure 3.16).

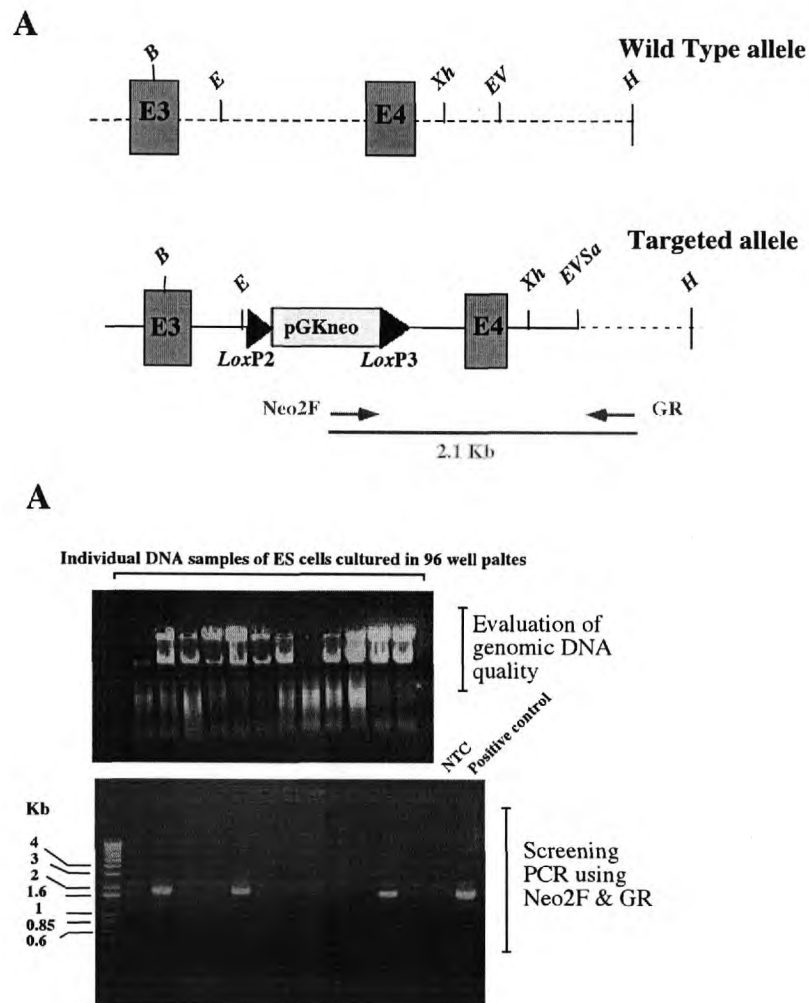


Figure 3.17.- Assessment of homologous recombination of the targeting vector in the *Ctla-4* locus by a PCR on the 3' end. The figure shows in A, the location of the primers used to amplify the 2.1 Kb segment. In B, it illustrates a representative PCR amplification of 12 individual ES cell cultures grown in a 96 well plate format. In the top panel, 1 $\mu$ l of freshly extracted genomic DNA of each ES cell culture was subjected to 1% agarose gel electrophoresis to determine the integrity of the template. The bottom panel shows an electrophoresis of the PCR performed with the primers indicated. This PCR will only amplify a product if the construct undergoes homologous recombination with the *Ctla-4* allele as this event will provide a suitable template for the PCR to proceed. Lanes 13 and 14 show: the non-template control (NTC) and a positive control for the PCR (sample previously identified as positive).

Recombination through a single crossover event, could introduce all the construct components and duplicate the size of the allele. This situation could still produce the suitable 2.1 Kb template for the PCR, despite being an undesirable targeting mutation.

The screening strategy included a PCR across the 5' arm area of the locus, produced after amplification with primers 5'pF and Neo2R. The product size expected for this reaction was 7.3 Kb (see figure 3.16) but if the construct integrated by a single crossover, the template of the PCR will increase in size and it is unlikely that a product will be amplified. After the screening of only ten ES cell samples, out the fourteen found to be positive for the initial PCR, five ES cell DNA samples produced the expected 7.3Kb fragment. The four outstanding samples could not be properly analyzed at this stage due to a shortage of genomic DNA template.

Figure 3.18 shows a set of amplified products of ten ES cell DNA samples. The conditions of this PCR are reported in chapter 2 and no positive control was included due to the lack of a DNA known, *a priori*, to be positive for this required sequence.

No product was observed when using WT mouse genomic DNA as template (data not shown).

A second round of PCR amplification was carried using primers 5'pF and Neo2R and the product digested with *EcoR1* and *HindIII*. The rationale behind this was to confirm that recombination through two crossover events introduced the entire area of homology of the vector. If the crossover on the 5' arm of homology is proximal to exons 2 and 3 and distal from exon 1, the replacement of *Ctla-4* by the construct may be incomplete and therefore a critical element of the whole strategy; the first *loxP* site will not be integrated, (see figure 3.19).

To do this, the PCR products, from all 10 ES cell cultures previously identified, were ethanol-precipitated and resuspended in TE. The DNA obtained was divided into 2 fractions and one each subjected to a restriction digest with the two enzymes mentioned.

Figure 3.20 shows a diagram of the different restriction fragments produced after digesting a PCR product corresponding to an ES cell sample where the entire construct replaced the WT *Ctla-4* region, or a product where only the area of homology downstream the *loxP* site recombined. A representative agarose gel electrophoresis of 10 PCR products digested is shown in the bottom panel of the figure.

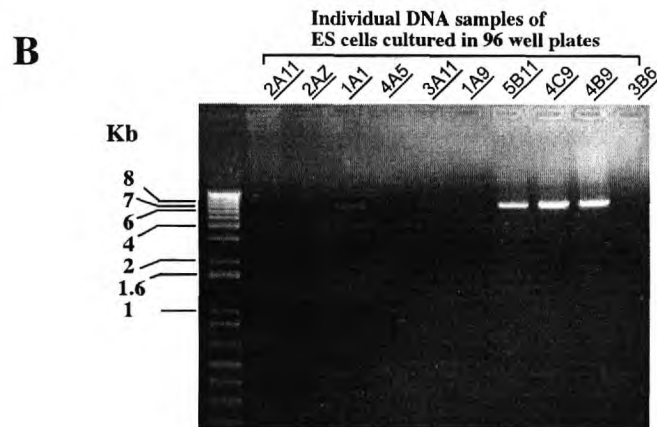
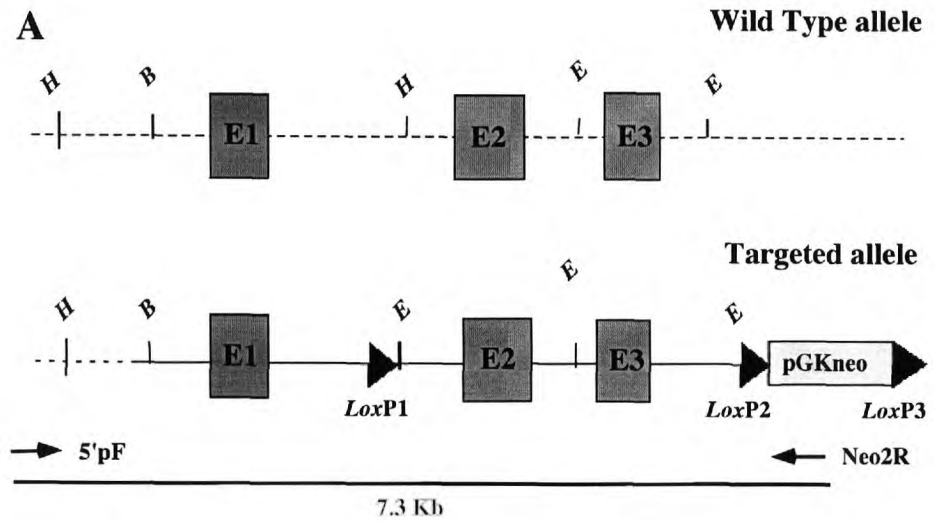


Figure 3.18.- PCR amplification of a 7.3 Kb region across the 5' region of the *Ctla-4* locus. The figure shows in A, the location of the primers used and in B, it shows a 0.8% agarose gel electrophoresis of the PCR amplification corresponding to 10 individual ES cell cultures grown in a 96 well plate format. Non-template controls were always included to exclude any amplification on contaminant or carried-over DNA template (sample not shown in the picture). *EcoRI*: E, *HindIII*: H, *BamHI*: B.

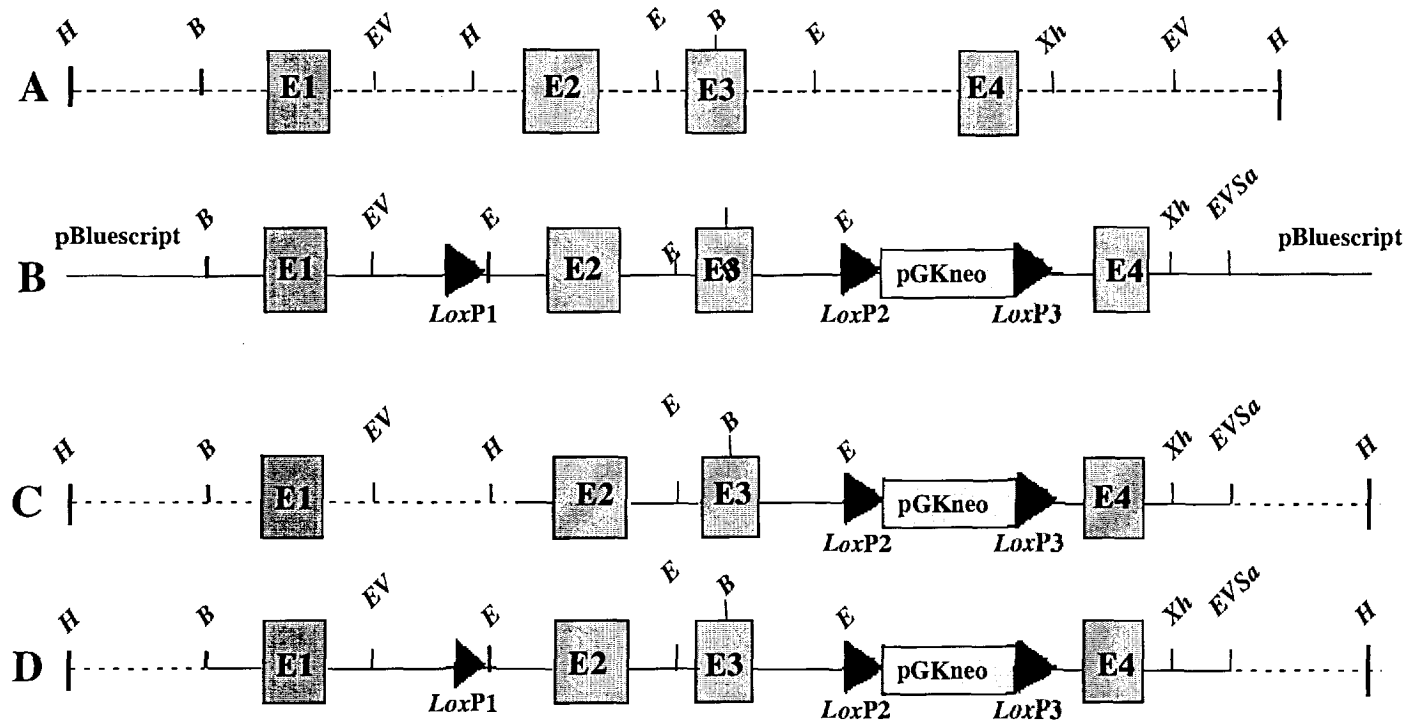


Figure 3.19.- Diagram of insertion of the regions of homology of pLoxCTLA-4 by homologous recombination into the *Ctla-4* allele. In A, the *WT Ctla-4* allele is shown (dashed horizontal lines). B, illustrates the linear pLoxCTLA-4 (continuous line). In C, the figure shows a representation of the partial insertion of a segment of the construct. (D) Insertion of the entire construct homology. *HindIII*: H, *BamHI*: B, *EcoRI*: E, *EcoRV*: EV, *XhoI*: Xh, *EcoRI-SalI*: EVSa

The results of the PCR screening indicated the following: 2 ES cell samples out of 221 (designated according to their location in the culture multi-well plate) as 1A1, 5B11, showed amplification at both ends of the *Ctla-4* locus as well as a pattern of restriction digest suggesting the presence of the *loxP* site downstream exon 1. Consistent with the entire vector having undergone the desired homologous recombination event.

In addition, the amplification of the 7.3 Kb 5' area by PCR in these ES cell colonies, strongly suggests that no insertions in 3' duplicate have occurred. There were four remaining samples (1A12 and 1B11, 4A11 and 3B5) that could not be fully analyzed at this stage and were only selected on the basis of a positive PCR evidence at the 3' end of the locus. The complete set of six samples were considered for further PCR and Southern blot analysis.



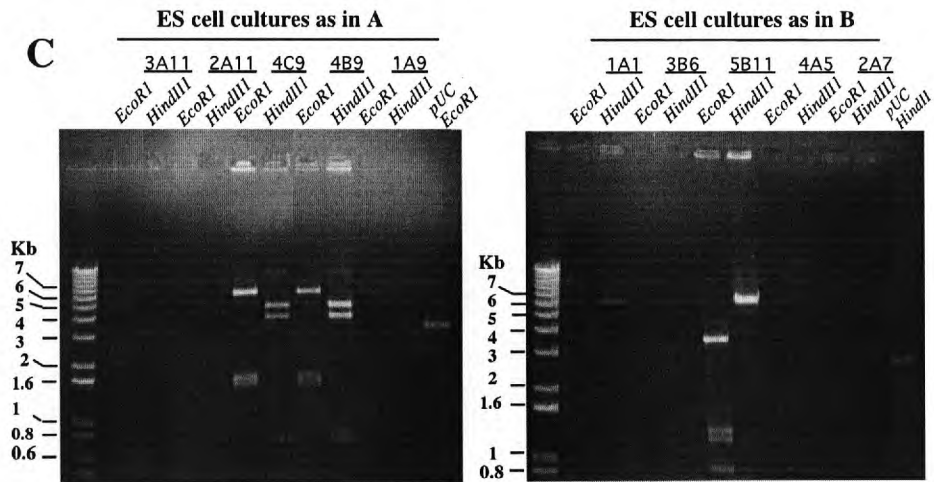
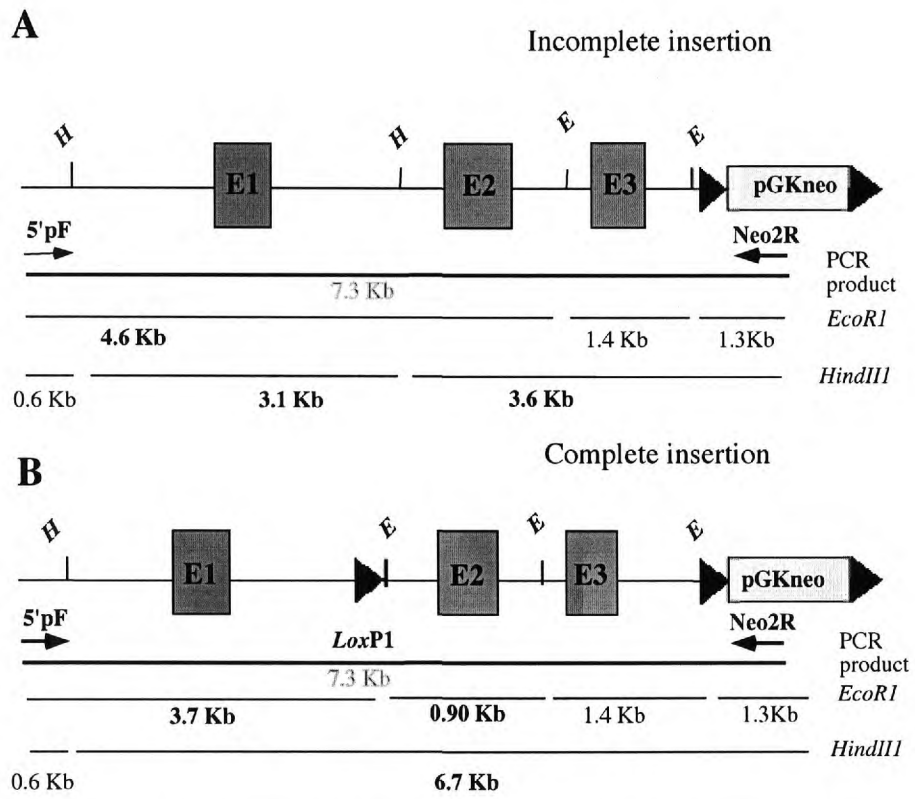


Figure 3.20.- Assessment of a complete or partial insertion of pLoxCTLA-4 into the *Ctla-4* allele. A second round of PCR amplification using primers 5'pF and Neo2R, was performed on ES cell samples previously identified for homologous recombination and the corresponding 7.3 Kb product obtained was subjected to *EcoR1* and *HindIII* restriction digest. The presence of the *LoxP* can be assessed in this restriction digest, because of the new *EcoR1* site engineered downstream the sequence of this *loxP* site and the absence of the *HindIII* site, originally located in that region of the locus, therefore the restriction pattern of a PCR product with or without such *loxP* site will be different. In A, a diagram shows the *Ctla-4* locus after an incomplete insertion of the construct. In B, the figure shows the insertion the entire construct and therefore the presence of the first *loxP* site. The location of the PCR product and the sizes of the expected restriction fragments are represented by horizontal. In C, the figure illustrated an agarose gel electrophoresis (1%) of 10 ES cell DNA samples amplified. The presence of a 0.9 Kb *EcoR1* fragment and a 6.7Kb *HindIII* fragment (panel on the left) represent the expected pattern following complete insertion of the construct. A 4.6Kb *EcoR1* fragment and a 3.6 Kb *HindIII* fragment were obtained when only a segment of the construct has undergone homologous recombination (panel on the right). *EcoR1*: E, *HindIII*: H. pUC digested with the correspondent enzymes was used to control the digest conditions and viability of the enzyme.

### 3.6. Screening for a single gene replacement by Southern blot analysis, Chimera production and germ-line transmission analysis.

#### 3.6.1 Screening for a single gene replacement by Southern blot analysis

The final selection of the ES cells exhibiting a single *Ctla-4* gene replacement by homologous recombination required the development of a strategy able to confirm that the complete sequence of the targeting vector has undergone homologous recombination and that such cells have no random pLoxCTLA-4 integrations. The technique implemented to select such ES cells was Southern blotting and it aims at identifying restriction fragments that will be specifically altered by the gene targeting. A scheme of the strategy is shown in figure 3.21, the length of the restriction fragments produced after digestion of genomic DNA with *EcoR1* and *HindIII* were calculated and mapped with reference of the CTLA-4 sequence published (NCBI Ac#AF142145).

2 probes located within the *Ctla-4* genomic region but external or non-homologous to the construct, one on each end of the locus were used. Such a probes will detect changes in restriction fragment lengths generated by a homologous recombination event, but will not hybridize to the targeting vector itself and thus will not illuminate random integration events. The main modifications that can be detected upon homologous recombination of pLoxCTLA-4 are an increase in the length of the targeted allele, as compared with the wt allele, due to the presence of the neo-cassette. The other modifications correspond to changes in size of restriction fragments due to modifications introduced with the sequence of the *loxP* site downstream exon 1. A third probe, was specific for a part of the sequence of the neo-cassette. This probe is internal to the construct and therefore can also to detect events of random integration.

The 5' external probe and the internal neo-specific probe were the result of PCR amplifications (see materials and methods). Suitable primers were designed to amplify, in the case of the 5' probe, a fragment of 750 bp homologous to an area adjacent to the *HindIII* site upstream exon 1 but outside the area of homology of pLoxCTLA-4. For the internal probe another PCR was designed and a 630 bp product specific for the sequence of the neomycin transferase amplified. The third probe (external 3') was a 1 Kb product of the *EcoRV/HindIII* digest of the genomic CTLA-4 construct p4KBH4 (see figure 3.3 and 3.21 for the location of the probes).

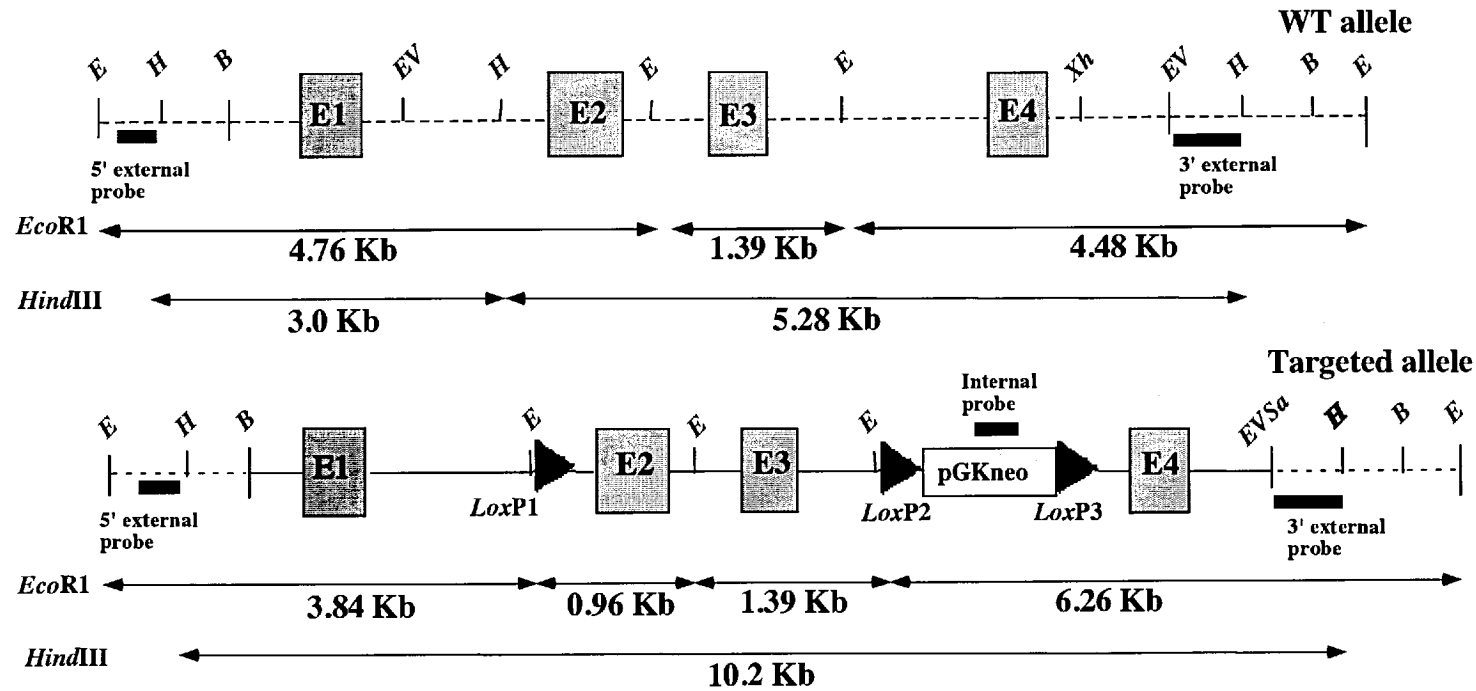


Figure 3.21.- Restriction map of the WT and targeted *Ctla-4* alleles for Southern blot analysis. The diagram shows the area of homology between the 3 probes selected (black boxes). The 5' and 3' external probes are homologous to the genomic *Ctla-4* sequence, outside the area of homology of the construct, (dashed lines) and the internal probe is homologous to the sequence of the PGK-neo in the construct. The expected *EcoR1* and *HindIII* restriction fragments are shown as horizontal arrows.

ES cell samples 1A1, 5B11, 1A12, 1B11 were cultured in 24 multi-well tissue culture plates for a greater scale genomic DNA extraction at genOway. These ES cell samples were sent to out laboratory and DNA extraction was performed. The genomic DNA obtained was then subjected to the above-mentioned Southern blotting method.

Figure 3.22 and 3.23 show the hybridization of the 5' and 3' external probes, to ES cell genomic DNA that was respectively digested with either *EcoR1* or *HindIII*.

WT mouse DNA was used as a control to reveal the location of the WT allele.

Figure 3.22 revealed for samples 5B11 and 1A1, a pattern of hybridization indicating the integration of at least the 5' end of the construct by HR to one of the *Ctla-4* alleles. Samples 1B11 and 1A12 show no modifications in their *EcoR1* restriction digest pattern indicating the absence of recombination.

The previous PCR evidence obtained for samples 1A12 and 1B11 on the 3' end (positive for the 2.1 Kb PCR product), suggested that at least the end of construct had integrated by HR, however, as shown by the Southern blot analysis (figure 3.22), incomplete insertion of the 5' end may have happened in this samples. No insertions in 5' duplicate or concatamers were observed for these samples as no bands of unexpected sizes appeared.

In figure 3.23 a hybridization of genomic DNA digested with *HindIII* was performed using the 3' external probe, for the same set of samples. Only sample 1A1 showed the correct restriction digest pattern and all the evidence gathered so far indicates that in this sample, the construct integrated its entire homologous sequence by HR.

Samples 1B11 and 5B11 showed hybridization of a genomic fragment greater than 10Kb, suggesting the integration of the construct in a 3' duplicate. Interestingly, this type of insertion was permissive to the amplification and correct restriction digest of the 7.3 Kb PCR, possibly indicating concomitant homologous recombination of the entire sequence of the construct and an insertion in 3' duplicate for this sample.

Sample 1A12 shows hybridization to a 7 Kb fragment indicating incomplete insertion of the construct by homologous recombination and therefore the lack of the *loxP* site downstream exon 1.

Figure 3.24 shows two independent hybridizations of the internal probe to DNA from the 4 ES cells samples, one after the digest with *EcoR1*, and the other after *HindIII*. For samples 1A12 and 1B11 multiple events of random integration were detected in both

Southern hybridizations. Sample 5B11 showed once more a single band greater than 10Kb indicating the possibility of an integration in 3' duplicate. This is consistent with what it was observed in previous Southern blots.

In conclusion after the screening by PCR and Southern blot analysis only sample sample 1A1 was chosen for amplification and blastocyst injection as it displays a single gene replacement at 1 allele of the *Ctla-4* locus and no random integration events.

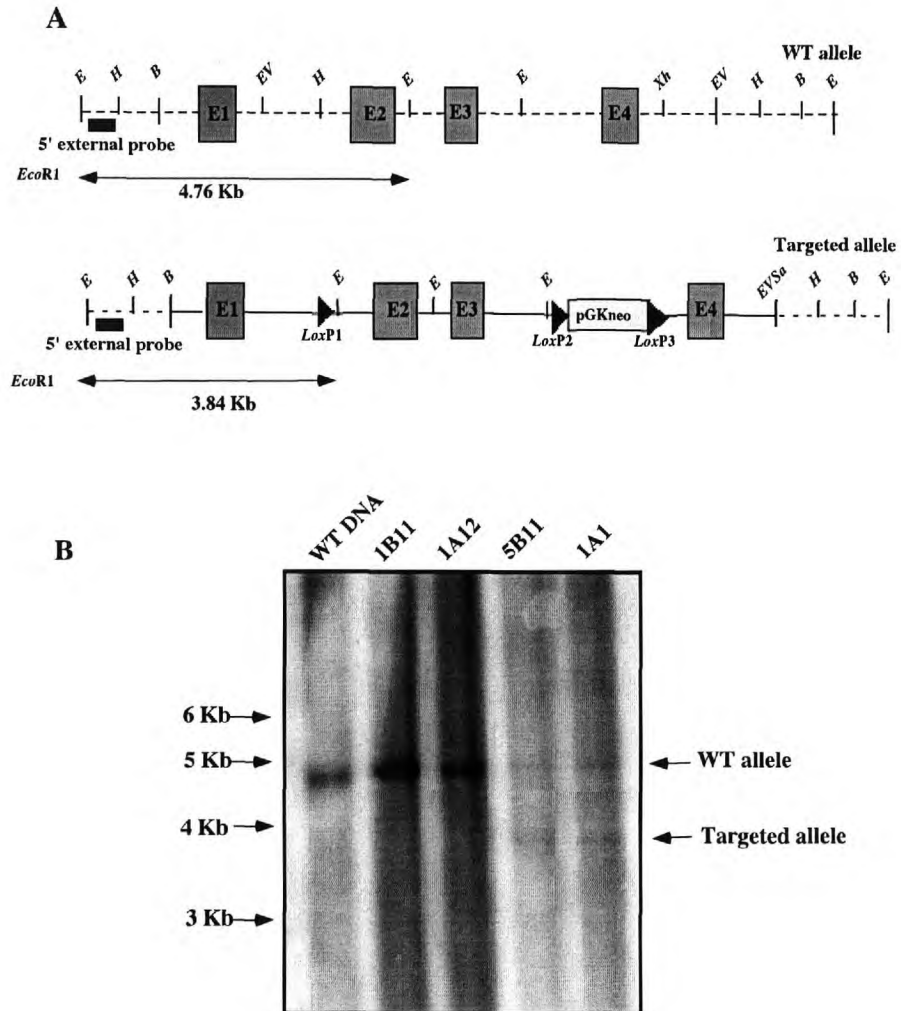


Figure 3.22.- Southern blot analysis using the 5' external probe hybridized to ES cell genomic DNA digested with *EcoR*I. The figure shows in A, a diagram of the location of the probe and the expected restriction fragments illuminated by the probe. In B, a autoradiograph of the genomic DNA on a nylon support membrane, showing the hybridization patterns of samples (5B11, 1A1, 1B11, 1A12). Corresponding WT and targeted restriction fragment size is indicated by the arrows.

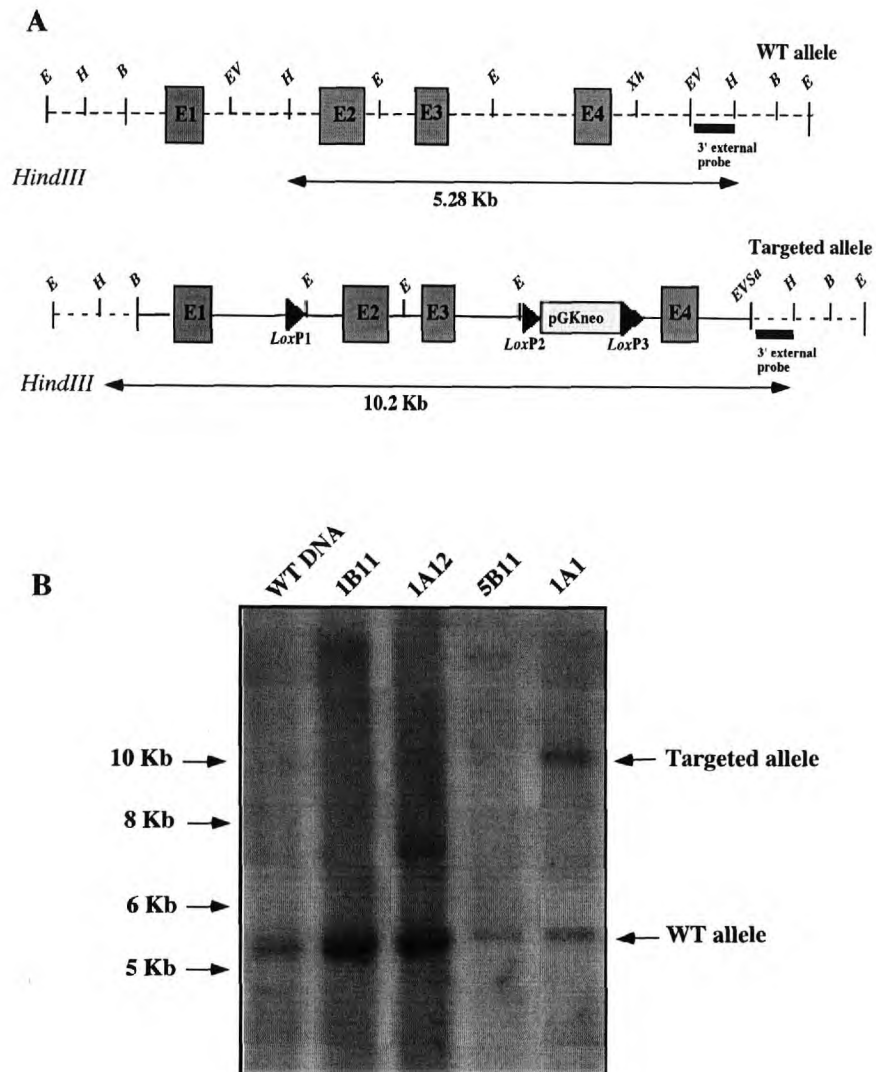


Figure 3.23.- Southern blot analysis using the 3' external probe hybridized onto ES cell genomic DNA digested with *HindIII*. The figure illustrates in A, a diagram of the location of the probe and the expected restriction fragments illuminated. In B, a autoradiograph of the genomic DNA on a nylon support membrane, showing the hybridization pattern of the samples (5B11, 1A1, 1B11, 1A12). WT and targeted restriction fragment size is indicated by the arrows.



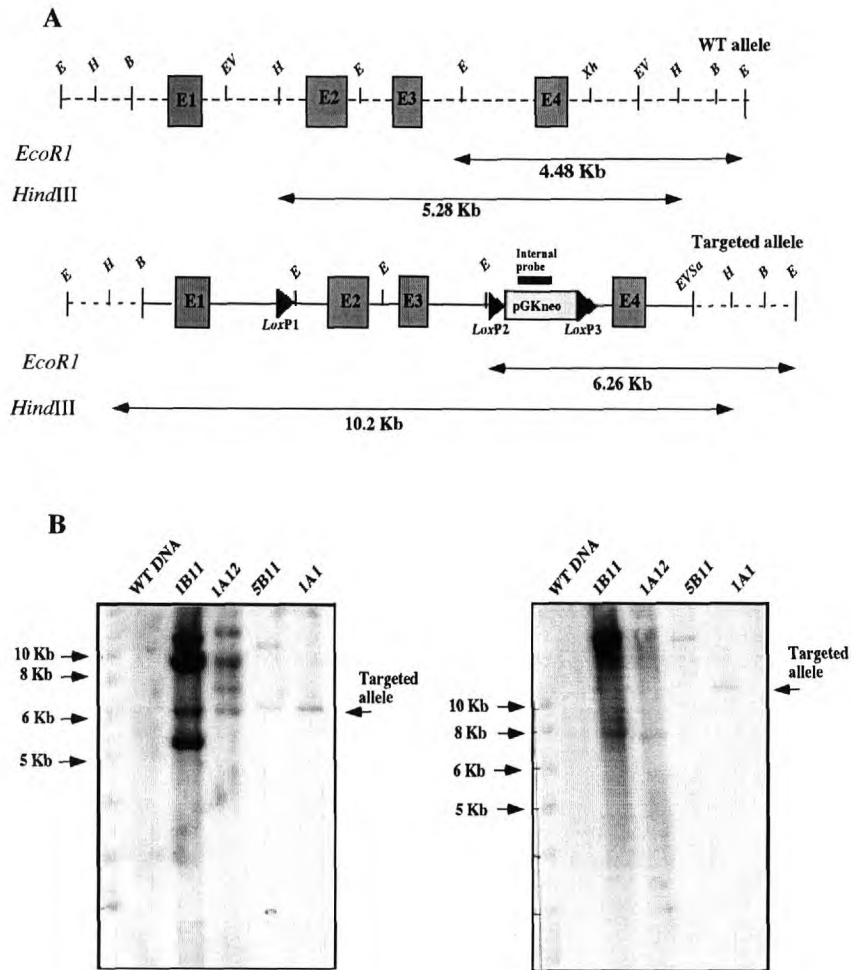


Figure 3.24.- Southern blot analysis using the internal probe hybridized to ES cell genomic DNA digested with *EcoR1* (left) and *HindIII* (right). The figure illustrates in A, the location of the probe and the expected restriction fragments illuminated. In B, 2 autoradiographs of the genomic DNA on a nylon support membrane, showing the hybridization pattern of samples 5B11, 1A1, 1B11, 1A12. The size of the expected targeted allele is indicated by an arrow.

### 3.6.2 Chimera production from ES cell sample 1A1 and analysis of germ line transmission.

The ES cells from sample 1A1 were further amplified and injected to recipient blastocysts isolated from C57BL/6 females (with specific pathogen free health status) and re-implanted into OF1 pseudopregnant females (specific and opportunistic pathogen health status). Table 3.1 summarizes the results of the blastocyst injections performed for ES cell sample 1A1.

Injection sessions	Blastocysts	Foster mothers implanted	Pregnant foster mothers	Number of pups	Chimeras obtained and %
1st	75	5	4	18	2, 5% & 20%
2nd	28	2	nil	nil	nil
3rd	52	4	nil	nil	nil

Table 3.1 Blastocyst injection sessions performed with ES cell sample 1A1 and chimeras produced.

The likelihood that ES cells from sample 1A1 had contributed to the germline of the mouse was estimated to be small in this experiment. This is because only a 5% and a 20% chimeric animals were produced. To test such contribution and their ability to transmit, the *Ctla-4* targeted mutation, the chimera possessing a 20% agouti coat colour, was bred with 3 C57BL/6 females and only black pups were born. This indicated that the ES cells from sample 1A1 did not contribute to the germline of the chimera and no further crosses were performed. In light of this results we asked genOway to amplify ES cell samples 4A11 and 3B5 as well as to re-amplify sample 1A1 for further confirmatory analysis.

### 3.6.3 Screening for a single gene replacement by Southern blot analysis of ES cell samples 4A11 and 3B5.

A second batch containing ES cell samples 4A11 and 3B5, as well as a new lysate from sample 1A1 was received in our lab for analysis. PCR across the 5' region of the locus together with restriction digests, were initially performed, to rapidly determine if ES cell samples 4A11 and 3B5 had a single *Ctla-4* gene replacement. In this experiment, DNA from sample 1A1, previously identified positive for this PCR was included and no product was detected. This observation may indicate the loss of the cells containing the targeted mutation.

Figure 3.25 shows a diagram of the PCR, its expected restriction fragments and two agarose gel electrophoresis showing the amplification of the 7.3Kb PCR product for each sample including 1A1 (Figure 3.25 C) and the restriction digest analysis performed on samples 4A11 and 3B5 (Figure 3.25 D). The pattern corresponding to an insertion of the entire construct into the *Ctla-4* allele by homologous recombination was observed in both samples.

Southern blot analysis was carried out on ES samples 4A11 and 3B5 to confirm the evidence observed by PCR. Sample 1A1 was also included in this analysis to further determine if the cells bearing the targeted mutation were truly lost. Figure 3.26 shows a hybridization of the 5' external probe on DNA digested with *EcoR1*. Both ES samples (4A11 and 3B5) produced the expected restriction fragment pattern, corresponding to the insertion of the 5' arm of homology into the *Ctla-4* locus. No other types of insertion were observed. In this experiment, the restriction fragment corresponding to the targeted allele was not detected in sample 1A1.

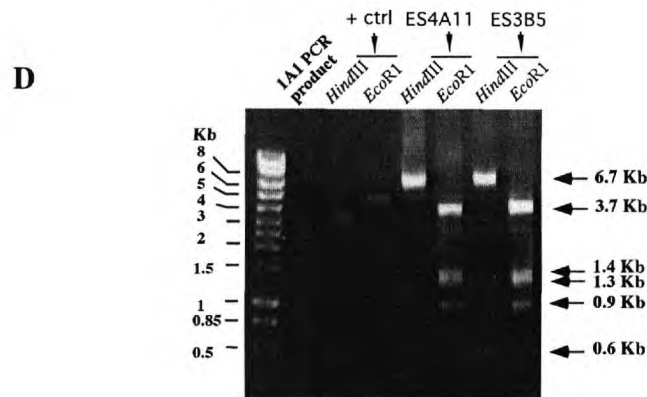
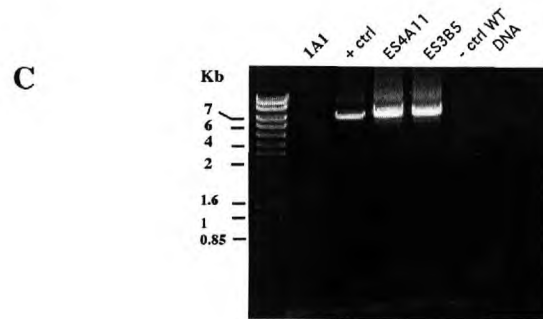
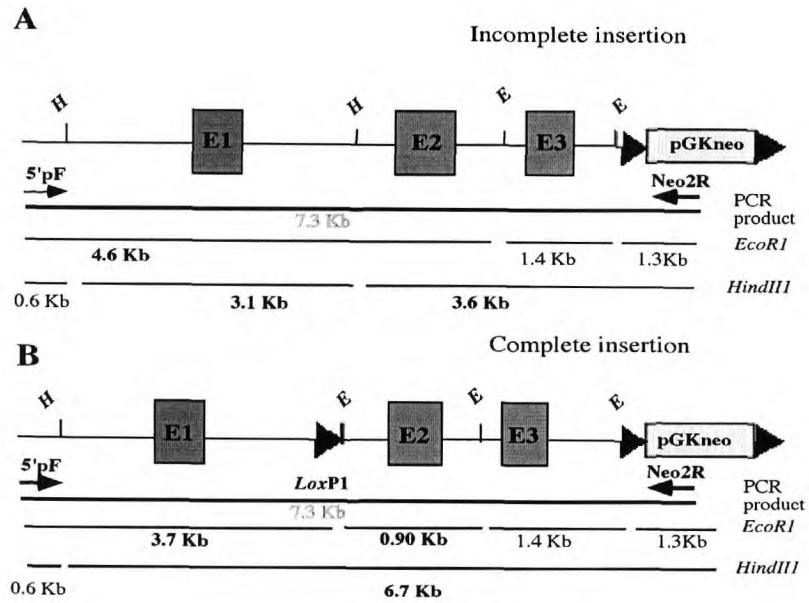


Figure 3.25.- Assessment of complete or partial insertion of pLoxCTLA-4 into *Ctla-4*. A PCR amplification using primers 5'pF and Neo2R, was performed on ES cell samples 4A11, 3B5 and 1A1. The 7.3 Kb product obtained was subjected to an *EcoR*I and a *Hind*III restriction digest to detect the presence of the *LoxP*. In A, a diagram shows the *Ctla-4* locus after incomplete insertion of the construct. In B, the figure shows the insertion of the entire construct including the first *loxP* site. The location of the PCR product, the sizes of the expected restriction fragments that differentiate an event of HR of the entire vector versus the insertion of only the 3' end, are represented by horizontal lines. An agarose gel electrophoresis (1%) of the PCR before digest is shown in C, and the electrophoresis of the resulting restriction fragments in D. Sample 1A1 was included in this analysis (C). Further ethanol/salt precipitation of that PCR reaction is also performed (D) to confirm that no product was produced at levels under the detection limit of the electrophoresis. *EcoR*I: E, *Hind*III: H.

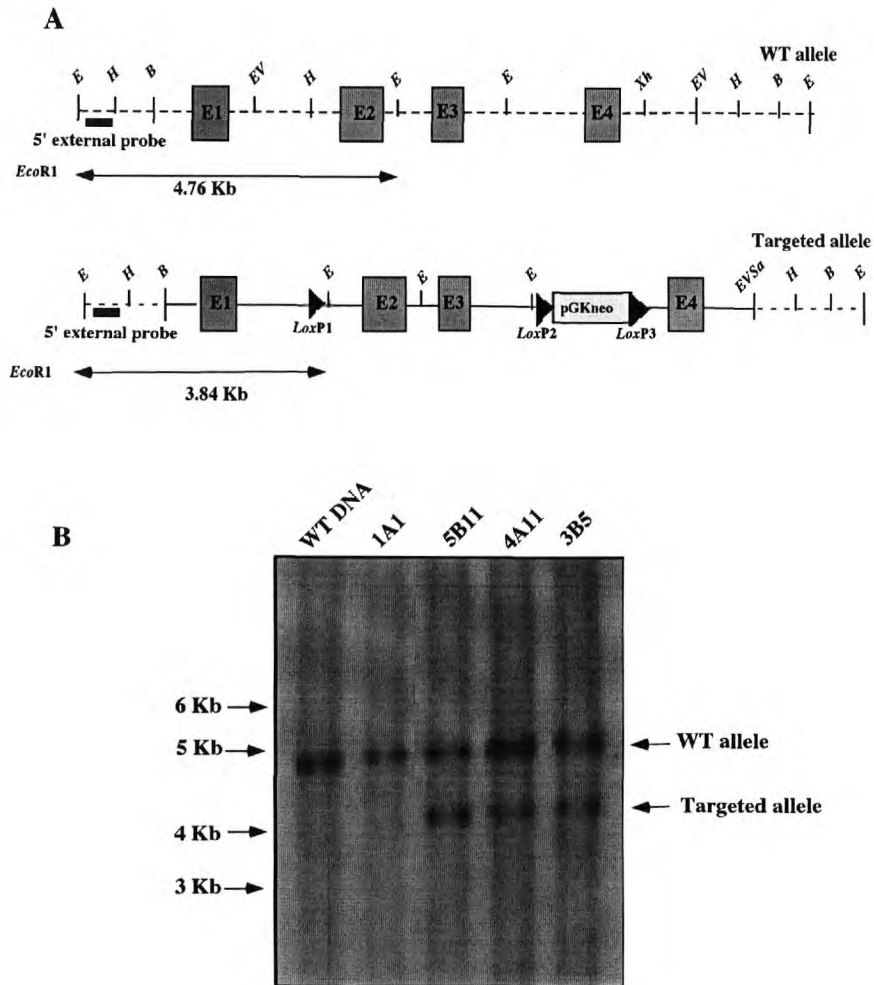


Figure 3.26.- Southern blot analysis using the 5' external probe hybridized to ES cell genomic DNA digested with *EcoRI*. The figure illustrates in A, a diagram of the location of the probe and the expected restriction fragments illuminated. In B, an autoradiograph of the genomic DNA on a nylon support membrane, showing the hybridization patterns of samples 4A11 and 3B5. DNA from sample 1A1 was also included to confirm what was observed by PCR (see figure 3.25). An aliquot of DNA from sample 5B11 was included in this blot as a control to show the location of the targeted allele. WT DNA was also included as in previous analyses.

Southern blot analysis using the 3' and internal probes were also performed on samples 4A11 and 3B5. The two samples displayed the restriction fragments corresponding to both a targeted and a WT allele with neither, undesired integrations in duplicate, nor random integrations (see figures 3.26, 3.27 and 3.28). Sample 1A1 was included in these analyses and no signal corresponding to the targeted allele was detected. This strongly indicates that the cells bearing the targeted mutation in this sample were lost, possibly during the culturing of the ES cells from 96 well plates to 24 well plates before Southern analysis or blastocyst injection.

In a Southern blot analysis, the bands corresponding to the WT and targeted allele should appear with similar intensity. Homologous recombination rarely occurs in both of the alleles of diploid ES cells and if each ES cell clone identified, is collected and further cultured under appropriate conditions, it should remain as a clonal population during amplification. It can be observed in figures 3.26 and 3.27, that this was certainly not the case, and for both samples 4A11 and 3B5, there are differences in intensity between the WT and targeted alleles, being the WT the brightest band.

The greater abundance of genomic DNA fragments corresponding to the WT allele, compared with the targeted allele can be explained if the correct concentration of G418 was not constantly used in the culture of ES cells after transfection, or if the initial period of selection was not long enough (generally not less than 15 days).

These two circumstances may have affected the selection of the ES cells giving rise to a mixed population of neo-resistant ES cells as well as neo-sensitive cells. The problem in this scenario is that the first group of cells will proliferate and out-compete cells bearing targeted mutations. This could have been the cause for the complete loss of clone 1A1.

Samples 4A11 and 3B5 showed the expected hybridization pattern corresponding to ES cells samples bearing a targeted *Ctla-4* allele with no random integrations of the construct. However both show a considerable degree of contamination with WT ES cells and this situation will become an obstacle to produce reliable chimeric animals where targeted ES cells can contribute to the germline and further transmit our targeted mutation. In order to minimize the chances of such phenomena, both ES cell samples (4A11 and 3B5) were amplified for blastocyst injection, in the presence of G418.

An aliquot of genomic DNA was sent to our laboratory before the injection sessions and a final Southern blot was performed. In order to minimize the loss of recombinant ES cells in the mixed samples (4A11 and 3B5) the amplification of cells before blastocyst injection was performed in the presence of G418.

An aliquot of genomic DNA was sent to our laboratory before the injection sessions and a final Southern blot was performed .

The results of this analysis is shown in figure 3.29. No significant improvement on the differences in intensity between alleles was observed for both ES cell samples.



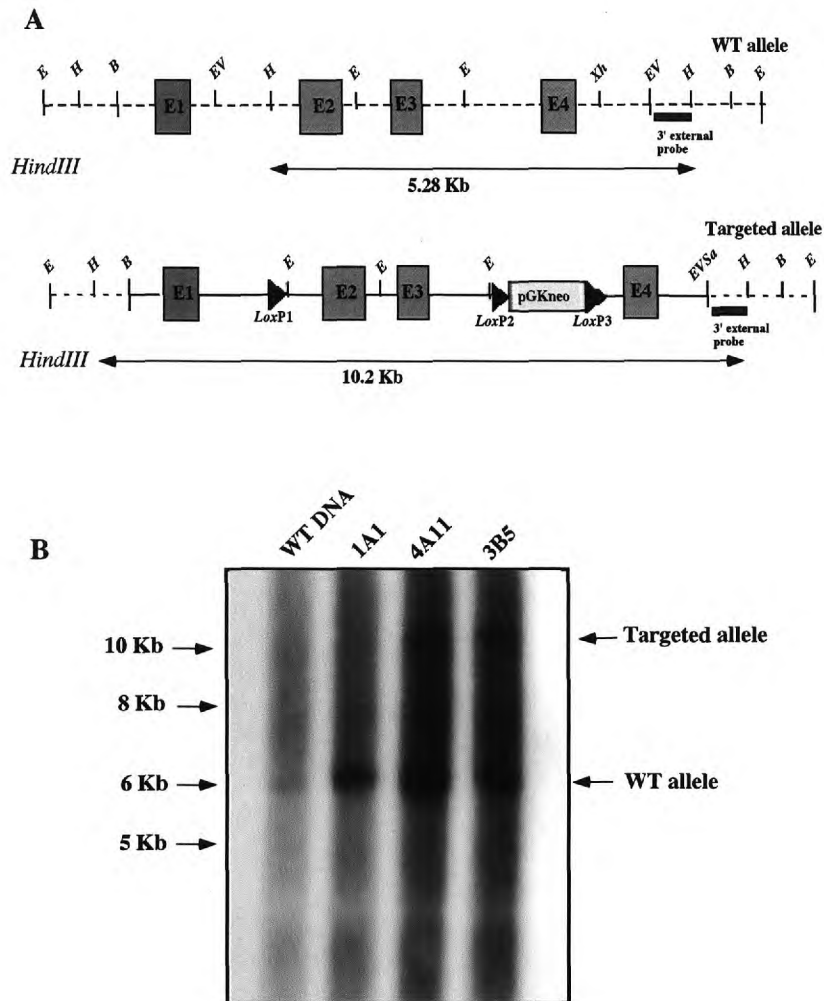


Figure 3.27.- Southern blot analysis using the 3' external probe hybridized onto ES cell genomic DNA digested with *HindIII*. The figure shows in A, a diagram of the location of the probe and the expected restriction fragments illuminated. In B, a autoradiograph of the digested genomic DNA on a nylon support membrane, showing the hybridization pattern for samples 4A11 and 3B5. Sample 1A1 was also included in this analysis. WT genomic DNA was included in lane one to indicate the size of this allele.

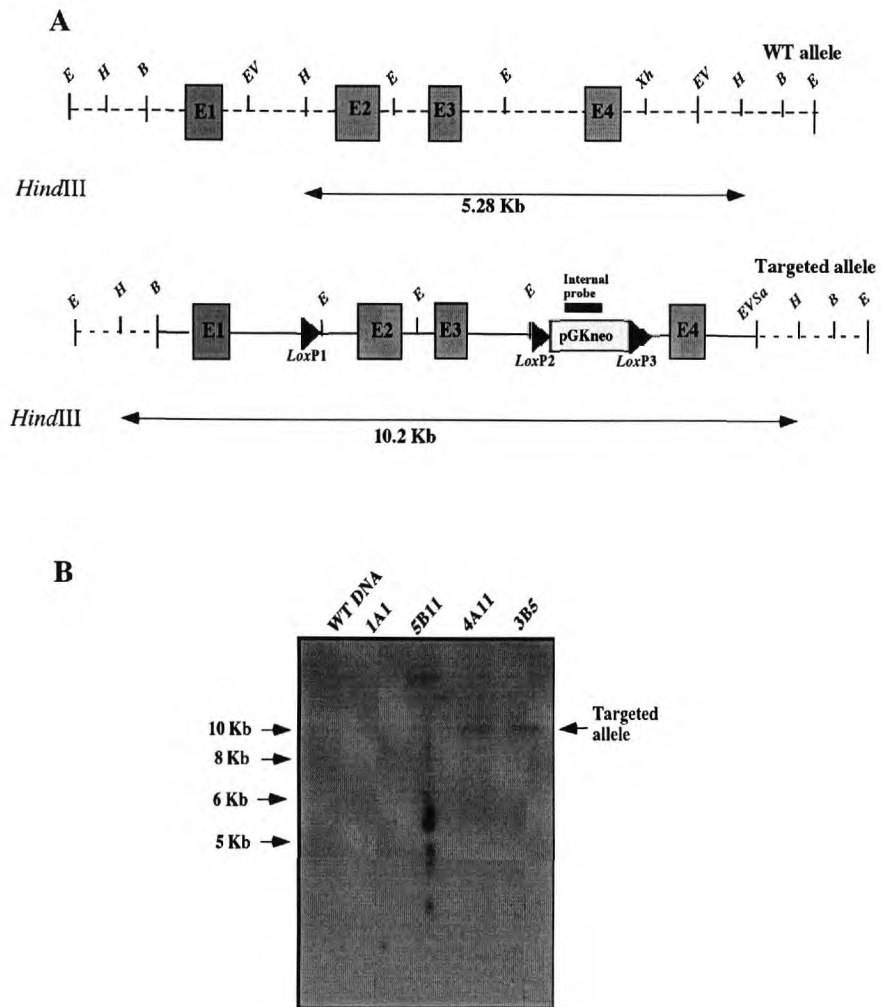


Figure 3.28.- Southern blot analysis using the internal probe hybridized onto ES cell genomic DNA digested with *HindIII*. The figure illustrates in A, a diagram of the location of the probe and the expected restriction fragments illuminated. In (B) an autoradiograph of the digested genomic DNA on a nylon support membrane, showing the hybridization pattern for both samples 1A1, 4A11 and 3B5.

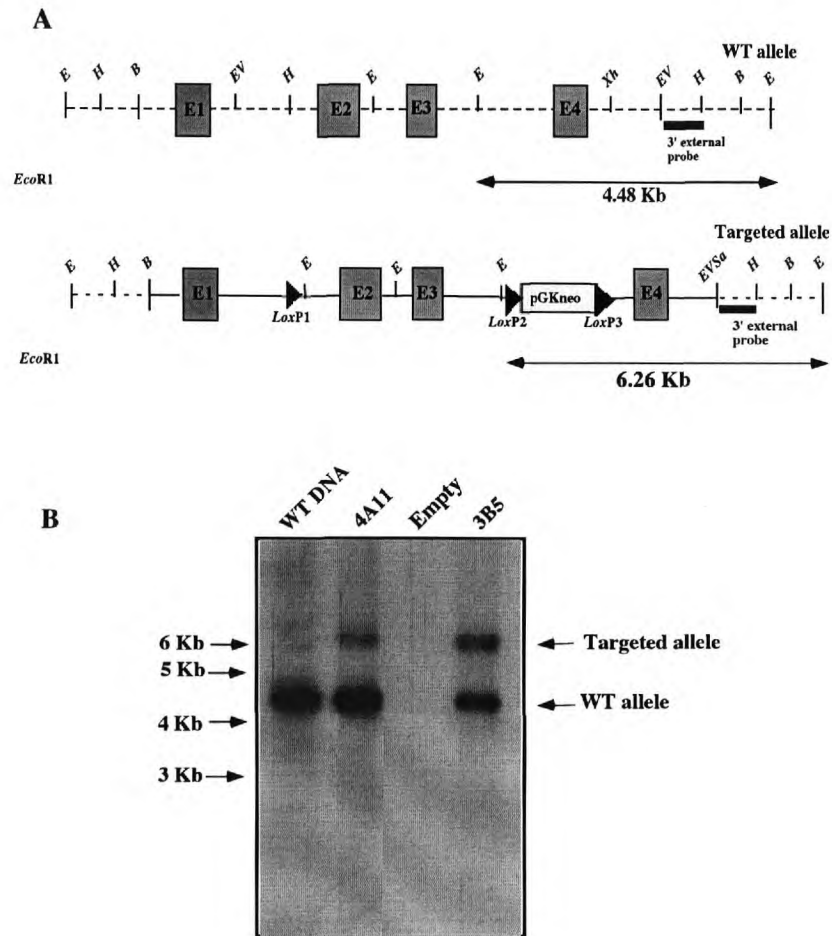


Figure 3.29.- Southern blot analysis using the 3' external probe, performed on genomic DNA digested with *Eco*R1 from ES cells after amplification and before blastocyst injection. The figure illustrates in A, a diagram of the location of the probe and the expected restriction fragments which it hybridizes to. In B, an autoradiograph of the genomic DNA of samples 4A11 and 3B5. Sizes for both the targeted and WT alleles are shown and WT genomic DNA was used as control.

### 3.6.4 Chimera production from ES cell samples 4A11 and 3B5 and analysis of germ line transmission.

The ES cells from both 4A11 and 3B5 ES cell samples were injected to recipient blastocysts isolated from C57BL/6 females. Table 3.2 summarizes the results of the blastocyst injections performed for ES cell sample 4A11.

Total injection sessions	Blastocysts	Foster mothers implanted	Pregnant foster mothers	Number of pups	Male Chimeras obtained
3	137	9	5	24	4 (80% 30%60% 50%)

Table 3.2.- The results of the blastocyst injections performed with ES cells from sample 4A11.

Chimeras with 80%, 50% and 60% were mated with 3 C57BL/6 females and they produced only 19 pups. From these animals 9 were agouti (two from the 50% chimera and seven from the 60%). Non of the agouti offspring produced from these chimeras possessed a targeted allele (figure 3.30). This demonstrates that the targeted ES cells did not contribute to the germline and/or the ES cells that contributed to the germline were of a WT *CTLA-4* genotype, possibly coming from the “contaminant” fraction of wt ES cells described before.

Table 3.3 shows the results obtained from the blastocyst injections with ES cells from sample 3B5.

Total injection sessions	Blastocysts	Foster mothers implanted	Pregnant foster mothers	Number of pups	Male chimeras obtained
5	255	20	8	24	3 (5%,30% and 90%)

Table 3.3.- The results of the blastocyst injections performed with ES cells from sample 3B5.

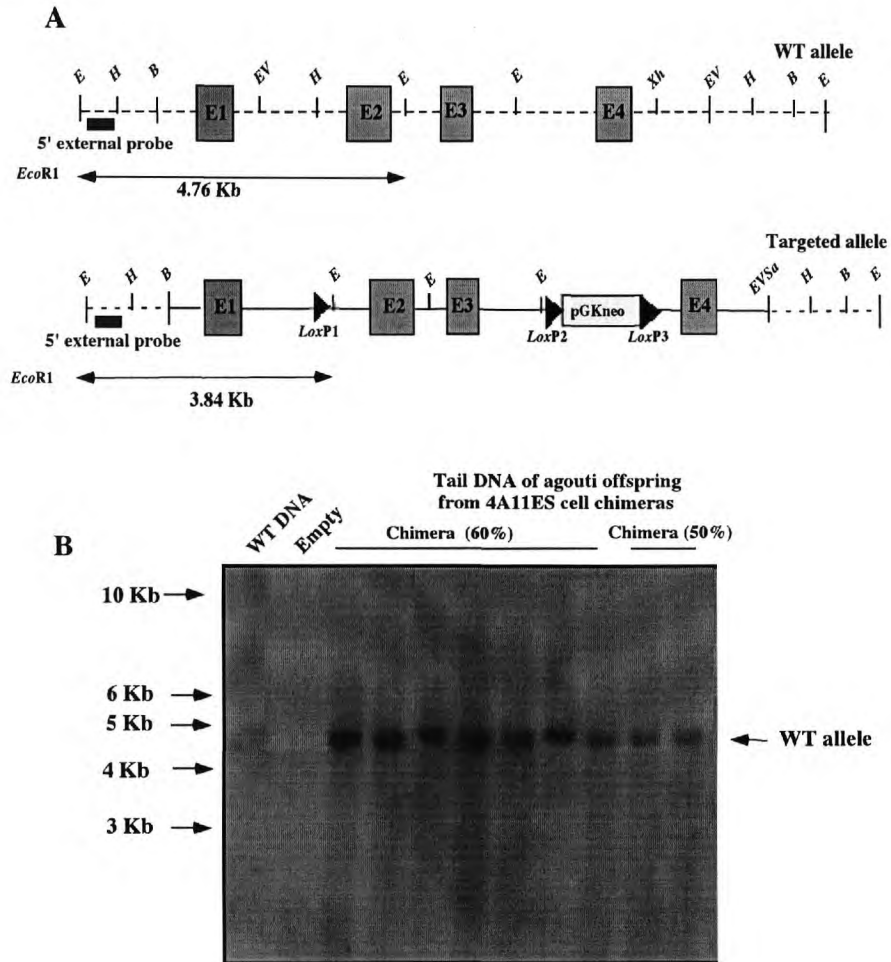


Figure 3.30.- Southern blot analysis of tail genomic DNA of agouti offspring from chimeric animals generated by blastocyst injections of ES cell sample 4A11. In (A) the figure illustrates a diagram showing the *EcoRI* restriction digest performed and the expected restriction fragments. The probe used in this analysis was the 5' external probe.

From the blastocyst injections of sample 3B5, two of the chimeras (90% and 30%) were mated with 2 C57BL/6 females and 42 pups were produced. 26 of those were agouti (14 from the 30% chimera and 12 from the 90%), and after Southern blot analysis of tail genomic DNA from these animals, only 5 agouti pups showed a targeted allele, all coming from the 90% chimera. This indicates that the targeted ES cells contributed to the germline of this animal. The transmission of the targeted mutation was subsequently assessed by Southern blot (figure 3.31). After evaluating the germline transmission of the targeted mutation, the number of agouti pups obtained from this 90% chimera was close to the statistical frequency of targeted offspring expected (50%). ES cells have only one targeted allele therefore, 1 out of every 2 pups should bear a targeted allele.

In this 90% chimera there was no apparent effect of the WT ES cells present in the original sample injected, on the transmission of the targeted mutation.

The lack of targeted agouti pups from the breeding of the 30% chimera is still an indication that WT ES cells in the original “mixed” sample injected have contributed to the germline of this animal.

Figure 3.31 shows the Southern blot analysis performed on tail DNA, from the agouti offspring born from the cross of a C57BL/6 female and the 90% agouti chimera. The analysis was performed to confirm the presence of a targeted allele using the external 5' probe. In addition, to further determine that no random integrations are present in the genome of these animals, a Southern analysis was carried out using the internal probe. The animals having a targeted *Ctla-4* targeted allele showed no random integrations. This analysis established the founders of a targeted *Ctla-4* line.

The genotype of these animals will be further modified, particularly by Cre-mediated recombination in the germline. Those genetic modifications and the analysis of their phenotypes are reported in the subsequent chapters of this thesis.

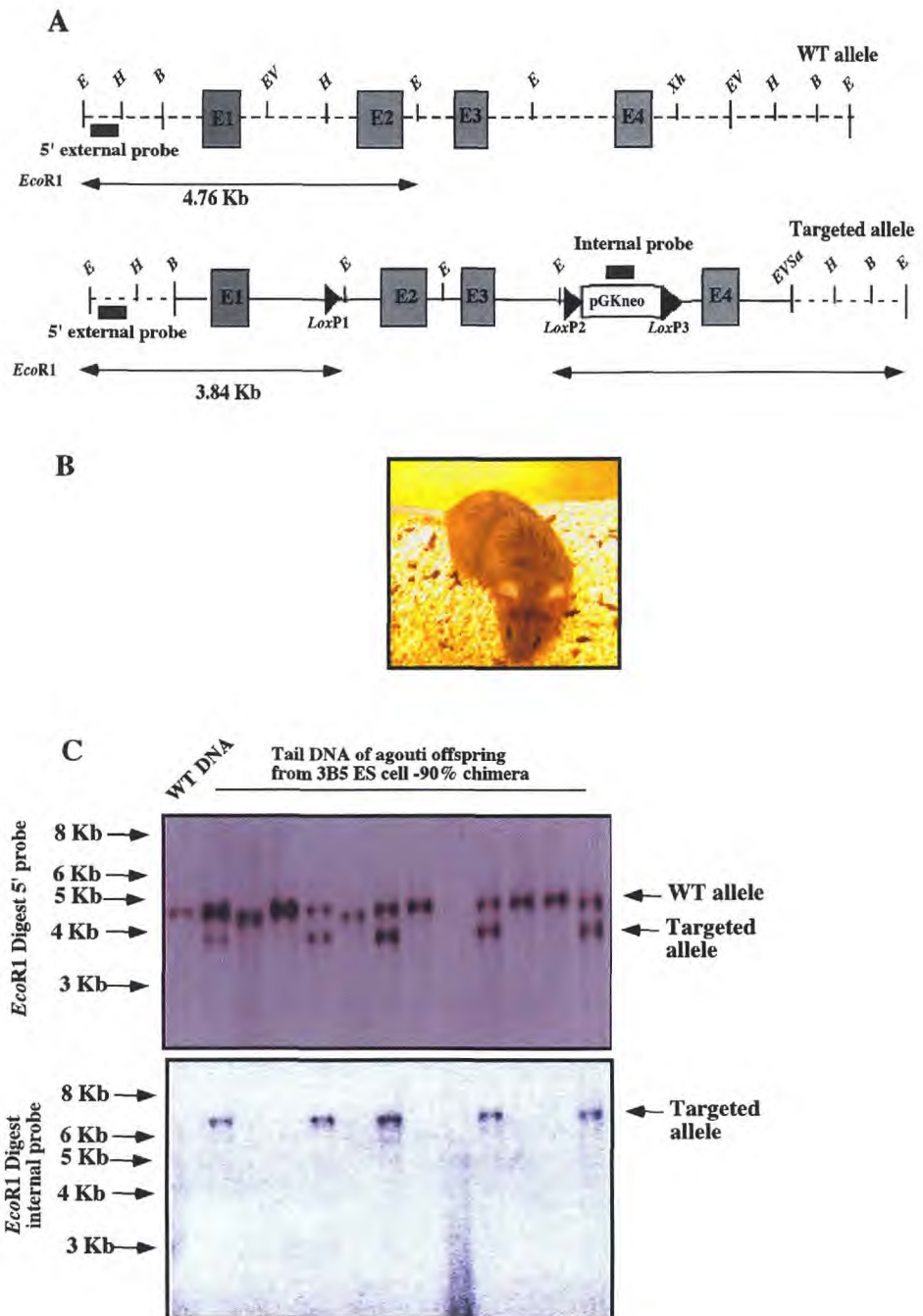


Figure 3.31.- Southern blot analysis of agouti animals heterozygous for the *Ctla-4* targeted allele. In A, a scheme shows the *EcoRI* restriction digests performed and the sizes of the expected restriction fragments. The location of the 5' external probe as well as the internal probe are indicated. In B, a photograph of the 90% chimera that transmitted the targeted mutation. The figure shows in C, (Top panel) hybridization using the 5' probe on DNA digested with *EcoRI*. The bottom panel corresponds to hybridization using the internal probe to analyze random integrations in these mice.

### 3.7 Concluding remarks.

#### 3.7.1 Estimation of the frequency of homologous recombination at the *Ctla-4* locus.

Values of the frequency of recombination are not often reported in gene targeting experiments. Previous knowledge of expected frequencies are useful to design future targeting experiments on previously mutated alleles as they can provide valuable information to decide, for instance; how many ES cell clones will be screened for homologous recombination and how such screening step should be performed.

*Ctla-4* has been targeted three times in the past (see chapter 1) but so far the frequencies observed have not been reported.

Here we found that three out of 221 individual ES cell samples were identified, initially by PCR and then confirmed by Southern blot, to have a single gene replacement of the entire targeting vector at the *Ctla-4* locus. This suggests an estimated 1.3% frequency of homologous recombination at this locus.

Further estimations, like the absolute frequency of recombination, are difficult to determine in this targeting experiment, as none of our ES cell samples were true clones, therefore the genotypes observed by PCR or Southern may not be a faithful reflection of the genotypes of all the individual ES cells in the sample.

#### 3.7.1 Towards a model for conditional inactivation of *Ctla-4*.

We have successfully generated and characterized by Southern blot, mice heterozygous for a *Ctla-4* targeted allele. This targeted mutation includes 3 Cre-recombinase sites, located in specific intronic regions of the *Ctla-4* locus, to allow further deletion by inducible recombination *in vivo*. The design of this targeting experiment, responds to the overall aim of generating mice possessing an allele in which exons 2, 3 and the neo cassette have been deleted, together with a further modification in the remaining allele, comprising the sole deletion of the neo cassette. This will leave exons two and three



(that code for the extracellular ligand binding and the transmembrane domains respectively) flanked by loxP sites (see figure 3.2). Mice with this genetic modification can be further crossed with a inducible Cre transgenic, such as Mx-Cre, (Khun. *et al* 1995) to generate a model for conditional inactivation of this regulatory gene.

### **3.7.3 Phenotypic analysis of mice bearing a targeted *Ctla-4* allele prior to any modification.**

*Ctla-4* has polymorphic variants that have shown to be significantly relevant for the function of this molecule. Sequence changes in either coding and non-coding segments of the gene have been implicated in alterations in the normal splicing and expression levels of the molecule. In fact there is ever-growing evidence that correlate such sequence variations to autoimmune disease in humans and mice (reviewed in Gough., *et al* 2005). For this reason we decided not to eliminate the selection cassette from targeted ES cells, for instance using transient transfection of Cre .

The genetic modification performed in this targeting experiment may generate an interesting phenotype in homozygous animals which can help to elucidate how *Ctla-4* is regulated.

In the next chapter we describe the data corresponding to a phenotypic characterization of heterozygous and homozygous *Ctla-4* targeted mice.

***Chapter 4. The phenotype of Ctlα-4 targeted mice***

## 4.1 Background.

Antibiotic selection cassettes such as the neomycin resistance gene driven by the PGK-1 promoter (PGK-neo), are invaluable tools as markers for homologous recombination in embryonic stem cells and transfected cell lines. As previously discussed, their sequences also serve as elements to disrupt the open reading frame of functionally important coding regions, when knock out mice are generated. This last methodology requires the retention of the selection marker, but that can often yield unexpected phenotypes. A striking example was illustrated by the myogenic basic helix-loop-helix gene (MRF4) knock outs. In this case, a range of targeting vectors was designed to produce knock outs. Homozygous animals generated from these mice showed a dramatic range of phenotypes; from complete viability to lethality. Further analysis demonstrated that the selection markers used altered the expression of downstream MRF genes in the cluster (Olson., *et al* 1996), generating a hypomorphic allele.

Other examples have also been reported in which the expression of neighbouring genes is affected by the insertion of selection cassettes, and they underscore the unpredictability of the phenotypes that can be caused by the retention of selectable markers.

The mechanisms that determine these effects are poorly understood, nonetheless the induction of neighbour effects have sometimes been useful to bypass the lethality produced when the gene of interest is involved in a vital biological process. Hypomorphic alleles have been recently used to study mice bearing a disruption in transport factor genes. These genes are crucial for development and embryos die early. To overcome the problem, a series of mouse mutants have been generated with varied levels of expression of this genes allow some mice to survive and therefore be studied (Dawlaty., *et al* 2006).

It would be of interest to generate mice bearing a hypomorphic allele of CTLA-4 for two reasons. First, two important and related molecules share a locus with *Ctla-4*. *Cd28* and in particular *Icos* are not only functionally related but also, they located closely upstream and downstream of *Ctla-4* respectively, possibly within range for a neighborhood effect.

Second, is the very well documented phenomena that discrete sequence variations, such as, single basepair changes in the coding and non-coding regions of this gene, can have important implications for its function, as well as being correlated with autoimmune disease (reviewed in Gough., *et al* 2005).

It has been reported that the existence of a polymorphism in exon 2 of the mouse *Ctla-4* correlates with diabetes in NOD mice (Vijaykrishnan., *et al* 2004). This sequence modification is believed to alter the splicing of CTLA-4 altering the production of an isoform highly expressed in diabetes resistant mice.

Taking into consideration all these aspects, we decided to generate homozygous and heterozygous mice bearing all the elements of the targeting vector (see chapter 3), with the aim of evaluating if the insertion of the *loxP* sites and particularly the PGK-neo cassette can alter the expression of *Ctla-4* or its neighbours and if that leads to a detectable phenotype.

The aims of this chapter are:

- Generate homozygous and heterozygous mice bearing targeted *Ctla-4* alleles.
- Characterize any possible phenotype developed by these mice by histologic analysis of the vital organs including secondary lymphoid tissue.
- To study the phenotype of their thymocytes and peripheral T cells either *ex vivo* or in culture, this in terms of surface markers and the expression of CTLA-4.
- Analyze the expression of the main CTLA-4 splice variants.

## **4.2 Generation of heterozygous and homozygous mice bearing a targeted *Ctla-4* allele.**

Gene targeting in ES cells was used to create mice having a targeted CTLA-4 allele (Chapter 3). This genetic alteration comprised the insertion of a floxed neomycin cassette in intron number 4 and a *loxP* site in intron 2 downstream exon 1. A germ-line transmitting chimera was bred to C57BL/6 females and progeny heterozygous for the CTLA-4 mutation produced. We then performed an intercross of two heterozygotes and the genotyping of the progeny resulted in the expected three allele combinations (figure 4.1).

Homozygous mice develop normally, show no obvious signs of disease and have a normal life span.

A PCR across the *loxP* site located downstream exon 1 was used throughout for genotyping. This reaction is able to selectively amplify a product from both alleles, thus allowing the detection of the presence and absence of the *loxP* site as a marker of the targeted allele see figure 4.1.

For all subsequent experiments animals of at least 16 weeks of age were used. All the experimental groups were selected using only littermates.

## **4.3 Histological analysis of CTLA-4 targeted mice.**

CTLA-4 knock out mice develop a lethal phenotype characterized by a severe interstitial infiltration of macrophages, neutrophils and lymphocytes. These mice show significant tissue damage in most organs (except kidney) but most lesions are dramatically observed in the pancreas and the heart. In the previous; destruction of both the islets and the glandular tissue is observed, and in the later, a mononuclear infiltrate and myocarditis observed.

The lymphoproliferation that characterizes this phenotype is evident in splenic histological sections of these mice. Normal spleen morphology is lost with only remnants of red pulp within an extended white pulp (Tivol., *et al* 1995).

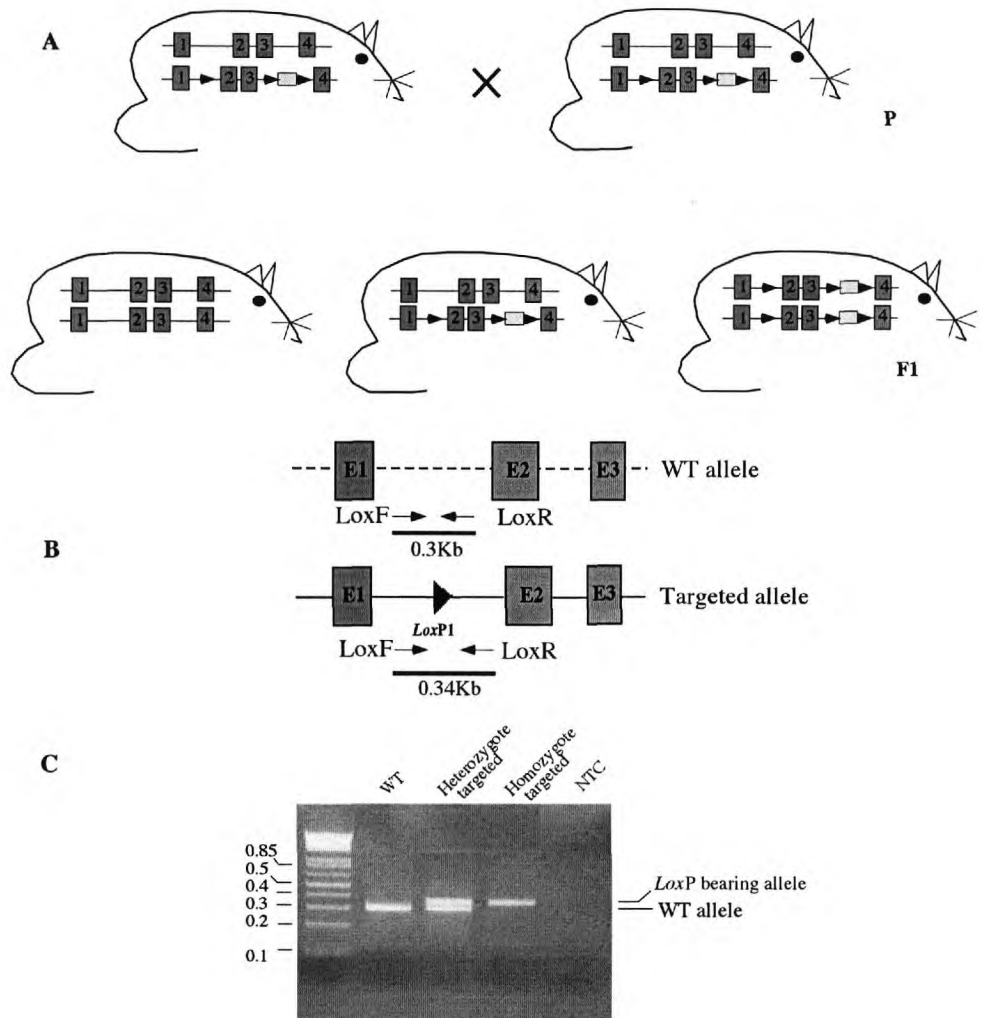


Figure 4.1.- Intercross of heterozygous animals bearing a targeted *Ctla-4* allele to produce homozygote mutants. Agouti littermates from the cross of the chimeric male and C57BL/6 females, were intercrossed as it is schematically shown in A, The genotype of the resulting offspring was determined by amplifying a 0.3Kb region downstream exon 2 of *Ctla-4*, using primers flanking the *LoxP* site in the region (B). PCR products were resolved on 2% agarose gels to discriminate between a product produced after amplification of an allele bearing a *loxP* site (targeted; 0.34Kb), and the corresponding WT allele lacking this sequence. Non template control (NTC) (C).

In contrast, microscopic analysis of Haematoxylin-Eosin (H&E) histologic sections revealed no malformation, infiltration or tissue damage when the organs of heterozygote and homozygote CTLA-4 targeted mice are compared with wild type littermates (figure 4.2). In addition, no signs of myocarditis and infiltration was observed in the heart or the pancreas, the organ that shows perhaps the most damage in the CTLA-4 knock outs and indeed in our mice where a full deletion of the gene has been produced ( Chapter 5). A normal morphology in the spleen was also observed with white and red pulps clearly defined. No signs of infiltration or altered morphology was detected in the kidney and thymus, that could suggest pathology. CTLA-4 knock outs show no infiltration or damage in the kidney (Waterhouse., *et al* 1995).

During the dissection of mice, homozygous individuals were observed to possess enlarged lymph nodes and Peyer's patches when compared with wt littermates (see figure 4.3 A). Lymph node tissue from homozygotes showed enlarged follicles and clear germinal centres. The Peyer's patches in this mice showed a greater cell density in the follicular area (figure 4.2 arrowed). Both observations may indicate an accumulation of B cells. Despite this accumulation in the Peyer's patches, no infiltration or damage was observed in the neighbouring bowel.

Throughout the analysis heterozygous individuals showed no differences when compared with wild type.

#### **4.4 Homozygous *Ctla-4* targeted mice develop lymphadenopathy.**

The increase in size of the lymph nodes from homozygous animals (figure 4.3 A) was reflected in an increase in the number of total lymphocytes that could be isolated.

Lymph node cells collected after dissections were counted and viable cell numbers directly compared between animals. The increased cellularity observed in lymph nodes of homozygous animals, as compared with wild type and heterozygous littermates, was statistically significant  $p < 0.05$  (figure 4.3).

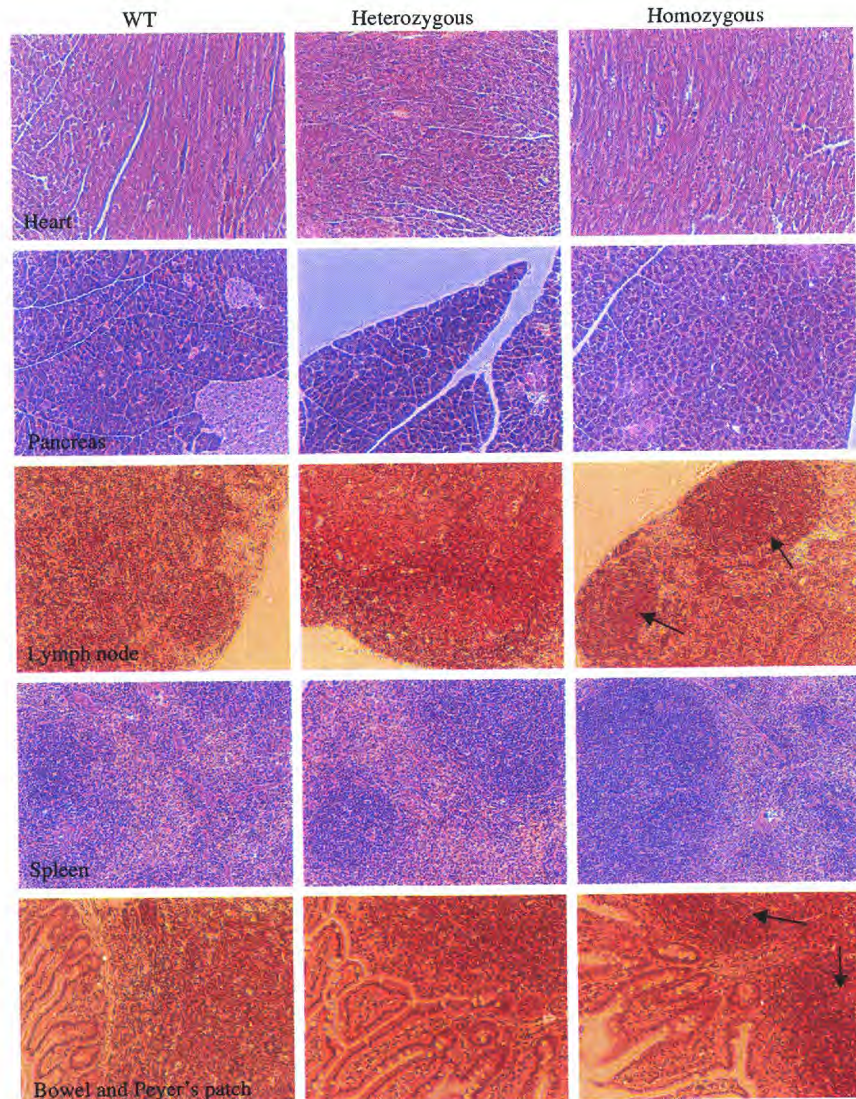


Figure 4.2.- Hystologic analysis of organs from *Ctla-4* targeted mice. Tissue sections from parafin embedded organs were stained with H&E and visualized under optical microscopy. All photographs are mignified 10X. Areas of greater cell density are shown with arrows.



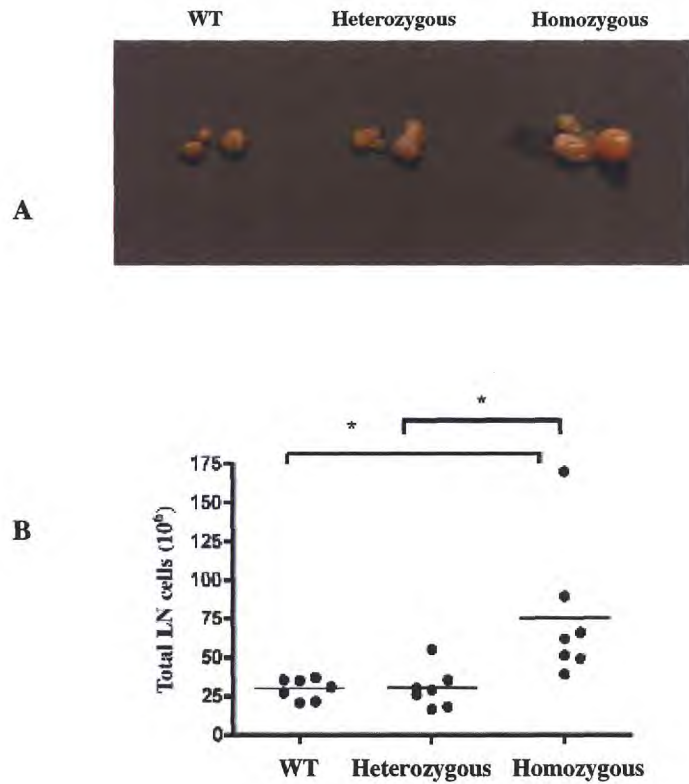


Figure 4.3.- The lymphadenopathy observed in homozygous mice is reflected in increased cell numbers. In A, the comparative sizes of three lymph nodes (brachial, mecenteric and inguinal) extracted from wild type, homozygous and heterozygous mice. In B, Total viable lymph node cells were counted after gentle masceration of nodes. The mean cell count of 7 independent observations (horizontal lines) are compared between genotypes (\* $p < 0.05$ ).

Cellularity of the spleens of these mice was also evaluated and no significant differences were observed between genotypes. There was a considerable variability in the data from different animals perhaps due to the extraction methods employed for this tissue. The data shown in figure 4.4 corresponds to counts from 4 different mice.

The possibility that the increased cellularity seen in the lymph nodes of homozygous mice could be the result of an altered proportion of different lymphocyte populations, was suggested by the observation that greater cell density was evidenced in areas restricted to B cells. Flow cytometry was used to assess the proportions of T cells and B in the lymph nodes of these mice. This analysis demonstrated a greater percentage of B cells, reflected in a greater absolute number of CD19<sup>+</sup> positive cells in homozygous when compared to wt and heterozygous-targeted littermates. Those differences were statistically significant ( $p < 0.05$ ). (see figure 4.5).

The expected proportion of T cells in the mouse lymph node is about 60% to 70% and for B cells the normal percentage is lower being; between 15% to 20%, as observed here in WT mice, Mice homozygous for the targeted *Ctla-4* allele, besides having a slight but not significantly lower percentage of T cells, show no significant differences in the absolute numbers of these cells when compared WT littermates. Further phenotypic analysis of the T cell compartment is necessary to determine if these cells are involved in the increased B cells activation seen in homozygous mice.

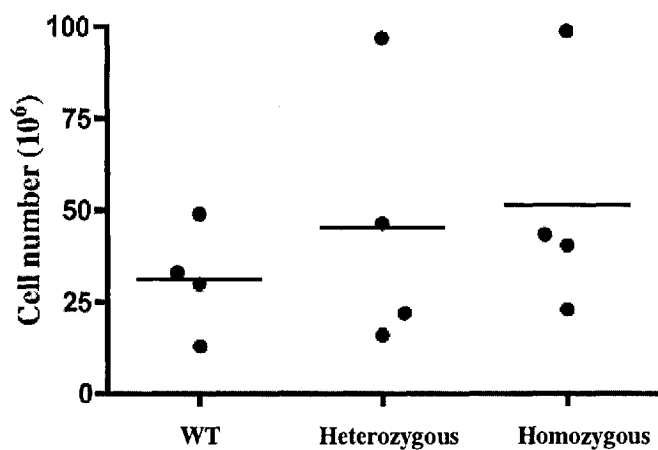


Figure 4.4.- Total cell counts in the spleen of wild type, heterozygous and homozygotes animals. The mean of 4 independent observations (horizontal lines) are compared between genotypes.

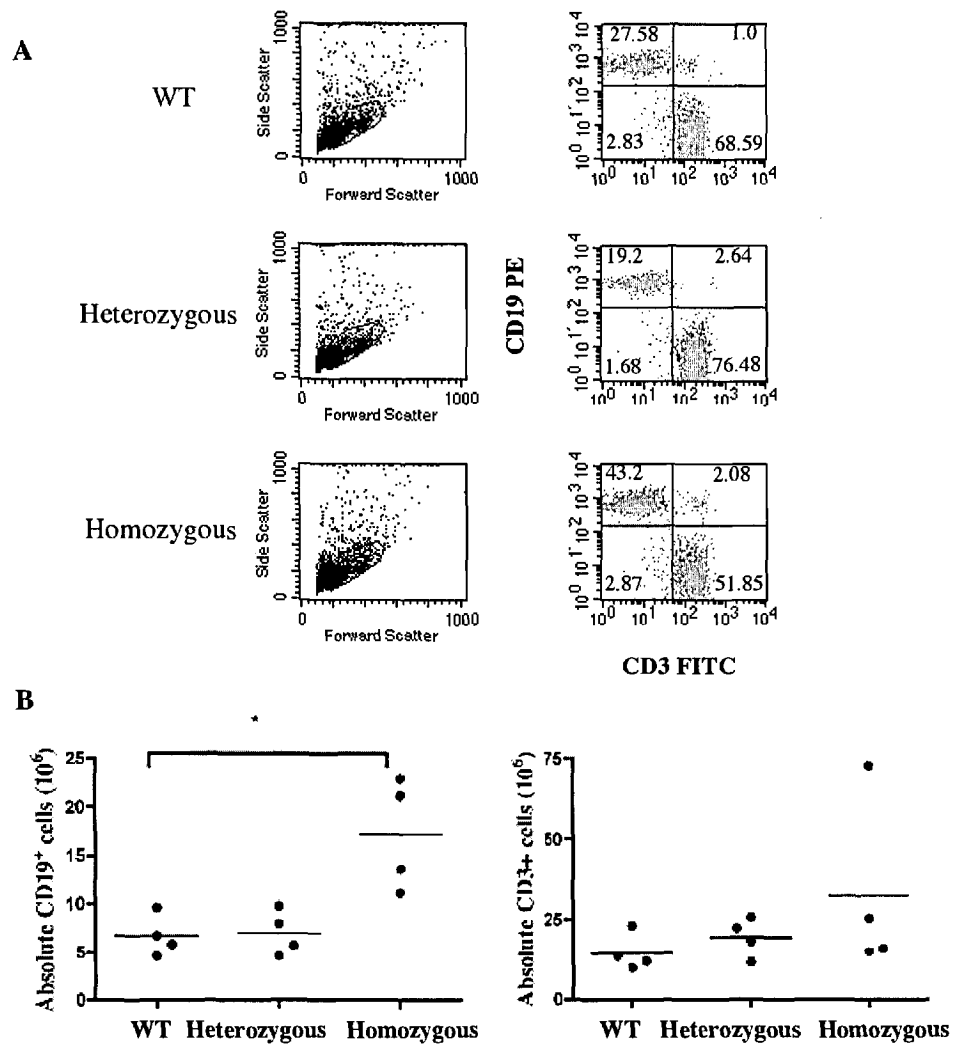


Figure 4.5.- Increased lymph node cellularity observed in homozygous *Ctla-4* targeted mice results from an increased proportion of B cells.

In A, CD19 vs CD3 scatter plots gated on live cells on the basis of SSC and FSC.

In B, the plots shown are representative of 4 independent experiments (\* $p < 0.05$ ), differences for the absolute numbers of CD19<sup>+</sup> cells were analyzed by a one-way ANOVA with Dunnett's post test.

## **4.5 Homozygous mice have an increased proportion of CD4 single positive thymocytes and lower numbers of double positive thymocytes.**

Thymi were harvested and analyzed to test for alterations in the development of T cells as this could alter the proportion of T cells populating the periphery.

The thymocytes of homozygous mice when compared to wild type and heterozygous individuals showed a moderate but consistent trend of an increased percentage of single CD4 positive thymocytes, together with an overall reduced proportion of CD4, CD8 double positive cells. Variations in CD8 single positives and double negative thymocytes were not consistent between independent experiments.

Figure 4.5 shows a comparative set of representative CD4 vs CD8 scatter plots of mice with the three genotypes of interest.

It is important to consider that this data is preliminary and the variations observed may not be greater than what expected by chance. Further analyses of these subpopulations on a larger sample are required to determine if these differences are real.

The same analysis was performed on lymph node cells of the experimental animals, but there was no indication of an alteration in the T cell compartment of this organ. Figure 4.7 shows this as a dispersion plot of data cumulative of 4 independent experiments.

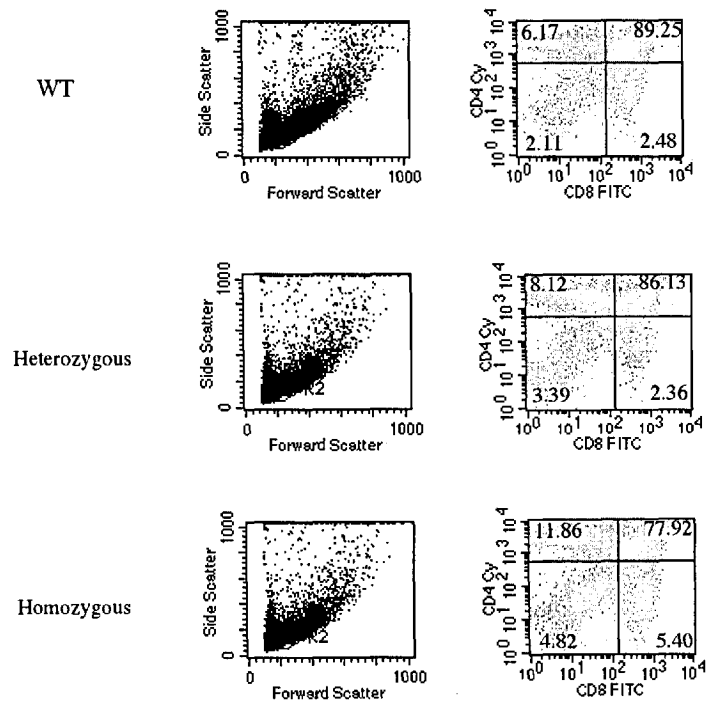


Figure 4.6.- Homozygous animals have a distinct CD4-CD8 profile in thymus when compared to WT or heterozygous individuals. The figure shows CD4 vs CD8 scatter plots gated on live thymocytes on the basis of SSC and FSC. The data is representative of 3 independent experiments and the percentage of cells in each quadrant correspond to gated events.

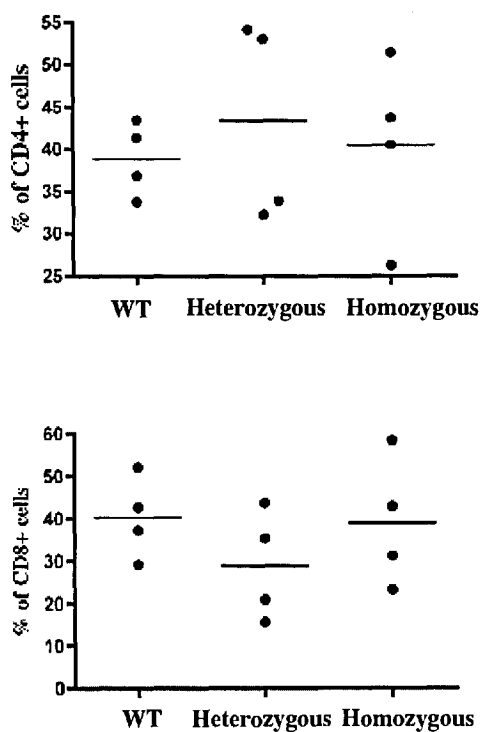


Figure 4.7.- Percentage of CD4<sup>+</sup> and CD8<sup>+</sup> T cells in lymph nodes from CTLA-4 targeted mice. The data is cumulative of 4 independent experiments and represents a percentage of either CD4 or CD8 positive cells from a gate of live cells determined by their parameters of FSC and SSC.

## **4.6 *Ex vivo* analysis of the activation state of T cells from experimental animals.**

The activation status of T cells from experimental animals immediately *ex vivo* was then examined. CD69 is an early marker of activation not present constitutively in the surface of peripheral blood T cells but expressed upon activation. This marker is useful for our analysis as its expression may indicate the presence of a “recent” or maybe continuous activation signal in the lymph nodes of this mice. This may seem unlikely from the data already described but important in view of the increased proportion of B cells observed in the lymph nodes of homozygous animals. CD25 is upregulated later after activation when compared with CD69 and if present differentially on the T cells of homozygous mice, may serve as evidence to suggest an increased T cell activation state in this mice.

As shown in figure 4.8 the percentage of cells expressing either CD69 or CD25 in cells extracted from lymph nodes from homozygote animals, are similar to the values observed for wild type and heterozygous T cells. This observation suggest that T cell activation in homozygotes remains normal, and this is consistent with the observations that the percentages of T cells in the enlarged lymph nodes of homozygous animals are within normal levels or even lower (figure 4.5)



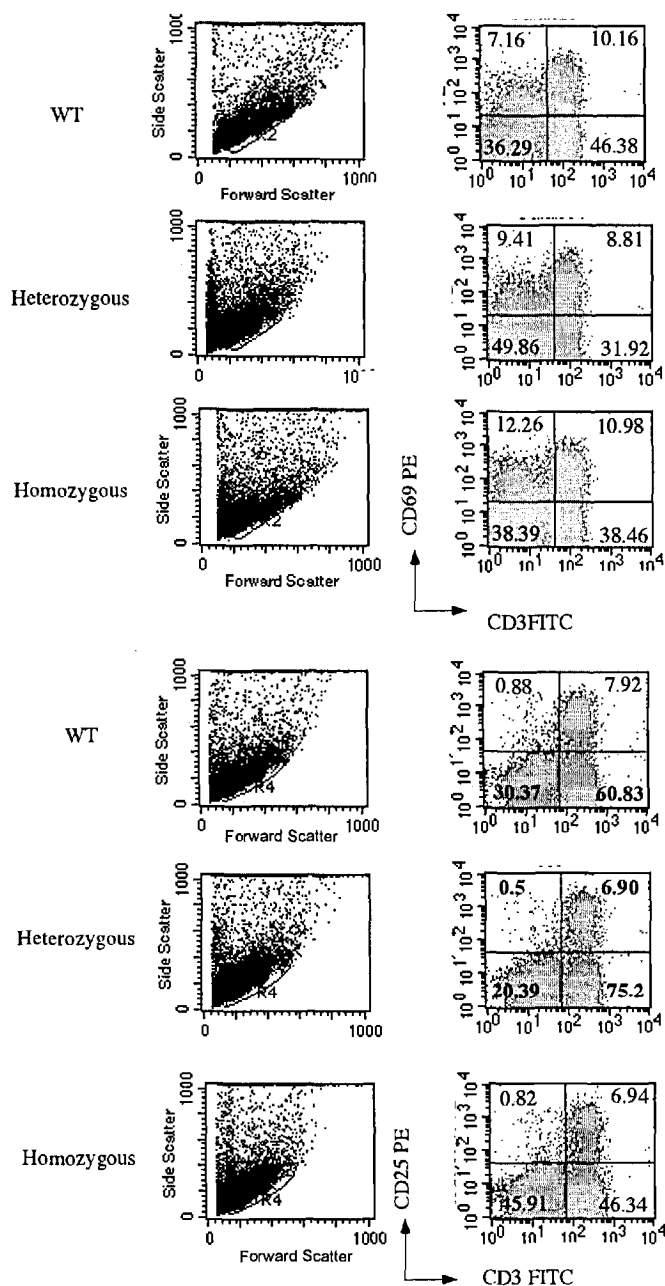


Figure 4.8;- Percentage of lymph node cells expressing the activation markers CD69 and CD25 is similar between experimental animals. Freshly isolated cells from lymph nodes were double stained with antibodies specific for CD3, CD69 and CD25. The percentages of CD3<sup>+</sup> CD69<sup>+</sup> cells (top three panels) and CD3<sup>+</sup> CD25<sup>+</sup> cells (bottom panels) are reported and correspond to gated events. These data are representative of 5 independent experiments.

## **4.7 T cells from homozygous mice over-express CTLA-4 upon polyclonal activation.**

As described in section 4.1 there are reasons to think the modifications we have performed to the genomic CTLA-4 sequence in the targeting process can alter the genetic regulation of this important gene. It has been reported that naturally occurring single nucleotide modifications can modify the expression of splice variants of this molecule and in general, ever-growing evidence point that these sequence variations can associate with autoimmunity (reviewed in Gough., *et al* 2005). Our observations in homozygous animals indicate a mildly abnormal phenotype.

With this in mind, the levels of expression of CTLA-4 in the different genotypes of the targeted CTLA-4 mice were therefore assessed. CTLA-4 is only expressed in T cells following activation and direct surface staining has proved difficult due to the dynamic regulation and internalization that controls the levels of membrane expression of this molecule. Intracellular staining, using fixed and saponin-permeabilized cells, was therefore performed.

At resting, freshly extracted total lymphocytes from lymph nodes of the mice, did not express CTLA-4 (figure 4.9), data consistent with the reported kinetics of expression of this molecule, but at day 3 and day 5 of culture (1 $\mu$ g/ml anti CD3) very significant over expression in cells from homozygotes as compared with wt littermates was observed. Heterozygous mice showed an intermediate level of expression when compared with homozygous and wt littermates, and this trend was observed more clearly at day 3 ( $p < 0.01$ ) than at day 5 ( $p < 0.05$ ). Data cumulative of at least 4 independent observations is shown in figure 4.10. The same phenomena was observed on CD3 purified T cells (figure 4.11) when costimulation was not provided by APC but by using CD28 antibody (figure 4.12).

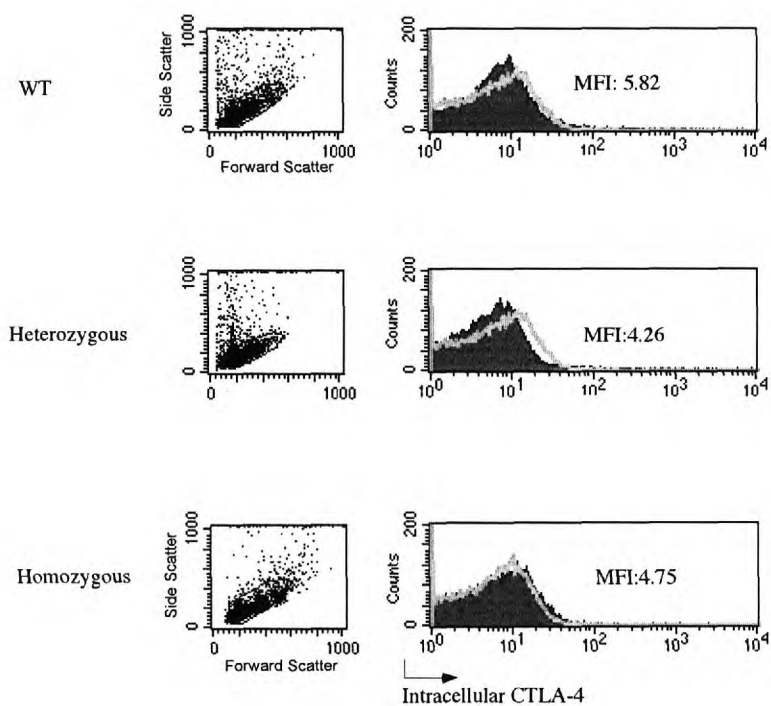


Figure 4.9.- Resting total lymph node cells do not express CTLA-4 intracellularly. The figure compares the expression of intracellular CTLA-4 of freshly extracted lymph node cells from wild type, heterozygous and homozygous mice. The mean fluorescence intensity reported corresponds to the value of all gated live cells. Intracellular isotype control stain is overlaid. The data is representative of 5 independent observations

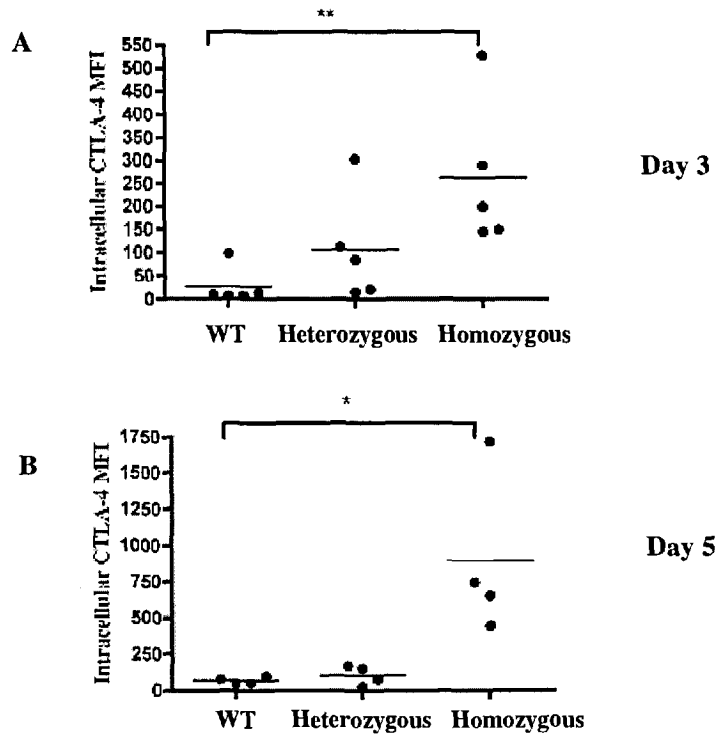


Figure 4.10.- Lymphocytes of homozygous mice over-express intracellular CTLA-4 upon activation. The graphs show the CTLA-4 intracellular expression on activated total lymphocytes (1 $\mu$ g/ml anti CD3) in culture at day 3 (A) or day 5 (B). The expression is reported as the mean fluorescence intensity of the total gated live cells. \*\*( $p < 0.01$ ) \* ( $p < 0.05$ ) as determined by a Kruskal Wallis test with Dunn's post test.

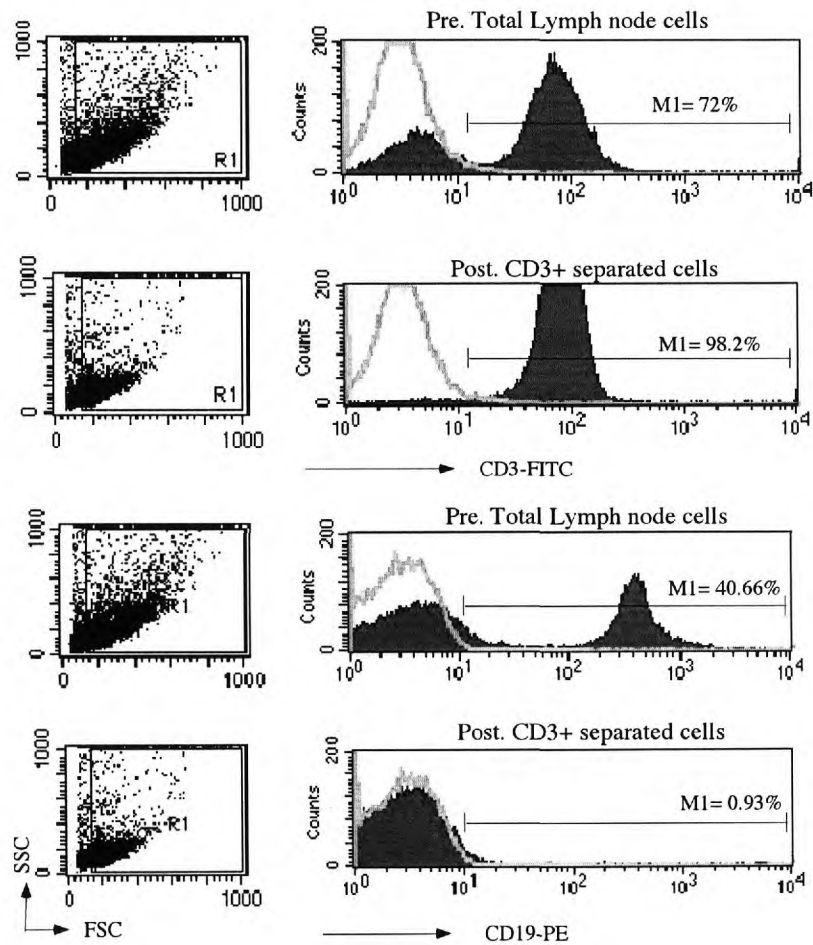


Figure 4.11 Purity assesment after CD3+ T cell negative isolation with paramagnetic beads. The histograms show the intensity of fluorescence of either total LN cells (pre) or isolated CD3+ T cells (post). Purity is expressed as % of cells gated for viability and either positive for CD3 (T, NK cells), or negative for CD19 (B cells) (see M1). The overlay correspond to the isotype control. All experiments were performed with purities not lower that 98%.

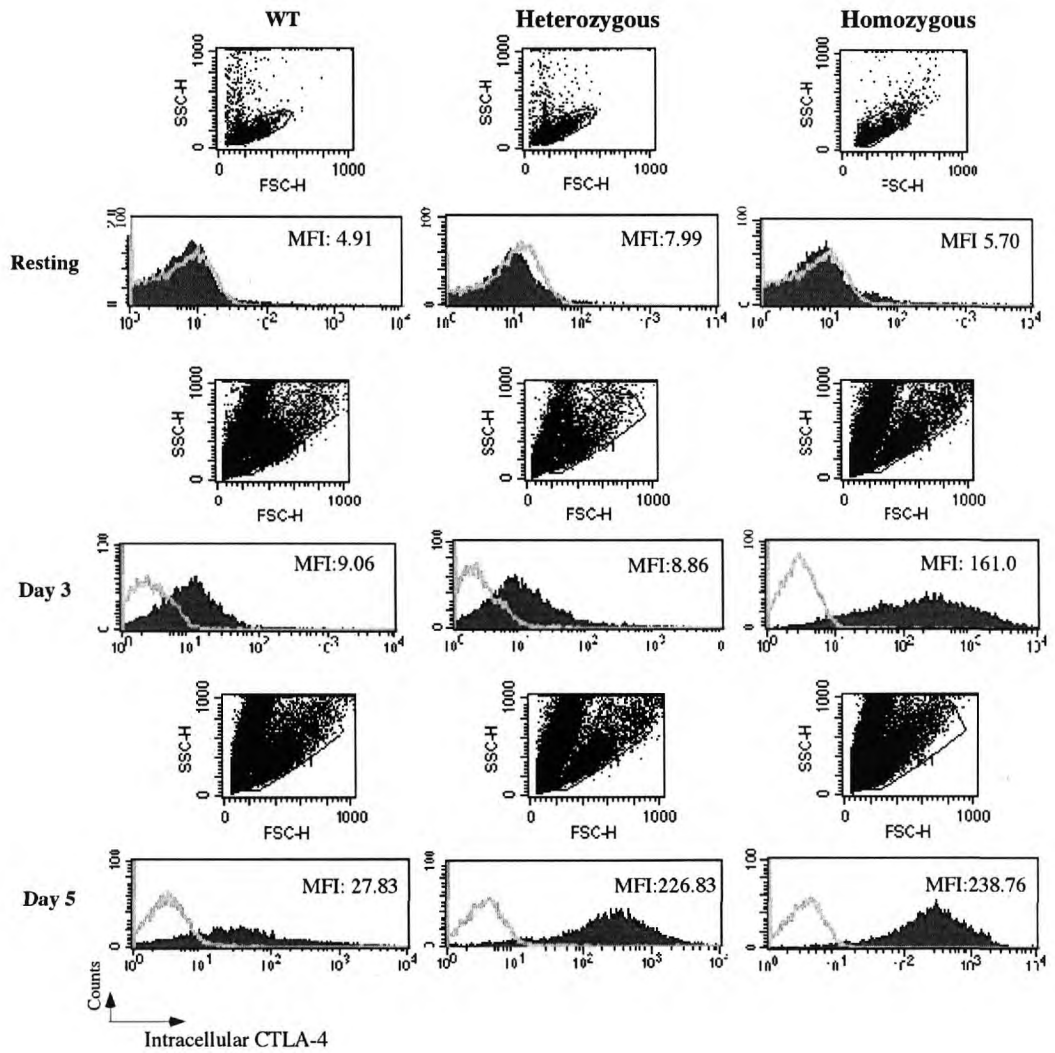


Figure 4.12.- Intracellular expression of CTLA-4 increased in homozygotes as compared with littermates. Side scatter vs forward scatter plots and histograms show the intracellular expression of CD3<sup>+</sup> T cells in culture over a period of 5 days. Plots report the MFI of the gated live cell population and overlaid with the corresponding isotype control. The data are representative of 4 independent experiments.

## **4.8 CTLA-4 over-expression is not associated with heterogeneity in background.**

The CTLA-4 targeted mouse line originally established, which we have used for the vast majority of the phenotypic characterization reported here, possesses a heterogeneous genetic background being descendants of the F1 from the 129Sv-B6 chimera (Chapter 3) and C57BL/6 females. The mix of genetic information of the strains 129SvPAS (ES cells) and C57BL/6 in the mice analyzed, is not desirable as it can influence the phenotypes observed. In order to determine if the phenotypic characteristics previously observed in the *Ctla-4* targeted mice were influenced by the genetic heterogeneity, we generated a new line of targeted mice possessing the same genetic modification but on a pure 129 background.

These mice were produced by crossing the 129 chimera with WT 129SvPAS females and by subsequently establishing the germline transmission of the targeted mutation by Southern blot analysis of all the progeny of this cross (figure 4.13).

The F1 offspring from heterozygous targeted mice, on the 129SvPAS pure background, were genotyped using a PCR across the *loxP* site downstream of exon 1.

Once homozygous and heterozygous targeted mice were obtained, we performed dissections and as before, enlarged lymph nodes were observed. CTLA-4 expression on total lymph node cells of these animals was evaluated and as shown in figure 4.15, the lymph node cells from these mice show the CTLA-4 over-expression previously observed in mice on a mixed background. This rules out the possibility that the effect observed could be influenced by genetic heterogeneity. It is nevertheless important to mention that so far only one observation has been recorded, and further analysis of this new genetically modified line is required.

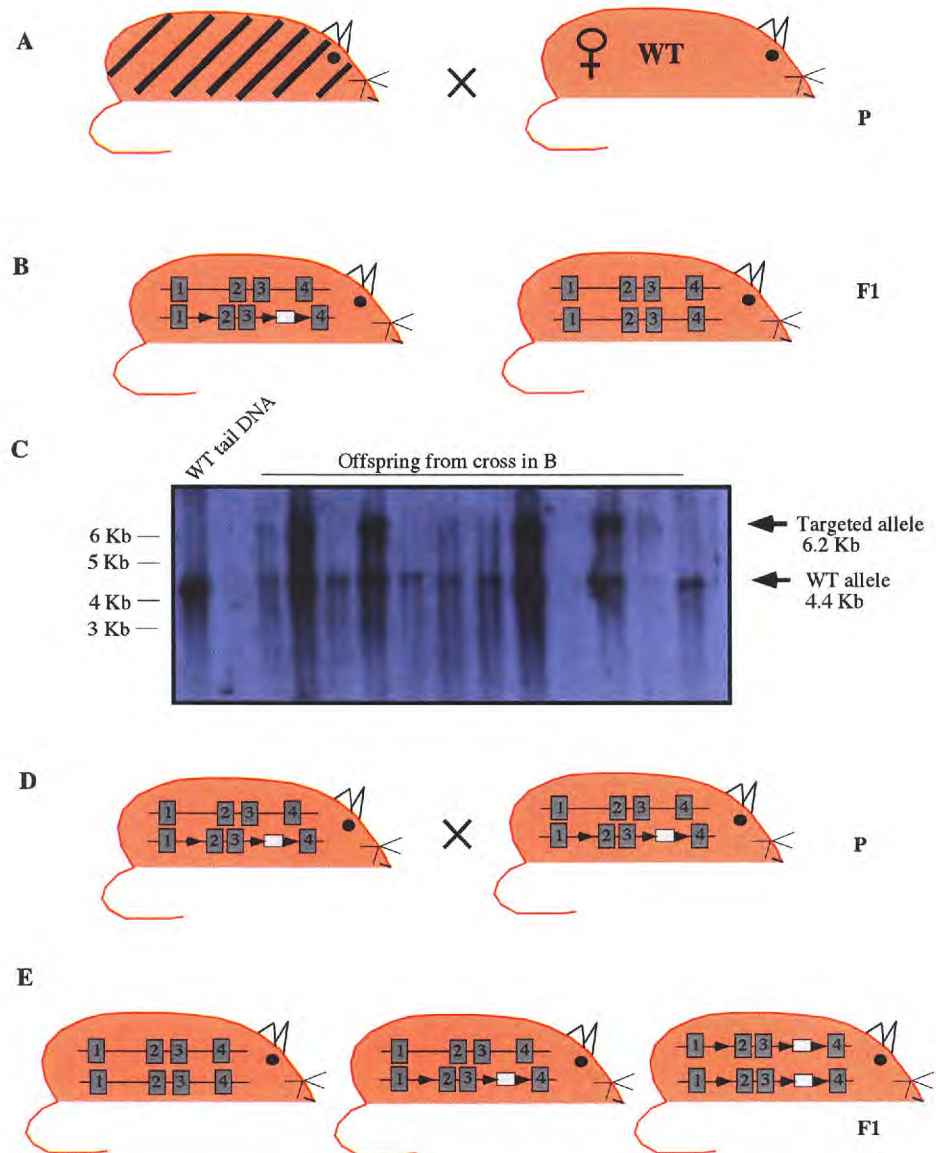


Figure 4.13.- Generation of a line of CTLA-4 targeted mice on a 129SvPAS (of agouti coat colour) pure background. (A). The 129-B6 chimera (see chapter 3) was crossed with 129Sv PAS wild type females to transmit the targeted CTLA-4 mutation through the germline of a pure 129Sv background. Southern analysis from tail DNA of the all the offspring (B) was performed to establish germline transmission. CTLA-4 targeted founders were inter-crossed (D) to obtain mice bearing the CTLA-4 targeted allele in homozygosity (E).



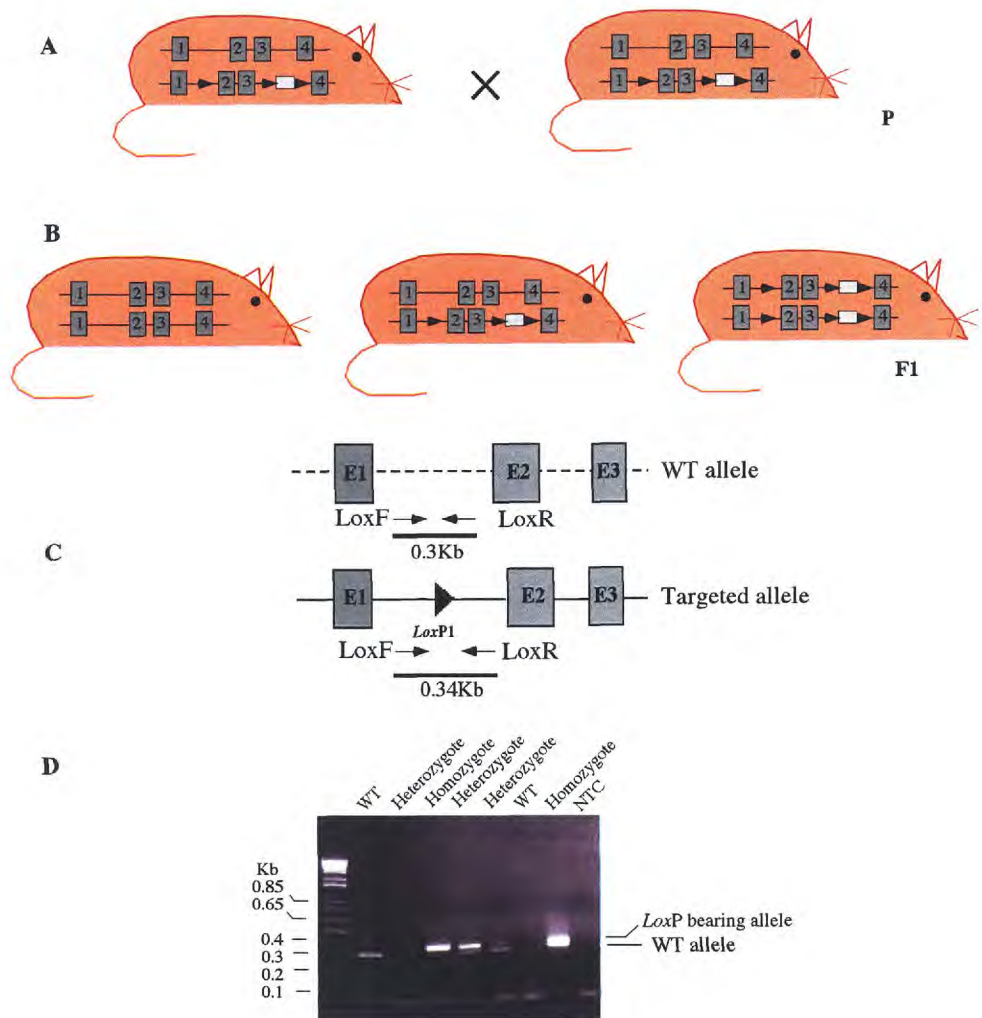


Figure 4.14.- Intercross of heterozygous animals bearing a targeted *Ctla-4* allele to on a 129SvPAS background to produce homozygote mutants (A). The genotype of the resulting offspring (B) was determined by amplifying a 0.3Kb region downstream exon 2 of *Ctla-4*, using primers flanking the *LoxP* site in the region (C). PCR products were resolved on 2% agarose gels to discriminate between a product produced after amplification of an allele bearing a *loxP* site (targeted; 0.34Kb), and the corresponding WT allele lacking this sequence. Non template control (NTC) (D).

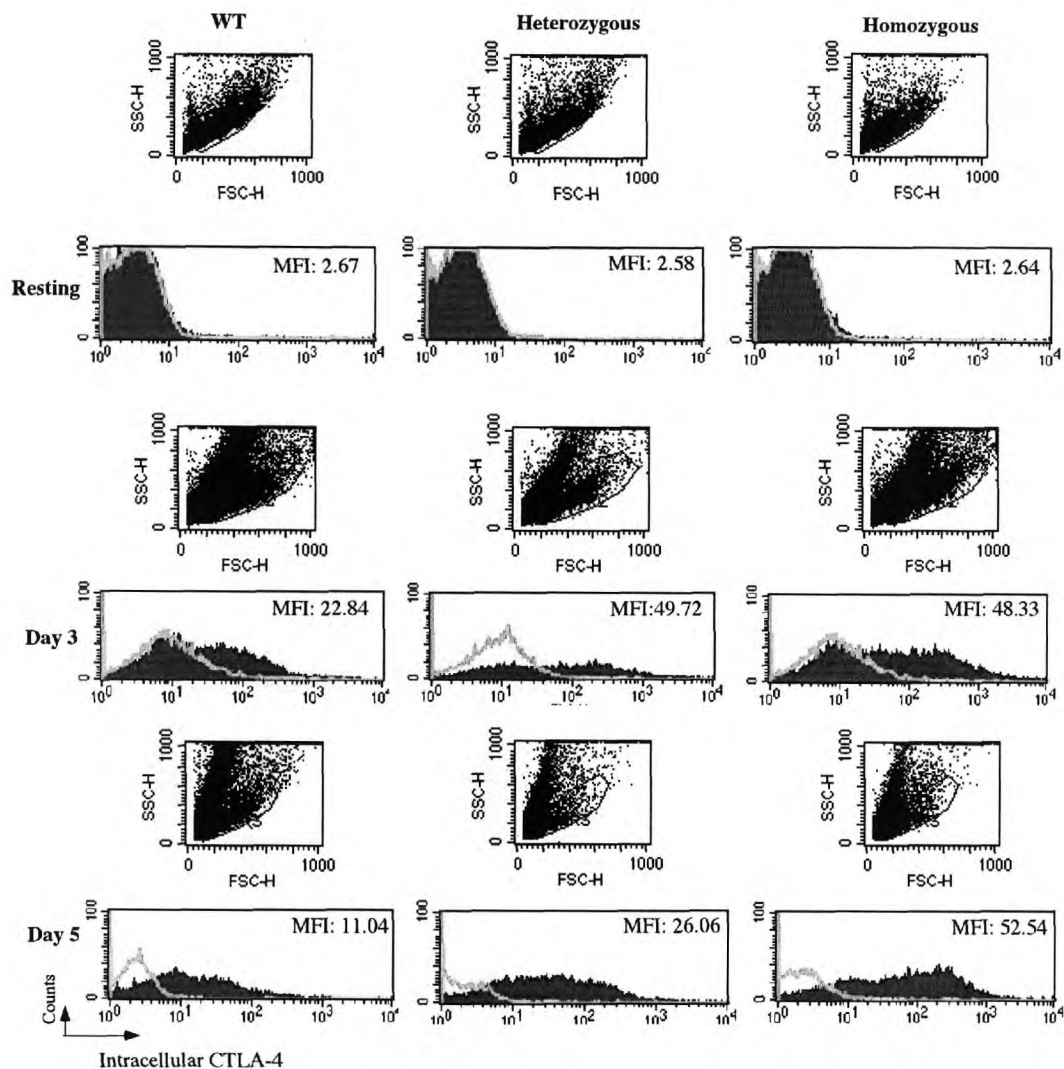


Figure 4.15.- Intracellular expression of CTLA-4 is also increased in 129SvPAS homozygotes as compared with littermates. Side scatter vs forward scatter plots and histograms show the intracellular expression of LN cells in culture over a period of 5 days. Plots report the MFI of the gated live cell population and overlaid with the corresponding isotype control. The data corresponds to a single observation.

#### **4.9 Activated lymph node cells from homozygous mice express higher levels of CD25 but do not proliferate differentially.**

Upon activation, homozygous mice express higher levels of intracellular CTLA-4 compared to wild type or heterozygous littermates. In order to evaluate if this had a functional outcome, we compared the ability of lymph node cells to proliferate *in vitro* under the standard conditions of polyclonal stimulation use throughout this analysis. We first observed that after a period of 72h of polyclonal stimulation with antibodies (anti CD3 and anti CD28 both at 1µg/ml), CD3<sup>+</sup> cells of homozygous mice expressed greater levels of CD25 as compared to wild type littermates. Heterozygous animals showing an intermediate level of expression. This observation suggested that cells from homozygotes are able to reach a higher level of activation, however this was not reflected in proliferation as measured by tritiated thymidine incorporation.

Figure 4.15 shows a comparative analysis of the expression of CD25 by CD3<sup>+</sup> cells from lymph nodes in culture. Homozygous mice showed increased CD25 expression, measured as percentage of positive cells and intensity of fluorescence, although there are no clear differences in the proliferation of CD3<sup>+</sup> cells, as assessed by <sup>3</sup>H-Thymidine incorporation, from this mice when compared with the littermates.

Altogether these observations suggest that the CTLA-4 over expression seen in homozygous mice, may have a potential functional implication inhibiting T cell proliferation. This evidence is consistent with the lack of irregular T cell proportions in the lymph node of these mice.

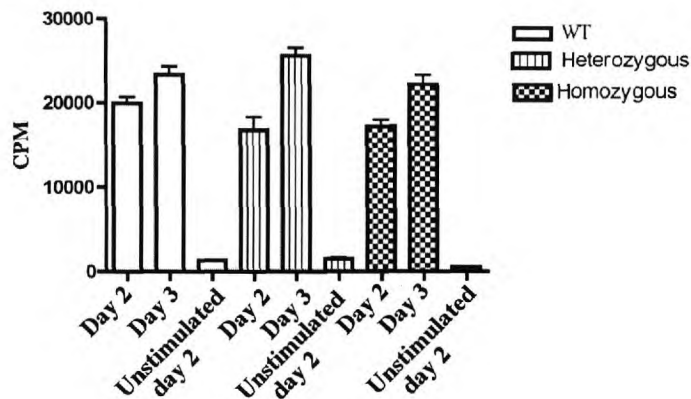
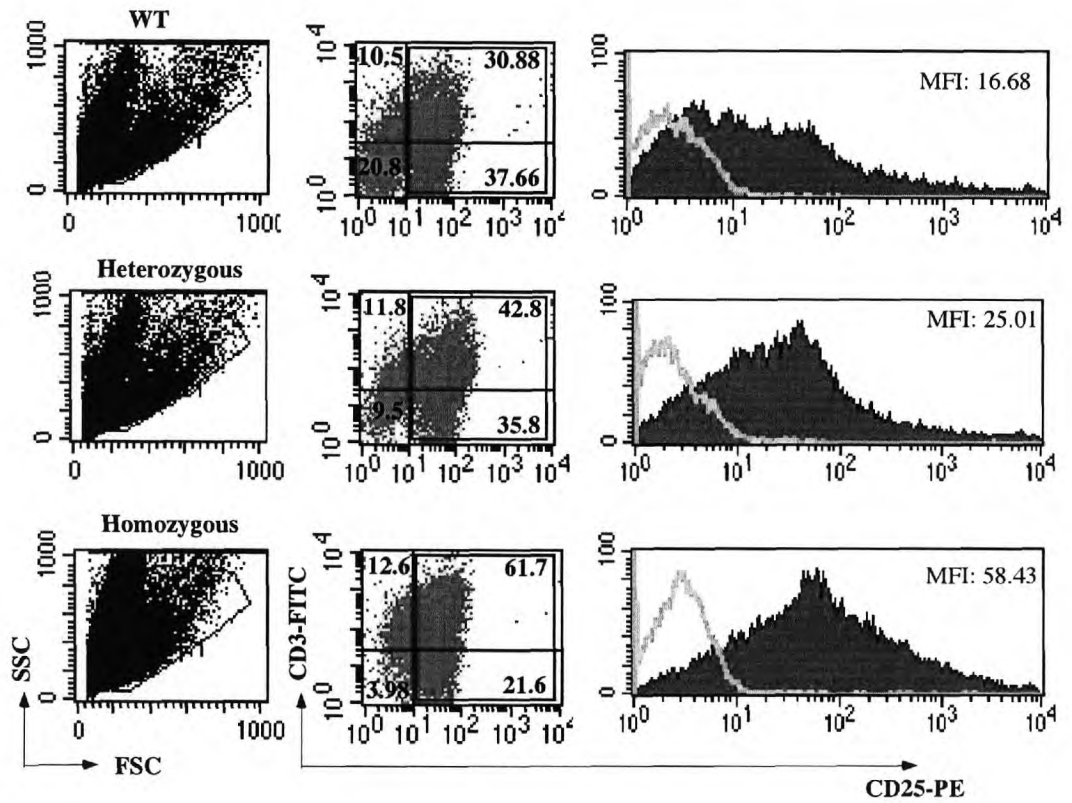


Figure 4.16.- Homozygous CD3<sup>+</sup> cells express higher levels of CD25 but does not proliferate differentially. Top panels show a comparative flow cytometry analysis of the CD25 expression of viable CD3<sup>+</sup> cells from lymph nodes. The expression is reported in percentage of positive cells or intensity of fluorescence and the data is representative of 5 independent observations. The graph at the bottom shows the comparative proliferative responses of total lymph node cells stimulated with 1 µg/ml of anti CD3 and anti CD28. The data is representative of 2 experiments. Percentiles show the SEM calculated from the triplicates in the assay.

## 4.10 Analysis of the expression of known *Ctla-4* splice variants.

It has been recently postulated that changes in the expression patterns of functional CTLA-4 splice variants may contribute to the control of autoimmunity (Ueda., *et al* 2003 & Vijayakrishnan., *et al* 2004). One of the functional splice variants in mice is LiCTA-4, an isoform produced after skipping exon 2, its open reading frame therefore lacking the B7 binding domain. The expression of this isoform on lymph node cells from of our mice was therefore evaluated by Western blot using a polyclonal antibody specific for intracellular domain of CTLA-4 (C19).

The analysis was restricted to resting lymphocytes because, in contrast to full length CTLA-4, LiCTLA-4 shows maximal expression on resting T cells (Vijayakrishnan., *et al* 2004). No differences in the expression of LiCTLA-4 were observed between homozygous and heterozygous or wt littermates, suggesting normal levels of expression of this isoform at least at resting (figure 4.17).

The expression kinetics of all known CTLA-4 splice variants was then explored by RT-PCR. Using primers published in (Vijayakrishnan., *et al* 2004) (figure 4.18) all the known CTLA-4 splice variants were amplified from cDNA produced from either resting or activated purified CD3<sup>+</sup> T cells from the lymph nodes of targeted mice.

Striking differences were observed between the homozygotes and wild type or heterozygote in terms of the relative levels of expression of Fl-CTLA-4, sCTLA-4 and LiCTLA-4 mRNA.

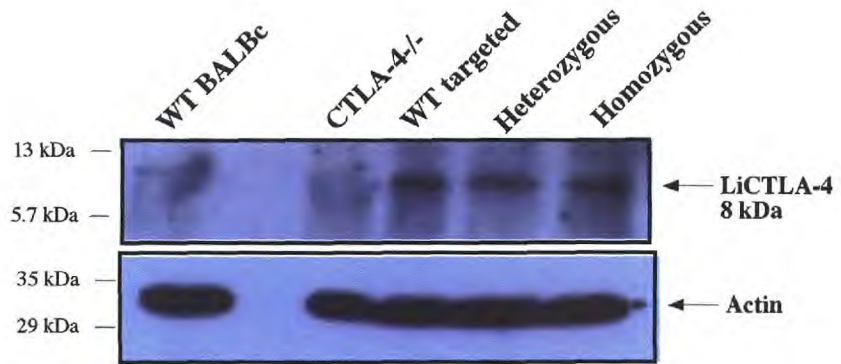


Figure 4.17.- Li-CTLA-4 expression is similar in homozygous targeted mice as compared to littermates. 10ug of total protein from lysed resting lymphocytes was separated by SDS-PAGE and transferred to PVDF membrane for blotting with an anti CTLA-4 antibody, specific for the intracellular domain (C19). Positive (BALBc total lymph node cells) and negative controls (CTLA-4<sup>-/-</sup> cells) were also analyzed. Equivalent amounts of protein were loaded to the gel as shown by the actin expression levels. Data representative of one single observation.

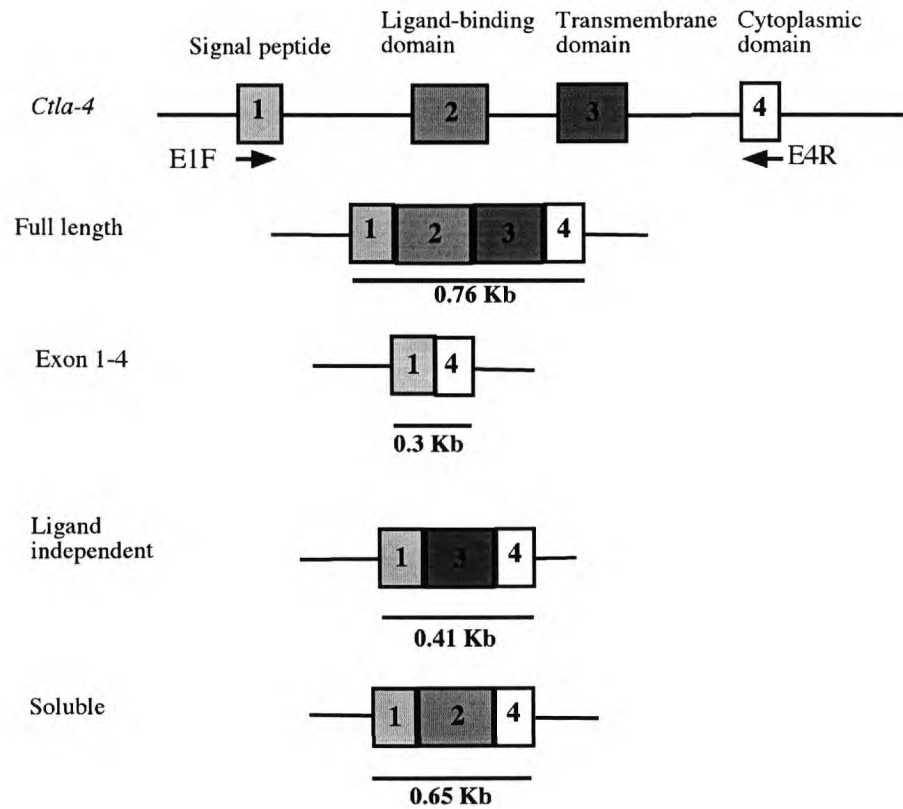


Figure 4.18.- *Ctla-4* and its splice variants. *Ctla-4* has four exons encoding different polypeptide chains (top). Four different splice variants have been identified at the level of mRNA and RT-PCR products product can be amplified using primers homologous for exon one and four.

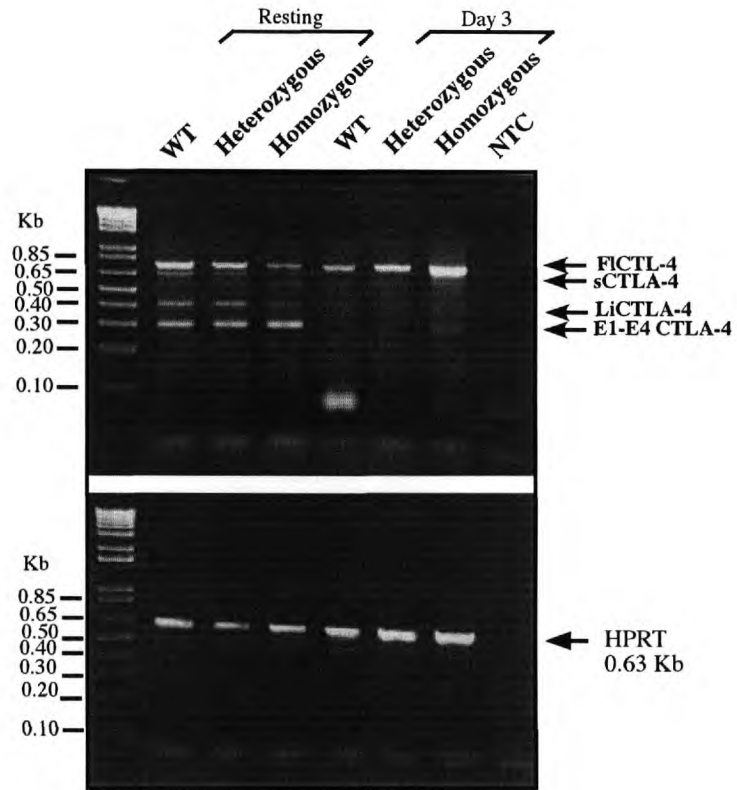


Figure 4.19.- The kinetics of expression of all splice variants are altered in homozygous targeted mice as compare with littermates. The figure shows PCR amplifications from cDNA of either resting or activated CD3<sup>+</sup> T cells from targeted mice. Polyclonal activation was performed with CD3, anti CD28 mAb both at 1 $\mu$ g/ml in culture for a period of 3 days. Top panel shows the amplification of all *Ctla-4* splice variants in one reaction. The bottom panel shows an amplification of HPRT as a qualitative control for the amount of RNA used to reverse transcribe to cDNA. Samples with no template were used as negative controls. The products are resolved in a 1.8% agarose. Data representative of two independent experiments.



Using a non-quantitative RT-PCR performed on cDNA from either resting or activated CD3<sup>+</sup> T cells differences in the abundance of three of the four splice variants of CTLA-4 were observed. Resting T cells from homozygous mice showed apparently lower levels of FlCTLA-4 as compared to WT or Heterozygotes after 3 days of activation. These T cells produced increased levels of this variant as compared with its littermates. This is consistent with the differences obtained by flow cytometry. In contrast PCR indicates lower transcript levels corresponding to sCTLA-4 and LiCTLA-4 in homozygotes than those produced by the littermates at resting. After activation, homozygous mice appear to produce slightly higher levels of both variants as compared with the littermates at that time point (see figure 4.19).

No absolute comparisons can be drawn from this analysis as this RT-PCR used is not quantitative. Nonetheless, it is possible to suggest that homozygous individuals have a differential ratio of expression between splice variants. Confirmation of this results by quantitative RT-PCR is essential.

## 4.11 Discussion.

The insertion of a PGK-neomycin cassette located in an intronic region downstream the coding region for the transmembrane domain of CTLA-4 may interfere with the networks of gene regulation and alter not only the gene that contains the sequences but also neighbouring genes as far as 100Kb. (Pham., *et al* 1996). A second smaller modification in the form of the loxP containing sequence of 50 bp was introduced downstream exon 1 and despite its size, this could also alter the normal mechanisms of CTLA-4 gene regulation since even single nucleotide variations can alter the function of this gene (Gough., *et al* 2005). For these reasons, mice retaining the neo cassette were therefore produced. Producing an altered CTLA-4 allele may provide insights on how these gene is regulated.

Homozygous mice bearing a targeted CTLA-4 allele were generated (figure 4.1), developed and lived normally throughout an average life span. Direct inspection through necropsy, however, demonstrated that homozygotes developed enlarged lymph nodes with no signs of tissue damage or inflammatory disease. Histologic sections showed no organ deterioration yet, the lymph nodes and Peyer's patches developed areas with greater cell density, localized in compartments corresponding mainly to B lymphocytes (lymph node cortex and follicular areas).

Total cellularity in the lymph nodes was significantly increased, but B and not T cell absolute numbers were increased. The same was not observed in the spleen. The data for the spleen is variable and additional experiments are required to analyze any possible differences.

It would be very valuable to analyze the activation state of B cells in the lymph nodes of homozygous mice, and this can be done using flow cytometry and double staining of lymph node cells for CD19 vs CD80 and CD86, as the expression of these markers indicates that B cells are activated and able to provide costimulation. Another readout to assess B cell effector activity could be the measurement of immunoglobulin in serum obtained by extraction of blood through cardiac puncture.

CTLA-4 knock out mice show increased levels of B7 receptors in the surface of B cells and also higher levels of basal Ig in sera. These mice also develop B cell infiltrates (Waterhouse., *et al* 1995) and it has been postulated that B cell activation, and in general

the whole pathology in homozygous knockouts, is mediated by dysregulated CD4<sup>+</sup> helper T cells. A similar crosstalk between lymphocyte subsets may be happening in homozygous mice bearing CTLA-4 targeted allele, but more experiments are required to confirm this. The slight skew observed towards an increased CD4 single positive cells in the thymus suggests that this must be worth pursuing, although no major alterations in the percentage of CD4 and CD8 T cells were observed in the lymph node. A greater sample of animals should to be analyzed to determine if there are subtle differences in this lymphoid organ. Regardless of the altered B cell numbers and enlarged lymph nodes, there is no apparent tissue damage or inflammation.

T cells in these mice are not in a pre activated state as observed in CTLA-4 knock outs. However, upon *in vitro* activation, either with APC or anti CD3, anti CD28 mediated costimulation, T cells of homozygous mice express up to ten fold more intracellular CTLA-4 than wild type littermates.

Masteller, E.L., et al, reported that a CTLA-4 transgenic strain lacking the intracellular domain, when crossed with CTLA-4 deficient mice, showed a long life span but a very similar phenotype, associated with a moderate lymphadenopathy (Mateller., *et al* 2000). They concluded that the cytoplasmic signaling domain was important for CTLA-4 to exert its inhibitory function and in the present studies, it is possible that the availability of an specific splice variant is altered, resulting in a similar effect.

An important finding is that the CTLA-4 over expression seen here in homozygous individuals is not influenced by the genetic background as targeted animals in a 129 pure background show the same increased CTLA-4 expression upon activation as seen in mice on a mixed background (figure 4.15).

The CTLA-4 over expression observed in homozygous mice, may have functional implications. *In vitro* activated CD3<sup>+</sup> cells express higher levels of CD25 indicating a greater level of activation, nevertheless these cells do not proliferate at a greater extent than cells from wt or heterozygous littermates. This suggests that the over expression of CTLA-4 in this cells is keeping them regulated probably by inhibiting IL-2 production or by inducing apoptosis. It would be very interesting to assess apoptosis in these T cells, and this can be performed relatively to their proliferation, by flow cytometry using the dye CFSC and simultaneously staining for phosphatidyl serine with Annexin V.

A possible explanation for the differences in CTLA-4 expression observed in homozygotes is the altered pattern of expression of 3 of the 4 splice variants of CTLA-4. Genetic as well as functional studies by others support the idea that genetic variation that results in changes in the expression of the isoforms of CTLA-4 (sCTLA-4, LiCTLA-4 and FLCTLA-4), contributes to the genetic control of autoimmunity (Ueda., *et al* 2003). It is unlikely however that LiCTLA-4, previously associated with T cell signalling and protection against diabetes (Vijaykrishnan., *et al* 2004), could play an important role in our model, as its expression in the homozygotes is similar to that seen in wt littermates (figure 4.17).

The ratio between FLCTLA-4 and, for instance, soluble CTLA-4 was different in resting T cells from homozygous mice when compared with its littermates (figure 4.19). Lower levels of soluble CTLA-4, when compared with FLCTLA-4, have been correlated with homozygous individuals, susceptible to auto immunity, and that the possible mechanism of action of this secreted form of CTLA-4 could be the regulation of T cell activity by inducing IDO production (reviewed in Gough., *et al* 2005). Further data on these mice is required, particularly through quantitative PCR, but if we are able to confirm this variations, our model is consistent with the observations in humans.

After 3 days of activation cells from homozygous individuals still express detectable levels of LiCTLA-4, despite the reported early kinetics of expression (Vijaykrishnan., *et al* 2004)). This leaves us with the question as to whether the expression of this splice variant may be linked to the over expression of FL-CTLA-4 also observed at that time point. Finally another CTLA-4 isoform was also detected in our assays which corresponds to transcript lacking exons 2 and 3 and to which no function has been assigned. This splice variant is expressed in resting T cells but disappears upon activation in wt mice, but not in homozygous animals after activation.

Taking together all these data, it is tempting to speculate that a possible trigger of the phenotype observed in homozygous mice could be a dysregulation in the expression of a CTLA-4 splice variant (for instance FLCTLA-4) at the resting state altering the required availability of this molecule to maintain T cell homeostasis. Furthermore more experiments are required to confirm this hypothesis.

Finally it can be postulated that an alteration in the levels of expression of *Cd28* or *Icos*, (located in close proximity to *Ctla-4*) caused perhaps by the insertion of a neo-cassette, may be driving the phenotype observed in mice homozygous for the targeted mutation. It has been recently reported that CTLA-4 knock out mice over express ICOS (van Berkel., *et al* 2005) and in these knock out model homozygous mutants retained the neo cassette in a similar position as the mice here reported. In addition, costimulation by ICOS seams to be critical for an efficient T cell-mediated B cell response (Coyle., *et al* 2000), in which case an alteration in its levels of expression in this mice could, be responsible for the increased proportion of CD19<sup>+</sup> cells observed in the lymphnodes of homozygous *Ctla-4* targeted mice. Analysis of the surface ICOS and CD28 expression of T cells in these mice by flow cytometry is essential to test this hypothesis.

***Chapter 5. Cre-mediated recombination and CtlA-4***

## **5.1. Background.**

The value of generating a mouse model that can provide us the possibility to gain temporal control of the *Ctla-4* inactivation has been described. The lethal phenotype developed by CTLA-4<sup>-/-</sup> mice, generates important limitations to study the peripheral immune system in the absence of this molecule at stages later than 1 month after birth. In addition, it would also be very desirable to have access to particular T cells subsets, such as regulatory T cells or CD45RB<sup>+</sup> memory T cells, in which the deletion of this gene can be induced *in vivo or ex vivo*, to then use them in culture assays or in adoptive transfer experiments.

Mice bearing 3 Cre recombinase (*loxP*) sites and a neo cassette have been generated. The location of these sites within the CTLA-4 intronic sequences, allows selective modifications of this locus and not only the elimination of the neo cassette, but also the generation of mice having two *loxP* sites flanking the sequences that encode for two domains critical for the function of this molecule. Further modification of this locus allows the elimination of the sequences corresponding to the ligand binding and transmembrane domains of CTLA-4 (exons 2 and 3), thus generating an animal deficient for this molecule, similar to those previously reported where CTLA-4 has been disrupted (Tivol., *et al* 1995 and Waterhouse., *et al* 1995), ( Figure 5.1)

All the modifications to the *Ctla-4* locus can be achieved using transgenic mice able to deliver active Cre in germ cells. After recombination, the resulting modified forms of the gene can be inherited.

The aims of this chapter are:

- Generate mice bearing 2 *loxP* sites, flanking exons 2 and 3 by inducible Cre-mediated recombination in germ cells.
- Generate mice homozygous and heterozygous for a modified *Ctla-4* allele lacking exons 2 and 3 as a new model of null expression of this molecule.
- Analyze the phenotype of mice lacking exons 2 and 3.

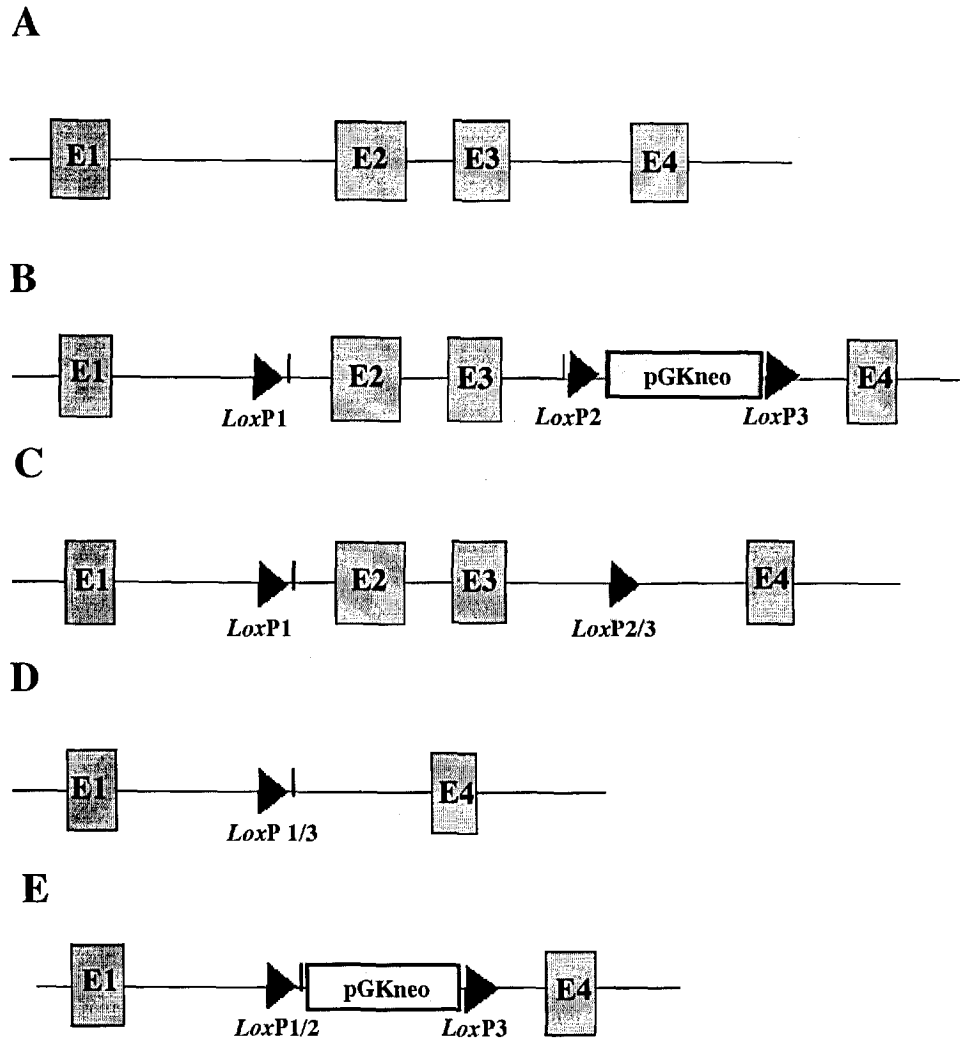


Figure 5.1.- Outcomes of Cre-mediated recombination on the *Ctla-4* targeted allele. Cre recombinase is able to excise a sequence of DNA that is flanked by 2 of its recombination sites (*loxP*). The position of the 3 *loxP* sites in the intronic sequence of *Ctla-4* can therefore produce 3 different alleles two of which are of interest in this chapter (C, D). In A, the figure illustrates the intron-exon configuration of *Ctla-4*, in B the targeted allele. The 3 possible deletion products are shown in C, D and E.



## **5.2. The generation of mice bearing two *loxP* sites flanking exons 2 and 3 of *Ctla-4*.**

In order to generate mice with a modifications of *Ctla-4*, as shown in figure 5.1 C, a Cre transgenic mouse that expresses a fusion protein of Cre with mutated estrogen receptor domains was used. In these mice (strain  $\beta$ -70) , the expression of the Cre fusion is driven by the chicken  $\beta$ -actin promoter providing potentially ubiquitous expression although in practice the expression and the activity of the recombinase varies between tissues (Dr Laurence Bugeon personal communication). It has been reported, however, that in these mice, Cre is expressed and functional in germ cells (Tolmachova., *et al* 2006), thus making them a useful germ-line deleter strain.

To produce the mice with the *Ctla-4* genotypes of interest, we crossed a  $\beta$ -70 mouse with an animal heterozygous for a targeted allele. The resulting offspring (heterozygous for the *Ctla-4* targeted allele and either possessing the Cre transgene or not) were assayed for both genotypes by PCR. Figure 5.2 summarizes the breeding and tamoxifen induction strategy and figure 5.3 shows representative PCR data corresponding to the genotyping.

As shown in figure 5.3, mice heterozygous for the *Ctla-4* targeted allele and positive for the Cre were identified. A series of tamoxifen inductions were performed (see materials and methods) to induce deletion of *Ctla-4* in the germline of these mice followed by crossing induced animals with WT C57BL/6 mice. The offspring was genotyped for the various deletion products that could have occurred after Cre mediated recombination in the germ cells of their progenitors. To discriminate between the 3 different CTLA-4 alleles produced by recombination, a set of PCR reactions was designed which amplified junctional regions specific for each deletion product. Together with this analysis the previously described PCR that amplifies an area downstream exon 1, around the 5'-most *loxP* site in the targeted allele was used. Figure 5.4 shows a scheme of this PCR strategy, the characteristics of the PCR specific for the area downstream exon 1 has been described before (chapters 3 and 4), a “close up” of the location for this PCR is however shown when appropriate.

After several attempts and variations of in the scheme of tamoxifen administration mice bearing a *Ctla-4* locus where exons 2 and 3 are flanked by *loxP* sites or also called “floxed” was generated. Another genotype obtained corresponded to an allele in which exons 2, 3 and the neo cassette were deleted (“deleted allele”). Figure 5.5 shows a representation of the PCR analysis performed to identify the above mentioned genotypes. So far we have not identified the third possible modified allele (“neo allele”) but we do not require mice with such genotype.

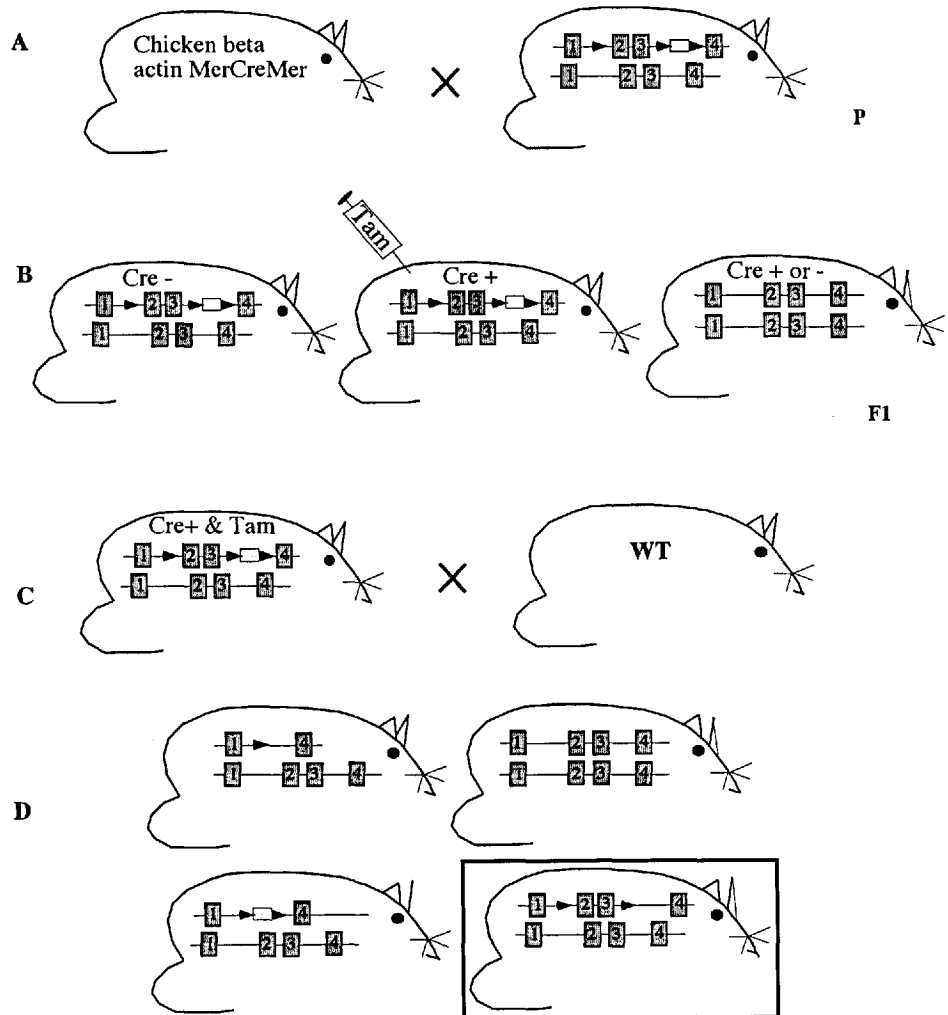


Figure 5.2.- Generation of mice bearing loxP sites flanking exons 2 and 3 for use in experiments for conditional inactivation of CTLA-4 (in box). Heterozygous *Ctla-4* targeted mice were crossed with a Cre transgenic, able to express an inducible form of Cre in the germ cells (A). Cre positive offspring bearing the targeted *Ctla-4* allele was induced with tamoxifen (B) and crossed with WT C57BL/6 mice (C). Heterozygous offspring bearing a *Ctla-4* allele with various deletions were analysed (D) and animals with loxP sites flanking exons 2 and 3 were identified.

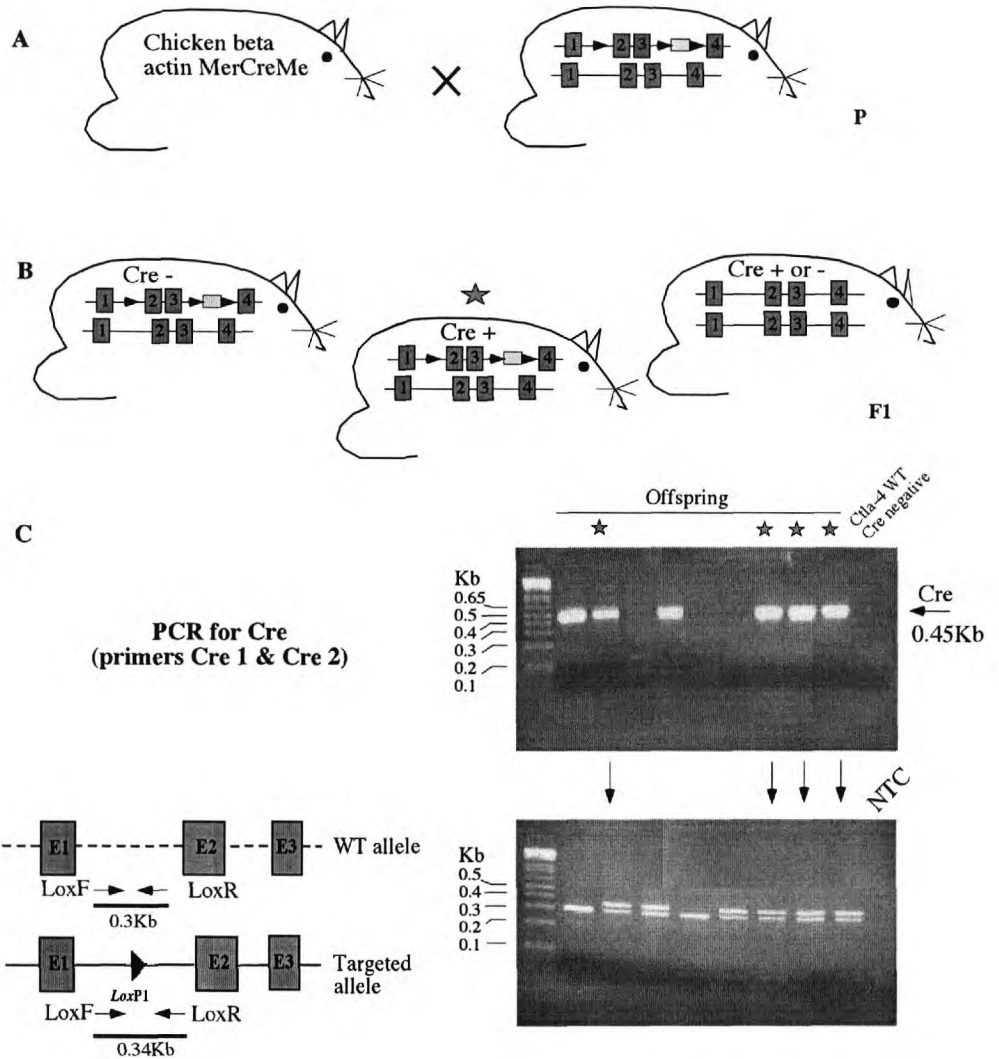


Figure 5.3.- Generation of mice heterozygous for a targeted *Ctla-4* allele and positive for a transgene encoding an inducible form of Cre (MerCreMer). Heterozygous *Ctla-4* targeted mice were crossed with a Cre transgenic, able to express an inducible form of Cre in the germ cells (A). Cre positive offspring (B) were analysed by PCR to select *Ctla-4* targeted, Cre positive individuals (C). This animals can be induced with tamoxifen to perform the desired *Ctla-4* deletion.

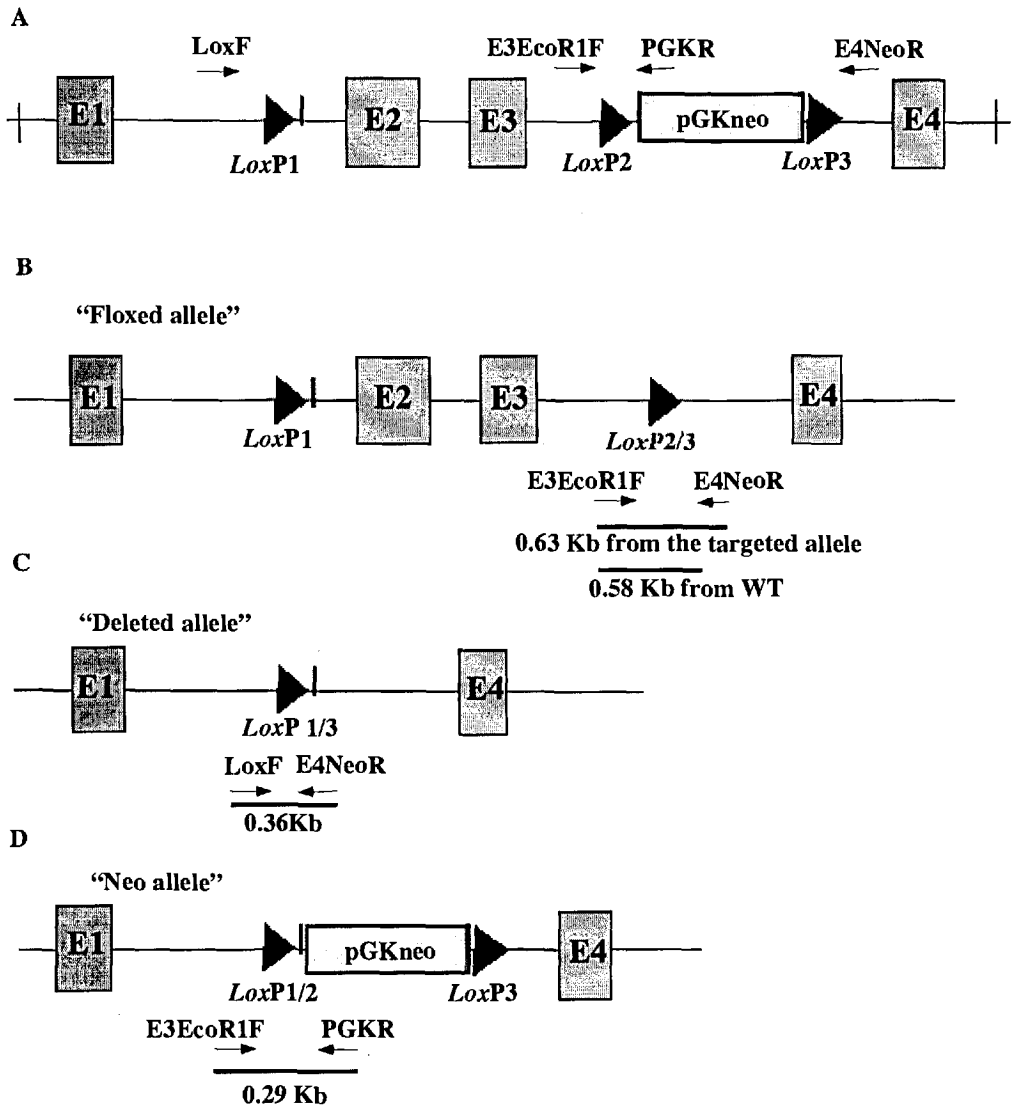


Figure 5.4.- Schematic representation of the PCR strategy to detect Cre-mediated deletion of *Ctla-4*. A, shows a representation of the targeted allele and the location of the 4 primers used. If recombination happens between loxP sites 2 and 3 (B), the deletion product will allow primers E3EcoR1F and E4NeoR to amplify a product on the allele, an additional product on a wt allele is also expected. If recombination proceeds between loxP sites 1 and 3 (C) or 1 and 2 (D), the corresponding PCR products should also be amplified.

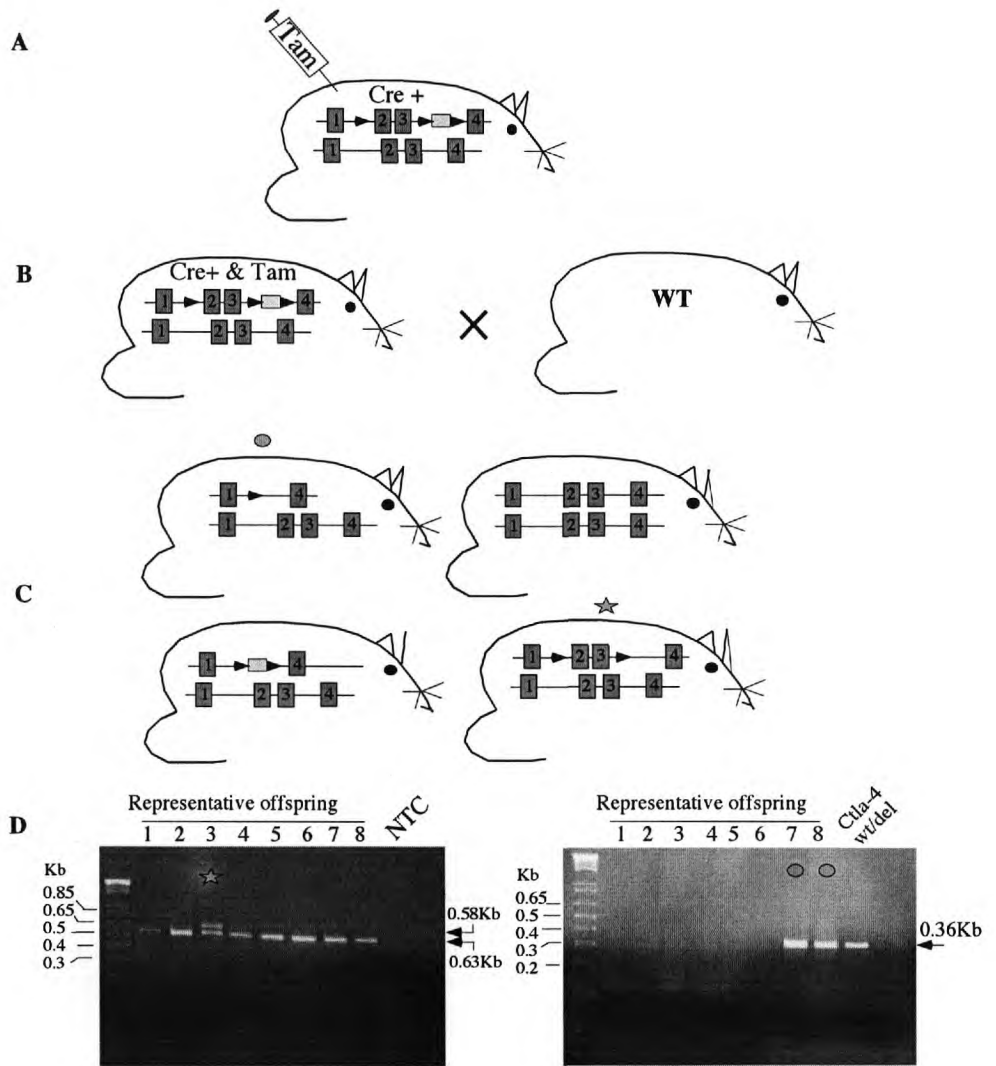


Figure 5.5.- In vivo inducible Cre mediated deletion of *Ctla-4*. Heterozygous *Ctla-4* targeted mice, positive for a tamoxifen-inducible form of Cre (A), were induced by intraperitoneal injection or orally (1mg-5mg of tamoxifen, see materials and methods) and subsequently crossed with wt C57BL/6 animals (B). The offspring (C) was genotyped using PCR as described in figure 5.4. D shows two representative PCRs to detect; a "floxed allele" (left) and a "deleted allele" (right). The rest of the offspring was tested and found not positive for the third type of deletion "neo allele".

### **5.3. Generation of mice with a *Ctla-4* allele lacking exons two and three.**

In parallel to the experiments reported in section 5.2, a second system to modify *Ctla-4* was employed to rapidly generate mice having a deletion in exons 2 and 3. The rationale of this modification was the generation of a novel CTLA-4 knock out line, one lacking a neo cassette and perhaps showing a variable phenotype to the models published (Tivol., *et al* 1995 and Waterhouse., *et al* 1995).

The transgenic system used this time was a mouse that also delivers Cre-mediated recombination. PGK-Cre transgenics express Cre under the PGK-1 promoter and under dominant maternal control. This means that Cre in these mice is expressed early in oogenesis, so when male mice having a gene flanked by *loxP* sites are crossed with PGK-Cre females, even animals that do not inherit the Cre gene, show efficient deletion. This happens because of the high and early expression of Cre due to the strong PGK-1 promoter, therefore active concentrations of the enzyme, present in the cytoplasm and pronucleus of the oocyte can act on any “floxed” target DNA in the male pronucleus (Lallemant, Y., *et al* 1988). This transgenic strain (kindly provided by Dr Tomalchova at the Seabra Lab, Imperial College) was mated with homozygous *Ctla-4* targeted mice and as expected, all the offspring of this cross were heterozygous for a “deleted allele” thus Cre mediated recombination proceeded between *loxP* 1 and 3 (figure 5.1), this probably is due to the high concentrations of Cre expressed in the embryos at early stages as a result of the strength of the PGK-1 promoter.

Further intercrosses between offspring with such genotype were set up and littermates wild type, heterozygous and homozygous for the mutation were generated, figure 5.6 summarizes this strategy. To genotype the mice produced after the intercross the PCR previously selected to detect a “deleted allele” was used in conjunction with the PCR specific for Cre, so only pups that had not inherited Cre were intercrossed Figure 5.7 shows representative genotyping data. As expected 100% of the progeny from the cross described in figure 5.7 possessed the deleted *Ctla-4* genotype.

For simplicity in nomenclature, from now and during the characterization of the phenotype of mice bearing a deletion at the *Ctla-4* locus, wild type littermates will be referred as wt/wt heterozygous mutants, wt/del and homozygous del/del.

Previously generated mice with a disruption in exons 2 and 3 due to the insertion of a neo cassette (Tivol., *et al* 1995 and Waterhouse., *et al* 1995) will be referred to as CTLA-4 knockouts.



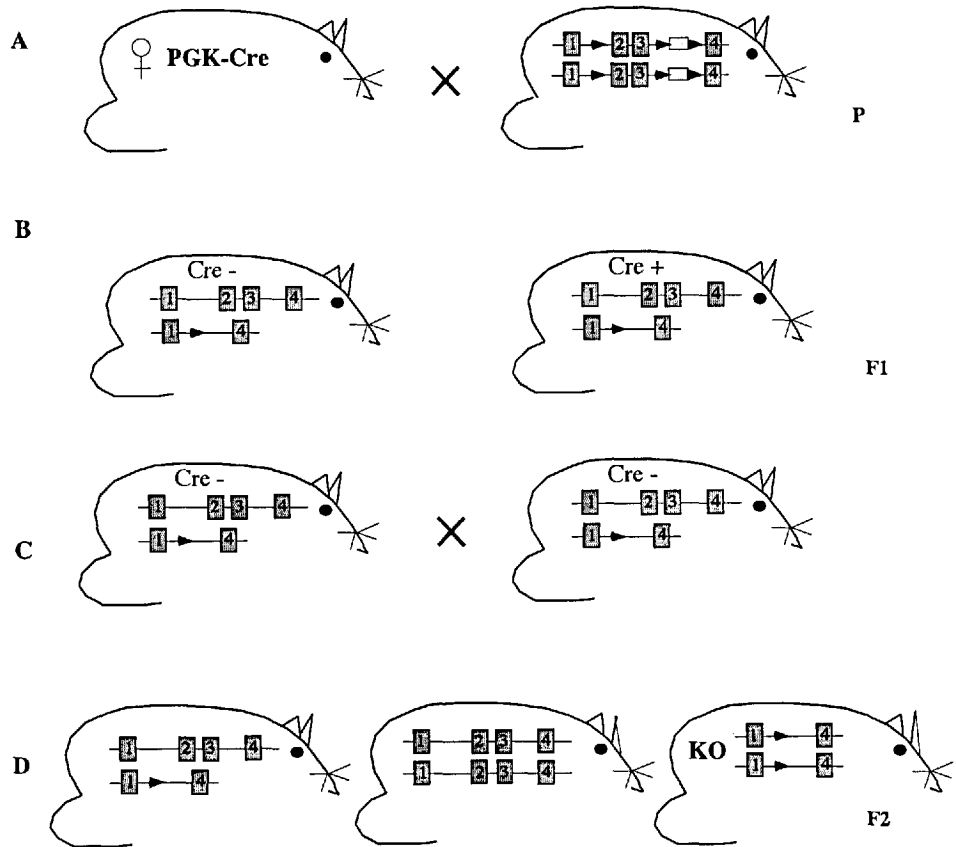


Figure 5.6.- Generation of *Ctla-4* del/del mice by Cre mediated deletion. Mice homozygous for the *Ctla-4* targeted allele were crossed with a transgenic strain that expresses Cre under the PGK-1 promoter (A). High expression of active Cre early in oocytes exerts complete deletion of the *Ctla-4* targeted in embryos, resulting in mice with a heterozygous deleted genotype at the *Ctla-4* locus (B). An intercross of Cre negative offspring allows the production of mice homozygous for *Ctla-4* deleted allele therefore theoretically deficient for this molecule.

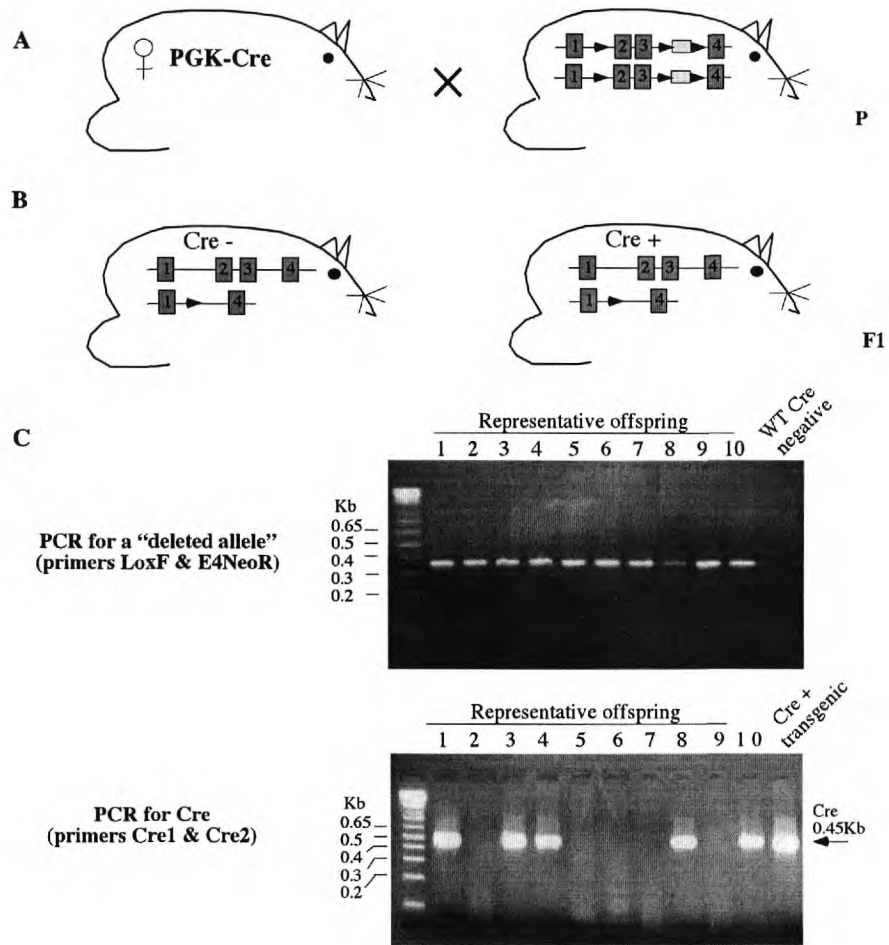


Figure 5.7.- Generation of mice bearing a deleted *Ctla-4* allele by Cre mediated recombination. Mice homozygous for the *Ctla-4* targeted allele were crossed with a transgenic strain that expresses Cre under the PGK-1 promoter (A). This cross resulted in mice with a heterozygous deleted genotype at the *Ctla-4* locus (B). This was confirmed by performing a PCR using primers LoxF and E4NeoR.

#### **5.4. Analysis of the phenotype of del/del mice.**

Del/del mice were generated as mentioned in section 5.3, genotyping of this line was performed using an PCR specific for the sequence downstream exon 1 where *loxP* site number 1 is located, together with the PCR designed to identify a “deleted allele”.

With this PCR combination, it was readily possible to discriminate between genotypes, as DNA from wt/wt mice should not produce a product when amplifying for the deleted allele and, in contrast, DNA from del/del mice should do so. Wt/del mice are expected to produce a product in both reactions. Figure 5.8 shows representative PCR data. All individuals used in experiments were genotyped accordingly, del/del mice were always screened again *post mortem*.

del/del mice developed normally and were born healthy at a normal Mendelian frequency. However significant lag in growth when compared with the littermates and signs of disease developed within the first two weeks of life. After about 3 weeks they become moribund. Following some initial qualitative observations survival data was collected and figure 5.9 shows a curve from 13 individuals. Wt/del individuals survived as wt littermates and showed no signs of disease.

The survival of del/del mice is a first indication that these mice developed a phenotype similar to the reported CTLA-4 knock outs generated by a disruption of exons 2 and 3 by the insertion of a neo cassette (Tivol., *et al* 1995 and Waterhouse., *et al* 1995). But before pursuing characterization, the levels of expression of CTLA-4 by lymphocytes using intracellular antibody staining and flow cytometry, together with a western blot from total resting lymph node cells were performed.

No expression of CTLA-4 was observed in del/del mice when compared with the littermates, this result confirms that the mutation generated in these mice substantially abrogates CTLA-4 expression (figure 5.10). CTLA-4 expression of wt/del animals is comparative to that of wt/wt littermates.

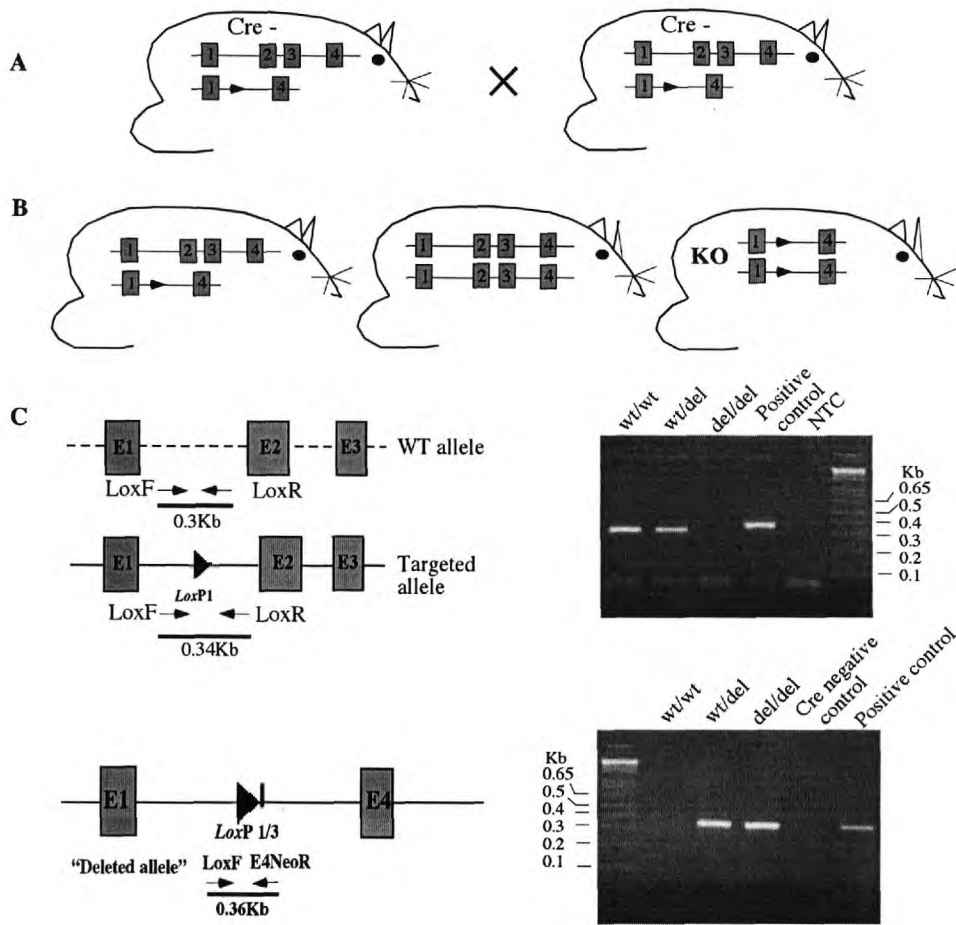


Figure 5.8.- Genotyping of *Ctla-4<sup>del/del</sup>* mice. Mice heterozygous for a deleted *Ctla-4* allele and negative for Cre, were intercrossed (A). The result of this intercross (B) were mice homozygous for *Ctla-4* deleted allele therefore theoretically deficient for this molecule. wt/wt and wt/del littermates were also produced for comparisons. These genotypes were confirmed by a PCR amplification of a region around the loxP site downstream exon 1 (C top) and the PCR designed to detect a "deleted allele" (C bottom) (see figure 5.2).

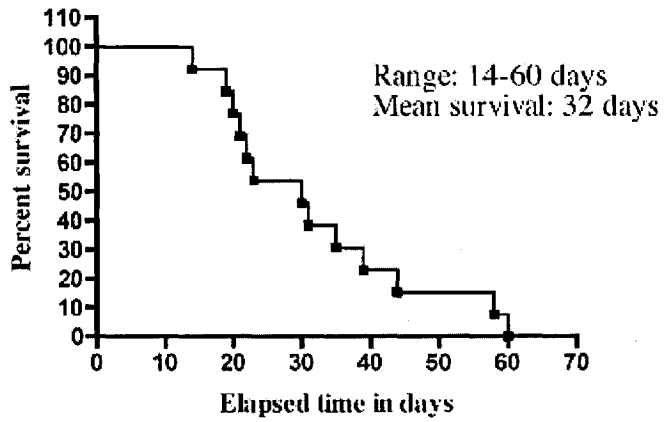


Figure 5.9.- *del/del* mice show a lethal phenotype and die 4 weeks after birth. The curve shows the percentage survival of *del/del* mice (n=13) from a single breeding pair. Mean survival and range are indicated.

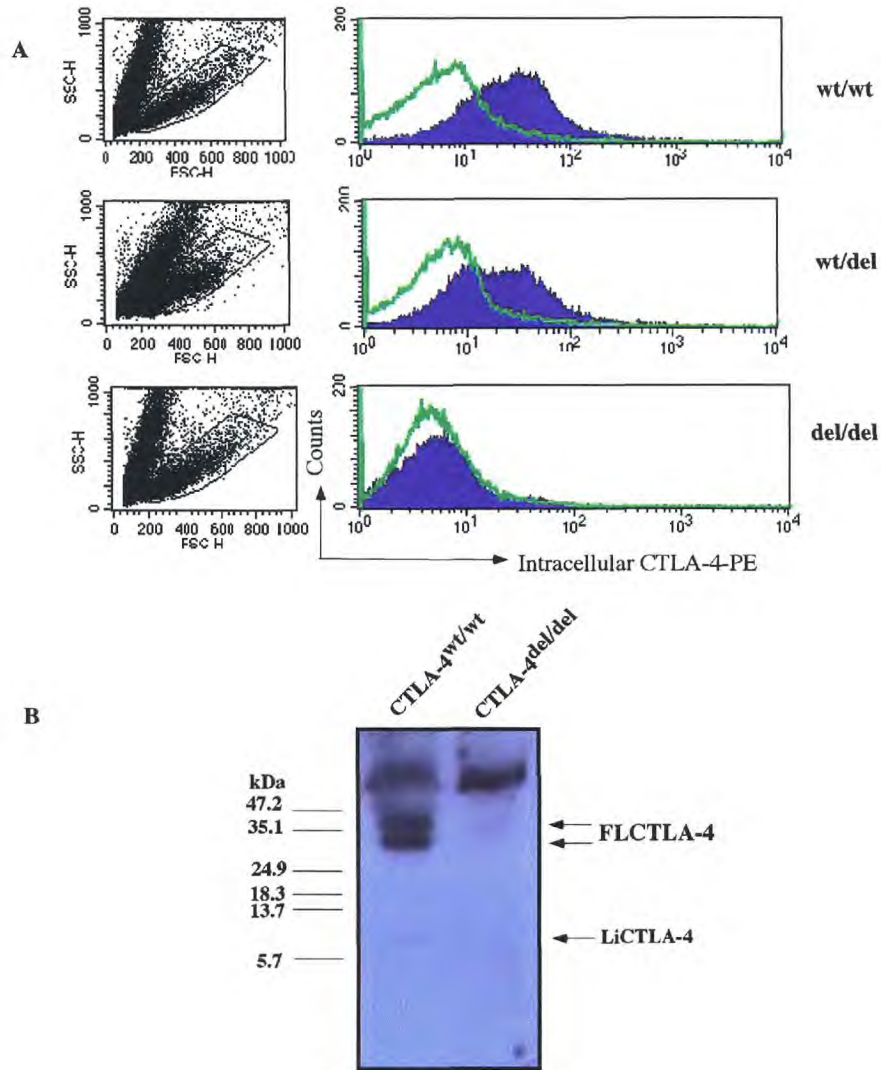


Figure 5.10. CTLA-4 expression analysis by flow cytometry and Western blot of cells from *del/del* mice compared with *wt/wt* and/or *wt/del* littermates. Approximately  $3 \times 10^6$  cells from lymph nodes were cultured for 3 days under polyclonal stimulation ( $1 \mu\text{g/ml}$  anti CD3) and harvested for surface CD3 and intracellular CTLA-4 antibody stains. Comparative CTLA-4 expression in the mice is reported as intensity of fluorescence (filled histograms), isotype control stains are overlaid (in green). In B, the figure illustrates a Western blot of total resting lymph node cells comparing the expression of CTLA-4 between animals.  $10 \mu\text{g}$  of protein separated by SDS-page transferred and blotted with an antibody (C19) specific for the intracellular portion of CTLA-4. Two bands, corresponding to 2 isoforms of the molecule can be detected (LiCTLA-8 at 8kDa and FLCTLA-4 between (30-35kDa). Two bands are detected for FLCTLA-4 due to differences in glycosylation.

During the dissection it was possible to observe dramatic differences in the sizes of lymph nodes from *del/del* individuals when compared with their littermates and this was reflected to the cellularity of these organs as *del/del* mice showed at least 20 fold more total cells than *wt/wt* or *wt/del* littermates (see table below).

<i>wt/wt</i>	<i>wt/del</i>	<i>del/del</i>
13x10 <sup>6</sup>	14x10 <sup>6</sup>	286x10 <sup>6</sup>
19x10 <sup>6</sup>	18x10 <sup>6</sup>	625x10 <sup>6</sup>

Table 5.1.- Viable cell count from lymph nodes of *wt/wt*, *wt/del* and *del/del* mice. Data corresponds to 2 independent observations.

Comparative histologic analysis of *del/del* mice showed a dramatic infiltrate and tissue destruction particularly in the pancreas where morphology was completely compromised. Organs on *wt/wt* and *wt/del* appeared normal. In contrast with the published CTLA-4 knock out histologic data, moderate infiltrate was observed for *del/del* individuals in organs in which greater damage is reported for such knock outs. For instance, in the heart a moderate infiltrate with no apparent signs of myocarditis was detected (see figure 5.11). Myocarditis was reported for the CTLA-4 knock out mice. Another interesting difference was that the spleen of *del/del* mice does not show a morphology of extended white pulp and compromised red pulp as observed in CTLA-4 knock outs and indicative of lymphoproliferation in this organ. Consistent with the literature for the CTLA-4 knock outs, *del/del* mice show no damage or infiltration in the kidney. *wt/del* mice showed no histologic signs of damage or infiltration.

The proportion of CD4 and CD8 cells in lymph nodes and in thymus were also analyzed in experimental animals by flow cytometry (figure 5.12 and 5.13). Interestingly the CD4/CD8 ratio in *del/del* mice was altered as compared with *wt* littermates, favouring a greater number of CD4 positive cells in the former group. Early reports suggested that this was not the case for CTLA-4 knock outs and their *wt* littermates (Waterhouse., *et al* 1995). However later it was demonstrated that there was indeed a change in the ratio of these subsets due to a preferential activation of CD4<sup>+</sup> T cells, as antibody depletion of these cells rescuing CTLA-4 knock outs from their phenotype (Chambers., *et al* 1997).

No clear changes in the numbers of CD4 and CD8 cells were observed in wt/del animals when compared to wt/wt littermates.

In the thymus of del/del mice, a gross variation was observed in CD4 to CD8 profile when compared with littermates (figure 5.12). An increased proportion of CD4 single positives and a decrease in double positives is consistent with previous reports indicating that this does not correspond to a dysregulated thymocyte development but a technical issue (Chambers., *et al* 1997). During the harvesting of thymi, the discrimination between this organ and the parathymic lymph nodes is not always straight forward and it seems likely we had harvested both organs and our single cell suspensions are mixed with lymphocytes other than from thymus. More careful dissections are required to determine a precise thymus CD4-CD8 profile.

As expected, CD3 positive cells in del/del mice showed a phenotype of early and constitutive activation as determined by the surface expression of CD69 and CD25 by flow cytometry. Lymph node cells from these mice showed a higher percent of cells positive for the two markers as compared with wt/w and wt/del littermates.

The proportion of T cells in the lymph node of del/del animals was not increased as compared to littermates, however due to the dramatic differences in cellularity in the lymph nodes, total numbers of T cells are indeed increased. In contrast CD19<sup>+</sup> cells showed an increased percentage when compared with wt/wt and wt/del. These data was determined by staining freshly extracted lymph node cells for CD3 and CD19. The expression of activation markers is consistent with the previous CTLA-4 knock out reports (see figure 5.13).



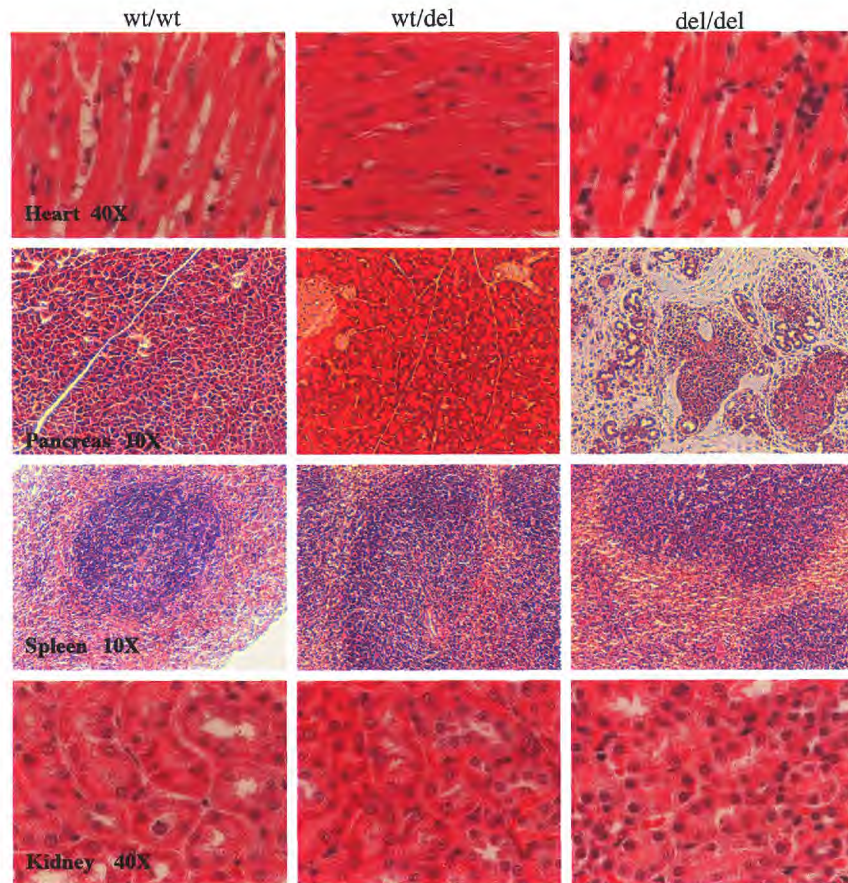


Figure 5.11- Histologic analysis of organs from del/del mice as compared the littermates. Sections from parafin embedded tissues were stained with H&E and observed by optical microscopy. All photographs shown are magnified as indicated.

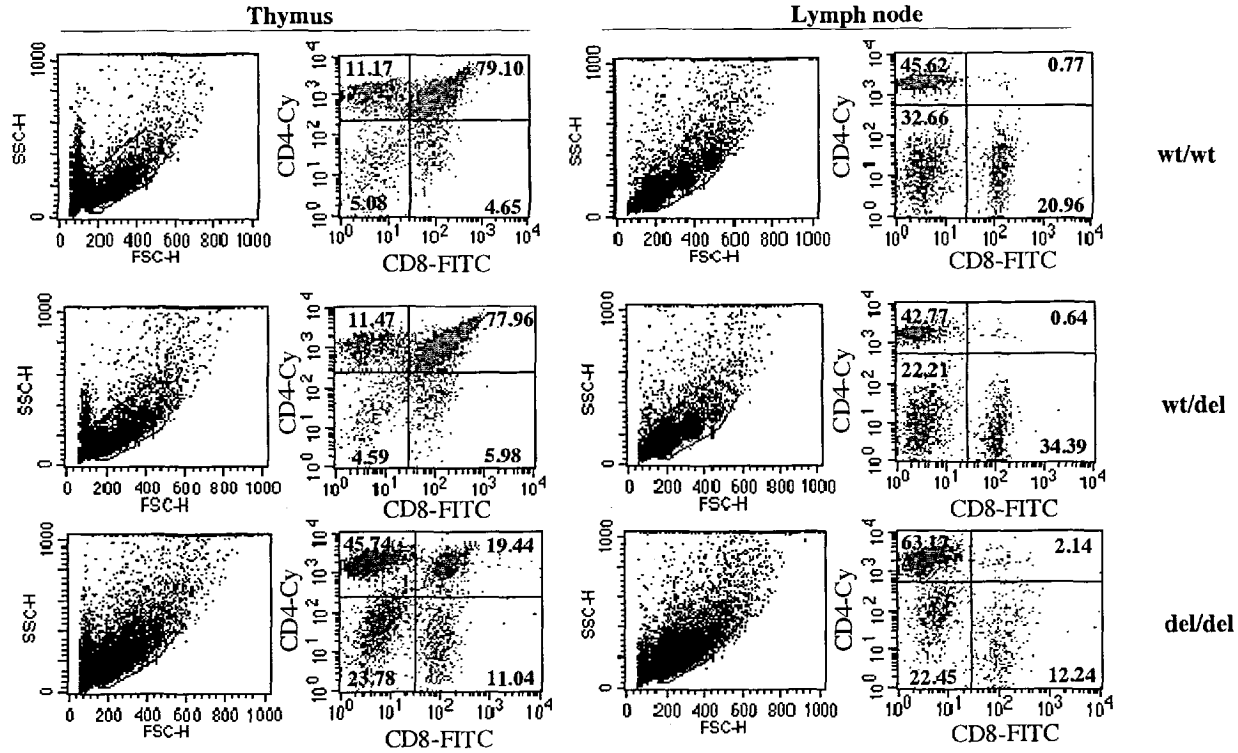


Figure 5.12.- Flow cytometric analysis of thymocytes and lymph node cells from *Ctla-4<sup>del/del</sup>* mice as compared with littermates. The dot plots show; SSC vs FSC and a double CD4 - CD8 stain of thymocytes and lymph node cells, percent cells in each quadrant is shown. Data representative of two experiments.

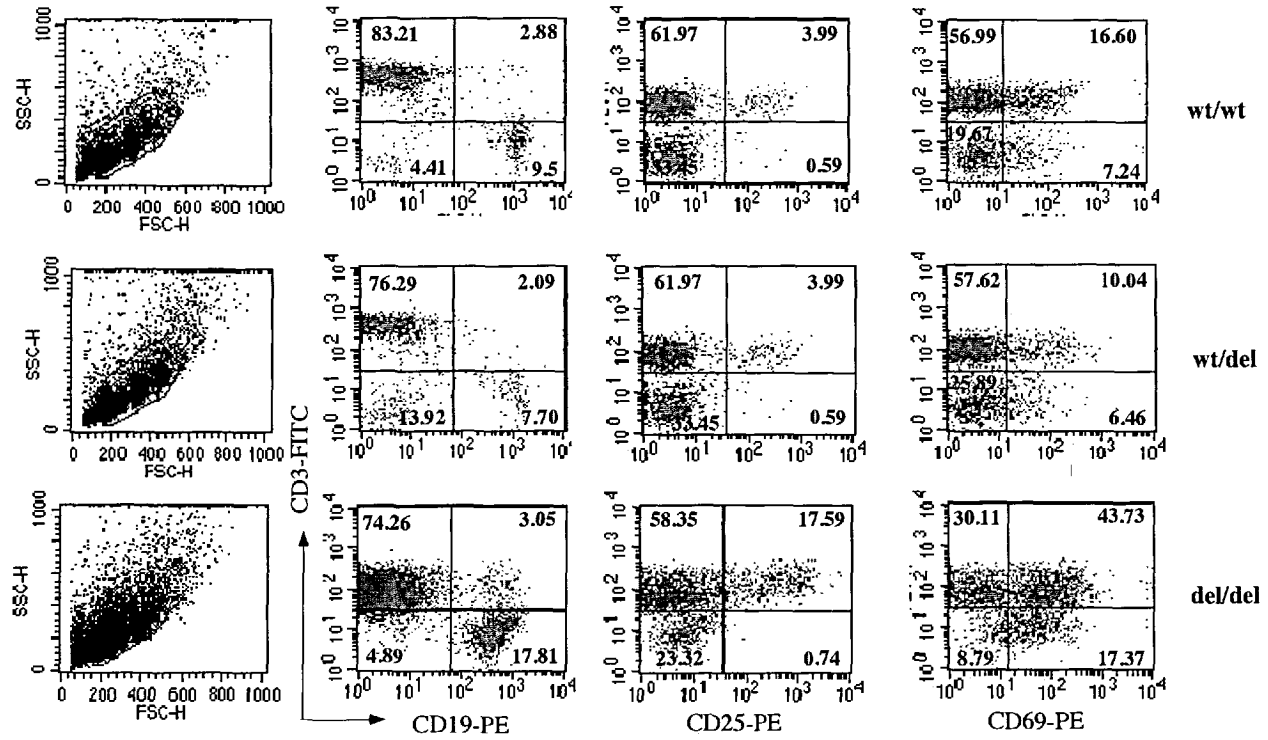


Figure 5.13.- Flow cytometry analysis of lymph node cells from del/del mice compared with wt and wt/del littermates. The plots show the percentage of cells expressing the lymphocyte markers CD19, CD25 and CD69, percent cells in each quadrant is indicated. To the left, a representative FSC vs SSC plots. Results are representative of two experiments.

## **5.5. Discussion.**

### *i. Generation of a model for conditional inactivation of CTLA-4*

Animals with two main modifications at the *Ctla-4* locus after Cre mediated recombination were generated. These mice were obtained by Cre recombination in germ cells using either a transgenic line that expresses Cre in an inducible fashion,  $\beta$ -70 MerCreMer (Produced in the Dallman Laboratory Imperial College London and used by Tolmachova., *et al* 2006 and unpublished data), or another transgenic mouse that is able to deliver high levels of Cre early in fertilization due to the PGK-1 promoter (Lallemand., *et al* 1988).

For the overall relevance of this project the most important *Ctla-4* genotype obtained is an animal bearing an allele with only two *loxP* sites, one upstream of exon 2 and the second downstream of exon 3, and lacking the sequence of the neo cassette. This animal is the precursor of mice in which conditional inactivation of *Ctla-4* can be induced. The simple crosses required to produce which mice are shown in figure 5.14.

A model for conditional inactivation through the Cre-*loxP* system, requires a transgenic animal able to express Cre in an inducible fashion and in the cell type of interest, in our case we can use animals that express Cre under the control of the Mx-1 promoter in which interferon alfa induces Cre expression (Khun, R. *et al* 1995). These mice are available in our lab and the advantages and disadvantages together with other mice that can be employed will be discussed in the next chapter. Overall and as confirmed in previous sections of in this chapter, all the animals required to inactivate CTLA-4 conditionally are now generated and this is the main future branch of the work reported in this thesis.

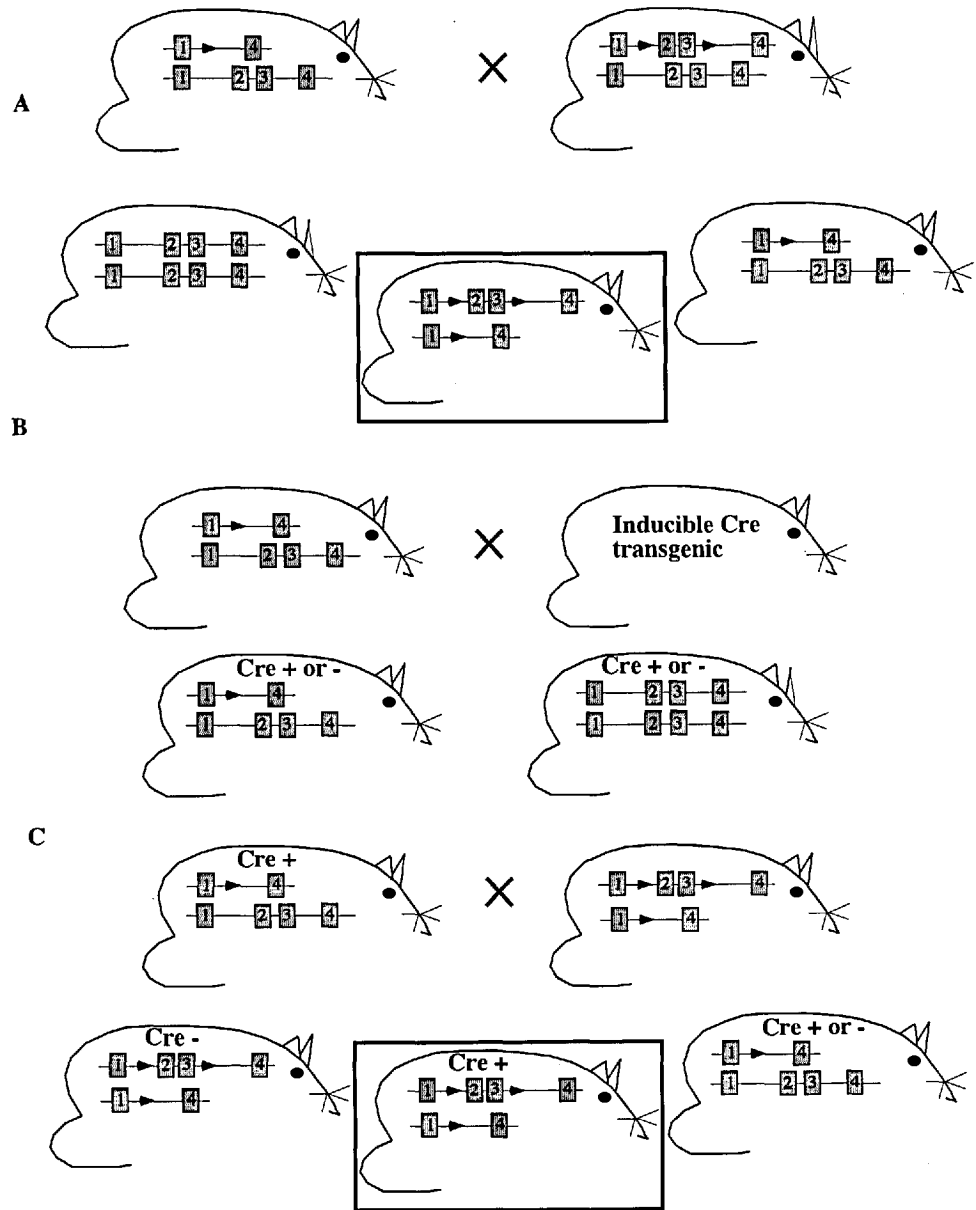


Figure 5.14.- Breeding strategy to generate mice suitable to conditionally inactivate CTLA-4. A first cross (A) between wt/del and an animal with the CTLA-4 exons 2 and 3 flanked by *loxP* sites, is required to generate mice with only one *Ctla-4* allele "floxed". In parallel wt/del mice need to be crossed with animals that express inducible Cre (B), to finally bring the two genotypes together (C) to generate an individual in which conditional inactivation can be achieved. Animals in boxes are genotypes of overall interest during the strategy.

***ii. The phenotype of mice lacking exons 2 and 3 of CTLA-4.***

Heterozygous and homozygous mice bearing a deletion of exons two and three of *Ctla-4* have also been created first by PGK-Cre mediated deletion and subsequently by intercrossing. These mice develop a phenotype very similar to the CTLA-4 knock outs made through conventional gene targeting (Tivol, E.A., *et al* 1995 and Waterhouse, P., *et al* 1995) as far as the phenotype of lymphocytes and thymocytes is concerned. However, mice generated here show a more moderate phenotype in terms of damage, lymphoproliferation and infiltration as analyzed by histology.

Consistent with the previous reports of CTLA-4 knock out mice the pancreas in *del/del* mice showed dramatic damage with a completely compromised morphology, nevertheless no signs of myocarditis or destructive lymphoproliferation was observed in the heart and the spleen respectively. No major damage was also observed in other tissues like Kidney, liver or gut (data not shown). Immunohistochemical analysis of tissue sections is required to confirm the absence or a lower level of cell specific infiltrate ( by T cells, B cells, or other leukocytes) in the heart and other tissues to establish if these mice have or not a milder phenotype.

***Chapter 6. Concluding discussion***

## 6.1. The rationale of generating a model for conditional inactivation of CTLA-4.

The overall aim of this project was to generate mice in which the inactivation of *Ctla-4* could be achieved under temporal control using the Cre-loxP system. The reasons why it would be very useful to have of such a model come, paradoxically, from the characteristics of perhaps the most important tool we have so far to understand the function of this molecule. CTLA-4 knock out mice have been essential to confirm the negative role of this T cell surface negative costimulator, yet the lethal phenotype these mice develop at early stages (Waterhouse., *et al* 1995, Tivol., *et al* 1995). This limits the study of the immune system in the absence of this molecule, and either the use of CTLA-4 deficient animals or only T cells from these mice for functional experiments, is limited to the first month of life of these animals.

The Cre-loxP system comprises two elements. One of them is a mouse having Cre recognition sites (loxP) flanking the sequences of the gene of interest that are critical for the function of the polypeptide. In the case of *Ctla-4* such animals were not available until now.

The strategy utilized to produce these genetically modified mice was the insertion, in intronic sequences of the gene, of a single loxP sequence downstream of exon 1 and a floxed neo cassette downstream of exon 3. These modifications to *Ctla-4* were introduced to the mouse genome via gene targeting in ES cells. Mice bearing these exogenous elements in a *Ctla-4* allele are not themselves useful to perform conditional inactivation experiments, as various outcomes of deletion can be obtained simultaneously after Cre recombination. Nonetheless these mice were generated in order to study animals bearing modifications at the *Ctla-4* locus that will not generate an allele with null expression, but that can alter the mechanisms of genetic control, for instance, by producing a hypomorphic allele. Effects on the expression of targeted genes or its neighbours have been reported in the past (Pham., *et al* 1996 and Olson., *et al* 1996), and the main candidate to cause this type of alterations is the neomycin cassette driven by strong promoters such as the phosphoglycerate-kinase promoter PGK-1.



In the case of *Ctla-4* even small modifications in the genomic sequence can result in an alteration of its expression and examples are comprehensively reported in the literature (reviewed in Gough., *et al* 2006). Sequence polymorphisms have been correlated with various autoimmune disorders and some specific single nucleotide polymorphisms (SNP) have even been associated with changes in the expression of functional splice variants of this gene (Vijayakrishnan., *et al* 2004).

Making a mouse having the mentioned modifications in the *Ctla-4* locus provided us also with the possibility of generating, through Cre-mediated deletion in germ cells, mice in which two of the most important coding sequences are flanked by *loxP* sites; the relevance of these two exons for the function of CTLA-4 has been revealed by the phenotype of the three knock out models already reported (Waterhouse., *et al* 1995; Tivol., *et al* 1995 and Chambers., *et al* 1997).

Mice having *loxP* sites flanking exons 2 and 3 also lack the neo cassette and in light of what we observed of the phenotype of mice possessing such antibiotic resistance sequence, retaining the cassette may complicate the analysis of any phenotype that can be obtained following conditional inactivation. Animals with this genotype have been generated and can now be considered for use in experiments for conditional inactivation.

A final genotype, also obtained after Cre-mediated recombination in germ cells, comprised the deletion of exons 2 and 3 and the neo cassette. Homozygous mice with this genotype were of interest because they are a novel knock out model that lacks a neo cassette, and it was of value to evaluate if these animals develop the lethal lymphoproliferation observed in mice generated by gene targeting and whether or not the phenotype observed varies from the published characterizations.

One recent and intriguing observation is that CTLA-4 deficient mice over express ICOS (van Berkel., *et al* 2005). This gene is a neighbor of CTLA-4 and the mice used by the authors retained the neo cassette disrupting exons 2 and 3. Therefore it seems likely that the overexpression could be the result of an effect of the neo cassette and this can be analyzed in the mice we have generated, in fact those experiments are now ongoing.

## 6.2. Key findings.

Mice having 3 loxP sites and a neo cassette developed lymphadenopathy as confirmed by visible enlarged lymph nodes and increased cellularity in homozygous mice as compared with heterozygotes or wt littermates. In addition the proportion of B cells, as defined by the expression for the surface marker CD19, was comparatively increased in homozygous. Furthermore histological analysis showed greater cell accumulation in areas of secondary lymphoid organs where B cells are the main cell type. In order to confirm an accumulation of B cells *in situ*, a B cell specific immunohistochemical analysis on such tissue sections should be performed.

The T cell compartment in the lymph node seemed not to be altered in the resting state. There were no significant differences in the absolute numbers of T cells, and those cells did not show a phenotype of activation as seen in CTLA-4 knock out mice (Tivol., *et al* 1995). Upon activation, total lymphocytes and more clearly CD3 enriched T cells from homozygous mice, over expressed CTLA-4 as defined by intensity of fluorescence (figures 4.12 and 4.15). The over expression of CTLA-4 was concomitant with greater expression of the activation marker CD25 (figure 4.16), suggesting at least a proportion of the T cells from homozygotes have been previously primed, this can be confirmed in future experiments by staining for Mel-14, a marker present in naive T cells. The over expression observed of both CD25 and CTLA-4 is in line with previous reports showing a relationship between these two molecules. Blockade of the IL-2R prevented CTLA-4 expression in T cells following activation (Alegre., *et al* 1996) and indirectly, the relationship between CTLA-4 and the IL-2 pathway is also demonstrated by the functional implications of a decreased CTLA-4 expression seen in IL-2 deficient mice and how transgenic over expression of CTLA-4 prevents autoimmune hemolytic anemia and inflammatory bowel disease (Schorle., *et al* 1991 and Hwang., *et al* 2004).

Interestingly, T cells from homozygous mice did not show proliferative responses greater than heterozygous or homozygous indicating the possibility that the CTLA-4 over expression seen in these mice can have a functional implication. It is of relevance to measure the ability of these T cells to produce IL-2 as another readout of this result.

The activation and quiescence of T cells is a tightly controlled phenomenon important for maintaining T cell homeostasis, in which CTLA-4 indeed plays a major role, and recently splice variants of this molecule have been implicated in this process.

The splice variant which has been characterized the most, is that which lacks the B7 ligand-binding domain. LiCTLA-4, but not FiCTLA-4, has been shown to have greater expression on regulatory and memory T cells from diabetic resistant congenic strains (Vijaykrishnan., *et al* 2004). We analyzed the expression of this splice variant in resting and activated lymphocytes and although qualitative differences were observed in the mRNA levels of this splice variant of homozygotes when compared with the littermates at resting, no differences were observed at the protein level as detected by Western blotting. Another interesting splice variant, that has been poorly studied in mice, is sCTLA-4 and lower expression of this variant has been associated with autoimmunity (Thyroid disease) in humans (Oaks., *et al* 2000). In our mice we have found qualitatively lower levels in the expression (as measured by non quantitative RT-PCR see figure 4.19) of this splice variant as well as FL-CTLA-4 in homozygotes when compared to littermates, all at resting. Altogether these data may indicate that a dysregulated expression of CTLA-4 splice variants may be the cause of the phenotype observed but these differences have to be confirmed using, for instance, quantitative RT-PCR.

Mice bearing a *Ctla-4* allele in which exons 2, 3 and the neo cassette have been excised by Cre-mediated recombination (figure 5.1), showed phenotype remarkably similar to the published CTLA-4 knock out mice. *Del/del* mice die 1 month after birth and develop a fatal tissue-destructive lymphoproliferation, particularly evidenced in the pancreas. While differences in the severity of the tissue damage were observed in these mice when compared with the published knock outs, it would be necessary to perform immunohistochemical analysis in order to firmly establish this.

### 6.3 Inducible Cre transgenics suitable to inactivate *Ctla-4*.

In order to conditionally inactivate *Ctla-4*, animals must be crossed with a transgenic animal that expresses Cre in the lymphoid tissue and under temporal control.

A relatively small number of inducible Cre transgenics have been generated that show expression and activity of Cre in lymphoid tissue. For instance we have used an inducible Cre transgenic line ( $\beta$ -70) to delete the *Ctla-4* floxed allele in germ cells. This strain expresses the tamoxifen inducible form of Cre under the control of an ubiquitous promoter (Chicken  $\beta$ -actin), but no expression of Cre has been observed in the T cells of this mice (Dr Laurence Bugeon personal communication).

Another now widely used strain is the Mx-Cre line. These mice express the recombinase under the control of the Mx-1 interferon inducible promoter, which requires the use of double stranded RNA or poly(I)-poly(C) for inducibility (Kuhn., *et al* 1995). Mx-Cre mice have been used to provide temporal control of gene inactivation in T cells. In an article by Huan Han at the Honjo Lab in Japan this interferon controlled Cre transgenic was used to eliminate the expression of the Notch pathway transcription factor, RBP-J. They measured the efficiency of recombination under their induction conditions (300 $\mu$ g of inducer daily and weekly) by Southern blot in various tissues. The spleen showed a relatively high percentage of recombination (80%) as compared with other non lymphoid tissues (around 40% in kidney) however recombination in the thymus was not as high (60%) (Han., *et al* 2002). This suggests that because in adult mice T cell numbers in the periphery depend on a constant and input from the thymus, experiments of conditional inactivation of CTLA-4 may require the use of thymectomized animals.

In another report Zhenyue, H., *et al* reported successful deletion of Fas using Mx-Cre mice and similar concentrations of poly(I)-poly(C). In this case they did not quantify the efficiency of deletion in their system, but they report a functional outcome of the deletion of Fas. Mice induced developed a Fas ligand-mediated T cell depletion (Zhenyue., *et al* 2004).

The efficiency of deletion using these mice is expected to be allele dependent. Pilot studies must therefore be performed to determine the efficiency of the system for *Ctla-4*. As reported for RBP-J, this can be done by Southern blot analysis and a strategy in place.

In Mx-Cre mice the molecule used for the induction of Cre activity, dsRNA or poly(I)-poly(C), is also a potent activator of antigen presenting cells through the Toll-like receptor 3 pathway. Stimulation of cells with dsRNA triggers the production of cytokines, like IFN- $\alpha$ , that can induce the response of cytotoxic cells, obscuring perhaps important features of a potential phenotype associated with the absence of CTLA-4. In this case littermates bearing a floxed *Ctla-4* allele but negative for the Mx-Cre transgene and induced with poly(I)-poly(C) transgene, will be required as critical controls.

#### **6.4. The uses and the value of a *Ctla-4* conditional knock out.**

Overall, the main advantage of gaining temporal control of the inactivation of CTLA-4 is the possibility of analyzing the peripheral immunity of mice at stages later than 1 month. Being able to trigger the excision of this gene at different stages in the lifetime of the mice would allow evaluation of whether the dramatic lymphoproliferation seen in *Ctla-4* deficient mice is reproduced later in life. If a similar phenotype is observed, studying the differences in the mechanisms underlying autoimmunity would be of outstanding relevance. In practice, upon induction of Cre mediated recombination of *Ctla-4*, the first set of experiments would most likely follow the lines of what was done to characterize the phenotype of conventional *Ctla-4* knock outs. These would include for instance: the analysis of potential tissue destruction by histology and immunohistochemistry and a comparative analysis of phenotype of T cells in the lymphoid organs of these mice by flow cytometry. These basic assays are very useful to determine potentially interesting characteristics that can be further pursued.

An enormous amount of data has now been accumulated to demonstrate the role of CTLA-4 in maintaining T cell homeostasis, although other inhibitory costimulatory molecules have been identified (PD-1 and BTLA), and they have been proven to have an independent inhibitory potential, as shown by the development of specific lymphoproliferative disorders in mice deficient for them (Nishimura., *et al* 2001 and Watanabe., *et al* 2003). Analyzing the expression and perhaps their functions in the context of an induced CTLA-4 inactivation, using blocking antibodies for cells in culture or as treat

ment for CTLA-4 conditional knock animals *in vivo*, could help to determine if these receptors have a potential to compensate for the lack of CTLA-4.

An additional advantage of controlling the CTLA-4 deficiency is the possibility to isolate and employ functionally distinct subsets of T cell in order to dissect the function of this molecule in such cells. In chapter 1 the limitations of using blocking antibody strategies have to address this questions was discussed. A very recent paper has come out to address this issue and to report that blocking CTLA-4 on CD4<sup>+</sup> CD25<sup>+</sup> regulatory T cells *in vivo*, abrogates its function by inhibiting T regs rather than effector CD25<sup>-</sup> T cells (Read, S., et al 2006). This together with more evidence available (reviewed in Sansom., *et al* 2006) establishes a critical role of CTLA-4 in T reg biology.

An interesting approach to further study this idea, would be to isolate CD25<sup>+</sup> T regs from CTLA-4 conditional knock outs to induce the deletion of the gene *in vitro*, by delivering Cre through retroviral transduction, or to isolate them from mice already induced and then use them in assays to determine their suppressive capacities.

Another approach would be to use them *in vivo* as a cell treatment for experimental mouse models of autoimmunity, like the diabetic susceptible strain NOD or autoimmune colitis, in which the effects of the treatment can be monitored in terms of progression of disease.

Conventional CTLA-4 knock outs have been used in conjunction with Rag1<sup>-/-</sup> Do11.10 transgenic mice designed to examine the mechanisms of tolerance of CD4<sup>+</sup> T cells, either to tissue restricted or systemic autoantigens (Lohr., *et al* 2005). As in any functional system that employs these knockouts, the power of the analysis that can be obtained, is affected by the age limitations imposed by the phenotype of CTLA-4 deficient mice. Using instead mice in which the inactivation of CTLA-4 can be controlled, could now allow to use these powerful transgenic models at stages beyond the ages at which CTLA-4 knock outs develop their fatal disorder in order to study the role of this molecule in establishing peripheral T cells tolerance to tissue restricted or systemic antigens.

*Bibliography*

- Agata, Y., Kawasaki, A., Nishimura, H., Ishida, Y., Tsubata, T., Yagita, H., et al. (1996). Expression of the PD-1 antigen on the surface of stimulated mouse T and B lymphocytes. *Int Immunol*, 8(5), 765-772.
- Akagi, K., Sandig, V., Vooijs, M., Van der Valk, M., Giovannini, M., Strauss, M., et al. (1997). Cre-mediated somatic site-specific recombination in mice. *Nucleic Acids Res*, 25(9), 1766-1773.
- Akbari, O., DeKruyff, R. H., & Umetsu, D. T. (2001). Pulmonary dendritic cells producing IL-10 mediate tolerance induced by respiratory exposure to antigen. *Nat Immunol*, 2(8), 725-731.
- Alegre, M. L., Noel, P. J., Eisfelder, B. J., Chuang, E., Clark, M. R., Reiner, S. L., et al. (1996). Regulation of surface and intracellular expression of CTLA4 on mouse T cells. *J Immunol*, 157(11), 4762-4770.
- Argos, P., Landy, A., Abremski, K., Egan, J. B., Haggard-Ljungquist, E., Hoess, R. H., et al. (1986). The integrase family of site-specific recombinases: regional similarities and global diversity. *Embo J*, 5(2), 433-440.
- Azuma, M., Ito, D., Yagita, H., Okumura, K., Phillips, J. H., Lanier, L. L., et al. (1993). B70 antigen is a second ligand for CTLA-4 and CD28. *Nature*, 366(6450), 76-79.
- Baroja, M. L., Luxenberg, D., Chau, T., Ling, V., Strathdee, C. A., Carreno, B. M., et al. (2000). The inhibitory function of CTLA-4 does not require its tyrosine phosphorylation. *J Immunol*, 164(1), 49-55.
- Bhatia, S., Edidin, M., Almo, S. C., & Nathenson, S. G. (2005). Different cell surface oligomeric states of B7-1 and B7-2: implications for signaling. *Proc Natl Acad Sci U S A*, 102(43), 15569-15574.
- Bhatia, S., Edidin, M., Almo, S. C., & Nathenson, S. G. (2006). B7-1 and B7-2: similar costimulatory ligands with different biochemical, oligomeric and signaling properties. *Immunol Lett*, 104(1-2), 70-75.
- Boise, L. H., Minn, A. J., Noel, P. J., June, C. H., Accavitti, M. A., Lindsten, T., et al. (1995). CD28 costimulation can promote T cell survival by enhancing the expression of Bcl-XL. *Immunity*, 3(1), 87-98.
- Bradley, A., Evans, M., Kaufman, M. H., & Robertson, E. (1984). Formation of germ-line chimaeras from embryo-derived teratocarcinoma cell lines. *Nature*, 309(5965), 255-256.
- Bradshaw, J. D., Lu, P., Leytze, G., Rodgers, J., Schieven, G. L., Bennett, K. L., et al. (1997). Interaction of the cytoplasmic tail of CTLA-4 (CD152) with a clathrin-associated protein is negatively regulated by tyrosine phosphorylation. *Biochemistry*, 36(50), 15975-15982.



- Broach, J. R., & Hicks, J. B. (1980). Replication and recombination functions associated with the yeast plasmid, 2 mu circle. *Cell*, 21(2), 501-508.
- Brocard, J., Warot, X., Wendling, O., Messaddeq, N., Vonesch, J. L., Chambon, P., et al. (1997). Spatio-temporally controlled site-specific somatic mutagenesis in the mouse. *Proc Natl Acad Sci U S A*, 94(26), 14559-14563.
- Brook, F. A., & Gardner, R. L. (1997). The origin and efficient derivation of embryonic stem cells in the mouse. *Proc Natl Acad Sci U S A*, 94(11), 5709-5712.
- Brunet, J. F., Denizot, F., Luciani, M. F., Roux-Dosseto, M., Suzan, M., Mattei, M. G., et al. (1987). A new member of the immunoglobulin superfamily--CTLA-4. *Nature*, 328(6127), 267-270.
- Carreno, B. M., & Collins, M. (2002). The B7 family of ligands and its receptors: new pathways for costimulation and inhibition of immune responses. *Annu Rev Immunol*, 20, 29-53.
- Cefai, D., Schneider, H., Matangkasombut, O., Kang, H., Brody, J., & Rudd, C. E. (1998). CD28 receptor endocytosis is targeted by mutations that disrupt phosphatidylinositol 3-kinase binding and costimulation. *J Immunol*, 160(5), 2223-2230.
- Chambers, C. A., Cado, D., Truong, T., & Allison, J. P. (1997). Thymocyte development is normal in CTLA-4-deficient mice. *Proc Natl Acad Sci U S A*, 94(17), 9296-9301.
- Chambers, C. A., Sullivan, T. J., & Allison, J. P. (1997). Lymphoproliferation in CTLA-4-deficient mice is mediated by costimulation-dependent activation of CD4+ T cells. *Immunity*, 7(6), 885-895.
- Chuang, E., Alegre, M. L., Duckett, C. S., Noel, P. J., Vander Heiden, M. G., & Thompson, C. B. (1997). Interaction of CTLA-4 with the clathrin-associated protein AP50 results in ligand-independent endocytosis that limits cell surface expression. *J Immunol*, 159(1), 144-151.
- Clark, G. J., & Dallman, M. J. (1992). Identification of a cDNA encoding the rat CD28 homologue. *Immunogenetics*, 35(1), 54-57.
- Collins, A. V., Brodie, D. W., Gilbert, R. J., Iaboni, A., Manso-Sancho, R., Walse, B., et al. (2002). The interaction properties of costimulatory molecules revisited. *Immunity*, 17(2), 201-210.
- Conne, B., Stutz, A., & Vassalli, J. D. (2000). The 3' untranslated region of messenger RNA: A molecular 'hotspot' for pathology? *Nat Med*, 6(6), 637-641.
- Copeman, J. B., Cucca, F., Hearne, C. M., Cornall, R. J., Reed, P. W., Ronningen, K. S., et al. (1995). Linkage disequilibrium mapping of a type 1 diabetes susceptibility gene (IDDM7) to chromosome 2q31-q33. *Nat Genet*, 9(1), 80-85.

- Coyle, A. J., Lehar, S., Lloyd, C., Tian, J., Delaney, T., Manning, S., et al. (2000). The CD28-related molecule ICOS is required for effective T cell-dependent immune responses. *Immunity*, 13(1), 95-105.
- Damle, N. K., Mohaghehpour, N., Hansen, J. A., & Engleman, E. G. (1983). Alloantigen-specific cytotoxic and suppressor T lymphocytes are derived from phenotypically distinct precursors. *J Immunol*, 131(5), 2296-2300.
- Damle, N. K., Doyle, L. V., Grosmaire, L. S., & Ledbetter, J. A. (1988). Differential regulatory signals delivered by antibody binding to the CD28 (Tp44) molecule during the activation of human T lymphocytes. *J Immunol*, 140(6), 1753-1761.
- Dariavach, P., Mattei, M. G., Golstein, P., & Lefranc, M. P. (1988). Human Ig superfamily CTLA-4 gene: chromosomal localization and identity of protein sequence between murine and human CTLA-4 cytoplasmic domains. *Eur J Immunol*, 18(12), 1901-1905.
- Darlington, P. J., Baroja, M. L., Chau, T. A., Siu, E., Ling, V., Carreno, B. M., et al. (2002). Surface cytotoxic T lymphocyte-associated antigen 4 partitions within lipid rafts and relocates to the immunological synapse under conditions of inhibition of T cell activation. *J Exp Med*, 195(10), 1337-1347.
- Darlington, P. J., Kirchhof, M. G., Criado, G., Sondhi, J., & Madrenas, J. (2005). Hierarchical regulation of CTLA-4 dimer-based lattice formation and its biological relevance for T cell inactivation. *J Immunol*, 175(2), 996-1004.
- Davis, S. J., Ikemizu, S., Evans, E. J., Fugger, L., Bakker, T. R., & van der Merwe, P. A. (2003). The nature of molecular recognition by T cells. *Nat Immunol*, 4(3), 217-224.
- Dawlaty, M. M., & van Deursen, J. M. (2006). Gene targeting methods for studying nuclear transport factors in mice. *Methods*.
- De Smedt, T., Pajak, B., Muraille, E., Lespagnard, L., Heinen, E., De Baetselier, P., et al. (1996). Regulation of dendritic cell numbers and maturation by lipopolysaccharide in vivo. *J Exp Med*, 184(4), 1413-1424.
- Deng, C., & Capecchi, M. R. (1992). Reexamination of gene targeting frequency as a function of the extent of homology between the targeting vector and the target locus. *Mol Cell Biol*, 12(8), 3365-3371.
- Doetschman, T. C., Eistetter, H., Katz, M., Schmidt, W., & Kemler, R. (1985). The in vitro development of blastocyst-derived embryonic stem cell lines: formation of visceral yolk sac, blood islands and myocardium. *J Embryol Exp Morphol*, 87, 27-45.
- Doetschman, T., Gregg, R. G., Maeda, N., Hooper, M. L., Melton, D. W., Thompson, S., et al. (1987). Targetted correction of a mutant HPRT gene in mouse embryonic stem cells. *Nature*, 330(6148), 576-578.

- Dymecki, S. M. (1996). Flp recombinase promotes site-specific DNA recombination in embryonic stem cells and transgenic mice. *Proc Natl Acad Sci U S A*, 93(12), 6191-6196.
- Eagar, T. N., Karandikar, N. J., Bluestone, J. A., & Miller, S. D. (2002). The role of CTLA-4 in induction and maintenance of peripheral T cell tolerance. *Eur J Immunol*, 32(4), 972-981.
- Eggena, M. P., Walker, L. S., Nagabhushanam, V., Barron, L., Chodos, A., & Abbas, A. K. (2004). Cooperative roles of CTLA-4 and regulatory T cells in tolerance to an islet cell antigen. *J Exp Med*, 199(12), 1725-1730.
- Evans, M. (1981). Origin of mouse embryonal carcinoma cells and the possibility of their direct isolation into tissue culture. *J Reprod Fertil*, 62(2), 625-631.
- Fallarino, F., Fields, P. E., & Gajewski, T. F. (1998). B7-1 engagement of cytotoxic T lymphocyte antigen 4 inhibits T cell activation in the absence of CD28. *J Exp Med*, 188(1), 205-210.
- Fallarino, F., Grohmann, U., Hwang, K. W., Orabona, C., Vacca, C., Bianchi, R., et al. (2003). Modulation of tryptophan catabolism by regulatory T cells. *Nat Immunol*, 4(12), 1206-1212.
- Feil, R., Brocard, J., Mascrez, B., LeMeur, M., Metzger, D., & Chambon, P. (1996). Ligand-activated site-specific recombination in mice. *Proc Natl Acad Sci U S A*, 93(20), 10887-10890.
- Finn, P. W., He, H., Wang, Y., Wang, Z., Guan, G., Listman, J., et al. (1997). Synergistic induction of CTLA-4 expression by costimulation with TCR plus CD28 signals mediated by increased transcription and messenger ribonucleic acid stability. *J Immunol*, 158(9), 4074-4081.
- Frauwirth, K. A., Alegre, M. L., & Thompson, C. B. (2000). Induction of T cell anergy in the absence of CTLA-4/B7 interaction. *J Immunol*, 164(6), 2987-2993.
- Frauwirth, K. A., Alegre, M. L., & Thompson, C. B. (2001). CTLA-4 is not required for induction of CD8(+) T cell anergy in vivo. *J Immunol*, 167(9), 4936-4941.
- Freeman, G. J., Lombard, D. B., Gimmi, C. D., Brod, S. A., Lee, K., Laning, J. C., et al. (1992). CTLA-4 and CD28 mRNA are coexpressed in most T cells after activation. Expression of CTLA-4 and CD28 mRNA does not correlate with the pattern of lymphokine production. *J Immunol*, 149(12), 3795-3801.
- Freeman, G. J., Long, A. J., Iwai, Y., Bourque, K., Chernova, T., Nishimura, H., et al. (2000). Engagement of the PD-1 immunoinhibitory receptor by a novel B7 family member leads to negative regulation of lymphocyte activation. *J Exp Med*, 192(7), 1027-1034.

- Garrick, D., Fiering, S., Martin, D. I., & Whitelaw, E. (1998). Repeat-induced gene silencing in mammals. *Nat Genet*, 18(1), 56-59.
- Gerbaud, C., Fournier, P., Blanc, H., Aigle, M., Heslot, H., & Guerineau, M. (1979). High frequency of yeast transformation by plasmids carrying part or entire 2-micron yeast plasmid. *Gene*, 5(3), 233-253.
- Gough, S. C., Walker, L. S., & Sansom, D. M. (2005). CTLA4 gene polymorphism and autoimmunity. *Immunol Rev*, 204, 102-115.
- Greene, J. L., Leytze, G. M., Emswiler, J., Peach, R., Bajorath, J., Cosand, W., et al. (1996). Covalent dimerization of CD28/CTLA-4 and oligomerization of CD80/CD86 regulate T cell costimulatory interactions. *J Biol Chem*, 271(43), 26762-26771.
- Greenwald, R. J., Freeman, G. J., & Sharpe, A. H. (2005). The B7 family revisited. *Annu Rev Immunol*, 23, 515-548.
- Grohmann, U., Orabona, C., Fallarino, F., Vacca, C., Calcinaro, F., Falorni, A., et al. (2002). CTLA-4-Ig regulates tryptophan catabolism in vivo. *Nat Immunol*, 3(11), 1097-1101.
- Grohmann, U., Orabona, C., Fallarino, F., Vacca, C., Calcinaro, F., Falorni, A., et al. (2002). CTLA-4-Ig regulates tryptophan catabolism in vivo. *Nat Immunol*, 3(11), 1097-1101.
- Gross, J. A., St John, T., & Allison, J. P. (1990). The murine homologue of the T lymphocyte antigen CD28. Molecular cloning and cell surface expression. *J Immunol*, 144(8), 3201-3210.
- Gross, J. A., Callas, E., & Allison, J. P. (1992). Identification and distribution of the costimulatory receptor CD28 in the mouse. *J Immunol*, 149(2), 380-388.
- Gu, H., Marth, J. D., Orban, P. C., Mossmann, H., & Rajewsky, K. (1994). Deletion of a DNA polymerase beta gene segment in T cells using cell type-specific gene targeting. *Science*, 265(5168), 103-106.
- Han, H., Tanigaki, K., Yamamoto, N., Kuroda, K., Yoshimoto, M., Nakahata, T., et al. (2002). Inducible gene knockout of transcription factor recombination signal binding protein-J reveals its essential role in T versus B lineage decision. *Int Immunol*, 14(6), 637-645.
- Harding, F. A., McArthur, J. G., Gross, J. A., Raulet, D. H., & Allison, J. P. (1992). CD28-mediated signalling co-stimulates murine T cells and prevents induction of anergy in T-cell clones. *Nature*, 356(6370), 607-609.
- Harper, K., Balzano, C., Rouvier, E., Mattei, M. G., Luciani, M. F., & Golstein, P. (1991). CTLA-4 and CD28 activated lymphocyte molecules are closely related in both mouse and human as to sequence, message expression, gene structure, and chromosomal location. *J Immunol*, 147(3), 1037-1044.

- Hasty, P., Rivera-Perez, J., Chang, C., & Bradley, A. (1991). Target frequency and integration pattern for insertion and replacement vectors in embryonic stem cells. *Mol Cell Biol*, 11(9), 4509-4517.
- Hasty, P., Rivera-Perez, J., & Bradley, A. (1991). The length of homology required for gene targeting in embryonic stem cells. *Mol Cell Biol*, 11(11), 5586-5591.
- Hathcock, K. S., Laszlo, G., Pucillo, C., Linsley, P., & Hodes, R. J. (1994). Comparative analysis of B7-1 and B7-2 costimulatory ligands: expression and function. *J Exp Med*, 180(2), 631-640.
- Hug, B. A., Wesselschmidt, R. L., Fiering, S., Bender, M. A., Epner, E., Groudine, M., et al. (1996). Analysis of mice containing a targeted deletion of beta-globin locus control region 5' hypersensitive site 3. *Mol Cell Biol*, 16(6), 2906-2912.
- Hutloff, A., Dittrich, A. M., Beier, K. C., Eljaschewitsch, B., Kraft, R., Anagnostopoulos, I., et al. (1999). ICOS is an inducible T-cell co-stimulator structurally and functionally related to CD28. *Nature*, 397(6716), 263-266.
- Hwang, K. W., Sweatt, W. B., Brown, I. E., Blank, C., Gajewski, T. F., Bluestone, J. A., et al. (2002). Cutting edge: targeted ligation of CTLA-4 in vivo by membrane-bound anti-CTLA-4 antibody prevents rejection of allogeneic cells. *J Immunol*, 169(2), 633-637.
- Hwang, K. W., Sweatt, W. B., Mashayekhi, M., Palucki, D. A., Sattar, H., Chuang, E., et al. (2004). Transgenic expression of CTLA-4 controls lymphoproliferation in IL-2-deficient mice. *J Immunol*, 173(9), 5415-5424.
- Ikemizu, S., Gilbert, R. J., Fennelly, J. A., Collins, A. V., Harlos, K., Jones, E. Y., et al. (2000). Structure and dimerization of a soluble form of B7-1. *Immunity*, 12(1), 51-60.
- Inaba, K., Witmer-Pack, M., Inaba, M., Hathcock, K. S., Sakuta, H., Azuma, M., et al. (1994). The tissue distribution of the B7-2 costimulator in mice: abundant expression on dendritic cells in situ and during maturation in vitro. *J Exp Med*, 180(5), 1849-1860.
- Jenkins, M. K., & Schwartz, R. H. (1987). Antigen presentation by chemically modified splenocytes induces antigen-specific T cell unresponsiveness in vitro and in vivo. *J Exp Med*, 165(2), 302-319.
- Jenkins, M. K., Ashwell, J. D., & Schwartz, R. H. (1988). Allogeneic non-T spleen cells restore the responsiveness of normal T cell clones stimulated with antigen and chemically modified antigen-presenting cells. *J Immunol*, 140(10), 3324-3330.
- Joyner, A., (Editor). (2001). *Gene Targeting: A practical Approach*. Oxford University Press. 2nd ed, 289pp.
- Judge, T. A., Wu, Z., Zheng, X. G., Sharpe, A. H., Sayegh, M. H., & Turka, L. A. (1999). The role of CD80, CD86, and CTLA4 in alloimmune responses and the induction of long-term allograft survival. *J Immunol*, 162(4), 1947-1951.

- June, C. H., Bluestone, J. A., Nadler, L. M., & Thompson, C. B. (1994). The B7 and CD28 receptor families. *Immunol Today*, 15(7), 321-331.
- Kanegae, Y., Takamori, K., Sato, Y., Lee, G., Nakai, M., & Saito, I. (1996). Efficient gene activation system on mammalian cell chromosomes using recombinant adenovirus producing Cre recombinase. *Gene*, 181(1-2), 207-212.
- Kaufman, R. M., Lu, Z. H., Behl, R., Holt, J. M., Ackers, G. K., & Ley, T. J. (2001). Lack of neighborhood effects from a transcriptionally active phosphoglycerate kinase-neo cassette located between the murine beta-major and beta-minor globin genes. *Blood*, 98(1), 65-73.
- Koller, B. H., Hagemann, L. J., Doetschman, T., Hageman, J. R., Huang, S., Williams, P. J., et al. (1989). Germ-line transmission of a planned alteration made in a hypoxanthine phosphoribosyltransferase gene by homologous recombination in embryonic stem cells. *Proc Natl Acad Sci U S A*, 86(22), 8927-8931.
- Kopf, M., Coyle, A. J., Schmitz, N., Barner, M., Oxenius, A., Gallimore, A., et al. (2000). Inducible costimulator protein (ICOS) controls T helper cell subset polarization after virus and parasite infection. *J Exp Med*, 192(1), 53-61.
- Krummel, M. F., & Allison, J. P. (1995). CD28 and CTLA-4 have opposing effects on the response of T cells to stimulation. *J Exp Med*, 182(2), 459-465.
- Krummel, M. F., & Allison, J. P. (1996). CTLA-4 engagement inhibits IL-2 accumulation and cell cycle progression upon activation of resting T cells. *J Exp Med*, 183(6), 2533-2540.
- Kuhn, R., Schwenk, F., Aguet, M., & Rajewsky, K. (1995). Inducible gene targeting in mice. *Science*, 269(5229), 1427-1429.
- Lafferty, K. J., & Cunningham, A. J. (1975). A new analysis of allogeneic interactions. *Aust J Exp Biol Med Sci*, 53(1), 27-42.
- Lafferty, K. J., Prowse, S. J., Simeonovic, C. J., & Warren, H. S. (1983). Immunobiology of tissue transplantation: a return to the passenger leukocyte concept. *Annu Rev Immunol*, 1, 143-173.
- Lakso, M., Pichel, J. G., Gorman, J. R., Sauer, B., Okamoto, Y., Lee, E., et al. (1996). Efficient in vivo manipulation of mouse genomic sequences at the zygote stage. *Proc Natl Acad Sci U S A*, 93(12), 5860-5865.
- Lallemand, Y., Luria, V., Haffner-Krausz, R., & Lonai, P. (1998). Maternally expressed PGK-Cre transgene as a tool for early and uniform activation of the Cre site-specific recombinase. *Transgenic Res*, 7(2), 105-112.
- Lee, K. M., Chuang, E., Griffin, M., Khattri, R., Hong, D. K., Zhang, W., et al. (1998). Molecular basis of T cell inactivation by CTLA-4. *Science*, 282(5397), 2263-2266.

- Lee, G., & Saito, I. (1998). Role of nucleotide sequences of loxP spacer region in Cre-mediated recombination. *Gene*, 216(1), 55-65.
- Lenschow, D. J., Sperling, A. I., Cooke, M. P., Freeman, G., Rhee, L., Decker, D. C., et al. (1994). Differential up-regulation of the B7-1 and B7-2 costimulatory molecules after Ig receptor engagement by antigen. *J Immunol*, 153(5), 1990-1997.
- Lenschow, D. J., Ho, S. C., Sattar, H., Rhee, L., Gray, G., Nabavi, N., et al. (1995). Differential effects of anti-B7-1 and anti-B7-2 monoclonal antibody treatment on the development of diabetes in the nonobese diabetic mouse. *J Exp Med*, 181(3), 1145-1155.
- Liang, S. C., Latchman, Y. E., Buhlmann, J. E., Tomczak, M. F., Horwitz, B. H., Freeman, G. J., et al. (2003). Regulation of PD-1, PD-L1, and PD-L2 expression during normal and autoimmune responses. *Eur J Immunol*, 33(10), 2706-2716.
- Lin, F. L., Sperle, K., & Sternberg, N. (1985). Recombination in mouse L cells between DNA introduced into cells and homologous chromosomal sequences. *Proc Natl Acad Sci U S A*, 82(5), 1391-1395.
- Lindsten, T., Lee, K. P., Harris, E. S., Petryniak, B., Craighead, N., Reynolds, P. J., et al. (1993). Characterization of CTLA-4 structure and expression on human T cells. *J Immunol*, 151(7), 3489-3499.
- Ling, V., Wu, P. W., Finnerty, H. F., Sharpe, A. H., Gray, G. S., & Collins, M. (1999). Complete sequence determination of the mouse and human CTLA4 gene loci: cross-species DNA sequence similarity beyond exon borders. *Genomics*, 60(3), 341-355.
- Ling, V., Wu, P. W., Spaulding, V., Kieleczawa, J., Luxenberg, D., Carreno, B. M., et al. (2003). Duplication of primate and rodent B7-H3 immunoglobulin V- and C-like domains: divergent history of functional redundancy and exon loss. *Genomics*, 82(3), 365-377.
- Linsley, P. S., Clark, E. A., & Ledbetter, J. A. (1990). T-cell antigen CD28 mediates adhesion with B cells by interacting with activation antigen B7/BB-1. *Proc Natl Acad Sci U S A*, 87(13), 5031-5035.
- Linsley, P. S., Brady, W., Urnes, M., Grosmaire, L. S., Damle, N. K., & Ledbetter, J. A. (1991). CTLA-4 is a second receptor for the B cell activation antigen B7. *J Exp Med*, 174(3), 561-569.
- Linsley, P. S., Greene, J. L., Tan, P., Bradshaw, J., Ledbetter, J. A., Anasetti, C., et al. (1992). Coexpression and functional cooperation of CTLA-4 and CD28 on activated T lymphocytes. *J Exp Med*, 176(6), 1595-1604.
- Linsley, P. S., Bradshaw, J., Urnes, M., Grosmaire, L., & Ledbetter, J. A. (1993). CD28 engagement by B7/BB-1 induces transient down-regulation of CD28 synthesis and prolonged unresponsiveness to CD28 signaling. *J Immunol*, 150(8 Pt 1), 3161-3169.

- Linsley, P. S., Greene, J. L., Brady, W., Bajorath, J., Ledbetter, J. A., & Peach, R. (1994). Human B7-1 (CD80) and B7-2 (CD86) bind with similar avidities but distinct kinetics to CD28 and CTLA-4 receptors. *Immunity*, 1(9), 793-801.
- Linsley, P. S., Nadler, S. G., Bajorath, J., Peach, R., Leung, H. T., Rogers, J., et al. (1995). Binding stoichiometry of the cytotoxic T lymphocyte-associated molecule-4 (CTLA-4). A disulfide-linked homodimer binds two CD86 molecules. *J Biol Chem*, 270(25), 15417-15424.
- Lohr, J., Knoechel, B., Kahn, E. C., & Abbas, A. K. (2004). Role of B7 in T cell tolerance. *J Immunol*, 173(8), 5028-5035.
- Magistrelli, G., Jeannin, P., Herbault, N., Benoit De Coignac, A., Gauchat, J. F., Bonnefoy, J. Y., et al. (1999). A soluble form of CTLA-4 generated by alternative splicing is expressed by nonstimulated human T cells. *Eur J Immunol*, 29(11), 3596-3602.
- Magistrelli, G., Jeannin, P., Herbault, N., Benoit De Coignac, A., Gauchat, J. F., Bonnefoy, J. Y., et al. (1999). A soluble form of CTLA-4 generated by alternative splicing is expressed by nonstimulated human T cells. *Eur J Immunol*, 29(11), 3596-3602.
- Mandelbrot, D. A., McAdam, A. J., & Sharpe, A. H. (1999). B7-1 or B7-2 is required to produce the lymphoproliferative phenotype in mice lacking cytotoxic T lymphocyte-associated antigen 4 (CTLA-4). *J Exp Med*, 189(2), 435-440.
- Mandelbrot, D. A., Oosterwegel, M. A., Shimizu, K., Yamada, A., Freeman, G. J., Mitchell, R. N., et al. (2001). B7-dependent T-cell costimulation in mice lacking CD28 and CTLA4. *J Clin Invest*, 107(7), 881-887.
- Manzotti, C. N., Liu, M. K., Burke, F., Dussably, L., Zheng, Y., & Sansom, D. M. (2006). Integration of CD28 and CTLA-4 function results in differential responses of T cells to CD80 and CD86. *Eur J Immunol*, 36(6), 1413-1422.
- Marron, M. P., Zeidler, A., Raffel, L. J., Eckenrode, S. E., Yang, J. J., Hopkins, D. I., et al. (2000). Genetic and physical mapping of a type 1 diabetes susceptibility gene (IDDM12) to a 100-kb phagemid artificial chromosome clone containing D2S72-CTLA4-D2S105 on chromosome 2q33. *Diabetes*, 49(3), 492-499.
- Martin, G. R. (1981). Isolation of a pluripotent cell line from early mouse embryos cultured in medium conditioned by teratocarcinoma stem cells. *Proc Natl Acad Sci U S A*, 78(12), 7634-7638.
- Martin, P. J., Ledbetter, J. A., Morishita, Y., June, C. H., Beatty, P. G., & Hansen, J. A. (1986). A 44 kilodalton cell surface homodimer regulates interleukin 2 production by activated human T lymphocytes. *J Immunol*, 136(9), 3282-3287.
- Martin, M., Schneider, H., Azouz, A., & Rudd, C. E. (2001). Cytotoxic T lymphocyte antigen 4 and CD28 modulate cell surface raft expression in their regulation of T cell function. *J Exp Med*, 194(11), 1675-1681.



- McAdam, A. J., Greenwald, R. J., Levin, M. A., Chernova, T., Malenkovich, N., Ling, V., et al. (2001). ICOS is critical for CD40-mediated antibody class switching. *Nature*, 409(6816), 102-105.
- Meyers, E. N., Lewandoski, M., & Martin, G. R. (1998). An Fgf8 mutant allelic series generated by Cre- and Flp-mediated recombination. *Nat Genet*, 18(2), 136-141.
- Moens, C. B., Auerbach, A. B., Conlon, R. A., Joyner, A. L., & Rossant, J. (1992). A targeted mutation reveals a role for N-myc in branching morphogenesis in the embryonic mouse lung. *Genes Dev*, 6(5), 691-704.
- Moustafa, L. A., & Brinster, R. L. (1972). Induced chimaerism by transplanting embryonic cells into mouse blastocysts. *J Exp Zool*, 181(2), 193-201.
- Munn, D. H., Sharma, M. D., & Mellor, A. L. (2004). Ligation of B7-1/B7-2 by human CD4+ T cells triggers indoleamine 2,3-dioxygenase activity in dendritic cells. *J Immunol*, 172(7), 4100-4110.
- Nagy, A., Moens, C., Ivanyi, E., Pawling, J., Gertsenstein, M., Hadjantonakis, A. K., et al. (1998). Dissecting the role of N-myc in development using a single targeting vector to generate a series of alleles. *Curr Biol*, 8(11), 661-664.
- Nakazawa, A., Dotan, I., Brimnes, J., Allez, M., Shao, L., Tsushima, F., et al. (2004). The expression and function of costimulatory molecules B7H and B7-H1 on colonic epithelial cells. *Gastroenterology*, 126(5), 1347-1357.
- Nishimura, H., Nose, M., Hiai, H., Minato, N., & Honjo, T. (1999). Development of lupus-like autoimmune diseases by disruption of the PD-1 gene encoding an ITIM motif-carrying immunoreceptor. *Immunity*, 11(2), 141-151.
- Nishimura, H., Okazaki, T., Tanaka, Y., Nakatani, K., Hara, M., Matsumori, A., et al. (2001). Autoimmune dilated cardiomyopathy in PD-1 receptor-deficient mice. *Science*, 291(5502), 319-322.
- Nishimura, H., & Honjo, T. (2001). PD-1: an inhibitory immunoreceptor involved in peripheral tolerance. *Trends Immunol*, 22(5), 265-268.
- Nistico, L., Buzzetti, R., Pritchard, L. E., Van der Auwera, B., Giovannini, C., Bosi, E., et al. (1996). The CTLA-4 gene region of chromosome 2q33 is linked to, and associated with, type 1 diabetes. *Belgian Diabetes Registry. Hum Mol Genet*, 5(7), 1075-1080.
- Oaks, M. K., Hallett, K. M., Penwell, R. T., Stauber, E. C., Warren, S. J., & Tector, A. J. (2000). A native soluble form of CTLA-4. *Cell Immunol*, 201(2), 144-153.
- Okamoto, N., Tezuka, K., Kato, M., Abe, R., & Tsuji, T. (2003). PI3-kinase and MAP-kinase signaling cascades in AILIM/ICOS- and CD28-costimulated T-cells have distinct functions between cell proliferation and IL-10 production. *Biochem Biophys Res Commun*, 310(3), 691-702.

- Okazaki, T., Maeda, A., Nishimura, H., Kurosaki, T., & Honjo, T. (2001). PD-1 immunoreceptor inhibits B cell receptor-mediated signaling by recruiting src homology 2-domain-containing tyrosine phosphatase 2 to phosphotyrosine. *Proc Natl Acad Sci U S A*, 98(24), 13866-13871.
- Olson, E. N., Arnold, H. H., Rigby, P. W., & Wold, B. J. (1996). Know your neighbors: three phenotypes in null mutants of the myogenic bHLH gene MRF4. *Cell*, 85(1), 1-4.
- Orban, P. C., Chui, D., & Marth, J. D. (1992). Tissue- and site-specific DNA recombination in transgenic mice. *Proc Natl Acad Sci U S A*, 89(15), 6861-6865.
- Ostrov, D. A., Shi, W., Schwartz, J. C., Almo, S. C., & Nathenson, S. G. (2000). Structure of murine CTLA-4 and its role in modulating T cell responsiveness. *Science*, 290(5492), 816-819.
- Paust, S., Lu, L., McCarty, N., & Cantor, H. (2004). Engagement of B7 on effector T cells by regulatory T cells prevents autoimmune disease. *Proc Natl Acad Sci U S A*, 101(28), 10398-10403.
- Perkins, D., Wang, Z., Donovan, C., He, H., Mark, D., Guan, G., et al. (1996). Regulation of CTLA-4 expression during T cell activation. *J Immunol*, 156(11), 4154-4159.
- Pham, C. T., MacIvor, D. M., Hug, B. A., Heusel, J. W., & Ley, T. J. (1996). Long-range disruption of gene expression by a selectable marker cassette. *Proc Natl Acad Sci U S A*, 93(23), 13090-13095.
- Ranheim, E. A., & Kipps, T. J. (1993). Activated T cells induce expression of B7/BB1 on normal or leukemic B cells through a CD40-dependent signal. *J Exp Med*, 177(4), 925-935.
- Sadowski, P. D. (1995). The Flp recombinase of the 2-microns plasmid of *Saccharomyces cerevisiae*. *Prog Nucleic Acid Res Mol Biol*, 51, 53-91.
- Sansom D.M, Walker L.S. (2006). The role of CD28 and cytotoxic T-lymphocyte antigen-4 (CTLA-4) in regulatory T-cell biology. *Immunol Rev*. 212, 131-48.
- Schorle, H., Holtschke, T., Hunig, T., Schimpl, A., & Horak, I. (1991). Development and function of T cells in mice rendered interleukin-2 deficient by gene targeting. *Nature*, 352(6336), 621-624.
- Schwartz, J. C., Zhang, X., Fedorov, A. A., Nathenson, S. G., & Almo, S. C. (2001). Structural basis for co-stimulation by the human CTLA-4/B7-2 complex. *Nature*, 410(6828), 604-608.
- Schwenk, F., Kuhn, R., Angrand, P. O., Rajewsky, K., & Stewart, A. F. (1998). Temporally and spatially regulated somatic mutagenesis in mice. *Nucleic Acids Res*, 26(6), 1427-1432.

- Shahinian, A., Pfeffer, K., Lee, K. P., Kundig, T. M., Kishihara, K., Wakeham, A., et al. (1993). Differential T cell costimulatory requirements in CD28-deficient mice. *Science*, 261(5121), 609-612.
- Sharpe, A. H., & Freeman, G. J. (2002). The B7-CD28 superfamily. *Nat Rev Immunol*, 2(2), 116-126.
- Shibata, H., Toyama, K., Shioya, H., Ito, M., Hirota, M., Hasegawa, S., et al. (1997). Rapid colorectal adenoma formation initiated by conditional targeting of the Apc gene. *Science*, 278(5335), 120-123.
- Sica, G. L., Choi, I. H., Zhu, G., Tamada, K., Wang, S. D., Tamura, H., et al. (2003). B7-H4, a molecule of the B7 family, negatively regulates T cell immunity. *Immunity*, 18(6), 849-861.
- Simpson, E. M., Linder, C. C., Sargent, E. E., Davisson, M. T., Mobraaten, L. E., & Sharp, J. J. (1997). Genetic variation among 129 substrains and its importance for targeted mutagenesis in mice. *Nat Genet*, 16(1), 19-27.
- Smithies, O., Gregg, R. G., Boggs, S. S., Koralewski, M. A., & Kucherlapati, R. S. (1985). Insertion of DNA sequences into the human chromosomal beta-globin locus by homologous recombination. *Nature*, 317(6034), 230-234.
- Sotomayor, E. M., Borrello, I., Tubb, E., Allison, J. P., & Levitsky, H. I. (1999). In vivo blockade of CTLA-4 enhances the priming of responsive T cells but fails to prevent the induction of tumor antigen-specific tolerance. *Proc Natl Acad Sci U S A*, 96(20), 11476-11481.
- Stack, R. M., Lenschow, D. J., Gray, G. S., Bluestone, J. A., & Fitch, F. W. (1994). IL-4 treatment of small splenic B cells induces costimulatory molecules B7-1 and B7-2. *J Immunol*, 152(12), 5723-5733.
- Stamper, C. C., Zhang, Y., Tobin, J. F., Erbe, D. V., Ikemizu, S., Davis, S. J., et al. (2001). Crystal structure of the B7-1/CTLA-4 complex that inhibits human immune responses. *Nature*, 410(6828), 608-611.
- Steinberger, P., Majdic, O., Derdak, S. V., Pfistershammer, K., Kirchberger, S., Klauser, C., et al. (2004). Molecular characterization of human 4Ig-B7-H3, a member of the B7 family with four Ig-like domains. *J Immunol*, 172(4), 2352-2359.
- Sternberg, N., Sauer, B., Hoess, R., & Abremski, K. (1986). Bacteriophage P1 cre gene and its regulatory region. Evidence for multiple promoters and for regulation by DNA methylation. *J Mol Biol*, 187(2), 197-212.
- Suemori, H., & Noguchi, S. (2000). Hox C cluster genes are dispensable for overall body plan of mouse embryonic development. *Dev Biol*, 220(2), 333-342.

- Suh, W. K., Gajewska, B. U., Okada, H., Gronski, M. A., Bertram, E. M., Dawicki, W., et al. (2003). The B7 family member B7-H3 preferentially down-regulates T helper type 1-mediated immune responses. *Nat Immunol*, 4(9), 899-906.
- Tafuri, A., Shahinian, A., Bladt, F., Yoshinaga, S. K., Jordana, M., Wakeham, A., et al. (2001). ICOS is essential for effective T-helper-cell responses. *Nature*, 409(6816), 105-109.
- Takahashi, S., Kataoka, H., Hara, S., Yokosuka, T., Takase, K., Yamasaki, S., et al. (2005). In vivo overexpression of CTLA-4 suppresses lymphoproliferative diseases and thymic negative selection. *Eur J Immunol*, 35(2), 399-407.
- Thomas, K. R., & Capecchi, M. R. (1987). Site-directed mutagenesis by gene targeting in mouse embryo-derived stem cells. *Cell*, 51(3), 503-512.
- Thomas, K. R., Deng, C., & Capecchi, M. R. (1992). High-fidelity gene targeting in embryonic stem cells by using sequence replacement vectors. *Mol Cell Biol*, 12(7), 2919-2923.
- Tivol, E. A., Borriello, F., Schweitzer, A. N., Lynch, W. P., Bluestone, J. A., & Sharpe, A. H. (1995). Loss of CTLA-4 leads to massive lymphoproliferation and fatal multiorgan tissue destruction, revealing a critical negative regulatory role of CTLA-4. *Immunity*, 3(5), 541-547.
- Tivol, E. A., & Gorski, J. (2002). Re-establishing peripheral tolerance in the absence of CTLA-4: complementation by wild-type T cells points to an indirect role for CTLA-4. *J Immunol*, 169(4), 1852-1858.
- Tolmachova, T., Anders, R., Abrink, M., Bugeon, L., Dallman, M. J., Fütter, C. E., et al. (2006). Independent degeneration of photoreceptors and retinal pigment epithelium in conditional knockout mouse models of choroideremia. *J Clin Invest*, 116(2), 386-394.
- Ueda, H., Howson, J. M., Esposito, L., Heward, J., Snook, H., Chamberlain, G., et al. (2003). Association of the T-cell regulatory gene CTLA4 with susceptibility to autoimmune disease. *Nature*, 423(6939), 506-511.
- Vaidya, B., Oakes, E. J., Imrie, H., Dickinson, A. J., Perros, P., Kendall-Taylor, P., et al. (2003). CTLA4 gene and Graves' disease: association of Graves' disease with the CTLA4 exon 1 and intron 1 polymorphisms, but not with the promoter polymorphism. *Clin Endocrinol (Oxf)*, 58(6), 732-735.
- Valle, A., Aubry, J. P., Durand, I., & Banchereau, J. (1991). IL-4 and IL-2 upregulate the expression of antigen B7, the B cell counterstructure to T cell CD28: an amplification mechanism for T-B cell interactions. *Int Immunol*, 3(3), 229-235.
- van Berkel, M. E., Schrijver, E. H., Hofhuis, F. M., Sharpe, A. H., Coyle, A. J., Broeren, C. P., et al. (2005). ICOS contributes to T cell expansion in CTLA-4 deficient mice. *J Immunol*, 175(1), 182-188.

- van der Merwe, P. A., & Davis, S. J. (2003). Molecular interactions mediating T cell antigen recognition. *Annu Rev Immunol*, 21, 659-684.
- Vasioukhin, V., Degenstein, L., Wise, B., & Fuchs, E. (1999). The magical touch: genome targeting in epidermal stem cells induced by tamoxifen application to mouse skin. *Proc Natl Acad Sci U S A*, 96(15), 8551-8556.
- Vijaykrishnan, L., Slavik, J. M., Illes, Z., Greenwald, R. J., Rainbow, D., Greve, B., et al. (2004). An autoimmune disease-associated CTLA-4 splice variant lacking the B7 binding domain signals negatively in T cells. *Immunity*, 20(5), 563-575.
- Vooijs, M., Jonkers, J., & Berns, A. (2001). A highly efficient ligand-regulated Cre recombinase mouse line shows that LoxP recombination is position dependent. *EMBO Rep*, 2(4), 292-297.
- Walunas, T. L., Lenschow, D. J., Bakker, C. Y., Linsley, P. S., Freeman, G. J., Green, J. M., et al. (1994). CTLA-4 can function as a negative regulator of T cell activation. *Immunity*, 1(5), 405-413.
- Walunas, T. L., & Bluestone, J. A. (1998). CTLA-4 regulates tolerance induction and T cell differentiation in vivo. *J Immunol*, 160(8), 3855-3860.
- Wang, L., Fraser, C. C., Kikly, K., Wells, A. D., Han, R., Coyle, A. J., et al. (2005). B7-H3 promotes acute and chronic allograft rejection. *Eur J Immunol*, 35(2), 428-438.
- Watanabe, N., Gavrieli, M., Sedy, J. R., Yang, J., Fallarino, F., Loftin, S. K., et al. (2003). BTLA is a lymphocyte inhibitory receptor with similarities to CTLA-4 and PD-1. *Nat Immunol*, 4(7), 670-679.
- Waterhouse, P., Penninger, J. M., Timms, E., Wakeham, A., Shahinian, A., Lee, K. P., et al. (1995). Lymphoproliferative disorders with early lethality in mice deficient in Ctl4. *Science*, 270(5238), 985-988.
- Witmer-Pack, M. D., Olivier, W., Valinsky, J., Schuler, G., & Steinman, R. M. (1987). Granulocyte/macrophage colony-stimulating factor is essential for the viability and function of cultured murine epidermal Langerhans cells. *J Exp Med*, 166(5), 1484-1498.
- Wu, Y., Guo, Y., Huang, A., Zheng, P., & Liu, Y. (1997). CTLA-4-B7 interaction is sufficient to costimulate T cell clonal expansion. *J Exp Med*, 185(7), 1327-1335.
- Yanagawa, T., Hidaka, Y., Guimaraes, V., Soliman, M., & DeGroot, L. J. (1995). CTLA-4 gene polymorphism associated with Graves' disease in a Caucasian population. *J Clin Endocrinol Metab*, 80(1), 41-45.
- Yoshinaga, S. K., Whoriskey, J. S., Khare, S. D., Sarmiento, U., Guo, J., Horan, T., et al. (1999). T-cell co-stimulation through B7RP-1 and ICOS. *Nature*, 402(6763), 827-832.

Zhenyue, H., Brigitte, H., Hideo, Y., Rajewsky, K. (2004). T Cell-Specific Ablation of Fas Ligand-mediated Lymphocyte Depletion and Inflammatory Pulmonary Fibrosis. *J Exp Med*, 199 (10), 1355-1365.

Zinkernagel, R. M., & Doherty, P. C. (1974). Restriction of in vitro T cell-mediated cytotoxicity in lymphocytic choriomeningitis within a syngeneic or semiallogeneic system. *Nature*, 248(450), 701-702.